The phytochemical therapeutic potential of *Doliocarpus dentatus* Red and White Ecotypes: Metabolomics, phytohormone profiles and Antioxidant Properties

A Thesis Submitted to the Committee on Graduate Studies

in Partial Fulfilment of the Requirements

for the Degree of

Doctor of Philosophy

in the Faculty of Arts and Science

TRENT UNIVERSITY

Peterborough, ON, Canada

Environment and Life Sciences Ph.D. Graduate Program

May 2025

ABSTRACT

The phytochemical therapeutic potential of *Doliocarpus dentatus* Red and White Ecotypes: Metabolomics, phytohormone profiles and Antioxidant Properties

Ewart Anthony Smith

The study examines the phytochemical and phytohormone profiles of two ecotypes of *Doliocarpus dentatus* (Capadulla) from Guyana with an emphasis on their potential therapeutic applications, particularly in the context of erectile dysfunction. The research concentrates on the red and white ecotypes, which are visibly differentiated by the colouration of their inner and outer bark; moreover, the red ecotype is widely regarded by traditional knowledge to be more efficacious in treating erectile dysfunction. The study seeks to provide much-needed scientific evidence to support the traditional medicinal uses of *D. dentatus* and aims to accomplish this by providing semi-targeted and targeted analysis of its bioactive compounds.

The thesis employs a multi-faceted approach, commencing with Chapter 2, an examination of the international and national frameworks that govern natural product research in Guyana, thereby ensuring ethical and sustainable practices. Chapter 3, Liquid chromatography-mass spectrometry-based metabolomics was utilized to analyze the phytochemical profiles of the red and white ecotypes of *D. dentatus*. Approximately 847 compounds were identified, with 138 tentatively classified as potentially therapeutic, particularly polyphenols exhibiting antioxidant properties.

Chapter 4 focus on the phytohormone profiling revealed that the red ecotype generally exhibited higher levels of active cytokinins, particularly trans-zeatin (*t*Z) and cis-zeatin (cZ), compared to the white ecotype. A strong correlation was identified between specific cytokinins and secondary metabolites such as flavonoids and alkaloids, suggesting complex interactions that may enhance the therapeutic potential of *D. dentatus*.

Chapter 5 further analysis of total phenolic content, flavonoid content, and their antioxidant capacities demonstrated differences between the red and white ecotypes, with the red ecotype generally showing higher levels of these compounds. Both ecotypes demonstrated significant antioxidant activity, with the red ecotype showing enhanced radical scavenging capacity. The study also revealed a diverse range of bioactive compounds, including flavonoids, terpenoids, and alkaloids, which may contribute to the plant's reported medicinal properties.

This semi-targeted and targeted analysis provides novel insights into the phytochemical and phytohormone profiles of *D. dentatus* ecotypes, offering a scientific basis for their traditional medicinal uses and potential therapeutic applications. The findings suggest that *D. dentatus*, particularly the red ecotype, may have significant potential for developing new drugs, especially in the context of erectile dysfunction therapy.

KEYWORDS

Doliocarpus dentatus, ecotypes (red and white), metabolomics, therapeutic properties, secondary metabolites; Nagoya protocol; Bioactive compounds, antioxidant, phenolic content; erectile dysfunction, liquid chromatography-electrospray ionization tandem mass spectrometry.

PREFACE

This thesis is presented in manuscript format. The contents of Chapters 1 and 2 are derived from a published review. Chapter 3 marks the initiation of the first experimental chapter. Chapters 2 and 3 have been published in the Journal of Academic Research and Essays and the Journal of Metabolites, respectively. Each chapter is either published or has been submitted for publication. Co-authors and their contributions are detailed in the preface of each chapter. Furthermore, all manuscript chapters (Chapters 4-6, inclusive) are the result of collaborative efforts, with collaborators acknowledged at the beginning of each chapter. Permissions from copyright holders for the published chapters are provided in Appendix 1.

ACKNOWLEDGEMENTS

Like many great journeys, mine began with having a love for plants and trees during my undergraduate studies—which set me on the path that led me here. Along the way, I have been fortunate to receive encouragement and support from many incredible people, and I extend my heartfelt thanks to each of you.

Initially, I would like to express my gratitude to my co-supervisors, Professor Neil Emery and Professor Suresh Narine for the privilege of conducting research in your laboratories. It has been a privilege and honour to learn from and work with you both, and your mentorship has influenced the researcher I am today. Additionally, I am appreciative of the guidance provided by my committee member, Professor Sanela Martic. To Linda Cardwell, Mary-Lynn Scriver, Angela Sikma and Chris Williams for their much-appreciated administrative direction over the years.

This journey has been enriched and made more enjoyable by the members of the Emery, Narine and Martic labs, both past and present—thank you all. I am especially grateful to Dr. Laziz Bouzidi, Dr. Ainsley Lewis, and Dr. Erin Morrison for their invaluable mentorship, guidance, friendship, and support over the years. I would particularly like to thank Dr. Ainsely for his mentorship, friendship, and encouragement, which have been essential to my development as a researcher. Additionally, I would like to express my gratitude to my colleagues, Chetwynd Osborne, Hamant France, Stacy James, Shaveshwar Deonarine, Josephine Esposto and Dr. Navindra Soodoo, for their unwavering support and friendship throughout the years.

I am grateful for the unwavering support, encouragement, and prayers of my family and friends. I am particularly appreciative of the unwavering support and affection of my wife and

mother Abiola Smith and Cheryl Small, who have served as the bedrock of this chapter of my life. To my sisters sheldine Gordon, Keyana Small, and Aslin Smith I am grateful for your unwavering support and friendship.

I am most grateful to my Lord and Savior, Jesus Christ, for the invaluable lessons and fortitude he has provided me during this experience. He is robust when I am frail.

Lastly, I would like to extend my gratitude to The University of Guyana and Trent University for allowing me to develop as a scientist and as a person. I have been genuinely fortunate to be a member of this community.

TABLE OF CONTENTS

LIST OF FIGURES

CHAPTER 1

CHAPTER 2

CHAPTER 3

CHAPTER 4

CHAPTER 5

LIST OF TABLES

CHAPTER 2

CHAPTER 3

CHAPTER 4

CHAPTER 5

CHAPTER 5

LIST OF ABBREVIATIONS

ABS	Access and Benefit Sharing
AST	Alanine Aminotransferase
CBD	Convention on Biological Diversity
CBPR	Community-Based Participatory Research
CKs	Cytokinins
CNA	Competent National Authority
cZ	cis-Zeatin
DW	Dry Weight
DZ	Dihydrozeatin
DZR	Dihydrozeatin Riboside
ED	Erectile Dysfunction
EPA	Environmental Protection Agency
ESI	Electrospray Ionization
GATS	General Agreement on Trade in Services
GATT	General Agreement on Tariffs and Trade
HPLC-PDA	High-Performance Liquid Chromatography-Photodiode Array
IP	Intellectual Property
IPRs	Intellectual Property Rights
IR	Infrared Spectroscopy
LC-MS	Liquid Chromatography-Mass Spectrometry
LCDS	Low Carbon Development Strategy
MAT	Mutually Agreed Terms
MIC	Minimal Inhibitory Concentration
MS	Mass Spectrometry
NBSAP	National Biodiversity Strategy and Action Plan
NFP	National Focal Point
NMR	Nuclear Magnetic Resonance

NP	Natural Products
PIC	Prior Informed Consent
R&D	Research and Development
SDGs	Sustainable Development Goals
TK	Traditional Knowledge
TRIPS	Trade-Related Aspects of Intellectual Property Rights
*t*Z	*t*rans-Zeatin
*t*Z7G	*t*rans-Zeatin-7-Glucoside
*t*Z9G	*t*rans-Zeatin-9-Glucoside
*t*ZR	*t*rans-Zeatin Riboside
UHPLC-HRMS	Ultra-High Performance Liquid Chromatography-High Resolution Mass Spectrometry
UNCBD	United Nations Convention on Biological Diversity
UNEP	United Nations Environment Program
UV-vis	Ultraviolet-visible
WTO	World Trade Organization

1. CHAPTER 1: GENERAL INTRODUCTION

Natural products derived from diverse plant families have played a crucial role in traditional medicine and drug development for centuries. Plant-based compounds have been a significant source of chemicals leading to the creation of numerous pharmaceutical drugs over the past 100 years (Gasmi et al., 2022; Veeresham, 2012). The World Health Organization (WHO) recognizes the widespread use of plant-based traditional medicines, particularly in developing countries where populations often rely on herbal remedies for primary health care (Gasmi et al., 2022).The use of plants in traditional medicine has been extensively documented, with plant extracts serving as natural remedies in various forms such as teas, potions, and oils (Aponte et al., 2008).

The Dilleniaceae family is a significant group of angiosperms with a pantropical distribution that extends into Australia (U.K.G. & M.L.A.M.S., 2024). It comprises 10−14 genera and approximately 500 known species of shrubs, lianas, and occasionally trees or herbaceous plants (Acevedo-Rodriguez, 2018; Bruniera & Groppo, 2010).

The family has a broad distribution across tropical and subtropical regions worldwide as shown in Fig 1.1, with significant diversity in Southeast Asia, Australia, Africa, and the Americas (Lu et al., 2024). These plants are commonly found in tropical, subtropical rainforest forests, savannas, and montane areas (Zhang et al., 2009). In the Americas, particularly in Central and South America, Dilleniaceae species are well-represented by climbing plants, such as the lianas in the *Doliocarpus* genus (Takahashi et al., 2023).

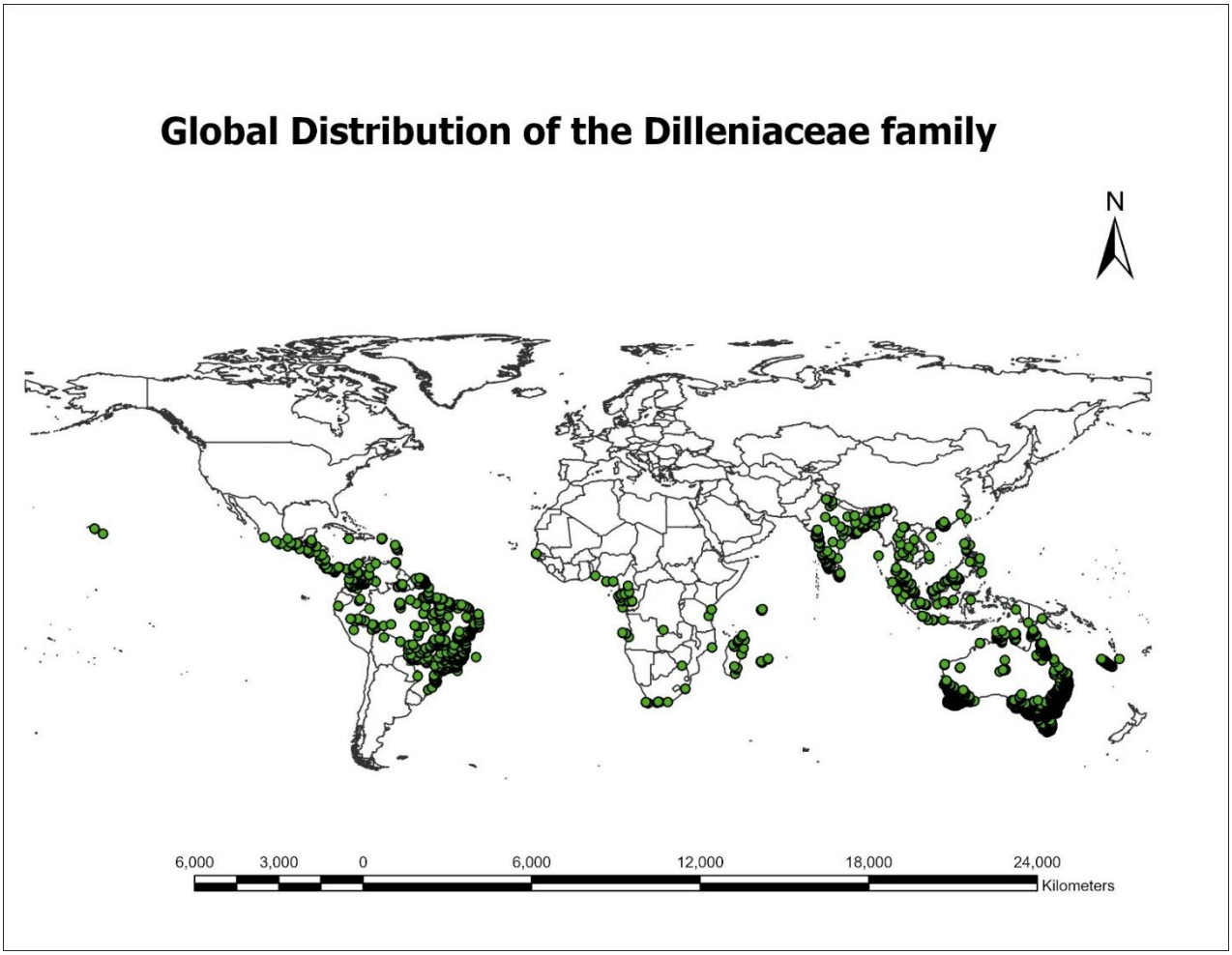

Figure 1. 1 Global Distribution of the Dilleniaceae family, green circles on the map on the continents. Image using ArcGIS Pro. The data was generated by the Global Biodiversity Information Facility (GBIF) on October 17, 2024, (User, 2024).

1.1. Phytochemical profile of Dilleniaceae

Studies indicate that the phytochemical profile of the Dilleniaceae family is diverse and extensive, with over 130 compounds isolated from various species. The major classes of compounds found in this family include flavonoids, terpenoids, lignans, anthraquinones, and other

phenolic derivatives. Flavonoids are particularly abundant, with 76 different compounds identified, including flavones, flavonols, dihydroflavonols, and isoflavones (Lima et al., 2014). Terpenoids are another important group for which 33 compounds have been identified, including phytosteroids and triterpenes with different structural skeletons (Lima et al., 2014).

The Dilleniaceae family displays a wide range of biological activities across its various genera and species. Researchers have documented several notable effects, including antimicrobial properties, where species such as *C. americana, D. indica*, and *Tetracera* show antibacterial, antifungal, and antimycobacterial activities against different pathogens (Biso et al., 2010). Other significant activities include anti-inflammatory, analgesic, antioxidant, antidiabetic, anticancer, gastroprotective, hepatoprotective, antihypertensive, antileishmanial, immunomodulatory, and xanthine oxidase inhibitory activities, largely attributed to their rich content of flavonoids, terpenoids, and phenolic compounds (Alam et al., 2012; Kushima et al., 2009; Sauvain et al., 1993).

The Dilleniaceae family exhibits remarkable pharmacological potential, supported by ethnomedicinal practices, traditional medicinal use and robust scientific evidence (Lima et al., 2014). However, despite their promising bioactive profiles of the Dilleniaceae species , only seven out of nineteen studied species have been rigorously analyzed for therapeutic properties (Barua et al., 2018; Lima et al., 2014; Sabandar et al., 2017). This stark research gap highlights a largely untapped resource. Future studies may reveal even more diverse and potent applications, particularly among under-investigated species such as *Doliocarpus dentatus* (Lima et al., 2014).

Dilleniaceae-derived chemicals show significant promise as sources of targeted therapeutics, supported by both traditional uses and modern pharmacological research. Notably, compounds such as betulinic acid and koetjapic acid, isolated from species like *Dillenia indica* and Dillenia serrata, have demonstrated potent anticancer activity. These triterpenoids induce apoptosis in cancer cells by modulating critical signaling pathways, including Akt/mTOR, NF-κB, and JAK/STAT3, which are involved in cell survival, inflammation, and metastasis (Jalil et al., 2015; Nordin et al., 2017). Betulinic acid, in particular, has shown selective toxicity toward cancer cells with minimal effects on normal cells, making it a promising candidate that has already advanced to preclinical trials (Nordin et al., 2017).

In addition to their anticancer potential, Dilleniaceae extracts have exhibited strong anti-inflammatory and analgesic properties. For example, extracts from *Dillenia serrata* have been shown to inhibit prostaglandin E2 production at levels comparable to standard anti-inflammatory drugs like indomethacin (Nordin et al., 2017). Similarly, *D. dentatus* contains betulin and betulinic acid, which provide analgesic and anti-inflammatory effects in animal studies without genotoxicity (Branquinho et al., 2021; Lima et al., 2014; Sauvain et al., 1993). The family also offers antidiabetic and antioxidant benefits, as seen with *D. indica* fruit extracts, which help regulate blood glucose and reduce oxidative stress in diabetic models. These effects are attributed to the presence of flavonoids and triterpenoids and have even led to patents for diabetes-related formulations (Jalil et al., 2015; Lima et al., 2014; Nordin et al., 2017).

1.2. *Doliocarpus dentatus* (Aubl.) Standley

Doliocarpus dentatus (Aubl.) Standley, hereafter referred to as *D. dentatus* is a species within the Dilleniaceae family. It is used in traditional medicine for various therapeutic properties. It is well-known for its role in treating conditions such as venereal disease and skin ulcers (Branquinho, Verdan, et al., 2021a; Van Andel T, 2000).

The two ecotypes of *D. dentatus*, which can be found in Guyana, are the most utilized in traditional medicine (Branquinho, Verdan, et al., 2021a; Branquinho, Verdan, Silva-Filho, et al., 2021; van Andel, 2000). While anecdotal evidence is abundant for their beneficial effects on specific illnesses such as leishmanial ulcers, erectile dysfunction (ED) and for promoting overall health and wellness, no scientific evidence has been provided to back up the claims. Accounts of intended benefits are publicized on popular online platforms such as YouTube since news journals, the Guyana Chronicle journal in 2013 popularized *D. dentatus* ethnomedical and pharmacological properties. An acceptable and much-publicized claim is that *D. dentatus* acts as a natural aphrodisiac, earning it the nickname 'local Viagra' due to its widespread informal use for this purpose. Nonetheless, these claims remain unsupported by scientific evidence.

1.3. Botanical Description

D. dentatus morphological features are shown in (Fig 1.2). The outer barks and mature leaves of *D. dentatus* red ecotype are shown in (Fig 1.3). *D. dentatus* red ecotype consists of bark that is greyish brown, smooth with circular plates. In cross-section, the cambia producing alternating concentric rings of xylem and phloem, either cylindrical or slightly asymmetrical (Fig 1.3). The white ecotype is characterized by bark that is greyish brown and has a papery, flaky, or

peeling texture with rectangular plates. In cross-section, it features successive cambia that produce alternating concentric rings of xylem and phloem, which are either cylindrical or slightly asymmetrical.

The inner bark of the white ecotype is light red to orange while the inner bark of the red ecotype is dark red both having alternated concentric rings of xylem and phloem, either cylindrical or slightly asymmetrical (Fig 1.3). The younger parts of the stem, petioles, and major leaf veins are covered with appressed, long slender trichomes, which become less prominent as the plant matures.

The leaves have dentate margins, a feature reflected in the species name "*dentatus*". As the plant ages, its stems and leaves become glabrate, or nearly hairless. *D. dentatus* is a woody climbing vine that is well-adapted to tropical forest habitat. Its woody stem ascends and spreads throughout the canopy. The seeds are typically two in number, reniform, and black, each encased in a white aril (a specialized structure for seed dispersal), which may be either membranous or fleshy (Aymard & Gerardo, 2000). The inflorescences are characterized by their arrangement in fascicles or glomerules.

The woody stem is ascended and spread through the canopy. The seeds are typically two, reniform, black, covered by a white arillode (specialise structure for seed dispersal) this is membranous or fleshy. (Aymard & Gerardo, 2000). Inflorescences of fascicles or glomerules. The flowers exhibit bisexuality and actinomorphic. The calyx is composed of 3–6 free, subequal sepals, with the inner sepals generally larger, imbricate, and persistent. The petals, which number between 2 and 6, are free, white, and early caducous. The stamens are numerous, characterized by unequal

filaments that may be flexuous or reflexed and the anthers dehisce via longitudinal sutures. The ovary is superior and unicarpellate, housing two basal ovules. The style is terminal and filiform, while the stigma varies from punctiform to peltate (Aponte et al., 2008; Raissa Borges Ishikawa et al., 2017; Oliveira et al., 2002; Sharma et al., 2001) .

Doliocarpus dentatus **red ecotype (A)**

Doliocarpus dentatus **leaves (both ecotypes) (B)**

Doliocarpus dentatus **white ecotype (C)**

Figure 1. 2 . Barks and mature leaves of *D. dentatus* (red and white ecotypes). A. *D. dentatus* red ecotype. B. *D. dentatus* mature leaves of red and white ecotypes. C. D. dentatus white ecotype. Photos by Ewart Smith - (21N0261909 – 0578704) (Potaro Siparuni, Region 8, Guyana, August 2022).

***Doliocarpus dentatus* red ecotype (A)**

***Doliocarpus dentatus* Fruit (both ecotypes) (B)**

***Doliocarpus dentatus* white ecotype (C)**

Figure 1. 3. *D. dentatus* red and white ecotypes morphological characteristics used to determine its selection for known therapeutic benefits. A. *D. dentatus* red ecotype, B. *D. dentatus* fruits (red and white). C. *D. dentatus* white. Photos by Ewart Smith (Potaro Siparuni (21N0261909 – 0578704), Region 8, August 2022, Guyana).

1.4. Ecology and Distribution

The Doliocarpus genus comprises 50 species, mostly woody climbers, known as lianas, that thrive in tropical regions of Central and South America and parts of the Caribbean shown in (Fig 1.4) (Bhatia et al., 2014; Huang et al., 2021; Kumar et al., 2007; Sasidharan et al., 2011). In Guyana, *D. dentatus* is frequently found as a large canopy liana in undisturbed mixed forests (Van Andel T, 2000). The species plays a vital role in forest regeneration and is ecologically important, but its conservation is critical due to habitat loss and degradation (Aymard-Corredor & Monzoli, 2024; Aymard, 1997; Dalziell et al., 2018).

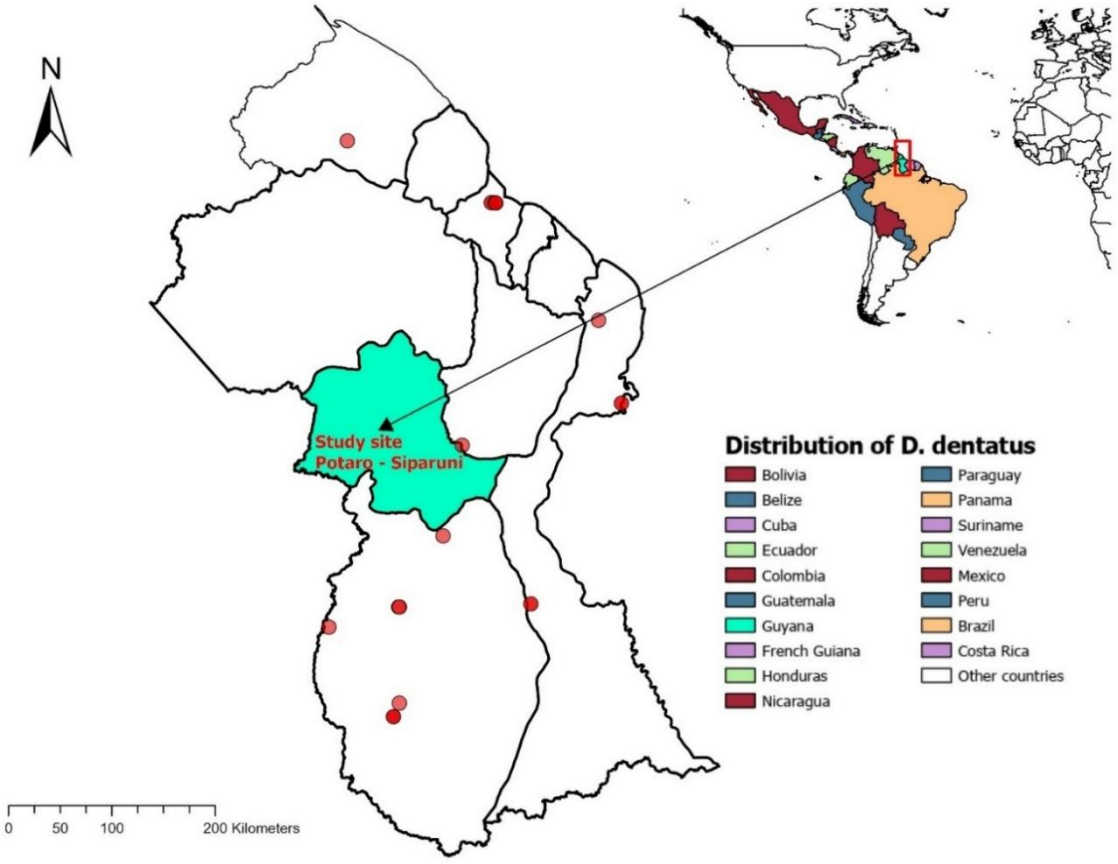

Figure 1. 4. illustrates the distribution of *D. dentatus* across Guyana. The distribution in Guyana (red circles on the map) is known for its therapeutic benefits. The Potaro-Siparuni region of Guyana, where our studies are conducted is highlighted in cyan in the map.

1.5. Phytochemical and Phytohormone Profiles *D. dentatus*

The phytochemical composition of *D. dentatus* exhibits a diverse range of bioactive compounds include flavonoids, tannins, alkaloids and terpenoids (Raissa Borges Ishikawa et al., 2017; R. Jagessar et al., 2013; Lima et al., 2014; Sousa et al., 2020), similar to other members of

the Dilleniaceae family (Aponte et al., 2008; De Toledo et al., 2011; Endringer et al., 2010; Lima et al., 2014).

D. dentatus may contain a variety of phytohormones with distinct effects that can influence its phytochemical composition and can enhance antioxidant and anti-inflammatory properties. Phytohormones are traditionally viewed as plant produced compounds that occur at $<10^{-8}$M; minute levels (Aoki et al., 2024; Hoyerová et al., 2006; Kisiala et al., 2019) and function in complex networks of signaling interactions that impact the growth and development of plants (El-Showk et al., 2013). Phytohormones aid in control diverse aspects of plant growth and development, including embryogenesis, organ size, pathogen defence, stress tolerance, and reproductive development (Han & Kahmann, 2019; Vondrakova et al., 2018; Z. Wang et al., 2016). These processes are influenced by a complex network of interactions among various plant hormones such as auxins, cytokinins, gibberellins, abscisic acid, ethylene, brassinosteroids, jasmonic acid, and salicylic acid (Choudhary & Kumari, 2021; Ma & Ma, 2016; Arpan Mukherjee et al., 2022; Stroud et al., 2022; Van der Does et al., 2013).

Phytohormones play a crucial role in the regulation of secondary metabolites in plants, which can enhance antioxidant and anti-inflammatory properties (Divekar et al., 2022; Lv et al., 2021b). These hormones, including JA, CKs and SA are recognized for their ability to modulate secondary metabolism in plants (Bernabé-Antonio et al., 2023). They can trigger transcriptional reprogramming, resulting in an increased synthesis of secondary metabolites such as phenylpropanoids, terpenoids, and alkaloids. Specifically, JA signaling is known to regulate the biosynthesis of terpenoid indole alkaloids and phenylpropanoids, while SA and CKs may induce the production of anthocyanins and phenolics (Bernabé-Antonio et al., 2023).

Phytohormones have the capacity to enhance antioxidant defenses by modulating the activities of both enzymatic and non-enzymatic antioxidants. For example, SA and ET can stimulate the production of antioxidants, thereby aiding plants in scavenging reactive oxygen species (ROS) and alleviating oxidative stress (Bernabé-Antonio et al., 2023). This mechanism is essential for safeguarding plants against abiotic stressors, such as ozone exposure, as an increased antioxidant capacity contributes to plant survival. The augmented antioxidant capacity is primarily attributed to the enhanced production of secondary metabolites with antioxidant properties, including flavonoids, which are recognized for their antioxidant, anti-inflammatory, and anticarcinogenic effects (Roy, 2017).

CKs are a group of evolutionarily significant molecules, renowned for their pivotal roles in signaling, where they coordinate various aspects of plant growth and development (Kisiala et al., 2019; Mok & Mok, 2001; Mok, 2019; Svolacchia & Sabatini, 2023). Chemically, these molecules are N^6 adenine derivatives, and they display a broad phylogenetic occurrence, extending from bacteria to humans, with both shared and divergent roles, such as promoting growth and influencing virulence (Aoki et al., 2024; Kieber & Schaller, 2018; Pils & Heyl, 2009). This diverse functionality underscores the complex and multifaceted nature of CKs across different kingdoms of life.

While phytohormones do not directly exhibit anti-inflammatory properties, the secondary metabolites they regulate can have significant anti-inflammatory effects. Phytochemicals such as flavonoids and phenolic acids, which are influenced by phytohormones, have been shown to modulate immune responses and reduce inflammation in various models (Mohammed et al., 2014; Nisar et al., 2023). For instance, flavonoids such as luteolin and kaempferol have been found to

suppress chronic inflammation by inhibiting pro-inflammatory CK and pathways (Nisar et al., 2023). These compounds can target multiple pathways involved in inflammation, thereby providing potential therapeutic benefits. Thus, the indirect role of phytohormones in enhancing anti-inflammatory properties occurs through the regulation of these beneficial secondary metabolites (Mohammed et al., 2014; Nisar et al., 2023).

Despite the vast majority of phytohormone studies have investigated production by and action in plants, current research is highlighting the importance of CKs, their conjugates, their interaction and influence on the biosynthesis of secondary metabolites such as terpenoids, phenylpropanoids and alkaloids in *D. dentatus* ecotypes that may contribute to its efficacy for treatment for ED.

The investigation of phytochemicals and their potential interactions with CKs in *D. dentatus* ecotypes presents significant opportunities for the discovery of bioactive compounds that may serve as treatments for ED. Examining the interplay between phytochemicals and CKs could enhance our understanding of plant-based remedies and their therapeutic applications. This topic is further elaborated upon in Chapter 3, 4 and throughout the remainder of the thesis.

1.6. Thesis Format and Research Objective, hypotheses and predictions

At the onset of research presented in this thesis, very little was known about the phytochemical and phytohormone profiles and phenolic and flavonoid content of the two ecotypes of the *D. dentatus* red and white, known in Guyana as Capadulla. While *D. dentatus* is regarded as a powerful aphrodisiac, key questions remain: What phytochemicals are present in the stem of *D. dentatus* red and white ecotypes? And is there a difference between the phytohormone profiles,

phenolic and flavonoid content and cytokinin profiles of *D. dentatus* red and white ecotypes? The overall objective of this thesis is a spectrometry-based metabolomics investigation of *D. dentatus* ecotypes from Central Guyana with a focus on the therapeutic potential of various biomarkers for erectile dysfunction therapy. This thesis is presented as a compilation of four manuscripts, each representing a single chapter; followed by a general discussion in which the overall findings and future directions are discussed.

The research objectives, hypotheses and predictions of this thesis were to:

1. **Examine international and national policy frameworks governing natural product research in Guyana.**

1.1. $H_{O:}$ the implementation of strong international and national policy frameworks in Guyana increases transparency, accountability, and sustainability in natural product research, thereby enhancing the country's ability to derive economic benefits from its biodiversity while ensuring environmental conservation and social equity.

1.2. Based on the current trends and policies in Guyana, it is predicted that the country will continue to strengthen its international and national policy frameworks governing natural product research. This will likely involve further implementation of agreements like the National Policy on Access to Genetic Resources and Fair and Equitable Sharing of Benefits to better regulate access to its rich biodiversity and ensure equitable benefit sharing with local stakeholders and international partners.

2.0. **Determine the general profile and target bioactive compounds of taxonomic origin of *D. dentatus* ecotypes in response to erectile dysfunction (ED) therapy**.

2.1. H_O: The red ecotype of *D. dentatus* contains higher levels of flavonoids, such as epicatechin methyl gallate, catechin gallate, and proanthocyanidin A2, compared to the white ecotype, which will correlate with enhanced therapeutic potential for erectile dysfunction. This higher flavonoid content is associated with enhanced antioxidant activity which reduces reducing oxidative stress and inflammation, thereby improving therapy for ED.

2.2.H_O: The metabolic pathways involved in the biosynthesis of flavonoids and other polyphenols in the *D. dentatus* red ecotype are more active, contributing more to its higher therapeutic efficacy for erectile dysfunction compared to the white ecotype.

3. **Determine the phytohormone levels in *D. dentatus* red and white ecotypes.**

3.1. H_O: The red ecotype of *D. dentatus* contains higher cytokinin levels compared to the white ecotype, leading to enhanced secondary metabolites with antioxidant and anti-inflammatory properties, contributing to its greater therapeutic efficacy for ED.

It is predicted that the *D. dentatus* red ecotype will contain higher levels of CKs than the white ecotypes of *D. dentatus*. The differences in CK levels may be linked to its secondary metabolites with antioxidant and anti-inflammatory properties, contributing to its greater therapeutic efficacy for ED.

4. **Assess the phenolic, flavonoid content and antioxidant capacities of *D. dentatus* red and white ecotypes**

4.1.H_O: The red ecotype of *D. dentatus* contains higher concentrations of total phenolic and flavonoid compounds compared to the white ecotype, which is associated with greater antioxidant activity, as measured by assays such as 2,2-diphenyl-2-picrylhydrazyl (DPPH).

It is predicted that both ecotypes of *D. dentatus* red exhibit significant levels of phenolic and flavonoid compounds, contributing to their antioxidant capacities. The red ecotype, given its higher metabolic profile, pigmentation and flavonoid content, is likely to show higher antioxidant activity compared to the white ecotype. This will be discussed in chapter 5.

To achieve these objectives, I examined the international legal framework and instruments that facilitate the development of trust, protection of biological resources, benefit sharing and connections between developing countries rich in biodiversity with research and development users. I further focused on the legal Framework of Guyana for protecting Biodiversity Resources and provides an understanding of the legal framework implemented in Guyana South America to protect biodiversity resources (chapter 2). Chapter 2 provided guided compliance with ethical and legal standards for natural product research, especially when it involves the collection of biological material from Indigenous communities in Guyana South America. It has emphasised building trust and establishing partnerships with local communities to ensure ethical and sustainable collection practices and capacity building and knowledge sharing to empower local communities and promote their participation in the research process (Chapter 2). The information gathered in

Chapter 2 was used to design a protocol for collecting biological material in a standardised and ethical manner. Once the protocol was finalised, it was tested and refined through a pilot study before being implemented in the main study. Overall, chapter 2 was crucial in ensuring the study's success by providing a solid foundation for collecting high-quality biological material.

In Chapter 3, I collected samples of *D. dentatus* red and white ecotypes from the Guyana rainforest. Samples were analysed in positive and negative electrospray ionisation (ESI) modes using liquid chromatography-mass spectrometry in full scan mode with a minor modification. All acquired untargeted mass spectrometry data were analysed using XCMS Online, XCalibur software, MetaboAnalyst (5.0 and 6.0), and Metaboquest and database. This analysis was done for methanolic extracts of *D. dentatus* red (treatment) and *D. dentatus* white (control) to understand the phytochemical profiles of the two ecotypes and to identify potential bioactive compounds in the different ecotypes. Approximately 847 compounds were identified through the metabolomic screening, with 138 compounds tentatively identified as potentially therapeutic—particularly polyphenols, which are known to have antioxidant properties.

Polyphenols emerged as the dominant class of compounds in both ecotypes, accounting for 63.9 % of the identified metabolites. This abundance of polyphenols, particularly in the red ecotype, underscores the potential therapeutic value of *D. dentatus*, given the well-documented health benefits of these compounds, including antioxidant and anti-inflammatory properties.

Chapter 4 focuses on the phytohormone profiles of *D. dentatus* red and white ecotypes. The screening was conducted to determine whether there is difference between the phytohormone profiles of *D. dentatus* red and white ecotype. The screening of these ecotypes reveals that, red ecotype generally exhibited higher levels of active CKs, particularly trans-zeatin (*t*Z) and cis-

zeatin (*c*Z), compared to the white ecotype. Notably, the red ecotype showed a remarkable accumulation of certain glucoside forms, especially *t*Z7G, suggesting a potential reservoir of inactive cytokinins that could be converted to active forms under specific conditions. A strong correlation was identified between specific cytokinins (e.g., *t*ZR, *t*Z9G, DZR, DZ) and secondary metabolites such as flavonoids and alkaloids, suggesting a complex interaction that may enhance the therapeutic potential of *D. dentatus*.

Chapter 5 is more targeted and functional testing approach, and builds on the data from Chapters 3 and 4 to examine the total phenolic and flavonoid content and antioxidant capacity of *D. dentatus* red and white ecotypes. Polyphenols represent the predominant class of secondary metabolites identified in both red and white ecotypes. Furthermore, other significant superclasses of compounds encompass benzenoids, phenylpropanoids, polyketides, lipids, and lipid-like molecules. This chapter seeks to enhance our understanding of the specific compounds present in *D. dentatus* ecotypes, with particular emphasis on the concentrations of phenolic compounds and antioxidants within these ecotypes.

The red and white ecotypes of *D. dentatus* reveals significant differences in their phytochemical profiles and antioxidant capacities. The red ecotype exhibits higher total phenolic content, averaging 119.70 mg/g, compared to the white ecotype's 61.08 mg/g. Similarly, the red ecotype contains more flavonoids, with an average of 4.146 mg/g, while the white ecotype averages 1.584 mg/g. FTIR analysis shows distinct spectral patterns, with the red ecotype displaying stronger peaks indicative of higher hydroxyl and amine functional groups. The red ecotype also demonstrates superior antioxidant activity, as evidenced by its ability to scavenge reactive oxygen species more effectively. These findings suggest that the red ecotype may offer

greater health benefits due to its enhanced antioxidant potential, supporting its traditional use in herbal medicine.

This PhD research revealed novel insights into the widespread application of *D. dentatus*, a plant species found in the South American rainforest especially Guyana with potential medicinal properties that can be used to develop new drugs.

1.7. REFERENCES

Acevedo-Rodriguez, P. (2018). Guide to the genera of lianas and climbing plants in the neotropics: Sapindaceae.

Alam, M. B., Rahman, M. S., Hasan, M., Khan, M. M., Nahar, K. N., & Sultana, S. S. (2012). Antinociceptive and antioxidant activities of the Dillenia indica bark.

Aoki, M. M., Kisiala, A. B., Mathavarajah, S., Schincaglia, A., Treverton, J., Habib, E., Dellaire, G., Emery, R. J. N., Brunetti, C. R., & Huber, R. J. (2024). From biosynthesis and beyond-Loss or overexpression of the cytokinin synthesis gene, iptA, alters cytokinesis and mitochondrial and amino acid metabolism in Dictyostelium discoideum. *Faseb j*, *38*(1), e23366. https://doi.org/10.1096/fj.202301936RR

Aponte, J. C., Vaisberg, A. J., Rojas, R., Caviedes, L., Lewis, W. H., Lamas, G., Sarasara, C., Gilman, R. H., & Hammond, G. B. (2008). Isolation of cytotoxic metabolites from targeted Peruvian Amazonian medicinal plants. Journal of Natural Products, 71(1), 102-105. https://doi.org/10.1021/np070560c

Aymard-Corredor, G. A., & Monzoli, J. V. L. (2024). A new species of Doliocarpus (Dilleniaceae, Doliocarpoideae) from the Amazon forests and an updated key for the Colombian species. Harvard Papers in Botany, 29(1), 37-44.

Aymard, C., & Gerardo, A. (2000). Dilleniaceae Novae Neotropicae: XI. A new subandean species of Doliocarpus. Brittonia, 52(2), 196-199. https://doi.org/10.2307/2666523

Aymard, G. A. (1997). Dilleniaceae Novae Neotropicae, V. El Genero Doliocarpus En Colombia. Anales del Jardin Botanico de Madrid, 55(1), 17-30.

Bernabé-Antonio, A., Castro-Rubio, C., Rodríguez-Anda, R., Silva-Guzmán, J. A., Manríquez-González, R., Hurtado-Díaz, I., Sánchez-Ramos, M., Hinojosa-Ventura, G., & Romero-Estrada, A. (2023). Jasmonic and Salicylic Acids Enhance Biomass, Total Phenolic Content, and Antioxidant Activity of Adventitious Roots of Acmella radicans (Jacq.)

R.K. Jansen Cultured in Shake Flasks. *Biomolecules*, *13*(5). https://doi.org/10.3390/biom13050746

Bhatia, H., Sharma, Y. P., Manhas, R. K., & Kumar, K. (2014). Ethnomedicinal plants used by the villagers of district Udhampur, J&K, India. Journal of Ethnopharmacology, 151(2), 1005-1018. https://doi.org/10.1016/j.jep.2013.12.017

Biso, F. I., Rodrigues, C. M., Rinaldo, D., dos Reis, M. B., Bernardi, C. C., de Mattos, J. C. P., Caldeira-de-Araújo, A., Vilegas, W., de Syllos Cólus, I. M., & Varanda, E. A. (2010). Assessment of DNA damage induced by extracts, fractions and isolated compounds of Davilla nitida and Davilla elliptica (Dilleniaceae). Mutation Research/Genetic Toxicology and Environmental Mutagenesis, 702(1), 92-99. https://doi.org/10.1016/j.mrgentox.2010.07.013

Branquinho, L. S., Verdan, M. H., Santos, E. d., Neves, S. C. d., Oliveira, R. J., Cardoso, C. A. L., & Kassuya, C. A. L. (2021a). Aqueous extract from leaves of Doliocarpus dentatus (Aubl.) Standl. relieves pain without genotoxicity activity. Journal of Ethnopharmacology, 266, 113440. https://doi.org/10.1016/j.jep.2020.113440

Branquinho, L. S., Verdan, M. H., Silva-Filho, S. E., Oliveira, R. J., Cardoso, C. A. L., Arena, A. C., & Kassuya, C. A. L. (2021). Antiarthritic and antinociceptive potential of ethanolic extract from leaves of Doliocarpus dentatus (aubl.) standl. in mouse model. Pharmacognosy Research, 13(1), 1-8. https://doi.org/10.4103/pr.pr_76_20

Bruniera, C. P., & Groppo, M. (2010). Flora da Serra do Cipó, Minas Gerais: Dilleniaceae. Boletim de Botânica da Universidade de São Paulo, 28(1), 59-67. https://doi.org/10.11606/issn.2316-9052.v28i1p59-67

Choudhary, M., & Kumari, A. (2021). Understanding plant hormones: Mechanisms and functions in growth and development. Plant Science Archives, 6(1), 14. https://doi.org/10.51470/PSA.2021.6.1.14

Dalziell, E. L., Erickson, T. E., Hidayati, S. N., Walck, J. L., & Merritt, D. J. (2018). Alleviation of morphophysiological dormancy in seeds of the Australian arid-zone endemic shrub, Hibbertia glaberrima F. Muell. (Dilleniaceae). Seed Science Research, 28, 286-293. https://doi.org/10.1017/S0960258518000247

De Toledo, C. E., Britta, E. A., Ceole, L. F., Silva, E. R., De Mello, J. C., Dias Filho, B. P., Nakamura, C. V., & Ueda-Nakamura, T. (2011). Antimicrobial and cytotoxic activities of medicinal plants of the Brazilian cerrado, using Brazilian cachaça as extractor liquid. *Journal of Ethnopharmacology, 133*(2), 420-425.

Divekar, P. A., Narayana, S., Divekar, B. A., Kumar, R., Gadratagi, B. G., Ray, A., Singh, A. K., Rani, V., Singh, V., & Singh, A. K. (2022). Plant secondary metabolites as defense tools

against herbivores for sustainable crop protection. *International journal of molecular sciences*, *23*(5), 2690. https://doi.org/10.3390/ijms23052690

El-Showk, S., Ruonala, R., & Helariutta, Y. (2013). Crossing paths: cytokinin signalling and crosstalk. *Development*, *140*(7), 1373-1383. https://doi.org/10.1242/dev.087676

Endringer, D. C., Valadares, Y. M., Campana, P. R., Campos, J. J., Guimarães, K. G., Pezzuto, J. M., & Braga, F. C. (2010). Evaluation of Brazilian plants on cancer chemoprevention targets in vitro. Phytotherapy Research, 24(6), 928-933. https://doi.org/10.1002/ptr.3051

Gasmi, A., Chirumbolo, S., Peana, M., Noor, S., Menzel, A., Dadar, M., & Bjørklund, G. (2022). The role of diet and supplementation of natural products in COVID-19 prevention. Biological Trace Element Research, 200(1), 27-30. https://doi.org/10.1007/s12011-021-02623-3

Han, X., & Kahmann, R. (2019). Manipulation of phytohormone pathways by effectors of filamentous plant pathogens. *Frontiers in Plant Science*, *10*, 822. https://doi.org/ 10.3389/fpls.2019.00822

Hoyerová, K., Gaudinová, A., Malbeck, J., Dobrev, P. I., Kocábek, T., Šolcová, B., Trávníčková, A., & Kamínek, M. (2006). Efficiency of different methods of extraction and purification of cytokinins. *Phytochemistry*, *67*(11), 1151-1159. https://doi.org/ 10.1016/j.phytochem.2006.04.014

Huang, D., Dang, F., Huang, Y., Chen, N., & Zhou, D.-M. (2021). Uptake, translocation, and transformation of silver nanoparticles in plants. Environmental Science: Nano, 8(7), 1757-1778. https://doi.org/10.1039/D1EN00195G

Ishikawa, R. B., Leitão, M. M., Kassuya, R. M., Macorini, L. F., Moreira, F. M. F., Cardoso, C. A. L., Coelho, R. G., Pott, A., Gelfuso, G. M., Croda, J., Oliveira, R. J., & Kassuya, C. A. L. (2017). Anti-inflammatory, antimycobacterial and genotoxic evaluation of Doliocarpus dentatus. Journal of Ethnopharmacology, 204, 18-25. https://doi.org/10.1016/j.jep.2017.04.004

Jagessar, R., Hoolas, G., & Maxwell, A. (2013). Phytochemical screening, isolation of betulinic acid, trigonelline and evaluation of heavy metals ion content of Doliocarpus dentatus. Journal of Natural Products, 6, 5-16.

Kieber, J. J., & Schaller, G. E. (2018). Cytokinin signaling in plant development. *Development*, *145*(4), dev149344.

Kisiala, A., Kambhampati, S., Stock, N. L., Aoki, M., & Emery, R. N. (2019). Quantification of cytokinins using high-resolution accurate-mass orbitrap mass spectrometry and parallel reaction monitoring (PRM). *Analytical chemistry*, *91*(23), 15049-15056

Kumar, G., Jayaveera, K., Kumar, C., Sanjay, U. P., Swamy, B., & Kumar, D. (2007). Antimicrobial effects of Indian medicinal plants against acne-inducing bacteria. Tropical Journal of Pharmaceutical Research, 6(2), 717-723. https://doi.org/10.4314/tjpr.v6i2.14651

Kumari, J., Navas, M., Dan, M., & Rajasekharan, S. (2009). Pharmacognostic studies on Acrotrema arnottianum Wight — A promising ethnomedicinal plant. Indian Journal of Traditional Knowledge, 8(3), 334-337.

Kushima, H., Nishijima, C. M., Rodrigues, C. M., Rinaldo, D., Sassá, M. F., Bauab, T. M., Di Stasi, L. C., Carlos, I. Z., Brito, A. R. M. S., & Vilegas, W. (2009). Davilla elliptica and Davilla nitida: gastroprotective, anti-inflammatory immunomodulatory and anti-Helicobacter pylori action. Journal of Ethnopharmacology, 123(3), 430-438. https://doi.org/10.1016/j.jep.2009.03.031

Lima, C. C., Lemos, R. P. L., & Conserva, L. M. (2014). Dilleniaceae family: An overview of its ethnomedicinal uses, biological and phytochemical profile. Journal of Pharmacognosy and Phytochemistry, 3(2), 181-204.

Lu, J. Z., Pan, X., Scheu, S., & Maraun, M. (2024). Biogeography of oribatid mites (Acari) reflects their ancient origin and points to Southeast Asia as centre of radiation. Journal of Biogeography. https://doi.org/10.1111/jbi.14791

Lv, Z.-Y., Sun, W.-J., Jiang, R., Chen, J.-F., Ying, X., Zhang, L., & Chen, W.-S. (2021). Phytohormones jasmonic acid, salicylic acid, gibberellins, and abscisic acid are key mediators of plant secondary metabolites. *World Journal of Traditional Chinese Medicine*, *7*(3), 307-325.

Ma, K. W., & Ma, W. (2016). Phytohormone pathways as targets of pathogens to facilitate infection. *Plant Mol Biol*, *91*(6), 713-725. https://doi.org/10.1007/s11103-016-0452-0

Mohammed, M. S., Osman, W. J., Garelnabi, E. A., Osman, Z., Osman, B., Khalid, H. S., & Mohamed, M. A. (2014). Secondary metabolites as anti-inflammatory agents. *The Journal of Phytopharmacology*, *3*(4), 275-285.

Mok, D. W., & Mok, M. C. (2001). Cytokinin metabolism and action. *Annual review of plant biology*, *52*(1), 89-118. https://doi.org/10.1146/annurev.arplant.52.1.89

Mok, M. C. (2019). Cytokinins and plant development—an overview. *Cytokinins*, 155-166.

Mukherjee, A., Gaurav, A. K., Singh, S., Yadav, S., Bhowmick, S., Abeysinghe, S., & Verma, J. P. (2022). The bioactive potential of phytohormones: A review. *Biotechnology Reports*, *35*, e00748. https://doi.org/doi/10.1016/j.btre.2022.e00748

Nisar, A., Jagtap, S., Vyavahare, S., Deshpande, M., Harsulkar, A., Ranjekar, P., & Prakash, O. (2023). Phytochemicals in the treatment of inflammation-associated diseases: the journey from preclinical trials to clinical practice. *Front Pharmacol*, *14*, 1177050. https://doi.org/10.3389/fphar.2023.1177050

Oliveira, B. H. d., Santos, C. A., & Espíndola, A. P. D. (2002). Determination of the triterpenoid, betulinic acid, in Doliocarpus schottianus by HPLC. *Phytochemical Analysis: An International Journal of Plant Chemical and Biochemical Techniques*, *13*(2), 95-98.

Pils, B., & Heyl, A. (2009). Unraveling the evolution of cytokinin signaling. *Plant Physiol*, *151*(2), 782-791. https://doi.org/10.1104/pp.109.139188

Roy, A. (2017). A review on the alkaloids an important therapeutic compound from plants. *IJPB*, *3*(2), 1-9.

Sasidharan, S., Chen, Y., Saravanan, D., Sundram, K., & Latha, L. Y. (2011). Extraction, isolation and characterization of bioactive compounds from plants' extracts. African Journal of Traditional, Complementary and Alternative Medicines, 8(1), 1-10. https://doi.org/10.4314/ajtcam.v8i1.60483

Sauvain, M., Dedet, J. P., Kunesch, N., Poisson, J., Gantier, J. C., Gayral, P., & Kunesch, G. (1993). In vitro and in vivo leishmanicidal activities of natural and synthetic quinoids. Phytotherapy Research, 7(2), 167-171. https://doi.org/10.1002/ptr.2650070215

Sharma, H. K., Chhangte, L., & Dolui, A. K. (2001). Traditional medicinal plants in Mizoram, India. Fitoterapia, 72(2), 146-161. https://doi.org/10.1016/S0367-326X(00)00278-1

Soares, M., Rezende, M., Ferreira, H., Figueiredo, A., Bustamante, K., Bara, M., & Paula, J. (2005). Pharmacognostic characterization of the leaves of Davilla elliptica St.-Hil. (Dilleniaceae). Revista Brasileira de Farmacognosia, 15, 352-360. https://doi.org/10.1590/S0102-695X2005000400015

Sousa, J. N., Mafra, V., Guimarães, V. H. D., Paraiso, A. F., Lelis, D. d. F., & Santos, S. H. S. (2020). Davilla elliptica (Dilleniaceae) a. St.-Hil. Ethnomedicinal, phytochemical, and pharmacological aspects: A review. Phytochemistry Letters, 39, 135-143. https://doi.org/10.1016/j.phytol.2020.08.009

Stroud, E. A., Jayaraman, J., Templeton, M. D., & Rikkerink, E. H. (2022). Comparison of the pathway structures influencing the temporal response of salicylate and jasmonate defence hormones in Arabidopsis thaliana. *Frontiers in Plant Science*, *13*, 952301.https://doi.org/10.3389/fpls.2022.952301.

Svolacchia, N., & Sabatini, S. (2023). Cytokinins. *Current Biology*, *33*(1), R10-R13. https://doi.org/10.1016/j.cub.2022.12.002.

Takahashi, K., Nishikawa, H., Tanabe, R., & Tran, D. Q. (2023). Golden Camellia as a driver of forest regeneration and conservation: A case study of value-chain forestry with Camellia quephongensis in Que Phong, Nghe An, North-Central Vietnam. Forests, 14(3), 526. https://doi.org/10.3390/f14030526

U.K.G., A., & M.L.A.M.S., M. (2024). Pollen morphological studies on selected species of family Dilleniaceae in Sri Lanka. Proceedings of International Forestry and Environment Symposium.

Global Biodiversity Information Facility. (2024). Occurrence download. https://doi.org/10.15468/DL.QMSVK3

Van Andel T, T. R. (2000). Non-timber forest products of the North-West District of Guyana. Part II - A Field Guide. *Tropenbos-Guyana Series;8a, 8b*(NOVEMBER 2000). http://dspace.library.uu.nl/handle/1874/1168

van Andel, T. R. (2000). *Non-timber forest products of the North-West District of Guyana*. Utrecht University.

Van der Does, D., Leon-Reyes, A., Koornneef, A., Van Verk, M. C., Rodenburg, N., Pauwels, L., Goossens, A., Körbes, A. P., Memelink, J., Ritsema, T., Van Wees, S. C., & Pieterse, C. M. (2013). Salicylic acid suppresses jasmonic acid signaling downstream of SCFCOI1-JAZ by targeting GCC promoter motifs via transcription factor ORA59. *Plant Cell*, *25*(2), 744-761. https://doi.org/10.1105/tpc.112.108548

Veeresham, C. (2012). Natural products derived from plants as a source of drugs. Journal of Advanced Pharmaceutical Technology & Research, 3(4), 200–201. https://doi.org/10.4103/2231-4040.104709

Vondrakova, Z., Dobrev, P. I., Pesek, B., Fischerova, L., Vagner, M., & Motyka, V. (2018). Profiles of endogenous phytohormones over the course of Norway spruce somatic embryogenesis. *Frontiers in Plant Science*, *9*, 1283. https://doi.org/10.3389/fpls.2018.01283

Wang, Z., Li, N., Jiang, S., Gonzalez, N., Huang, X., Wang, Y., Inzé, D., & Li, Y. (2016). SCFSAP controls organ size by targeting PPD proteins for degradation in Arabidopsis thaliana. *Nat Commun*, *7*(1), 11192. https://doi.org/10.1038/ncomms11192

Zhang, Q., Yi, J.-Y., & Shang, X.-J. (2009). Reactive oxygen species and erectile dysfunction [Zuò yòng de yǎng huà jí yǔ bó qǐ zhàng'ài]. Zhonghua Nan Ke Xue = National Journal of Andrology, 15(12), 1124–1

CHAPTER 2

PREFACE

Title: **Compliance With International and National Frameworks Governing Natural Product Research in Guyana**

Authors: Ewart A. Smith, Ainsely Lewis, R. J. Neil Emery and Suresh Narine

Reference: Journal of Academic Research and Essays

Year: 2023

Copyright: See APPENDIX 1.

EAS conducted a desktop review (data collection from academic journals), analyzed reports, statistics, and policy documents from government agencies, created tables and figures, and wrote the manuscript. AL worked on modifications and editing. SN and RJNE conceived, directed, and obtained funding for the research presented in the study. EAS, AL, RJNE, and SN edited the manuscript before submission.

2. CHAPTER 2

Compliance with International and National Frameworks governing Natural Product Research in Guyana: Insight into the policies, guidelines and a Communication and Engagement strategy for sharing information.

Published in: Journal of Academic Research and Essays (2024)

ABSTRACT

The controversial utilisation of biological resources arises from the amalgamation of globalisation and biopiracy, both fueled by Intellectual Property Rights (IPRs). Historically, biodiversity exploration remained unhindered, devoid of legal or ethical repercussions. However, over time, extensive debates have taken place, culminating in pivotal agreements: the United Nations Convention on Biological Diversity (UNCBD), ratified during the Nairobi Conference on May 22, 1992; the Trade-Related Aspects of Intellectual Property Rights (TRIPS); and the Nagoya Protocol (NP), inked on October 29, 2010, in Nagoya, Japan, and globally enforced from October 12, 2014. These significant accords, including the Convention on Biological Diversity (CBD), uphold nations' sovereignty over natural resources and acknowledge Indigenous and rural communities' traditional knowledge concerning biodiversity. This assessment delves into the global legal framework and instruments that foster trust, protect biological resources, ensure equitable benefit sharing, and establish connections between biodiverse developing countries and research entities. It also highlights Guyana's legal framework, shedding light on its measures to safeguard biodiversity resources and conserve biodiversity within its jurisdiction.

Keywords: Guyana, Biological Resources; Intellectual Property; Stakeholder Engagement; Communication Framework; Trade-Related Aspects.

3. INTRODUCTION

The interaction of industrialisation, urbanisation, and unsustainable extraction of biological resources for Natural Products (NP) has led to the extinction of unique species (Pimm et al., 2014; Vellend et al., 2017). This has sparked controversy over the use of biological resources, resulting in the loss of phylogenetic and functional diversity, habitat degradation, species invasions, and environmental shifts, indicating impending species loss (Pimm et al., 2014). NP research relies on biological materials for novel drugs and chemical leads (Katz & Baltz, 2016; Tavares et al., 2020). However, the ongoing biodiversity decline jeopardizes NP research and its potential benefits. Moreover, cultural practices rooted in traditional knowledge tied to natural resources are impacted (Martins et al., 2014). This necessitates a sustainable approach that balances environmental and societal impacts through conservation, alternative resource methods, and preservation.

The core objective of natural product drug discovery is to isolate and understand the structures of natural compounds, known as secondary metabolites, for societal use (Katz & Baltz, 2016; Rosenthal & Katz, 2003). These molecules enhance the producing organism's survival [8]. Natural products possess biological activity due to their specific chiral forms, complementing synthetic molecules in drug development (Kinghorn et al., 2011). Over 60% of US-introduced chemical entities in the past 25 years have been natural product-based (David, 2008; Li et al., 2022). Despite advantages, NP drug discovery faces challenges, including complex structures, limited sources, ethical concerns, regulatory hurdles, cost, and limited mechanistic understanding (Atanasov et al., 2015; Barnes et al., 2016). Additionally, regulations and intellectual property complexities affect access, benefit-sharing even under the recently adopted Kunming-Montreal Global Biodiversity Framework (Digital Sequence Information on Genetic Resources), and

patentability (Brink & van Hintum, 2022; Decision, 2011; Heffernan, 2020; Hiemstra et al., 2019; Lyal, 2022; Sunderland et al., 2004). Guyana navigates international and national frameworks for access, trade, and benefit-sharing of biological materials yet confronts threats like biopiracy and climate change. This review aims to guide researchers on ethical access, Indigenous knowledge respect, and legal considerations in Guyana's biological material collection process. By adhering to these guidelines, researchers can ensure responsible practices that respect nature and communities. The findings may inform policymakers and stakeholders, facilitating sustainable biological material access strategies and equitable benefits sharing, aligning with the UNCBD principles

3.1. International Conventions that Contribute to Biodiversity Conservation and Sustainable Utilisation: International Instruments and Mechanisms

International efforts to conserve biodiversity and ensure sustainable resource utilization have given rise to significant international conventions, notably the Convention on Biological Diversity (CBD) and the Trade-Related Aspects of Intellectual Property Rights (TRIPs). These instruments have emerged as pivotal with global support (Rajam & Schovsbo, 2022). More than 190 nations have subscribed to these documents, aiming to safeguard biodiversity, including diverse ecosystems. The CBD commits globally to protecting biological diversity as well as upholding the rights of Indigenous peoples and local communities. It protects a country's biological resources and community rights, while TRIPs offer a baseline of intellectual property rights protection, specifically defending private rights (Rajam & Schovsbo, 2022). The CBD entered into force in 1993, responding to the growing importance of conserving and sustainably using biodiversity. In parallel, the TRIPs agreement, arising from the emergence of biotechnological

discoveries, has introduced private rights to various domains, including biotechnology. However, this has led to intricate legal complexities for biotechnology entities and researchers, prompting discussions on the balance between fostering innovation and ensuring public access to essential technologies (Lakshmi et al., 2012)

The UNCBD is a crucial component of these international efforts. Born out of the United Nations Environment Program (UNEP), it originated from the need to address environmental protection and its global implementation. The UNCBD was ratified in 1992 in Rio de Janeiro, Brazil, envisioning the preservation of biodiversity, responsible utilization of genetic resources, and equitable sharing of derived benefits (Farnsworth, 1988; McGraw, 2002). The CBD, via the Nagoya Protocol, introduces concepts such as "Prior Informed Consent (PIC)" and underscores sovereign rights in determining access criteria (Smagadi,2006). Furthermore, it acknowledges the intricate challenge of distinguishing tangible and intangible components of genetic resources, which affects property rights classifications.

Complementary to the CBD, the Nagoya Protocol, globally enforceable since 2014, seeks fair benefit sharing arising from genetic resource use. By addressing legal clarity and transparency in interactions between developed countries and developing countries, the Nagoya Protocol advances the preservation of biological diversity, contributing to its sustainable utilization (Buck & Hamilton, 2011; Kamau et al., 2010; Morgera et al., 2012). The scope of application of the Nagoya Protocol encompasses a wide range of biological entities, including plants, animals, microbes, and fungi, and pertains to their utilisation in both academic and commercial research and development endeavours (Denny, 2022).

Notably, Articles 2c, d, and e hold particular significance within this context. Article 2c emphasises the utilisation of genetic resources, emphasising research and development concerning the genetic and biochemical composition of these resources. This also includes the incorporation of biotechnology, as defined within Article 2c of the Convention (Denny, 2022). Articles 2d and 2e further clarify the protocol's scope by defining derivatives as naturally occurring biochemical molecules originating from genetic expression or biological resource metabolism. Articles 2d and 2e applied regardless of whether such derivatives contain functional units of heredity (Sherman & Henry, 2020). Importantly, the concept of Access and Benefit Sharing (ABS) is central to the Nagoya Protocol. ABS is concerned not with the monetary value of the biological resource, but rather with the additional value generated through research and development (R&D) conducted on that genetic resource. However, it is worth noting that the implementation of ABS, intended to promote equitable benefit sharing, might inadvertently stifle innovation due to the complexities of research taxation (Aubertin & Filoche, 2011; Denny, 2022). The Nagoya Protocol aims to balance fair remuneration for genetic resources with administrative processes that do not hinder innovation, fostering a favourable R&D environment, and fair benefit sharing to promote equity in genetic resource usage.

3.2. Trade-Related Aspects of Intellectual Property Rights (TRIPS)

Intellectual property rights (IPRs) are a dynamic landscape shaped by diverse national aims, beliefs, cultures, traditions, and political contexts, leading to varying levels of protection and enforcement. IPRs grant individuals exclusive rights over their creative or innovative creations, providing legal protection under national law (Correa, 2020). These rights cover a spectrum of creative works, from inventions to artistic expressions, with the primary goal of fostering

economic, social, and cultural progress. Patents, copyrights, and other forms of IPRs enable creators to profit from their contributions, stimulate innovation, and facilitate the dissemination of knowledge and technology (Munson, 2023; Strathern, 1999). The intellectual property system serves as a vital tool for public policy, cultivating a conducive environment for creativity, technological advancement, and the equitable distribution of benefits to society at large (Braga, 1989; Sople, 2016).

Early international efforts to establish a comprehensive framework for intellectual property protection resulted in the Paris Convention for the Protection of Industrial Property (1883) and the Berne Convention for the Protection of Literary and Artistic Works (1886). Subsequent agreements, such as the Rome Convention (1961) and the Budapest Treaty (1977), further expanded the scope of intellectual property protection. The World Trade Organization (WTO) was established to address trade-related aspects of IPRs, culminating in the Agreement on Trade-Related Aspects of Intellectual Property Rights (TRIPS) under the Uruguay Round negotiations. TRIPS is a comprehensive and transformative international agreement that bolsters intellectual property rights across various domains, including patents, copyrights, trademarks, and more. This landmark accord enhances global intellectual property standards, promotes fair competition, and fosters innovation on a worldwide scale (Arlidge et al., 2018; Chadha, 2000; Rheude et al., 2022; Walseth, 2002).

3.3. Objectives of Trade-Related Aspects of Intellectual Property Rights (TRIPs)

The Trade-Related Aspects of Intellectual Property Rights (TRIPs) agreement, an integral component of the WTO, applies universally to all WTO member nations. Reflecting principles similar to the General Agreement on Tariffs and Trade (GATT) and the General Agreement on Trade in Services (GATS), TRIPs establish essential foundations such as non-discrimination provisions, national treatment provisions, and the concept of most-favoured-nation status (Baranyanan, 2021; Busch & Reinhardt, 2003). Although predating TRIPs, the 1883 Paris Convention laid an initial groundwork for global intellectual property (IP) standards, yet it did not establish a comprehensive and uniform level of IP protection (Harris, 2010). In contrast, the TRIPs Agreement sets forth minimum IP protection and enforcement standards, applicable across WTO member states (Correa, 2022; Tyson & Frazier, 2022)By becoming parties to the WTO Agreement, nations commit to ensuring effective and appropriate worldwide protection of intellectual property rights (Murray et al., 2022; Simmons, 2010). TRIPs stand as a comprehensive global accord on intellectual property, covering diverse categories of IPRs and establishing fundamental prerequisites for their safeguarding. This entails delineating the administration and enforcement of IPRs and establishing mechanisms to address disputes among members regarding the adequacy of protection (Correa, 2000, 2022).

3.4. The TRIPs Agreement comprises six distinct sections:

1. Part I The initial section outlines broad terms and key concepts, including provisions related to national and most-favoured-nation treatment and IPR exhaustion (Baranyanan, 2021; Stone, 2011).

2. Part II outlines the core requirements for intellectual property protection that WTO members must embody. Sections I and II include substantive regulations to be incorporated into national legal systems.

3. Part III addresses the enforcement responsibilities of members, establishing general guidelines for intellectual property enforcement procedures and remedies.

4. Part IV outlines the procedures for acquiring and maintaining IP protection, and also provides mechanisms for resolving disputes transparently to safeguard rights (Murray et al., 2022; Tyson & Frazier, 2022).

5. Part V introduces provisions for transition, technological transfer, and technical cooperation.

6. Finally, Part VI addresses institutional structures and addresses specific challenges such as safeguarding existing subject matter (Simmons, 2010; Stone, 2011).

The preamble of the TRIPs Agreement played a crucial role in the negotiations during the Uruguay Round. The primary intention was to acknowledge intellectual property as private property rights and eliminate distortions and barriers in international trade. This signifies the practice of Intellectual Property Rights (IPRs) by holders rather than government authorities

(Busch & Reinhardt, 2003). Similarly, under Article 28, a patent right grants exclusive rights to the inventor, enabling them to prevent others from using, manufacturing, or selling the patented product (Singh, 2002). The objectives of the TRIPs Agreement are clearly delineated in Article 7, while Article 8 lays out its guiding principles. Both articles play a significant role in helping less developed nations balance their gains from the TRIPs negotiations. While emphasizing the importance of IPRs in promoting creativity and innovation, Article 7 also addresses concerns of potential negative impacts on social and economic development, striving to achieve a balanced approach to IP protection that considers both producers and users. Article 66 of the TRIPs Agreement contains provisions for technology transfer, particularly addressing the needs of least developed countries. These nations, facing economic and administrative limitations, are granted flexibility to establish a sustainable technical foundation. The agreement offers 10 years from the date of application, subject to restrictions outlined in Articles 3, 4, and 5. Additionally, Article 67 outlines extension options, further highlighting the council's role in safeguarding IPRs to stimulate technical innovation and facilitate the dissemination of technological advancements for social and economic welfare.

3.5. Relationships between the United Nations Convention on Biological Diversity (CBD), Nagoya Protocol (NP), and Local Laws

In contrast to India's Biological Diversity Act of 2002, the Environmental Protection Agency (EPA) of Guyana does not differentiate between local and foreign researchers regarding transaction costs for the exchange and utilisation of biological materials. The 2007 Guyana National Policy on Access to Genetic Resources and Fair Benefit-Sharing advocates for this inclusive approach. It emphasises that access to genetic resources and associated knowledge for research in biology,

agriculture, and biotechnology should be provided without causing harm to its citizens or impeding the country's wider interests, regardless of whether the research is for commercial or non-commercial purposes. The policy framework of Guyana focuses on actively managing national genetic resources. This framework aims to support the sustainable use and preservation of genetic resources, as well as to promote social, cultural, and economic growth. It emphasises involving relevant parties and providing support for developing skills to ensure successful participation in access and benefit-sharing agreements (Tables 1, 2 and 3). Furthermore, it stresses the importance of respecting the culture, traditions, customary laws, and community regulations of Amerindian and local communities, particularly when entering their territories (Fusi et al., 2019; Kamau, 2022; Mr Lilwah, 2007) which is aligned with the CBD..

3.6. Guyana Legal Framework for the Protection of medical biodiversity (natural products)

The preservation of Guyana's medical biodiversity (NPs) is anchored in the 1996 Environmental Protection Act and the 2000 Biodiversity and Access to Genetic Resources Regulations but is supported by other acts and legislative frameworks (Table 1). These legal instruments oversee the exploration, development, and commercial utilisation of biological resources and traditional wisdom and ensure the just and balanced sharing of benefits derived from these endeavours among resource providers and guardians. Moreover, these regulations uphold Indigenous communities' and local societies' rights and interests concerning their biological and cultural legacy. This overarching approach is pivotal for fostering sustainable progress and shielding vulnerable communities from exploitation. Furthermore, it underscores the paramount

importance of safeguarding biodiversity and ancestral wisdom for the well-being of future generations.

Table 2. 1. National Legislation for the Sustainable Use of Guyana's Natural Resources

National Policy, Legislative Framework, and Institutional Context	***Date***
1. *Environmental Protection Regulations*	2000
2. *Guyana Forestry Commission Act, Cap. 67:02*	2011
3. *Protected Areas Act, Act No. 14*	2013
4. *Wildlife Management and Conservation Regulations*	1999
5. *Species Protection Regulations*	2000
6. *Fisheries Act*	1996
7. *Iwokrama International Centre of Rainforest Conservation and Development Act.*	1919 2005
8. *Wild Birds Protection Act*	1919
9. *Plant Protection Act*	2011
10. *Mining Environmental Regulations*	2006
11. *Mining Act, Cap. 65:01*	1989

3.7. Exploring the Utilisation of Guyana's Enchanting Tropical Rainforest

In the heart of South America, Guyana's extensive tropical rainforests, comprising almost 85% of the country's geographical area, serve as a remarkable example of nature's resilience and human stewardship (Ter Steege et al., 2013; van den Boog et al., 2018). The historical preservation of these lush tropical forests can be attributed to factors such as Guyana's low population density, remote and inaccessible forest areas, and historically limited disturbances (Elias-Roberts, 2020; Steege et al., 1995). This preservation has nurtured a rich tapestry of biodiversity, offering refuge to unique species while also fostering a profound cultural connection between Indigenous communities and the forest (Hammond, 2005; Shah & Cummings, 2021). As history intertwines with the present, Guyana's approach strikes a harmonious balance between sustainable economic

development and ecological integrity, encompassing responsible timber harvesting and a strategic shift towards non-timber forest products (Clarke, 2006; Sizer, 1996; Ter Steege et al., 1999). This innovative strategy not only enhances local livelihoods but also contributes to global conservation efforts, showcasing Guyana's dedication to both its people and the planet (Ter Steege et al., 1999).

Amidst a broader global context, Guyana's commitment to environmental conservation extends beyond its borders, as evidenced by its participation in international agreements such as the United Nations Convention on Biological Diversity and many others (Table 2) (Soltis et al., 2003). This dedication highlights the nation's role as a responsible global citizen, offering financial and technical support to developing countries for biodiversity conservation (Soltis et al., 2003). Guided by a comprehensive framework of policies and strategies, Guyana's sustainable forest management approach emphasises the protection of diverse ecosystems, the promotion of equitable resource utilisation, and the cultivation of a resilient environment in the face of evolving challenges (Strauß et al., 2022). As the nation traverses the delicate terrain between preserving cultural traditions, pursuing economic aspirations, and safeguarding ecological well-being, its tropical rainforests stand as a living testament to the harmonious coexistence of humanity and nature (Strauß et al., 2022).

3.8. Navigating Biodiversity Conservation in Guyana: Challenges and Solutions

Guyana's commitment to biodiversity conservation preservation and environmental sustainability is underscored by its participation in international agreements Having signed the United Nations Convention on Biological Diversity (CBD) in 1992 and subsequently ratifying it in 1994, Guyana has embraced a global effort to protect its rich natural heritage (Soltis et al., 2003).

This Convention mandates the development of conservation strategies, plans, and programmes, integrating biodiversity protection into sectoral policies (Soltis et al., 2003). CBD Member nations, including Guyana, are also called upon to provide financial and technical support for biodiversity conservation in developing countries, promoting equitable and sustainable use of genetic resources (Soltis et al., 2003). The Convention also emphasises establishing protected areas and regulating access to genetic resources to ensure their sustainable and equitable utilisation (Table 2).

Since its CBD ratification, Guyana has taken significant strides toward the sustainable management of its natural resources weaving conservation principles into national decision-making processes (Table 2). Measures are in place to minimise adverse impacts on biological diversity, while customary use of natural resources is encouraged within compatible cultural practices (Soltis et al., 2003). The country's commitment extends beyond policy and legislation, as evident in its adherence to various international and national frameworks. These frameworks provide a solid foundation for Guyana's development of policies geared towards reducing carbon emissions, safeguarding wildlife habitats, and promoting sustainable development (Strauß et al., 2022).

Guyana's commitment to biodiversity preservation is translated into tangible action through a series of national policies, plans, and legislative frameworks. The National Forest Policy, National Land Use Policy, and Policy on Access to Genetic Resources emphasize sustainable utilization (Strauß et al., 2022). National strategies such as the Low Carbon Development Strategy (LCDS) and National Protected Areas Strategy contribute to biodiversity management (Strauß et al., 2022). The National Coordinating Committee on Biosafety and Biosecurity ensures Guyana's adherence to international agreements, while the Ministry of Natural Resources and the

Environment plays a pivotal role in harmonizing policy and management across natural resource sectors(Strauß et al., 2022).

Despite these commendable efforts, several challenges and gaps remain in Guyana's biodiversity conservation journey. The absence of a specific biodiversity policy poses a hurdle, potentially leading to deforestation and habitat loss (Clerici et al., 2020). The harmonization of diverse legislation is essential to ensure effective and efficient conservation efforts, avoiding conflicts and contradictions (Blind & Heß, 2023). Furthermore, the scarcity of baseline data hampers the establishment of adequate trends in biodiversity, urging the nation to invest in comprehensive monitoring mechanisms (McNellie et al., 2020). A robust monitoring system is crucial for evaluating interventions and demonstrating their impact (Maja & Ayano, 2021).

The lack of awareness of the National Biodiversity Strategy and Action Plan (NBSAP) among stakeholders underscores the need for targeted outreach and education(Shen & Jiang, 2021). Similarly, the absence of a single authoritative source of biodiversity and environmental data impedes informed decision-making and calls for the establishment of a centralized and transparent data-sharing mechanism (Shen & Jiang, 2021). Collaboration between academic institutions and government sectors is pivotal to bridging knowledge gaps and implementing sustainable practices (Kopnina, 2020).

Guyana's journey toward biodiversity conservation and sustainable development is marked by international commitments, national policies, and dedicated institutions. While challenges persist, they provide opportunities for growth and innovation. Through strategic policy development, harmonisation of legislation, robust monitoring, enhanced stakeholder engagement,

and collaborative efforts, Guyana can further solidify its position as a global steward of biodiversity and a model for sustainable resource management.

Guyana has adhered to international and national frameworks governing natural resources are important for ensuring the quality, safety and efficacy of natural products and their derivatives. These frameworks and adoption agreements from the CBD have been established since 1990. They have provided the foundation for Guyana to start its conversation on policies tailored to reducing carbon emissions, protecting wildlife habitats, and promoting sustainable development. By implementing these agreements, the country can contribute to global efforts to mitigate climate change and preserve biodiversity (Strauß et al., 2022).

Table 2.2: The Biodiversity-Related Conventions to Which Guyana Is a Party

Convention	***Ratification / Accession***
1. *The United Nations Convention on Biological Diversity (CBD)*	Signatory in 1992.
a. Cartagena Protocol on Biosafety	ratified in 1994.
2. *Nagoya Protocol on Access to Genetic Resources and the Fair and Equitable Sharing of Benefits Arising from their Utilization.*	Acceded to 2008
3. *Convention on International Trade in Endangered Species of Wild Fauna and Flora (1973).*	Acceded to 2014
4. *Cartagena Convention for the Protection and Development of the Marine Environment of the Wider Caribbean Region (1983)*	Ratified in 2010
5. *Specially Protected Areas & Wildlife (SPAW) Protocol (1990)*	Ratified in 2010
6. *International Plant Protection Convention (1952)*	Acceded to 1970
7. *Convention on the Protection of the World Cultural and Natural Heritage (1972)*	Acceded to 1977
8. *United Nations Convention on Climate Change*	Signatory in 1992; ratified in 1997.
9. *Montreal Protocol*	Acceded to 1993
10. *Kyoto Protocol*	Acceded to 2003
11. *Vienna Convention on the Protection of the Ozone Layer*	Acceded to 1993
12. *United Nations Convention to Combat Desertification*	Signatory in 1996; ratified in 1997
13. *International Convention for the Prevention of Pollution (MARPOL 73/78)*	Acceded to 1997
14. *Basel Convention on the Control of Trans-boundary Movement of Hazardous Waste and their Disposal*	Acceded to 2001
15. *Stockholm Convention on Persistent Organic Pollutants*	Acceded to 2007
16. *Rotterdam Convention on Prior Informed Consent for Certain Chemicals and Pesticides in International Trade*	Acceded to 2007
17. *Minamata Convention on Mercury*	Signatory in 2013

3.9. Applications to Guyana involved in Access to Benefit Sharing (ABS) initiatives, including the Nagoya Protocol

In the context of Guyana's engagement in Access to Benefit Sharing (ABS) initiatives, the Nagoya Protocol holds significant importance. The Protocol dictates that each nation appoints a National Focal Point (NFP) and a Competent National Authority (CNA) to facilitate access to genetic resources, ensuring Prior Informed Consent (PIC) and Mutually Agreed Terms (MAT). In Guyana, the EPA serves as the National Focal Point (NFP) and the Competent National Authority (CNA) responsible for facilitating access to genetic resources, ensuring Prior Informed Consent (PIC), and negotiating Mutually Agreed Terms (MAT) figure 1. However, Guyana's involvement in ABS, including the Nagoya Protocol, has been comparatively limited in contrast to other regions. This restricted engagement hampers its influence in shaping global ABS discussions, despite the crucial role of genetic resources for its Indigenous communities. Despite challenges in defining stakeholders and ensuring equitable engagement, efforts are being made to incorporate indigenous communities in ABS discussions, highlighting the pivotal role of Traditional Knowledge (TK) and the necessity for multidisciplinary approaches (Berger Filho & Maia, 2022; Karger & Scholz, 2021; Knight et al., 2022; Rakotondrabe & Girard, 2021; Sikor et al., 2014; Sirakaya, 2020; Suiseeya, 2014).

Regarding safeguarding research and development, the Nagoya Protocol emphasizes legal stability throughout the research process. It introduces the concept of International Certificates of Compliance, providing tangible evidence of due diligence and legal provenance in utilising genetic resources (Burton & Evans-Illidge, 2014) Guyana has adopted compliance measures from diverse member states, such as the EU, to inform its approach [68]. However, challenges persist in

stakeholder engagement and defining Indigenous communities, necessitating robust strategies for communication and collaboration. These endeavours aim to ensure equitable involvement within Community-Based Participatory Research (CBPR) frameworks and address concerns related to Traditional Knowledge and Intellectual Property (Cámara-Leret et al., 2014; Parks, 2018; Rakotondrabe & Girard, 2021; Sirakaya, 2020; Suiseeya, 2014; Zheng, 2021). The overall objective is to create a comprehensive and inclusive engagement plan that respects all stakeholders' rights and contributions while facilitating effective research and development Figure 2 (Leonidou et al., 2020; Stocker et al., 2020)

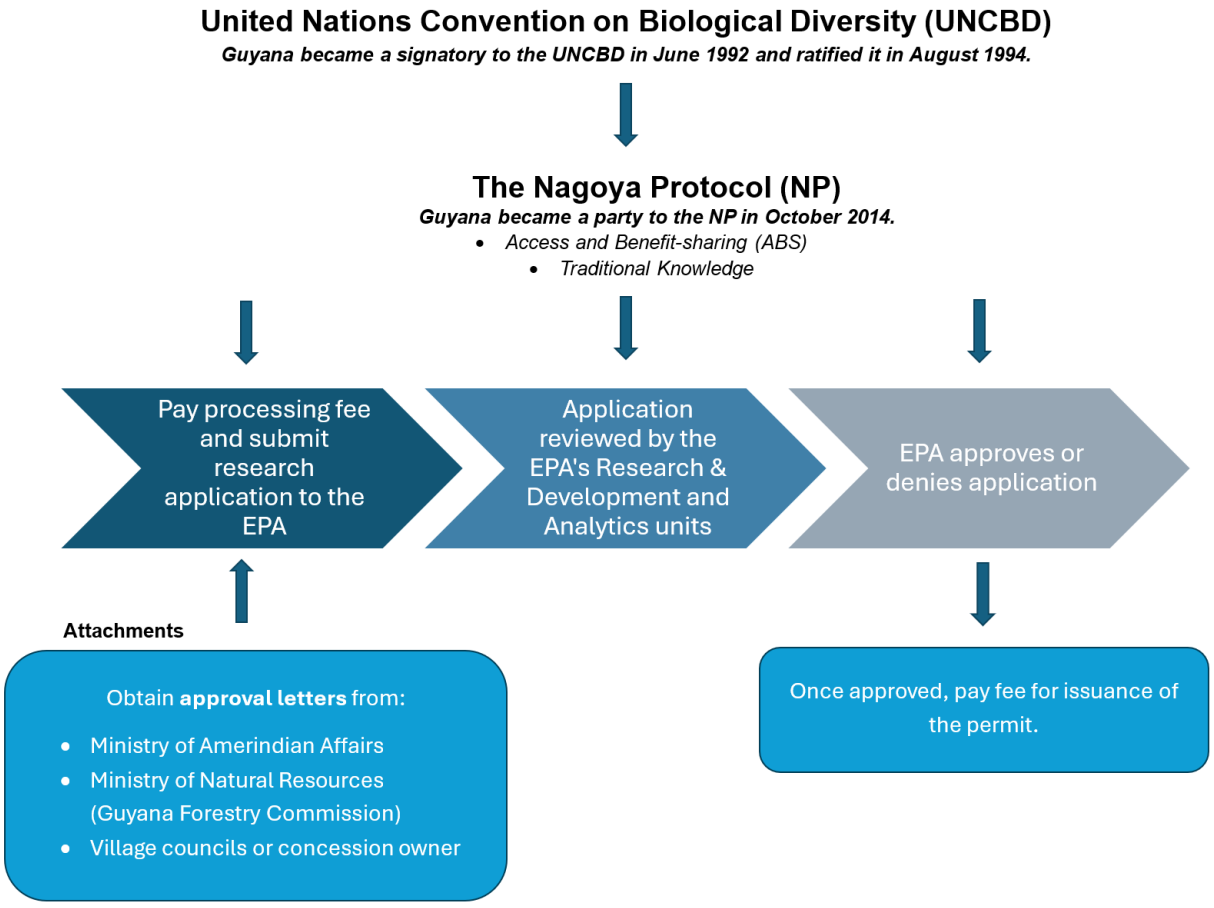

.

Figure 2. 1:Compliance Process for Collecting Biodiversity Material for Natural Product Research in Guyana

3.10. Protection for Research and Development

The research community requires legal stability that goes beyond just issuing access licenses. This involves establishing legal frameworks and mechanisms that provide clarity and consistency in terms of compliance with regulations, laws, and agreements related to access and benefit-sharing of genetic resources. By emphasising legal stability, the Nagoya Protocol aims to create an environment where researchers, institutions, and stakeholders can conduct their activities with confidence, knowing that they are operating within clear and predictable legal frameworks (Klymenko, 2022). To accomplish this, the contributing country's CNA issues International Certificates of Compliance and submits them to the Access and Benefit-Sharing Clearing House. Once deposited, these certificates become international documents that serve as publicly discoverable, tangible evidence of legal origin. The proof is publicly available and securely recorded, including information like the granting authority's date, unique provider identifier, covered content for commercial or non-commercial use, confirmation of previously informed consent (PIC), and mutually agreed terms (MAT) (Burton & Evans-Illidge, 2014).

3.11. The Guyana Approach to Compliance with International and National Policies Governing Biodiversity Research.

The "Guyana Approach to Compliance with International and National Policies Governing Biodiversity Research" aligns scientific endeavours with regulatory frameworks. Guyana ensures that its biodiversity research complies with both global and local policies. This approach promotes the advancement of scientific knowledge while upholding principles of sustainability, conservation, and benefit-sharing as outlined in international agreements such as the Convention on Biological Diversity (CBD). However, the lack of specificity in the Protocol's compliance responsibilities has allowed Guyana to adopt measures and guidelines from 28 EU member states to establish a standard for compliance procedures. The EU law provides specific details on user duties, the development of registries for genetic resource collections, and the appointment of competent authorities and focal points. It also establishes government monitoring of user compliance, recognition of best practices, and the imposition of sanctions (Burton & Evans-Illidge, 2014). Key attributes relevant to researchers are:

1. Users of genetic resources must undertake due diligence to ascertain that the genetic resources they use (and traditional knowledge associated with genetic resources) have been accessed following the laws or regulatory requirements of the providing country and that benefits have been shared as required.
2. If available, an international certificate issued by the providing country's CNA and lodged in the ABS Clearing House must be sought, held, and transferred as required.

3. Possessing a standard material transfer agreement of the Treaty on Plant Genetic Resources for Food and Agriculture for specific material covered by the Treaty meets the due diligence obligation.
4. Transfer and use of genetic resources and traditional knowledge can occur only if consistent with the Confirmation of Prior Informed Consent (PIC) and Mutually Agreed Terms (MAT)
5. Where provenance is unclear, users must either seek clarity by obtaining the necessary PIC and MAT or discontinue the use.
6. Users can rely on ex-situ material obtained from registered collections, as registration is contingent on the display being fully compliant with the CBD and the Nagoya Protocol.
7. Users receiving research funding will be requested to declare they have exercised due diligence.
8. Users must advise relevant National Competent Authorities that they have met their obligations whenever they reach the product approval stage. This information will be put on the Access and Benefit-sharing Clearing House.

3.12. Stakeholder Identification

In the realm of stakeholder identification, a primary hurdle arises from the absence of consensus in defining a community for a research project or pinpointing its constituents. Guided by the principles outlined by Brunger et al. [61], two key criteria were followed. Firstly, a community encompasses individuals who share the stipulated risks associated with the proposed research. Secondly, the community is not a pre-established entity but rather takes shape gradually in response to specific facets of the study and community engagement activities tied to the research

project. The process of characterising the community involves recognising stakeholders who genuinely hold interests in the study, be they individuals, groups, organisations, or agencies. This facilitates swift and effective engagement and facilitates the ongoing evaluation of community requirements, anticipating changes that might influence study conclusions or necessitate adjustments in community involvement strategies. For instance, before commencing data collection on Indigenous Forest land in Guyana, the research plan is to be presented to the EPA and discussions will be held with the Ministry of Amerindian Affairs regarding engagement with Amerindian villages/communities [Figure 1].

The commencement of stakeholder engagement begins with identifying stakeholder groups and delineating when they will be consulted throughout the research process. Stakeholders encompass those impacted by research activities during data collection or likely to be affected during research execution (research-affected parties). These stakeholders may experience positive or negative and direct or indirect impacts. Furthermore, stakeholders with interests in the study or influence over project outcomes (other interested parties) are also engaged. Consequently, an array of stakeholder groups is identified for consultation during research preparation. This includes government agencies at various levels, private sector entities, civil society organisations, local communities, indigenous villages, foresters, and members of the private sector. The engagement approach employs diverse methodologies and tools depending on research phases and stakeholder groups. The overarching aim is to foster substantial discussions, exchange of information, and viewpoints pertinent to the research endeavour. A pivotal initial step involves disseminating study details to enhance stakeholder awareness and encourage their assessment of potential impacts. This lays the groundwork for the subsequent element of the engagement plan—consultations—where

stakeholders actively engage with the researcher, offering feedback on challenges and providing suggestions (Table 2.3).

The stakeholder consultation process operates through a tripartite strategy to involve all pertinent stakeholders and gather feedback. Methodologies include public meetings, one-on-one discussions, interviews, and feedback solicitation. Public meetings facilitate information sharing and consultations with broad stakeholder groups. Conversely, one-on-one interactions, interviews, and focus groups facilitate in-depth and specific discussions, fostering open dialogue between stakeholders and the researcher. These engagements, though focused, enable stakeholders to seek clarifications on planned research activities and provide additional insights into resource use near the research site, thus identifying potential conflicts (Table 2.3).

The imperative organisation and reporting phase involve maintaining a stakeholder registry, methodically documenting interactions, and incorporating feedback into the research process. These steps ensure evidence preservation and meaningful consideration of feedback in the research progression. Furthermore, the feedback and recommendations from the stakeholder engagement process are shared with the EPA to guide future engagement initiatives, particularly those led by the company during project implementation. The process for organising and reporting feedback

Collected from the community and stakeholders is depicted in Table 3, highlighting the flow of communication and collaboration.

Table 2. 3: Process for Organizing and Reporting Stakeholder Feedback (From Outreach to Community Involvement Stages)

	Inform	**Consult**	**Involve**	**Collaborate**	**Co-lead**
The objective of the research approach	• To provide the public with information to assist them in understanding the purpose of the research and alternative solutions • Communication flows from one to the other to inform	• To gather feedback from targeted stakeholders on the research project goals, and process, share matrices, or strategies for changes • More community involvement	• To work directly with stakeholders continuously to ensure that concerns are consistently understood and considered • Community involvement • Community flow is bidirectional	• To partner with stakeholders in each aspect of the decision, including the development of alternatives and priorities • Community involvement	• To place final decision–making in the hands of stakeholders so that they drive decisions and implementation of the work. • Strong bidirectional relationship
Level of community involvement	• Some community involvement	• Communication flows to the community and then back from the community.	• Forms partnerships with the community on each aspect of two project, from development to solution • Entities from bidirectional communication channels	• Communication flow is bidirectional. • Entities form bidirectional communication channels.	• Final decision-making is at the community level. • Entities have formed a strong partnership structure.
Examples	Email Social media Send press releases announcing research milestone	• Ask for input on initiative strategies. • Invite to small groups or individual presentations about the initiative	• Invite to join working groups or an advisory body for the initiative • Partner in policy advocacy	• Appoint to the leadership role on a working group to help share strategies • Partnership building, trust building	• Invite to join the steering committee and/or similar body with decision-making power in the initiative. • Broader health outcomes affecting the broader community

The Second Voluntary National Review on the Sustainable Development Goals (SDGs) 2023 and the Low Carbon Development Strategy (LCDS) 2030 show that Guyana has made considerable progress in accordance with the international biodiversity framework. The EPA and other Competent National Authorities (CNAs) have highlighted the country's commitment to the agreements and guidelines of treaties like the Convention on Biological Diversity. This commitment is reflected in actions such as formulating biodiversity strategies and designating protected areas. Moreover, Guyana has scrutinized the efficacy of its compliance mechanisms, which encompass enforcement, monitoring, and accountability. The country also acknowledges the influence of socioeconomic and political elements, including power dynamics, the impact of multinational corporations, and the rights of Indigenous populations.

3.13. CONCLUSION

Overall, Guyana has achieved a comprehensive understanding of compliance with the international biodiversity framework necessitates a multidisciplinary approach encompassing legal, political, economic, and socio-cultural dimensions. This approach allows for a holistic assessment of the numerous factors that influence compliance with international biodiversity agreements. By considering the complex interplay of legal, political, economic, and socio-cultural factors, policymakers and stakeholders can better address the challenges and barriers to compliance. Ultimately, a multidisciplinary approach to understanding compliance with international biodiversity frameworks is crucial in promoting sustainable conservation efforts and protecting biodiversity for future generations.

ACKNOWLEDGEMENTS

All individuals, organisations, and partners who have contributed significantly to the success of the Sustainable Guyana programme have our deepest gratitude. This recognition extends to our visionary founding members, local communities, government agencies, nonprofit organisations, devoted volunteers, and benevolent donors. Your unwavering dedication, collaborative spirit, and financial assistance from The University of Guyana funded jointly by CGX Energy Inc. and Frontera Energy Corporation have propelled our mission to promote sustainability in Guyana, paving the way for a more resilient and prosperous future for the nation and generation.

Declarations

Competing interests: All authors declare that they have no competing interests.

Availability of data and material: All relevant data generated or analysed during this study and supplemental information are included in this published article. Other raw data will be available upon request.

3.14. REFERENCES

Arlidge, W. N. S., Bull, J. W., Addison, P. F. E., Burgass, M. J., Gianuca, D. T., Gorham, T. M., Jacob, C., Shumway, N., Sinclair, S. P., & Watson, J. E. M. (2018). A global mitigation hierarchy for nature conservation. BioScience, 68(5), 336–347. https://doi.org/10.1093/biosci/biy029

Atanasov, A. G., Waltenberger, B., Pferschy-Wenzig, E.-M., Linder, T., Wawrosch, C., Uhrin, P., Temml, V., Wang, L., Schwaiger, S., & Heiss, E. H. (2015). Discovery and resupply of pharmacologically active plant-derived natural products: A review. Biotechnology Advances, 33(8), 1582–1614. https://doi.org/10.1016/j.biotechadv.2015.08.001

Aubertin, C., & Filoche, G. (2011). The Nagoya Protocol on the use of genetic resources: One embodiment of an endless discussion. Sustentabilidade em Debate, 2(1), 51–64. https://doi.org/10.1590/S2179-38282011000100004

Baranyanan, S. D. (2021). Simplification of law regulations in copyright criminal act settlement. Journal of Human Rights, Culture and Legal System, 1(2), 80–91. https://doi.org/10.53955/jhcls.v1i2.15

Barnes, E. C., Kumar, R., & Davis, R. A. (2016). The use of isolated natural products as scaffolds for the generation of chemically diverse screening libraries for drug discovery. Natural Product Reports, 33(3), 372–381. https://doi.org/10.1039/C5NP00115K

Berger Filho, A. G., & Maia, B. G. (2022). The inclusion of the digital sequence information (DSI) in the scope of the Nagoya Protocol and its consequences. Revista de Direito Internacional, 19(1). https://doi.org/10.5102/rdi.v19i1.7891

Blind, K., & Heß, P. (2023). Stakeholder perceptions of the role of standards for addressing the sustainable development goals. Sustainable Production and Consumption, 37, 180–190. https://doi.org/10.1016/j.spc.2023.03.015

Braga, C. A. P. (1989). The economics of intellectual property rights and the GATT: A view from the South. Vanderbilt Journal of Transnational Law, 22, 243.

Brink, M., & van Hintum, T. (2022). Practical consequences of digital sequence information (DSI) definitions and access and benefit-sharing scenarios from a plant genebank's perspective. Plants, People, Planet, 4(1), 23–32. https://doi.org/10.1002/ppp3.10235

Buck, M., & Hamilton, C. (2011). The Nagoya Protocol on access to genetic resources and the fair and equitable sharing of benefits arising from their utilization to the Convention on

Biological Diversity. Review of European, Comparative & International Environmental Law, 20(1), 47–61. https://doi.org/10.1111/j.1467-9388.2011.00703.x

Burton, G., & Evans-Illidge, E. A. (2014). Emerging R and D law: The Nagoya Protocol and its implications for researchers. In Natural Products as Source of Molecules with Therapeutic Potential (pp. 477–493). American Chemical Society.

Busch, M. L., & Reinhardt, E. (2003). Developing countries and General Agreement on Tariffs and Trade/World Trade Organization dispute settlement. Journal of World Trade, 37(4), 719–735.

Cámara-Leret, R., Paniagua-Zambrana, N., Svenning, J.-C., Balslev, H., & Macía, M. J. (2014). Geospatial patterns in traditional knowledge serve in assessing intellectual property rights and benefit-sharing in northwest South America. Journal of Ethnopharmacology, 158, 58–65. https://doi.org/10.1016/j.jep.2014.10.033

Chadha, R. (2000). Understanding the WTO regime. In India's Foreign Trade (pp. 3–19). Allied Publishers.

Clarke, G. (2006). Law compliance and prevention and control of illegal activities in the forest sector in Guyana. Food and Agriculture Organization of the United Nations.

Clerici, N., Armenteras, D., Kareiva, P., Botero, R., Ramírez-Delgado, J., Forero-Medina, G., Ochoa, J., Pedraza, C., Schneider, L., & Lora, C. (2020). Deforestation in Colombian protected areas increased during post-conflict periods. Scientific Reports, 10(1), 4971. https://doi.org/10.1038/s41598-020-61805-6

Correa, C. (2020). Trade related aspects of intellectual property rights: A commentary on the TRIPS Agreement. Oxford University Press. https://doi.org/10.1093/oso/9780198862147.001.0001

Correa, C. M. (2000). Intellectual property rights, the WTO and developing countries: The TRIPS agreement and policy options. Zed Books.

Correa, C. M. (2022). Interpreting the flexibilities under the TRIPS Agreement. In Access to Medicines and Vaccines (pp. 1–23). Springer. https://doi.org/10.1007/978-3-030-83128-3_2

David, B. (2008). Natural product sources and the biodiversity convention. Planta Medica, 74(09), L3. https://doi.org/10.1055/s-0028-1084075

Convention on Biological Diversity. (2011). Conference of the Parties Decision X/1. Access to genetic resources and the fair and equitable sharing of benefits arising from their utilization. https://www.cbd.int/decision/cop/?id=12267

Denny, D. M. T. (2022). Bioeconomy and the Nagoya Protocol. Brazilian Journal of International Law, 19, 224-241. https://doi.org/10.5102/rdi.v19i1.8278

Elias-Roberts, A. (2020). Balancing environmental protection and offshore petroleum developments in Guyana. Global Energy Law and Sustainability, 1(1), 1-27. https://doi.org/10.3366/gels.2020.0004

Farnsworth, N. R. (1988). Screening plants for new medicines. In E. O. Wilson (Ed.), Biodiversity (pp. 81-99). National Academy Press.

Fusi, F., Welch, E. W., & Siciliano, M. (2019). Barriers and facilitators of access to biological material for international research: The role of institutions and networks. Science and Public Policy, 46(2), 275-289. https://doi.org/10.1093/scipol/scy062

Hammond, D. S. (2005). Tropical forests of the Guiana Shield: Ancient forests in a modern world. CABI Publishing.

Harris, D. (2010). TRIPS after fifteen years: Success or failure, as measured by compulsory licensing. Journal of Intellectual Property Law, 18, 367-400.

Heffernan, O. (2020). Why a landmark treaty to stop ocean biopiracy could stymie research. Nature, 580(7801), 20-22. https://doi.org/10.1038/d41586-020-00912-w

Hiemstra, S. J., Brink, M., & van Hintum, T. (2019). Digital Sequence Information (DSI): Options and impact of regulating access and benefit sharing-stakeholder perspectives. Centre for Genetic Resources, the Netherlands (CGN), Wageningen University & Research.

Kamau, E. C. (2022). Transformations in international law on access to genetic resources and benefit-sharing and domestic implementation. Introduction, synthesis, observations, recommendations and conclusions. In E. C. Kamau (Ed.), Global transformations in the use of biodiversity for research and development: Post Nagoya Protocol implementation amid unresolved and arising issues (pp. 3-45). Springer. https://doi.org/10.1007/978-3-030-95286-7_1

Kamau, E. C., Fedder, B., & Winter, G. (2010). The Nagoya Protocol on access to genetic resources and benefit sharing: What is new and what are the implications for provider and user countries and the scientific community. Law, Environment and Development Journal, 6(3), 246-262.

Karger, E. J., & Scholz, A. H. (2021). DSI, the Nagoya Protocol, and stakeholders' concerns. Trends in Biotechnology, 39(2), 110-112. https://doi.org/10.1016/j.tibtech.2020.09.008

Katz, L., & Baltz, R. H. (2016). Natural product discovery: Past, present, and future. Journal of Industrial Microbiology and Biotechnology, 43(2-3), 155-176. https://doi.org/10.1007/s10295-015-1723-5

Kinghorn, A. D., Pan, L., Fletcher, J. N., & Chai, H. (2011). The relevance of higher plants in lead compound discovery programs. Journal of Natural Products, 74(6), 1539-1555. https://doi.org/10.1021/np200391c

Klymenko, I. (2022). Nagoya Protocol on access and benefit sharing: An effective international instrument for safeguarding the indigenous peoples' rights or declarative rhetoric of double standards? [Master's thesis, UiT. The Arctic University of Norway]. UiT Open Research Archive. https://hdl.handle.net/10037/24963

Knight, J., Flack-Davison, E., Engelbrecht, S., Visagie, R., Beukes, W., Coetzee, T., Mwale, M., & Ralefala, D. (2022). A literature review analysis of engagement with the Nagoya Protocol, with specific application to Africa. South African Journal of Bioethics and Law, 15(2), 69-74. https://doi.org/10.7196/SAJBL.2022.v15i2.778

Kopnina, H. (2020). Education for the future? Critical evaluation of education for sustainable development goals. The Journal of Environmental Education, 51(4), 280-291. https://doi.org/10.1080/00958964.2019.1710444

Lakshmi, S. M., Nagasree, Y. B., Sreelekha, K., Madhavi, N., & Reddy, C. S. (2012). Aphrodisiac agents from medicinal plants: An ethnopharmacological and phytochemical review. Journal of Pharmacy Research, 5(2), 845-848.

Leonidou, E., Christofi, M., Vrontis, D., & Thrassou, A. (2020). An integrative framework of stakeholder engagement for innovation management and entrepreneurship development. Journal of Business Research, 119, 245-258. https://doi.org/10.1016/j.jbusres.2018.11.054

Li, Y., Zhao, H., Sun, G., Duan, Y., Guo, Y., Xie, L., & Ding, X. (2022). Alterations in the gut microbiome and metabolome profiles of septic rats treated with aminophylline. Journal of Translational Medicine, 20(1), 1–11. https://doi.org/10.1186/s12967-022-03342-6

Lilwah, P., & Mcclure, T. (2007). National policy on access to genetic resources and the fair and equitable sharing of benefits arising from their utilization. [Government report].

Lyal, C. H. C. (2022). Digital sequence information on genetic resources and the convention on biological diversity. In E. C. Kamau (Ed.), Global transformations in the use of

biodiversity for research and development (pp. 589–619). Springer. https://doi.org/10.1007/978-3-030-88711-7_21

Maja, M. M., & Ayano, S. F. (2021). The impact of population growth on natural resources and farmers' capacity to adapt to climate change in low-income countries. Earth Systems and Environment, 5, 271–283. https://doi.org/10.1007/s41748-021-00232-7

Martins, A., Vieira, H., Gaspar, H., & Santos, S. (2014). Marketed marine natural products in the pharmaceutical and cosmeceutical industries: Tips for success. Marine Drugs, 12(2), 1066–1101. https://doi.org/10.3390/md12021066

McGraw, D. M. (2002). The CBD—Key characteristics and implications for implementation. Review of European Community & International Environmental Law, 11(1), 17–28.

McNellie, M. J., Oliver, I., Dorrough, J., Ferrier, S., Newell, G., & Gibbons, P. (2020). Reference state and benchmark concepts for better biodiversity conservation in contemporary ecosystems. Global Change Biology, 26(12), 6702–6714. https://doi.org/10.1111/gcb.15383

Morgera, E., Buck, M., & Tsioumani, E. (2012). The 2010 Nagoya Protocol on access and benefit-sharing in perspective: Implications for international law and implementation challenges. Martinus Nijhoff. https://doi.org/10.1163/9789004243033

Munson, A. (2023). The United Nations Convention on Biological Diversity. In The Earthscan reader in sustainable development (pp. 55–62). Routledge. https://doi.org/10.4324/9781003403432-8

Murray, A. L., Speyer, L. G., Brown, R., Zhu, X., Yang, Y., Eisner, M., & Ribeaud, D. (2022). Advancing multi-timeframe developmental research through combining long-term cohort and ecological momentary assessment studies: The Decades-to-minutes (D2M) study. PsyArXiv. https://doi.org/10.31234/osf.io/yqust

Parks, L. (2018). Challenging power from the bottom up? Community protocols, benefit-sharing, and the challenge of dominant discourses. Geoforum, 88, 87–95. https://doi.org/10.1016/j.geoforum.2017.11.017

Pimm, S. L., Jenkins, C. N., Abell, R., Brooks, T. M., Gittleman, J. L., Joppa, L. N., Raven, P. H., Roberts, C. M., & Sexton, J. O. (2014). The biodiversity of species and their rates of extinction, distribution, and protection. Science, 344(6187), 1246752. https://doi.org/10.1126/science.1246752

Rajam, N., & Schovsbo, J. (2022). The protection of intangible cultural assets by trade secrets and unfair competition law. In I. Stamatoudi (Ed.), Research handbook on intellectual

property and cultural heritage (pp. 113–130). Edward Elgar Publishing. https://doi.org/10.4337/9781800376915

Rakotondrabe, M., & Girard, F. (2021). Protecting traditional knowledge through biocultural community protocols in Madagascar: Do not forget the "B" in BCP. Sustainability, 13(18), 10255. https://doi.org/10.3390/su131810255

Rheude, T., Pellegrini, C., Allali, A., Bleiziffer, S., Kim, W.-K., Neuser, J., Landt, M., Rudolph, T., Renker, M., & Widder, J. D. (2022). Multicenter comparison of latest-generation balloon-expandable versus self-expanding transcatheter heart valves: Ultra versus Evolut. International Journal of Cardiology, 357, 115–120. https://doi.org/10.1016/j.ijcard.2022.03.056

Rosenthal, J. P., & Katz, F. N. (2003). Natural products research partnerships with multiple objectives in global biodiversity hot spots: Nine years of the international cooperative biodiversity groups program. In A. T. Bull (Ed.), Microbial diversity and bioprospecting (pp. 458–466). ASM Press.

Shah, M., & Cummings, A. R. (2021). An analysis of the influence of the human presence on the distribution of provisioning ecosystem services: A Guyana case study. Ecological Indicators, 122, 107255. https://doi.org/10.1016/j.ecolind.2020.107255

Shen, W., & Jiang, D. (2021). Making authoritarian environmentalism accountable? Understanding China's new reforms on environmental governance. The Journal of Environment & Development, 30(1), 41–67. https://doi.org/10.1177/1070496520961136

Sherman, B., & Henry, R. J. (2020). The Nagoya Protocol and historical collections of plants. Nature Plants, 6(5), 430–432. https://doi.org/10.1038/s41477-020-0657-8

Sikor, T., Martin, A., Fisher, J., & He, J. (2014). Toward an empirical analysis of justice in ecosystem governance. Conservation Letters, 7(6), 524–532. https://doi.org/10.1111/conl.12142

Simmons, B. (2010). Treaty compliance and violation. Annual Review of Political Science, 13, 273–296. https://doi.org/10.1146/annurev.polisci.12.040907.132713

Singh, R. (2002). Implementation of intellectual property rights regime: The justification question. Social Scientist, 30(1/2), 61–82.

Sirakaya, A. (2020). A balanced ABS system: Stakeholder perception on ABS goals. Sustainable Development, 28(3), 495–503.

Sizer, N. (1996). Profit without plunder: Reaping revenue from Guyana's tropical forests without destroying them. World Resources Institute.

Soltis, D. E., Senters, A. E., Zanis, M. J., Kim, S., Thompson, J. D., Soltis, P. S., Ronse De Craene, L. P., Endress, P. K., & Farris, J. S. (2003). Gunnerales are sister to other core eudicots: Implications for the evolution of pentamery. American Journal of Botany, 90(3), 461–470. https://doi.org/10.3732/ajb.90.3.461

Sople, V. V. (2016). Managing intellectual property: The strategic imperative. PHI Learning Pvt. Ltd.

Steege, H. t., Boot, R., Brouwer, L., Hammond, D., Van Der Hout, P., Jetten, V., Khan, Z., Polak, A., Raaimakers, D., & Zagt, R. (1995). Basic and applied research for sound rain forest management in Guyana. Ecological Applications, 5(4), 904–910.

Stocker, F., de Arruda, M. P., de Mascena, K. M., & Boaventura, J. M. (2020). Stakeholder engagement in sustainability reporting: A classification model. Corporate Social Responsibility and Environmental Management, 27(5), 2071–2080. https://doi.org/10.1002/csr.1975

Stone, R. W. (2011). Controlling institutions: International organizations and the global economy. Cambridge University Press.

Strathern, M. (1999). What is intellectual property after? The Sociological Review, 47(1_suppl), 156–180.

Strauß, L., Baker, T. R., de Lima, R. F., Afionis, S., & Dallimer, M. (2022). Limited integration of biodiversity within climate policy: Evidence from the Alliance of Small Island States. Environmental Science & Policy, 128, 216–227. https://doi.org/10.1016/j.envsci.2022.01.016

Suiseeya, K. R. M. (2014). Negotiating the Nagoya Protocol: Indigenous demands for justice. Global Environmental Politics, 14(3), 102–124. https://doi.org/10.1162/GLEP_a_00239

Sunderland, T. C. H., Harrison, S. T., & Adu-Anning, C. (2004). Commercialisation of non-timber forest products in Africa: History, context and prospects. Forest Products, Livelihoods and Conservation, 2, 1–24.

Tavares, W. R., Barreto, M. d. C., & Seca, A. M. L. (2020). Uncharted source of medicinal products: The case of the Hedychium genus. Medicines, 7(5), 23. https://doi.org/10.3390/medicines7050023

Ter Steege, H., Lilwah, R., Ek, R., Van Der Hout, P., Thomas, R., Van Essen, J., & Jetten, V. (1999). Composition and diversity of the rain forest in Central Guyana. An addendum to 'Soils of the rain forest in Central Guyana'. Tropenbos Guyana Reports 99-2.

Ter Steege, H., Pitman, N. C. A., Sabatier, D., Baraloto, C., Salomão, R. P., Guevara, J. E., Phillips, O. L., Castilho, C. V., Magnusson, W. E., Molino, J.-F., Monteagudo, A., Vargas, P. N., Montero, J. C., Feldpausch, T. R., Coronado, E. N. H., Killeen, T. J., Mostacedo, B., Vasquez, R., Assis, R. L., Terborgh, J., … Silman, M. R. (2013). Hyperdominance in the Amazonian tree flora. Science, 342(6156), 1243092. https://doi.org/10.1126/science.1243092

Tyson, R. K., & Frazier, B. W. (2022). Principles of adaptive optics. CRC Press.

van den Boog, T., Bulkan, J., Tansey, J., & van Andel, T. R. (2018). Sustainability issues of commercial non-timber forest product extraction in West Suriname. Journal of Ethnobiology and Ethnomedicine, 14(1), 1–16. https://doi.org/10.1186/s13002-018-0244-5

Vellend, M., Baeten, L., Becker-Scarpitta, A., Boucher-Lalonde, V., McCune, J. L., Messier, J., Myers-Smith, I. H., & Sax, D. F. (2017). Plant biodiversity change across scales during the Anthropocene. Annual Review of Plant Biology, 68, 563–586.

Walseth, M. (2002). Reverse presumptions: Guillen v. Pierce County disregards reasonable constitutional interpretations of 23 USC 409. Washington Law Review, 77, 951.

Zheng, X. (2021). Empowering indigenous peoples and local communities: A human rights-based appraisal of the compliance mechanism of the Nagoya Protocol. Review of European, Comparative & International Environmental Law, 30(1), 61–72.

CHAPTER 3

PREFACE

Title: **Unlocking Potentially Therapeutic Phytochemicals in Capadulla (Doliocarpus dentatus) from Guyana Using Untargeted Mass Spectrometry-Based Metabolomics**

Authors: Ewart A. Smith, Ainsley Lewis, Suresh Narine and R. J. Neil Emery

Reference: Published in Metabolites (2023), 13 (1050)

Doi: https://doi.org/10.3390/metabo13101050

Contributions: EAS assembled metabolomics data, created figures and wrote the manuscript. AL worked on the modification of the workflow and experimental design. SN and RJNE conceived, directed and obtained funding for research present in the study. EAS, AL, RJNE and SN edited the manuscript before submission.

3. CHAPTER 3

Unlocking Potentially Therapeutic Phytochemicals in Capadulla (*Doliocarpus dentatus*) from Guyana Using Untargeted Mass Spectrometry-Based Metabolomics

Published in: Metabolites (2023), 13 (1050)

https://doi.org/10.3390/metabo13101050

ABSTRACT

Doliocarpus dentatus is thought to have a wide variety of therapeutic phytochemicals that allegedly improve libido and cure impotence. Although a few biomarkers have been identified with potential antinociceptive and cytotoxic properties, an untargeted mass spectrometry-based metabolomics approach has never been undertaken to identify therapeutic biofingerprints for conditions, such as erectile dysfunction, in men. This study executes a preliminary phytochemical screening of the woody vine of two ecotypes of *D. dentatus* with renowned differences in therapeutic potential for erectile dysfunction. Liquid chromatography–mass spectrometry-based metabolomics was used to screen for flavonoids, terpenoids, and other chemical classes found to contrast between red and white ecotypes. Among the metabolite chemodiversity found in the ecotype screens, using a combination of GNPS, MS-DIAL, and SIRIUS, approximately 847 compounds were annotated at levels 2 to 4. Level 4 annotations provided molecular formulas with multiple structural candidates, while level 2 annotations incorporated predictive or literature-supported structural evidence, such as diagnostic MS/MS fragmentation patterns. The majority of compounds falling under lipid and lipid-like molecules, benzenoids and phenylpropanoids, and polyketides, indicative of the contributions of the flavonoid, shikimic acid, and terpenoid biosynthesis pathways. Despite the extensive annotation, we report on 138 tentative compound

identifications of potentially therapeutic compounds, with 55 selected compounds at a level 2 annotation, and 22 statistically significant therapeutic biomarkers, the majority of which were polyphenols. Epicatechin methyl gallate, catechin gallate, and proanthocyanidin A2 had the greatest significant differences and were also relatively abundant among the red and white ecotypes. These putatively identified compounds reportedly act as antioxidants, neutralizing damaging free radicals, and lowering cell oxidative stress, thus aiding in potentially preventing cellular damage and promoting overall well-being, especially for treating erectile dysfunction (ED).

Keywords: Capadulla erectile dysfunction mass spectrometry metabolomics polyphenols antioxidants

3.1. INTRODUCTION

Doliocarpus dentatus, popularly known as Guyanese Capadulla, is an important medical woody stem belonging to the Dilleniaceae family (Gurni et al., 1981; Lima et al., 2014). The *D. dentatus* species is commonly found in tropical rainforests in Central and South America, from Mexico to South Brazil, and the Amazon region has the highest representation of the species (Branquinho, Verdan, dos Santos, et al., 2021). In Guyana, the woody vine of *D. dentatus* grows in mixed to evergreen lowland forests (Bhatia et al., 2014; Huang et al., 2021; Kumar et al., 2007; Sasidharan et al., 2011). The Capadulla woody vine is regarded locally as a powerful aphrodisiac (Andel & Banki, 2003; Andel et al., 2003). The stem of the *D. dentatus* is used to make tea or drink, which purportedly raises libido, cures impotence, and improves sexual desire in men (Van Andel T, 2003).

In Guyana, the traditional use of *D. dentatus* has involved treating specific symptoms of diabetes, Leishmanial ulcers and erectile dysfunction (ED) and supporting overall well-being (Singh et al., 2013; Van Andel, 2001). The differences between *D. dentatus* red and white ecotypes are recognized by their wood color instead of their botanical features, such as leaves and fertile organs (van Andel, 2000). Two ecotypes of *D. dentatus* (i.e., white and red) are used similarly as an aphrodisiac without reported noticeable differences in their efficacy by Guyanese locals. Informants have also indicated that the *D. dentatus red species is considered a better aphrodisiac than the Capadulla white ecotype and that "Capadulla red is considered a male species consumed by males". At the same time, "Capadulla white is regarded as the female species but is consumed when Capadulla red is in limited supply*".

In earlier studies on *D. dentatus*, using mass spectrometry, total phenolic (204.04 mg/g), flavonoid (89.17mg/g), tannins (12.05 mg/g) contents and sitosterol-3-O-D-glucopyranoside, kaempferol 3-O-L-aminopyranoside, betulinic acid and betulin were discovered in the ethanolic extract of *D. dentatus* leaves, which evaluated for widespread use against pain (Raissa Borges Ishikawa et al., 2017). Additional phytochemical analysis confirmed the presence of butyric acid, steroids, lactones, anthracensides, betulinic acid, tannins, flavones, and phenolic acids in this plant (R. C. Jagessar et al., 2013).

D. dentatus leaves' ethanolic extract was evaluated for widespread use against pain in animal models, and its toxicogenicity (Branquinho, Verdan, Dos Santos, et al., 2021). The results indicated that an ethnopharmacological dose of the aqueous extract from the leaves of *D. dentatus* decreased the pain response, indicating analgesic and anti-inflammatory actions. Furthermore, toxicogenic assays determined that the aqueous extract of *D. dentatus* does not have genotoxic potential and does not modify splenic phagocytosis (Branquinho, Verdan, Dos Santos, et al., 2021; Branquinho, Verdan, Santos, et al., 2021). Another study suggested that the extract from the leaves of *Capadulla* has antibacterial and anti-inflammatory properties, demonstrating that the leaves have phytochemical compounds that can treat various illnesses (R. B. Ishikawa et al., 2017; Raissa Borges Ishikawa et al., 2017; R. B. Ishikawa et al., 2018). The extract from the leaves of the *D. dentatus* is safe to use during the gestational period. It does not cause DNA damage and is not teratogenic (Raissa Borges Ishikawa et al., 2018).

In vitro studies of the biological activity of *D. dentatus* have shown that it is an antimicrobial against strains of *Escherichia coli*, *Klebsiella pneumoniae*, and *Staphylococcus aureus*; anti-inflammatory; cytotoxic in leukemic cells of the K562 lineage (R. B. Ishikawa et al., 2017). It is

effective against amastigotes of *Leishmania amazonenses* (Aponte et al., 2008; Sauvain et al., 1996) and does not cause genomic or chromosomal damage, implying that it is safe for use (Branquinho, Verdan, dos Santos, et al., 2021; Branquinho, Verdan, et al., 2021b; Raissa Borges Ishikawa et al., 2018; R. C. Jagessar et al., 2013; Rodrigues & de Carvalho, 2008).

Although many phytochemicals have been discovered in *D. dentatus leaves,* the woody vine of *Doliocarpus dentatus* has not been investigated using mass spectrometry-based metabolomics and other bioinformatics techniques. The objective of the current study is to determine the phytochemical profile of *D. dentatus* ecotypes utilizing untargeted and semi-targeted plant metabolomics using liquid chromatography (LC) coupled with electrospray ionization mass spectrometry (ESI-MS/MS). Liquid chromatography-electrospray ionization-mass spectrometry (LC-ESI-MS) is a sensitive technology for determining compound molecular masses. ESI-tandem mass spectrometry (MS/MS) can be utilized to get additional structural information on compound fragmentation patterns (Mari et al., 2015; Prabakaran et al., 2018). LC-MS-based metabolomics methods are commonly used to profile complex biological extracts such as those from plants (Feussner & Feussner, 2019; Shimizu et al., 2018), with non-targeted plant metabolomics being of particular interest, owing to the enormous plant kingdoms metabolite variety (Gorrochategui et al., 2016; L. Wang et al., 2018).

The goal of this work sought to do a preliminary investigation of the phytochemical profiles of *D. dentatus* that will provide additional information on the potential use of the compounds, compare compounds in both ecotypes and identify any unique or beneficial compounds present in *D. dentatus* using mass spectrometry-based metabolomics. This information can be used better to understand the physiology and ecology of this species and potentially inform conservation efforts.

It may also affect human health, as *D. dentatus* is a known source of bioactive compounds. Additionally, understanding the metabolic pathways of this plant could eventually help target new therapies for erectile dysfunction (ED) in men.

3.2. MATERIALS AND METHODS

3.2.1. Chemicals Used for Metabolite Extraction and Liquid Chromatography–Mass Spectrometry

HPLC-grade solvents, such as acetonitrile and methanol, were purchased from Fisher Scientific (Hampton, NH, USA). Water used for metabolite extraction and the mobile phase in liquid chromatography–mass spectrometry (LC-MS) was previously purified using a Milli-Q system (Millipore, Burlington, MA, USA). Benzyladenine and abscisic acid-labeled standards were acquired from OlChemim Ltd., Olomouc, Czech Republic.

3.2.2. Study Site and Plots–Eagle Mountain Forest Potaro–Siparuni, Guyana

The Eagle Mountain Forest is about 200 km south-southwest of Georgetown, Guyana's capital city (21N0261909 - 0578704). The Eagle Forest, located in an isolated area, is characterized by steep sandstone ridges ranging in height from 100m – 724.8m above sea level. Annual rainfall is very high (3500-4000 mm), with a noticeable peak in May and June. The study area is ecologically significant, supporting a high diversity of flora and fauna. It is dominated by Leguminosae/Fabaceae subfamilies (Mimosaceae, Caesalpiniaceae, and Papilionaceae) (Hammond, 2005; P. B. Matheny et al., 2003). *D. dentatus* liana was collected randomly after an inventory of all *D. dentatus* lianas had been carried out and their position recorded. The measurement point for all *D. dentatus* liana was 3-5cm representing seedlings, and poles, 20 cm and up, representing mature individuals in the diameter range, known to capture demography for

seedling poles and mature individuals (Castilla et al., 2022). In July 2022, we gathered a total of four biological samples, all of which were chosen at random from the *D. dentatus* liana population present at the Eagle Mountain study location. Collections included red and white *D. dentatus*, utilizing diameter classes (50 mm – 200 mm).

For every individual *D. dentatus* liana selected (N=3), a 20 mm disc was carefully extracted from various points along the woody vine, encompassing the ground level, an intermediate position, and an emergent point. The processed samples of the same ecotypes with similar diameter formed a composite sample (CS = 9). Following extraction, these samples were promptly placed in dry ice to maintain their metabolic integrity during transit. Subsequently, they were transported to the University of Guyana (Greater Georgetown, Guyana). Here, the samples underwent further processing to prepare them for in-depth analysis. Finally, the samples were sent to Trent University (Peterborough, Canada), where advanced metabolomic analysis was conducted.

3.2.3. Biological Sample Preparation and Metabolite Extraction

Metabolite extraction was performed as previously published (Nguyen et al., 2023a). Thirty mg of *D. dentatus* dried tissues were pre-weighed before the extraction. Tissues in 2 mL Eppendorf tubes with two zirconium grinding beads (Comeau Technique Ltd., Vandreuil-Dorion, Canada) were loaded into a Retsch MM300 ball mill (Haan, Germany) where they were shaken for five minutes at 25 Hz. The powder was suspended in 1 mL of ice-cooled 80% MeOH/20% double distilled water v/v and sonicated for 15 minutes. Tubes were centrifuged (Sorvall ST 16 centrifuge; ThermoScientific, Waltham, Massachusetts, USA) at 10,000 rpm for 10 minutes. 700 µL of sample supernatant was transferred to 0.2 µM PVDF centrifuge filters with 2 mL receiver tubes and spun down at 10,000 rpm for 5 minutes. Filtered extracts were dried at ambient

temperature in the Speed vacuum centrifuge (ThermoScientific Savant SpeedVac^{TM}, Rockford, IL, USA). Residues were redissolved in 400 µL 50% MeOH/water and spun down again at 10000 rpm. 300µL of supernatant was transferred to a 350 µL autosampler insert inside a 2 mL glass vial with a septa cap. 10 µL of benzyladenine and 27 µL of abscisic acid labeled standards (OlChemim Ltd., Olomouc, Czech Republic) were added to each vial to monitor retention time deviation across samples for positive and negative ionization modes, respectively.

3.2.4. Data Acquisition via Liquid Chromatography–Mass Spectrometry (LC-MS)

Extracts from both *D. dentatus* ecotypes (i.e., red and white) were analyzed by LC-MS (Nguyen et al., 2023b) with minor modifications. For an untargeted metabolomics analysis, the data were acquired using a Thermo Q-Exactive Orbitrap mass spectrometer (Thermo Scientific, San Jose, CA, USA) coupled to a Thermo Dionex Ultimate 3000 Liquid Chromatograph System (Thermo Scientific, San Jose, CA, USA). All samples were injected for analysis in a mixed mode (positive and negative electrospray ionization (ESI) modes) with an initial mass range of m/z 80−600 at a resolution of 140,000 at m/z 200 full width at half minimum (FWHM), with an automatic gain control (AGC) target of 3 × 106, and maximum injection time (IT) of 524 ms. The following conditions were used for the heated electrospray ionization (HESI) probe: capillary temperature, 250 °C; sheath gas, 30 arbitrary units; auxiliary gas, 8 units; probe heater temperature, 450 °C; S-Lens rf level, 60%; and capillary voltage, 3.9 kV.

Quality controls (QCs) composed of equal volumes of sample replicates, were used for data-dependent tandem mass spectrometry (ddms2). QCs were created with a mixture of all replicates from both ecotypes and also from each ecotype. Fragmentation using ddms2 was performed at a resolution of 17,500 with an AGC target of 5 × 105 within a narrower mass range

of 100 to 600 m/z. The fragmentation was triggered at a loop count of 10 (top 10 most intense peaks per scan), with a precursor isolation window of 1 m/z at a normalized collision energy (NCE) of 35 eV. The maximum IT was 64 ms.

The chromatographic separation was accomplished with an HGP-3400RS dual pump and WPS-3000 autosampler equipped with a Kinetex C18 column (2.1 i. d × 50 mm, 2.6 μm particle size, Phenomenex, Torrace, CA, USA) operated at an approximate room temperature of 22 °C. The instrument control was achieved with Chromeleon Chromatography Data System software version 6.8(ThermoScientific; Ottawa, ON, Canada). For the separation, component A comprised ddH20 with 0.1% formic acid, and component B comprised acetonitrile (CH3CN) with 0.1% formic acid, at a flow rate of 0.3 mL/min. Mobile phase B was held at 0% for 30 s, before increasing it to 100% over 3 min. Solvent B was then held at 100% for 2 min before returning to 0% over 4 min for column re-equilibration. The total runtime was 10 min, with a sample injection volume of 25 μL.

3.2.5. Data Processing of Untargeted Mass Spectrometry Data

The MS Convert utility (Version 3.0) of the open-source ProteoWizard program was used to convert raw mass spectrometric data to mzXML format (Chambers et al., 2012). As the LC-MS acquisition occurred in mixed ionization mode, negative and position ions were extracted separately by using the default for peak picking, and threshold peak filter with absolute intensity using the most intense ions (0.001 and above). Peak peaking, retention time correction, and peak grouping were all conducted using the default parameters of XCMS Online (Smith et al., 2006) which is included in the Supplemental Information. The pairwise option in XCMS Online was

used with the white ecotype as the control (Chong et al., 2019). After peak peaking, retention time correction, and peak grouping, the resulting peak intensities matrix was subjected to statistical analysis using MetaboAnalyst 5.0 (Chong et al., 2019). The data was normalized by sum and then log-transformed before principal component analysis (PCA) to visualize the overall clustering pattern of the samples. Additionally, partial least squares discriminant analysis (PLS-DA) was performed to identify metabolites that contributed most to the separation between sample groups. The significance of differential metabolites was determined using the t-test and fold change analysis.

D. dentatus red and white putative MS^1 m/z features were compared to databases of physiologically active substances in literature and with bioinformatics servers used in untargeted metabolomics such as KnapSack (Shinbo et al., 2006), KEGG (Kanehisa et al., 2019), Plant Metabolic Network using the PlantCyc database (https://plantcyc.org) (Hawkins et al., 2021), MetaboQuest (Fan et al., 2020), SciFinder (Hounguè et al.) and PubChem (Kim et al., 2022). In the processing module of XCalibur 4.1 (ThermoScientific, Waltham, MA, USA), we inputted the putative identities of key therapeutic compound families (i.e., flavonoids, terpenoids, and alkaloids). They extracted the exact masses of protonated or deprotonated compounds.

Putative identities of key therapeutic compounds families (i.e., flavonoids, terpenoids, and alkaloids) generated were inputted in the processing module in XCalibur 4.1 (ThermoScientific, Waltham, MA, USA) where the exact masses of protonated or deprotonated compounds were extracted. This semi-targeted approach was done to determine peak quality and to monitor peaks within samples for therapeutic compounds falling under polyphenolics, terpenoids, and alkaloids. Relative quantification of peak areas was done to determine up-or-downregulated compounds, by

the ratio of the averages of [Capadulla Red] / [Capadulla White]. If the ratio (fold change; FC)> 1, the samples are upregulated. The converse is downregulated if the ratio < 1 (Supplemental Fig3. 2). Metabolite AutoPlotter was used to generate images for tentative metabolites with corresponding peak areas (M. Pietzke & A. Vazquez, 2020). The workflow for data processing can be seen in Fig 3.1) for MS1 data.

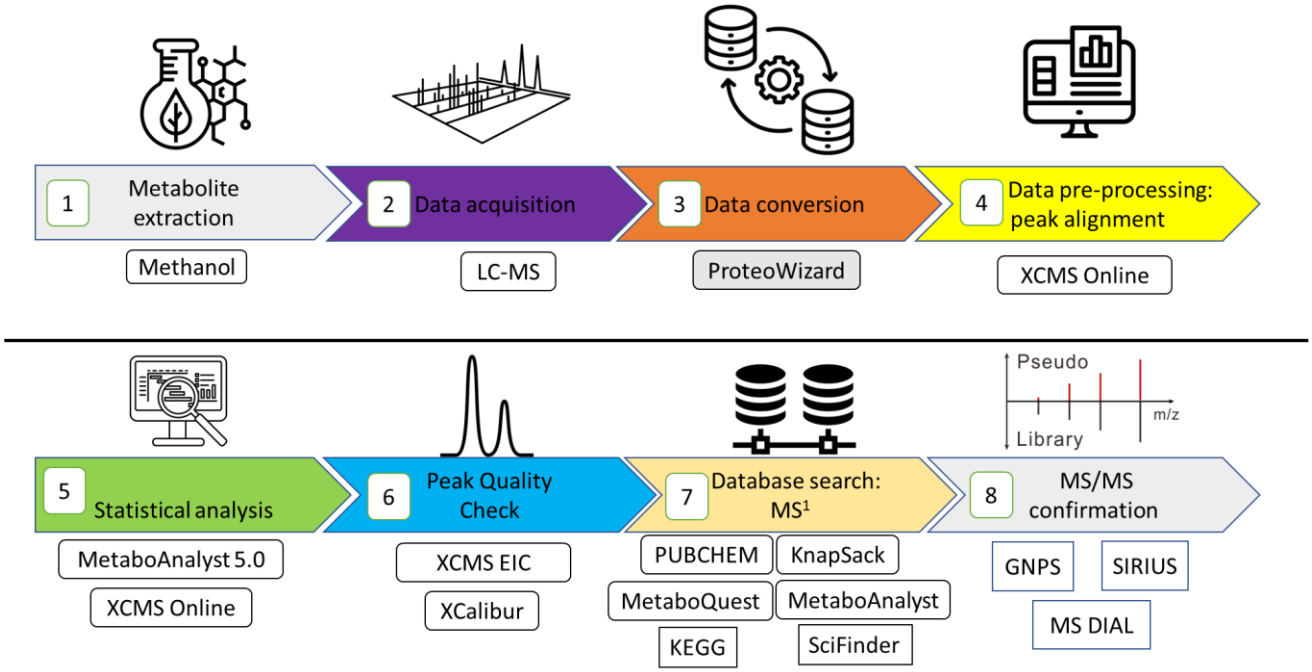

Figure 3. 1. Metabolomics workflow used for extracting, acquiring, and analyzing compounds present in *D. dentatus* ecotypes. The icons used are sourced from The Noun Project.

3.2.6. Statistical Analysis of Metabolomics Datasets

Untargeted metabolomic analyses generate complex multivariate datasets with thousands of tentative metabolites features and their corresponding intensities. Various dimensionality reduction procedures are employed to simplify the data and understand the relationships among samples based on these intensities. Metabolomic data analysis is characterized by high dimensionality, where the number of measured metabolite features exceeds the number of samples and collinearity among the features. These factors challenge traditional linear regression methods, necessitating statistical procedures capable of handling collinearity (Pezzatti et al., 2020).

Before any statistical analysis, preprocessing steps were applied to normalize the data to facilitate further analysis. This involved sum normalization, $\log_2$ transformation, and Pareto scaling to ensure the appropriate scaling of the obtained data using the MetaboAnalyst 5.0 platform [13] (www.metaboanalyst.ca, accessed from January 14, 2022, to June 10, 2023). By normalizing the data through sum normalization, applying a $\log_2$ transformation, and performing Pareto scaling, the dataset was prepared for subsequent statistical analysis. These preprocessing steps help to ensure that the data is appropriately scaled and standardized, allowing for meaningful comparisons and accurate statistical inference. We used ANOVA and the volcano plot to find metabolites strongly affected by the experimental factor, which is the difference between the red and white ecotypes.

The XCMS Online software tool was utilized to annotate the LC-MS dataset, which was subsequently analysed through the MetaboAnalyst 5.0 platform. The methodology employed to identify differential metabolites involved using the standard volcano plot, which integrates the t-test and fold-change techniques. The graph displays the logarithmic transformation of the fold-change values on the X-axis and the negative logarithmic transformation of the p-values obtained from the t-test on the Y-axis (H. Wang et al., 2013).

Furthermore, this analysis sought to uncover potential m/z biofingerprints that were elevated or downregulated in *D. dentatus* red and white ecotypes that may have therapeutic potential for erectile dysfunction. These statistical approaches, combined with the visual representation provided by the volcano plot, Principal Component Analysis (PCA), Partial Least-Squares Discriminant Analysis (PLS-DA) and hierarchical cluster analysis (HCA), offer valuable insights into the metabolomic variations between the *D. dentatus* red and white ecotypes.

Principal Component Analysis (PCA) and Partial Least-Squares Discriminant Analysis (PLS-DA) are commonly employed to reduce the dimensionality of the data and identify differences between groups. PCA aims to replace correlated variables with uncorrelated variables, known as principal components (PCs), which capture most of the variability in the original dataset. This allows for initial biological conclusions about the samples, which can be further verified using PLS-DA or orthogonal projections to latent structures DA (OPLS-DA). Despite having fewer samples than variables (metabolite features and intensities), multivariate statistical methods such as PCA (Houriet et al., 2022; Jiang et al., 2022), PLS-DA (Fonville et al., 2010) and hierarchical cluster analysis (HCA) (Granato et al., 2018) are appropriate for analyzing metabolomics datasets

(Bartel et al., 2013; Blaise et al., 2021; Böckel et al., 2021; Cambiaghi et al., 2017; Dias et al., 2012; Peris-Díaz et al., 2019; Roessner & Dias, 2013).

In our study, we performed PCA to examine the relationships among samples based on the relative intensities of all tentative metabolite features. PCA groups sample into clusters based on overall similarity or metabolite profile differences. Samples with similar profiles are grouped together on the PCA plot. PCA determines these relationships solely based on the metabolite features without considering sample descriptions such as species or treatment. Following determining sample relationships through PCA, we identified the top 25 significantly different features ($P \leq 0.05$) using PLS-DA or OPLS-DA. These features allow for separating samples into distinct groups, indicating significant differences in their accumulation among ecotypes and treatments.

Additionally, HCA was conducted to identify the top 25 statistically significant tentative metabolite features between the ecotypes in both positive and negative modes. Pearson's correlation was used to assess the relatedness of samples based on these 25 features (Figures 6 and 7). The results of HCA were visualized as a heatmap, with samples and features displayed on the X- and Y-axes, respectively, and relative metabolite intensities indicated by a color scale. The relationship among samples was depicted using a color-coded dendrogram atop the HCA plot. Similar to PLS-DA, HCA identifies metabolite features that separate samples into distinct clusters aligned with sample descriptions. Ward's clustering algorithm and Pearson's correlation were employed to construct the dendrograms, with the Euclidean distance indicated on the X-axis. All statistical analyses were performed using the MetaboAnalyst 5.0 platform (Pang et al., 2021).

3.2.7. Tandem Mass Spectrometry-Data Analysis for Metabolite Annotation

Using diverse bioinformatic tools can aid in metabolite annotation. Global Nature Production Social Molecular Networking (GNPS), SIRIUS and MS-DIAL were therefore used to query fragments for putative identification (Branquinho, Verdan, Santos, et al., 2021; Li et al., 2016). The metabolite annotation levels using these tools are level 2 for MS-DIAL, levels 2 and 3 for GNPS, and level 3 using the *in silico* fragmentation tool SIRIUS and were assigned these levels as recommended by the Metabolomics Standards Initiative (Sumner, 2007). The workflow for data analysis can be seen in (Fig.3.1).

3.2.8. Metabolite Annotation using MS-DIAL

Tandem mass spectrometry raw data were processed with MS-DIAL 5.1 (Tsugawa et al., 2015). Automatic feature detection was performed between retention times of 0 and 10 min for mass signal extraction in positive and negative ionization modes. MS^1 and MS^2 tolerance were set to 0.01 and 0.025 Da, respectively, in profile mode. Minimum feature height, mass slice width and the sigma window value were all set to the default of 1000 (AU; arbitrary units), 0.1 Da, and 0.5, respectively (Hu et al., 2019). Alignment for samples was done at 0.015 Da mass tolerance and 0.05 min for the retention time tolerance for MS^1. Database matches were done with the parameters of MS^1 and MS^2 at 0.01 and 0.05 Da, respectively (instructions as previously published (Perez de Souza et al., 2019)). Databases for both positive and negative ionization modes were downloaded and chosen for level 2 from the MS-DIAL website (<http://prime.psc.riken.jp/compms/msdial/main.html> accessed March 1, 2023).

3.2.9. Metabolite Annotation Using GNPS via Classical Molecular Networking

Raw data from quality control samples from each ecotypewere converted to mzXML via MSConvert option in Proteowizard and submitted to GNPS. A molecular network for both negative and positive ionization data was created using the online workflow (https://ccms-ucsd.github.io/GNPSDocumentation/) on the GNPS website (http://gnps.ucsd.edu). The data was filtered by removing all MS/MS fragment ions within +/- 17 Da of the precursor m/z. MS/MS spectra were filtered windows by choosing only the top 6 fragment ions in the +/- 50Da window throughout the spectrum. The precursor ion mass tolerance was set to 0.02 Da and a MS/MS fragment ion tolerance of 0.02 Da. A network was then created where edges were filtered to have a cosine score above 0.6 and more than 3 matched peaks. Further, edges between two nodes were kept in the network if and only if each of the nodes appeared in each other's respective top 10 most similar nodes. Finally, the maximum size of a molecular family was set to 100, and the lowest scoring edges were removed from molecular families until the molecular family size was below this threshold. The spectra in the network were then searched against GNPS' spectral libraries. The library spectra were filtered in the same manner as the input data. All matches kept between network spectra and library spectra were required to have a score above 0.6 and at least 3 matched peaks (M. Wang et al., 2016).

The workflow and results of Classical Molecular networking can be found in the following GNPS repositories for positive and negative ionization data (Task IDs = e06a20c58fa04355ba3630912077b3ea and 8ceaa322aac44c62a027d131b33dc4ce).

Dereplicator+ (Mohimani et al., 2018) and Network Annotation Propagation (NAP)(R. R. da Silva et al., 2018) were used in conjunction for enhanced annotation. Although

MolNetEnhancer (Ernst et al., 2019) is used a workflow used for combining results of CMN, Dereplicator+ and NAP, this function did not work for annotating our results for visualization of compound classes via Cytoscape (Shannon et al., 2003). However, overall visualization was done in Cytoscape 3.10.0 after merging networks of both negative and positive ionization modes (Choi et al., 2021) (included in Supplemental Information).

3.2.10. Metabolite Annotation Using GNPS via Feature-Based Molecular Networking

The mzMine 2.5.3 analysis pipeline (Olivon et al., 2017; Pluskal et al., 2010) was used to look for MS^1 features corresponding to MS^2 fragments. Data acquired from QC samples from each ecotype analyzed using $ddMS^2$ were converted to the mzXML format using the MSConvert option in Proteowizard, as mentioned previously. The peaks were aligned using the previously published parameters with modifications involving mass detection, chromatogram building, smoothing deconvolution, deisotoping, alignment and gap filling (Reveglia et al., 2022). All data (for MS^1 and MS^2) was used and stored in .mgf format with the corresponding .csv file.

A molecular network was created with the Feature-Based Molecular Networking (FBMN) workflow (Nothias et al., 2020) on GNPS (https://gnps.ucsd.edu)(M. Wang et al., 2016). The results from mzMine 2.5.3 were exported to GNPS for FBMN analysis. FBMN was used to resolve any isomers and also to check for any other annotations due to cleaning up data during mzMine preprocessing. The data was filtered by removing all MS/MS fragment ions within +/- 17 Da of the precursor m/z. MS/MS spectra were window filtered by choosing only the top 6 fragment ions in the +/- 50 Da window throughout the spectrum. The precursor ion mass tolerance was set to 0.02 Da and the MS/MS fragment ion tolerance to 0.02 Da. A molecular network was then created

where edges were filtered to have a cosine score above 0.6 and more than 3 matched peaks. Further, edges between two nodes were kept in the network if and only if each of the nodes appeared in each other's respective top 10 most similar nodes. Finally, the maximum size of a molecular family was set to 100, and the lowest scoring edges were removed from molecular families until the molecular family size was below this threshold. The spectra in the network were then searched against GNPS spectral libraries (Horai et al., 2010; M. Wang et al., 2016). The library spectra were filtered in the same manner as the input data. All matches kept between network spectra and library spectra were required to have a score above 0.6 and at least 3 matched peaks. The DEREPLICATOR was used to annotate MS/MS spectra (Mohimani et al., 2018). The molecular networks were visualized using Cytoscape software (Shannon et al., 2003).

The workflow and results of FBMN networking can be found in the following GNPS repositories for positive and negative ionization data (Task IDs = 39963758986b4f09b0b992d130489534 and 031003b2e66744fab8923d6ee405a5e2). Dereplicator+ and Network Annotation Proparagation (NAP) were used in conjunction for enhanced annotation. Although MolNetEnhancer is a workflow used for combining results of CMN, Dereplicator+ and NAP, this function did not work FBMN for annotating our results for visualization of compound classses via Cytoscape at that time. Dereplicator+ also did not work for FBMN annotation, revealing no hits. The workflow for FBMN processing can be seen in Supplemental Information (Fig 3.1).

3.2.11. Using SIRIUS as an In Silico Fragmentation Tool for Metabolite Annotation

mzXML files corresponding to quality controls for each ecotype and both positive ionization modes were imported into SIRIUS 5.6.2. Peaks were classified and their MS^2 fragmentation patterns tentatively annotated with the ZODIAC, CSI: FingerID, CANOPUS using ClassyFire and NPClassifier modules within SIRIUS 5.6.2 (Djoumbou Feunang et al., 2016; Duhrkop et al., 2019; Duhrkop et al., 2021; Duhrkop et al., 2015; Hoffmann et al., 2022; Kim et al., 2022). Default settings were used for the different modules, with Orbitrap being the instrument of choice, and MS^2 queried within 10 ppm error. For positive ion mode, $[M+H]^+$ and $[M+H-H_2O]^+$ adducts were used, with $[M-H]^-$ being the adduct used in negative ionization mode. All databases were used for tentative identification. For tentative identification, a combination of COSMIC and ZODIAC scores were both considered. Manual analysis of the matching substructures was conducted before structural assignment was made. If the fragmentation pattern did not match the structures proposed by CSI:FingerID, matching fragments from the proposed structures were considered when the class was assigned using CANOPUS. If the ZODIAC score was < 50%, no tentative identification was made. If the SIRIUS score was < 50% with no accompanying ZODIAC score, no identification was made. A combination of scores of > 90% for SIRIUS and > 70% for ZODIAC were used for screening (K. Blatt-Janmaat et al., 2023; K. L. Blatt-Janmaat et al., 2023; Peters et al., 2023).

3.2.12. Cheminformatics Using ClassyFire for Compound Class Groupings

For querying data in cleaning up tentative metabolite names, and to identify compounds not named from both GNPS and SIRIUS, the Pubchem Identifier service (https://pubchem.ncbi.nlm.nih.gov/idexchange/idexchange.cgi accessed September 18, 2023) was used to convert SMILES to InChiKeys for the batch compound classification tool in ClassyFire (Djoumbou Feunang et al., 2016). ClassyFire Batch Compound Classification (https://cfb.fiehnlab.ucdavis.edu/ accessed September 18, 2023) was used to categorize InChiKeys to compound classes. SMILES without corresponding InChiKeys, and InChiKeys not found not found in ClassyFire were not used in metabolite annotation. Also, duplicate data were deleted after checking InChiKeys. InChiKeys were used for structural information instead of SMILES format as they are standardized and are of fixed length, allowing for easy data processing (Ollivier et al., 2022)

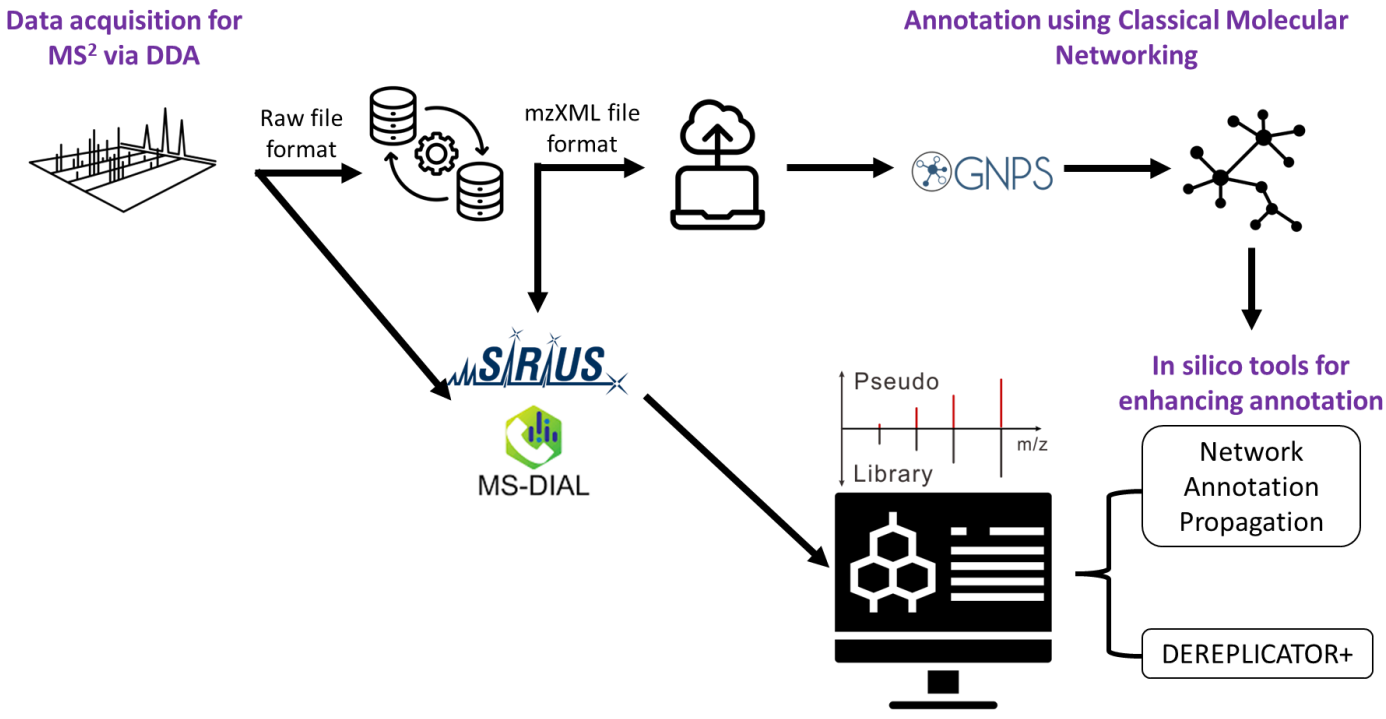

Figure 3. 2 : Processing of tandem mass spectrometry data using a combination of bioinformatics tools for level 2–3 annotations.

3.3. RESULTS

3.3.1. Untargeted Metabolomics: Analysis of *D. dentatus* Red and White Ecotypes

Metabolomics analyses of the woody vine *D. dentatus* red and white ecotypes in natural communities have not been previously undertaken. Therefore, in this study, we aimed to explore and describe the metabolomic differences between these ecotypes on a global level, specifically focusing on the occurrence of secondary metabolites, such as polyphenols (i.e., flavonoids), terpenoids, alkaloids, and other compounds, in the *D. dentatus* red ecotype compared to the *D. dentatus* white ecotype to identify potential biofingerprints and/or differentially expressed compounds that may have been a potential therapy for erectile dysfunction in men. This study represents one of the initial efforts to investigate and present the descriptive metabolomic results for these two ecotypes.

To investigate the dissimilarities in the metabolome between the *D. dentatus* red and white woody vine ecotypes, we conducted an untargeted metabolomics analysis using LC-MS/MS (liquid chromatography–tandem mass spectrometry). This allowed for the detection of 9562 tentative metabolite features that were further queried for exact and approximate matches in the databases of physiologically active substances in the literature and with bioinformatics servers used in untargeted metabolomics.

Among these detected features, we observed 2664 tentative metabolite features with positive ionizations [M+H] + and 2470 with negative ionizations [M-H] − in the *D. dentatus* red ecotype. Similarly, in the *D. dentatus* white ecotype, we identified 2316 tentative metabolite features with positive ionizations [M+H] +. These findings indicate variations in the metabolite profiles between the red and white ecotypes of *D. dentatus*, as demonstrated by the differing numbers of detected tentative metabolite features in each ecotype.

We utilized the "Functional Analysis" module and the Gene Set Enrichment Assay (GSEA) tool within MetaboAnalyst 5.0 to better understand the metabolic differences between the two ecotypes. The purpose was to compare the tentative metabolite features (9562) obtained from our analysis. Using the GSEA tool, we searched for metabolite features in the annotated *A. thaliana* metabolite database that closely matched our mass charge ratio (m/z) features. This allowed us to find similarities with the Kyoto Encyclopedia of Genes and Genomes (KEGG) database and other bioinformatics servers used in untargeted metabolomics.

Upon conducting the global metabolomic analysis, we found a total of 637 putative metabolite features that matched with the reference database. Among these, 107 features 16.79% were exclusive to the *D. dentatus* red ecotype, while 64 features belonged to the *D. dentatus* white ecotype 10.05%. Notably, approximately a portion % of these putative metabolite features, about 36.58%, were unique to the *D. dentatus* red or white ecotypes (Oliveros, 2007) (Fig. 3.3).

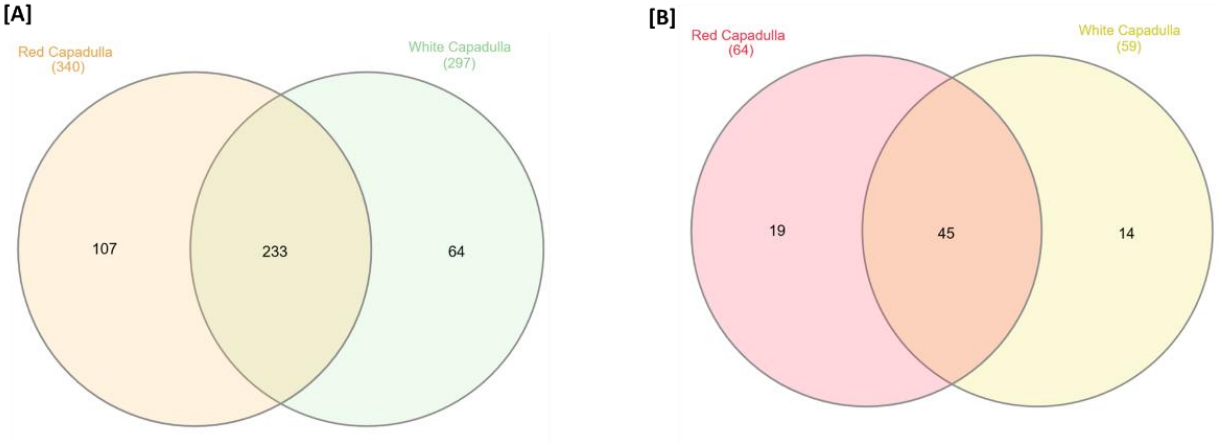

Figure 3. 3: Venn diagrams illustrating the comparisons of tentative metabolite features and tentatively attributed pathways between the *D. dentatus* red and white ecotypes. Venn diagram (A) consists of the common and unique tentative features grouped in *D. dentatus* red- and white-ecotype woody vines. Venn diagram (B) consists of the tentatively attributed metabolite features in each woody vine *D. dentatus* ecotype using features from both ionization modes.

Utilizing the abovementioned software tools and approaches, we successfully compared numerous metabolite features and identified the putative compounds that differed between the two ecotypes at levels 3 and 4 (Apendex 3) (Schrimpe-Rutledge et al., 2016). This comprehensive analysis provided valuable insights into the metabolic variations within these ecotypes, further enhancing our understanding of their distinct characteristics. For further validation, MS2 data processing revealed 55 selected compounds composed of flavonoids, terpenoids, and some alkaloids at a level 2 annotation level (Tables 3.1 and 3.2).

We utilized volcano plots to determine tentative features in *D. dentatus* red that exhibit up-regulation or down-regulation compared to the *D. dentatus* white control in both positive and negative ionization ionizationmodes. Several tentative m/z features deviated from the typical pattern within the volcano plot, indicating significant fold changes in regulating *D. dentatus* red

and white ecotypes (Figure 4). To validate these tentative m/z features, we referred to the Omics Craft database module MetaboQuest (http://tools.omicscraft.com/MetaboQuest/) (Oliveros, 2007; Schrimpe-Rutledge et al., 2016). The analysis revealed compounds such as Methocarbamol di-TMS derivative, Diosprin, Deoxycytosine, and others (Figure 4A). However, these putative compounds did not align with the biofingerprints of interest, particularly the polyphenolic compounds like catechin groups (Fig.3.6). The presence of polyphenols is noteworthy as they possess antioxidant, anticancer, anti-inflammatory, cytotoxic, and antimicrobial properties, primarily due to their radical-scavenging ability (Moon et al., 2021). These findings suggest that further exploration of polyphenolic compounds in *D. dentatus* red and white may hold potential as a therapeutic response for erectile dysfunction. Their beneficial effects, attributed to their diverse bioactivities, make them a promising area of interest for potential therapeutic interventions.

Table 3.1.tentative identification of selected compounds derived from a combination of classical molecular networking and feature-based molecular networking with fragmentation data grouped according to natural product classification (NP superclass). Tentative identification and/or ionization mode with an asterisk (*) were found in feature-based molecular networking.

Tentative Identification	Molecular Formula	Adduct	Precursor m/z	MS^2	NP Superclass
(R)-Norlaudanosoline	$C_{16}H_{17}NO_4$	M+H	288.12	123.04, 143.05, 149.00, 161.06, 164.0, 225.09	Alkaloids
Salsolinol	$C_{18}H_{24}N_2O_3$	M+H	180.102	117.07, 137.06, 145.0, 151.07	Alkaloids
Cinchonidine	$C_{19}H_{22}N_2O$	M-H	293.166	59.01, 96.96	Alkaloids
Coniferyl aldehyde	$C_{10}H_{10}O_3$	M+H	179.07	55.02, 91.06, 105.07, 119.05, 123.04, 147.0	Cinnamic acids and derivatives
3-Hydroxy-4-methoxycinnamic acid	$C_{10}H_{10}O_4$	M+H-H_2O	177.054	89.05, 117.03, 145.0, 149.06	Cinnamic acids and derivatives
6-Methylcoumarin	$C_{10}H_8O_2$	M+H	161.06	91.06, 105.07, 115.06, 119.0	Coumarins
Phloridzin	$C_{27}H_{30}O_{13}$	M+H	453.139	85.03, 123.04, 139.0, 163.04, 205.05, 273.08	Flavonoids
Kaempferol *	$C_{15}H_{10}O_6$	M+H	287.055	153.02, 165.02, 213.06, 287.0	Flavonoids
Quercetin	$C_{15}H_{10}O_7$	M+H	303.049	137.02, 151.0, 165.02, 229.05, 257.04	Flavonoids
		M-H	301.035	121.02, 151.0, 179.00	
Maesopsin	$C_{15}H_{12}O_6$	M-H	287.056	57.03, 83.01, 125.0, 151.00, 215.07, 259.06	Flavonoids
(-)-Epicatechin	$C_{15}H_{14}O_6$	M+H	291.086	115.0, 123.04, 139.04	Flavonoids
(+)-Catechin				123.04, 139.0, 147.04, 161.06, 165.05, 179.07, 207.07	Flavonoids
Epigallocatechin	$C_{15}H_{14}O_7$	M+H	307.081	84.08, 111.04, 123.04, 139.0, 151.04	Flavonoids
Gallocatechin		M-H	305.066	109.3, 125.0, 137.02, 161.02, 165.02,219.07	Flavonoids
Apigetrin [Cosmosiine]	$C_{21}H_{20}O_{10}$	M+H	433.113	256.73, 271.0	Flavonoids
Astragalin [Kaempferol-3-O-glucoside]	$C_{21}H_{20}O_{11}$	M+H *	449.108	85.03, 153.02, 287.0	Flavonoids
		M-H	447.091	227.03, 255.03, 284.0	Flavonoids
Kaempferol-4-glucoside		M+H	449.108	85.03, 97.03, 127.04, 287.0	Flavonoids
Isoquercetin *	$C_{21}H_{20}O_{12}$	M-H	463.088	151.00, 255.03, 271.02, 300.0	Flavonoids
6-Methoxyluteolin	$C_{21}H_{22}O_6$	M+H-H_2O	327.158	137.06, 151.0, 171.08, 203.11	Flavonoids
Phlorizin	$C_{21}H_{24}O_{10}$	M-H	435.13	125.02, 167.0, 179.03, 273.08	Flavonoids
		M+H *	289.092	85.03, 127.0	Flavonoids
(-)-Catechin gallate	$C_{22}H_{18}O_{10}$	M+H	443.096	123.04, 139.0, 153.02, 273.07	Flavonoids
Epicatechin gallate		M-H	441.08	109.03, 125.02, 169.0, 193.01, 245.08, 289.07	Flavonoids
		M+H *	443.097	139.0, 153.02, 165.05, 273.07, 291.09	Flavonoids
Rutin	$C_{28}H_{24}O_{15}$	M-H	599.105	125.02, 151.00, 169.0, 284.03, 285.04, 313.06	Flavonoids
Procyanidin B1	$C_{30}H_{26}O_{12}$	M-H	577.135	109.0, 125.0, 161.03, 203.07, 245.08, 289.07, 407.08	Flavonoids
Procyanidin B2		M+H	579.15	127.0, 139.04, 191.03, 233.04, 247.06, 271.06, 287.06, 409.09	Flavonoids
Isatin	$C_8H_5NO_2$	M+H	148.04	92.05, 120.0	Indoles and derivatives

Tentative Identification	Molecular Formula	Adduct	Precursor m/z	MS^2	NP Superclass
1,3,6-Tri-O-galloyl-β-D-glucose	$C_{20}H_{20}O_{14}$	M-H	483.078	125.02, 151.01, 169.0, 211.02, 271.04, 313.07	Phenolic acids
Chlorogenic acid	$C_{23}H_{30}O_{12}$	M-H	497.166	125.02, 169.0, 313.06, 331.07	Phenolic acids
Gallic acid	$C_7H_6O_5$	M+H-H_2O	153.018	79.02, 97.03, 107.0, 125.02	Phenolic acids
		M-H *	169.014	81.03, 97.03, 125.0, 169.01	
4-Allyl-2,6-dimethoxyphenol (Eugenol) *	$C_{10}H_{12}O_3$	M+H	195.102	107.0, 135.08, 154.06, 163.07, 195.10	Phenolic compounds
Genipin *	$C_{11}H_{14}O_5$	M+H-H_2O	209.081	121.0, 149.06, 177.06, 181.05, 209.08	Phenolic compounds
Coumaroyl quinic acid *	$C_{16}H_{18}O_9$	M-H	337.092	93.03, 163.04, 173.04, 191.0	Phenolic compounds
Protocatechuic acid *	$C_7H_6O_4$	M-H	137.024	93.03, 108.02, 109.03, 137.0	Phenolic compounds
p-Coumaric acid *	$C_9H_8O_3$	M+H-H_2O	147.044	91.05, 119.0, 123.96, 147.04	Phenolic compounds
Methyl gallate *	$C_8H_8O_5$	M+H	185.045	113.01, 126.03, 153.02, 185.0	Phenolic compounds (gallotannins)
Cuminyl alcohol *	$C_{10}H_{12}O_2$	M+H-H_2O	133.101	91.05, 105.07, 118.08, 133.1	Phenolic compounds (phenylpropanoids)
Alpha-Pinene *	$C_{10}H_{16}$	M+H	137.13	67.05, 79.05, 81.07, 95.09, 109.10, 137.10	Terpenoids
Ascaridole	$C_{10}H_{16}O_2$	M+H	195.102	95.05, 123.08, 149.06, 167.07	Terpenoids
(1R)- (-)-Nopol	$C_{11}H_{18}O$	M+H-H_2O	149.132	65.04, 81.07, 93.07, 107.09, 121.0	Terpenoids
Dianthoside	$C_{13}H_{20}O_8$	M+H	289.092	97.03, 127.0	Terpenoids
Dihydro-α-ionone	$C_{15}H_{22}O$	M+H	177.164	79.06, 81.07, 93.07, 95.09, 107.09, 1121.1, 149.06	Terpenoids
Farnesol *	$C_{15}H_{26}O$	M+H	223.205	69.07, 95.09, 83.09, 109.10, 121.10, 135.12, 205.20, 223.21	Terpenoids
Betulinic acid	$C_{30}H_{48}O_3$	M+H-H_2O	439.357	57.07, 81.07, 95.09, 109.10, 123.12, 137.13, 189.16, 241.19, 255.21	Terpenoids
Betulonic acid	$C_{30}H_{48}O_4$	M+H-H_2O	437.341	69.07, 95.09, 107.09, 121.10, 135.12, 189.16, 203.18, 215.18, 241.19, 255.21, 391.33	Terpenoids
Sumaresinolic acid	$C_{30}H_{48}O_4$	M+H-H_2O	455.352	57.07, 81.07, 95.09, 109.10, 137.13, 189.16, 203.18, 391.33, 409.35	Terpenoids
Betulin	$C_{30}H_{50}O_2$	M+H-H_2O	425.378	67.06, 81.07, 95.09, 109.10, 123.12, 137.13, 189.16, 201.16,215.18, 227.18, 255.21, 269.23	Terpenoids

Table 3.2. Tentative identification of compounds resulting from data analysis using MS DIAL grouped according to natural product classification (NP superclass). Tentative identifications that were not seen in the GNPS workflow are denoted by an asterisk (*).

Tentative Identification	Molecular Formula	Adduct	Precursor m/z	MS^2	NP Superclass
Epicatechin gallate	$C_{22}H_{18}O_{10}$	M+H	443.0972	139.039; 153.0184; 165.0548	Flavonoids (catechin gallates)
Quercetin	$C_{15}H_{10}O_7$	M+H	303.0499	137.0240, 229.0488	Flavonoids (flavonols)
Methylophiopogonanone A *	$C_{19}H_{18}O_6$	M+Na	365.1052	185.0422; 203.0528; 365.1057	Flavonoids (homoisoflavanones)
Emodin *	$C_{15}H_{10}O_5$	M-H	269.0452	201.0566; 241.0503; 269.0546	Phenolic compounds (hydroxyanthraquinones)
Catechol	$C_6H_6O_2$	M-H	109.0293	81.0345, 91.0189, 108.0217, 109.0294	Phenolic compounds
3-Coumaric acid *	$C_9H_8O_3$	M-H	163.0402	119.0499, 163.0034	Phenolic compounds (hydroxycinnamic acids)
p-Coumaric acid	$C_9H_8O_3$	M+H	165.0546	91.0540, 95.0858, 119.0493, 147.0442	Phenolic compounds (hydroxycinnamic acids)
Caffeic acid *	$C_9H_8O_4$	M-H-CO_2	135.0451	107.0499, 135.0450	Phenolic compounds (hydroxycinnamic acids)
2-[(2S,4aR,8aS)-2-hydroxy-4a-methyl-8-methylidene-3,4,5,6,7,8a-hexahydro-1H-naphthalen-2-yl] prop-2-enoic acid *	$C_{15}H_{22}O_3$	M-H	249.1495	205.1594, 249.1494	Terpenoids (eudesmane, isoeudesmane, or cyclic terpenoids)
Saikikogenin D *	$C_{30}H_{48}O_4$	M+H	473.3625	473.3460 (only MS^1 available)	Terpenoids (triterpenoids)

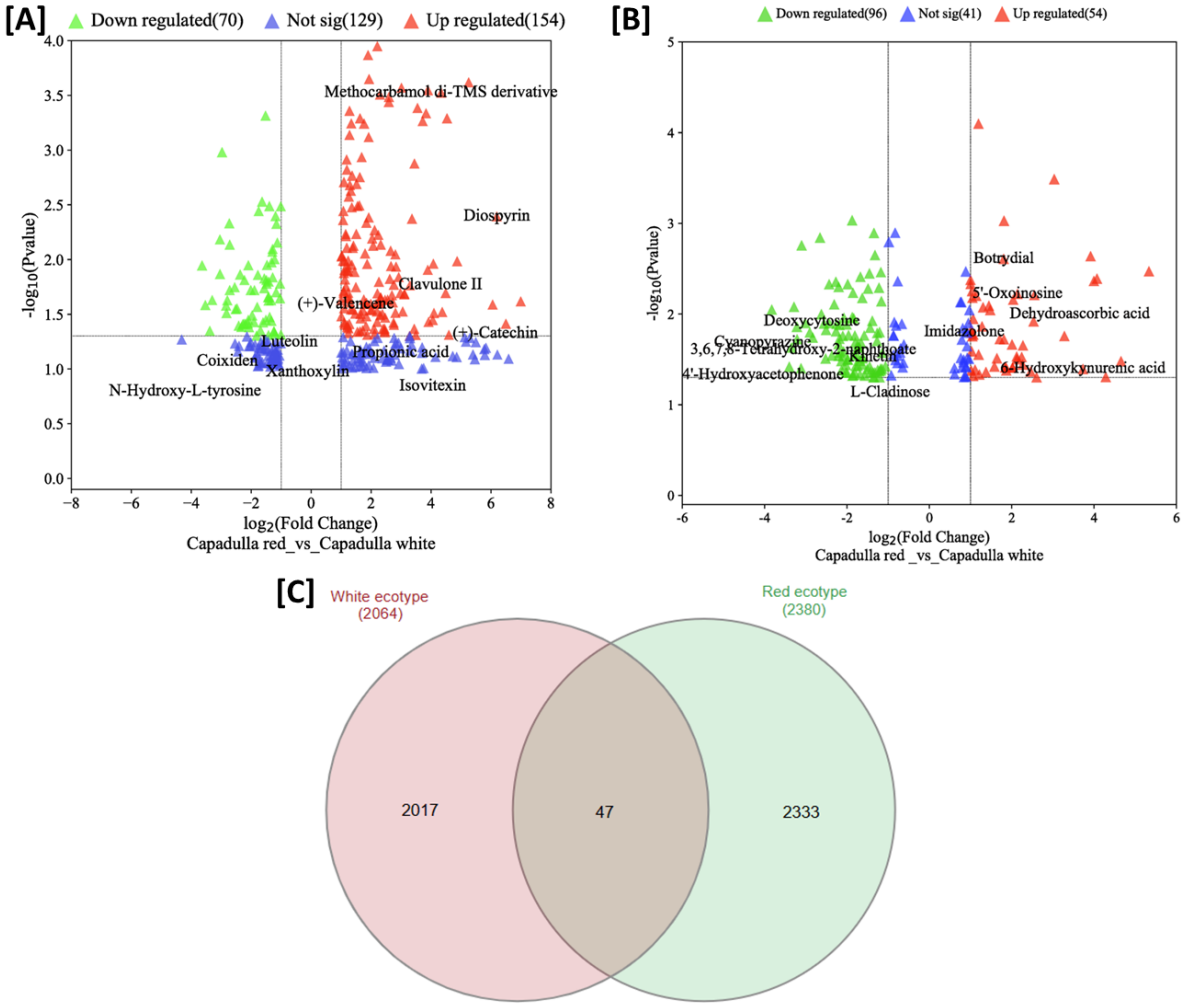

Figure 3. 4: (A) Volcano plot from the mass spectrometry data demonstrates the magnitude and significance of *D. dentatus* red compared with the control (*D. dentatus* white) in (A) the positive ionization mode and (B) the negative ionization mode. The horizontal dashed line shows where the p-value is 0.05 [- log10 (0.01) = 1.5], and the vertical lines show where the fold change is 2 [log2 (2) = 1] or 0.5 [log2 (0.5) = −1]. The two-fold change and p-value of 0.05 were used as the threshold cutoff. A total of 208 significantly upregulated, 166 downregulated, and 170 nonsignificant features were identified. (C) Venn diagram showing the repartition of the features obtained as statistical differences between *D. dentatus* red and white ecotypes combining both ionization modes (Oliveros, 2007).

3.1.1. Tentative Identification of the Significant Metabolites

To compare shared and unique tentative metabolite features among ecotypes, we utilized a Venn Diagram (Heberle et al., 2015). For predicting the pathways to which the tentatively identified metabolite features belong, we compared their accurate masses against the annotated metabolite database of *Arabidopsis thaliana* using the "Functional Analysis" module and the Gene Set Enrichment Assay (GSEA) tool within MetaboAnalyst 5.0 (Fig 3.1). The GSEA tool searches for similar metabolite features in the annotated *A. thaliana* metabolite database and provides a ranked list of statistically significant metabolic pathways enriched in these metabolites. The list includes corresponding p-values and adjusted p-values, indicating the significance level. GSEA employs a cut-off-free approach, searching for similarities between the metabolite features of the test species and *A. thaliana*. The resulting list ranks the metabolic pathways based on the similarity of metabolites and provides p-values derived from Kolmogorov-Smirnov tests (Chong et al., 2019; Pang et al., 2022).

3.1.2. Pathway Analysis of *D. dentatus* Ecotypes

A pathway analysis was performed to investigate the possible biomarkers within two separate ecotypes. This work aimed to elucidate the metabolic regulatory mechanisms that impacted the synthesis of diverse secondary metabolites and metabolic processes. A thorough analysis of the metabolic pathways was performed to identify the difference between the red and white ecotypes of *D. dentatus*. Databases, such as KEGG and HMDB, were used to analyze the obtained biomarkers.

The research utilized a range of techniques for visualizing and analyzing the data. The data were shown using a scatter plot, and an enrichment analysis was performed using Fisher's exact test. Furthermore, a topological study was conducted to examine the out-degree centrality. These methods were selected based on their statistical significance and capacity to evaluate the influence of routes.

The red ecotype of *D. dentatus* showed a statistical significance ($p \leq 0.05$) in the pathways related to the formation of sesquiterpenoids and triterpenoids, galactose metabolism, flavonoids, steroids, flavones, and flavonols. Additional data further substantiated these findings, demonstrating statistical significance values ranging from p = (0.000 to 0.01586) for the pathways mentioned above. The red ecotype of *D. dentatus* was statistically involved in the biosynthesis of sesquiterpenoid and triterpenoid, the biosynthesis of flavonoid, and galactose metabolism. The significance levels for these pathways ranged from p = (0.03 to 0.58). In contrast, the influence of limonene and pinene degradation, as well as the production of anthocyanin, an isoquinoline alkaloid, tropane, piperidine, and pyridine alkaloid, was shown to be relatively insignificant, as illustrated in (Fig 3.5 and appendix 2).

Regarding the *D. dentatus* white ecotype, the metabolic pathways that exhibited the highest importance were flavonoid biosynthesis, valine, leucine, and isoleucine biosynthesis. The statistical significance of these routes ranged from P = (0.0000 to 0.00046416). Additionally, the impact of these pathways varied, with significance levels ranging from P = 0.08 to 0.36. In contrast, the degradation of valine, leucine, and isoleucine, inositol phosphate metabolism, and tryptophan metabolism had reduced impacts, as depicted in Figure 5B and Supplementary Table 8. Given the preceding literature on the *D. dentatus* species, it is plausible that these metabolic pathways exert

substantial effects and can influence the taxonomic classification at distinct hierarchical levels (Kharazian & Mohammadi, 2014).

In the context of biochemistry and nutrition, interactions between compounds often yield various health benefits. These interactions are multifaceted and can result in enhanced outcomes. For example, antioxidants like Epicatechin methyl gallate, Catechin gallate, and Proanthocyanidin A2 can collaborate to neutralize harmful free radicals more effectively, extending protection against oxidative damage (Pang et al., 2022). Additionally, some compounds can improve the absorption and utilization of others, increasing the availability of essential nutrients like vitamins and minerals. Metabolic interactions can also occur, enhancing the effectiveness or duration of specific com-pounds (Kharazian & Mohammadi, 2014). Furthermore, compounds interacting with the same cellular pathways can regulate cellular processes cooperatively, leading to improved cell function and modulation of inflammation. Nutrient synergy is another aspect where certain compounds are more effective when consumed together, while balancing effects can mitigate adverse outcomes of specific com-pounds when consumed alone (Matysik & Liebisch, 2017).

These interactions are intricate and context-dependent, influenced by factors, such as the types of compounds involved, their concentrations, individual genetics, and overall dietary and lifestyle choices. Researchers continually explore these complex dynamics to better comprehend how compounds collectively impact health and well-being, especially in the case of ED. Principal component analysis was conducted on all the samples based on the LC-MS data. The overall relationship among the samples was assessed by PCA using all the tentative metabolite features identified for all the samples; on a PCA plot, samples that were spatially close to each other had

more similar metabolite profiles. The PCA generated two distinct clusters, each cluster corresponding to an ecotype of *D. dentatus*.

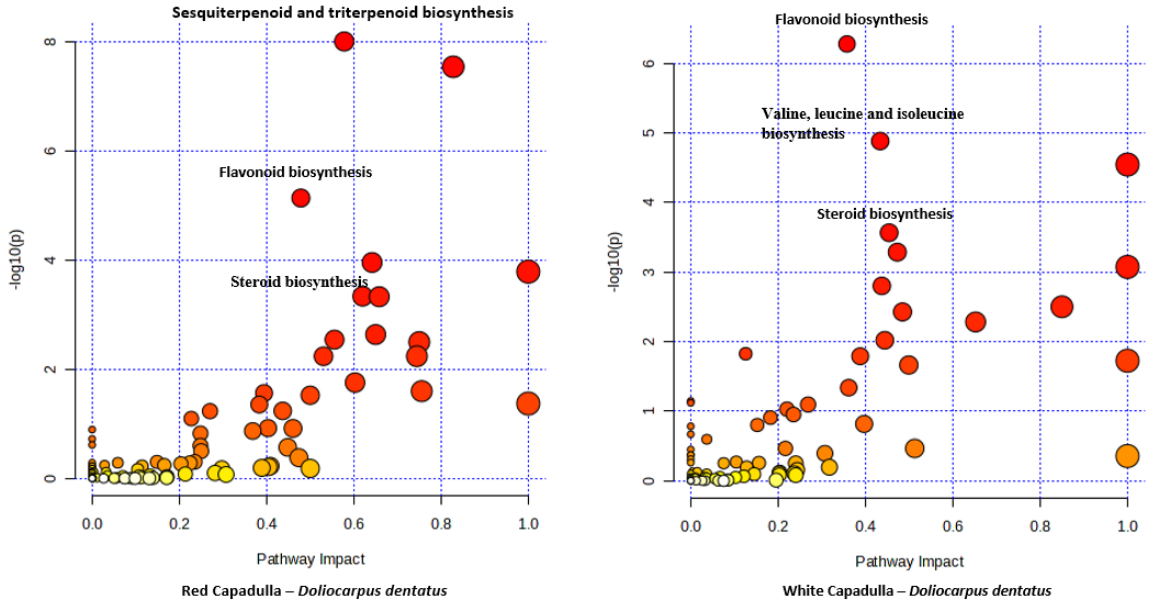

(**A**)

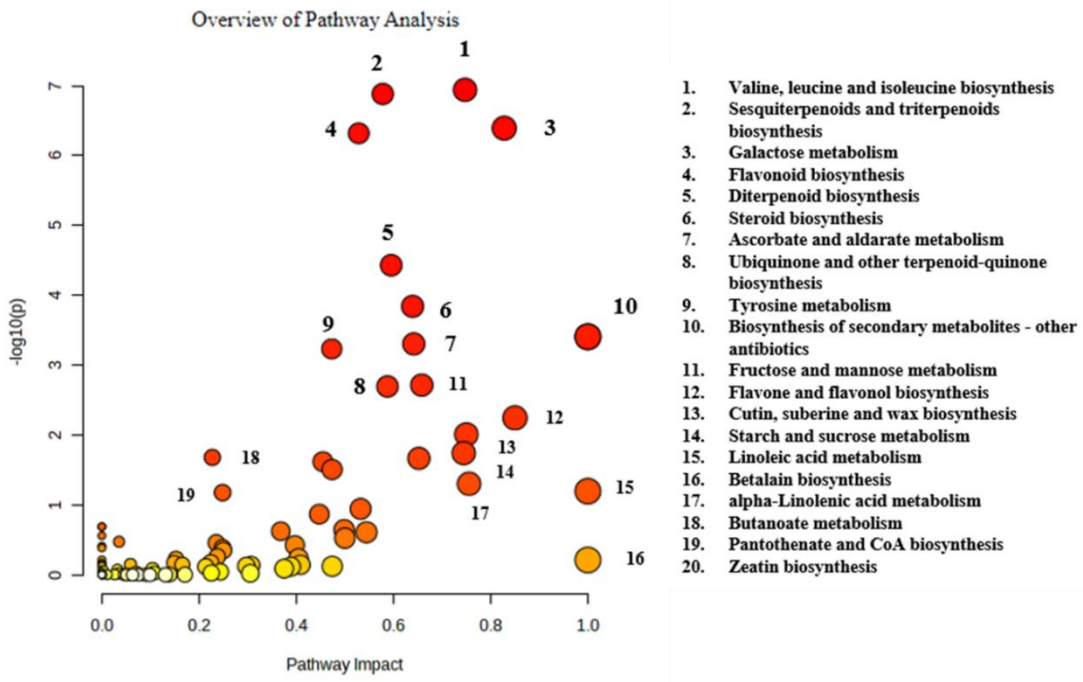

(**B**)

Figure 3. 5. (A) Overview of pathway analysis from all metabolic pathways (KEGG and HMDB) for D. dentatus red and white ecotypes. All the matched pathways were classified by p-values (y-axis) from the pathway enrichment analysis and pathway impact values (x-axis) from the pathway topology analysis. The node size exhibits the effect of impact values. The node colors exhibit different p-values. (B) Integrated pathway activity profile of significant ($p \leq 0.05$) metabolite features using both *D. dentatus* ecotypes linked to biosynthetic pathways as analyzed by MetaboAnalyst 5.0 (GSEA algorithm) using default parameters and the *Arabidopsis thaliana* pathway as the library. The colour gradient from yellow to red and the size of the dot indicate the statistical significance and impact of pathways.

3.1.3. Principal Component Analyses of *D. dentatus* Red and White Ecotypes

The first two principal components, PC1 and PC2, explained 60.3% and 13.9%, respectively, of the variability in the positive ionization mode. In contrast, 67% and 11% in the negative ionization mode of the total variability among the samples and the clusters that corresponded to the *D. dentatus* white ecotype and *D. dentatus* red ecotype, respectively, were closer to each other, indicating overall similarities in their metabolite profiles (Figures 6 and 7). The same pattern of relatedness was also observed in a dendrogram based on the Euclidean distance, on which the *D. dentatus* red and *D. dentatus* white ecotypes were grouped in the same clade (Fig.3.6 and 3.7).

The metabolic profiles of *D. dentatus* red and white ecotypes were examined with OPLS-DA to probe for metabolite features that separated the samples into distinct clusters corresponding to the ecotypes (Fig.3.6 and 3.7). The accumulation of the top 15 statistically significant metabolite features that separated the samples into the two main PLS-DA clusters was mainly influenced by the relative intensity of the sample and the ecotypes (Fig.3.6 and 3.7 and appendix). However, a close inspection of the relative abundance of some of the top statistically significant metabolite features indicated that species and treatment influenced their abundance (Fig 3.6 and 3.7). For

instance, the relative abundance of the flavonoids was significantly higher in the *D. dentatus* red ecotype than in the *D. dentatus* white ecotype (Figure 7; Supplemental Figures S2 and S5). The secondary metabolites putatively identified, such as alkaloids and terpenoids, were comparable between the ecotypes (Figure 5; Supplemental Figures S3 and S4).

3.1.4. Metabolite Annotation and Compound Class Contribution Using Tandem Mass Spectrometry Data

We annotated 847 compounds ranging from levels 2 to 4 by combining the usage of GNPS, MS DIAL, and SIRIUS, and compounds without fragmentation data (MS1). Approximately 12% of compounds annotated did not have fragmentation data and were placed at annotation level 4. In pooling contributions of red and white ecotypes, with ClassyFire used to categorize the compounds, most of the superclass of compounds fell into benzenoids, lipids, and lipid-like molecules, and phenylpropanoids and polyketides at 13.7, 37.9, and 20%, respectively (Figure 8). The phenolic compounds screened for therapeutic potential were majorly distributed in these categories. Although alkaloids were a superclass of interest, they were the second lowest contributor to the annotated compound pool at 0.6%.

In investigating phenylpropanoids and polyketides, the flavonoid class dominated the pool at 63.9%, followed by macrolides and monologues at 5.9%, with equal contributions of cinnamic acids and derivatives, isoflavonoids, and linear 1,3-diarylpropanoids at 5.3% each (Figure 9). Under lipids and lipid-like molecules, the fatty acyl class contributed most to the pool at 45.5%, followed by prenol lipids at 38%, and steroids and steroid derivatives at 6.54%. Terpenoids, another category of interest for therapeutic potential, fell into prenol lipids.

With respect to the biosynthetic pathways, using the Mummichog algorithm under MetaboAnalyst 5.0 for the initial screening of MS1 data, the pathway analysis results aligned with the annotated compounds, especially with high contributions of compounds belonging to both flavonoid and terpenoid biosynthesis pathways (Figures 5A, B).

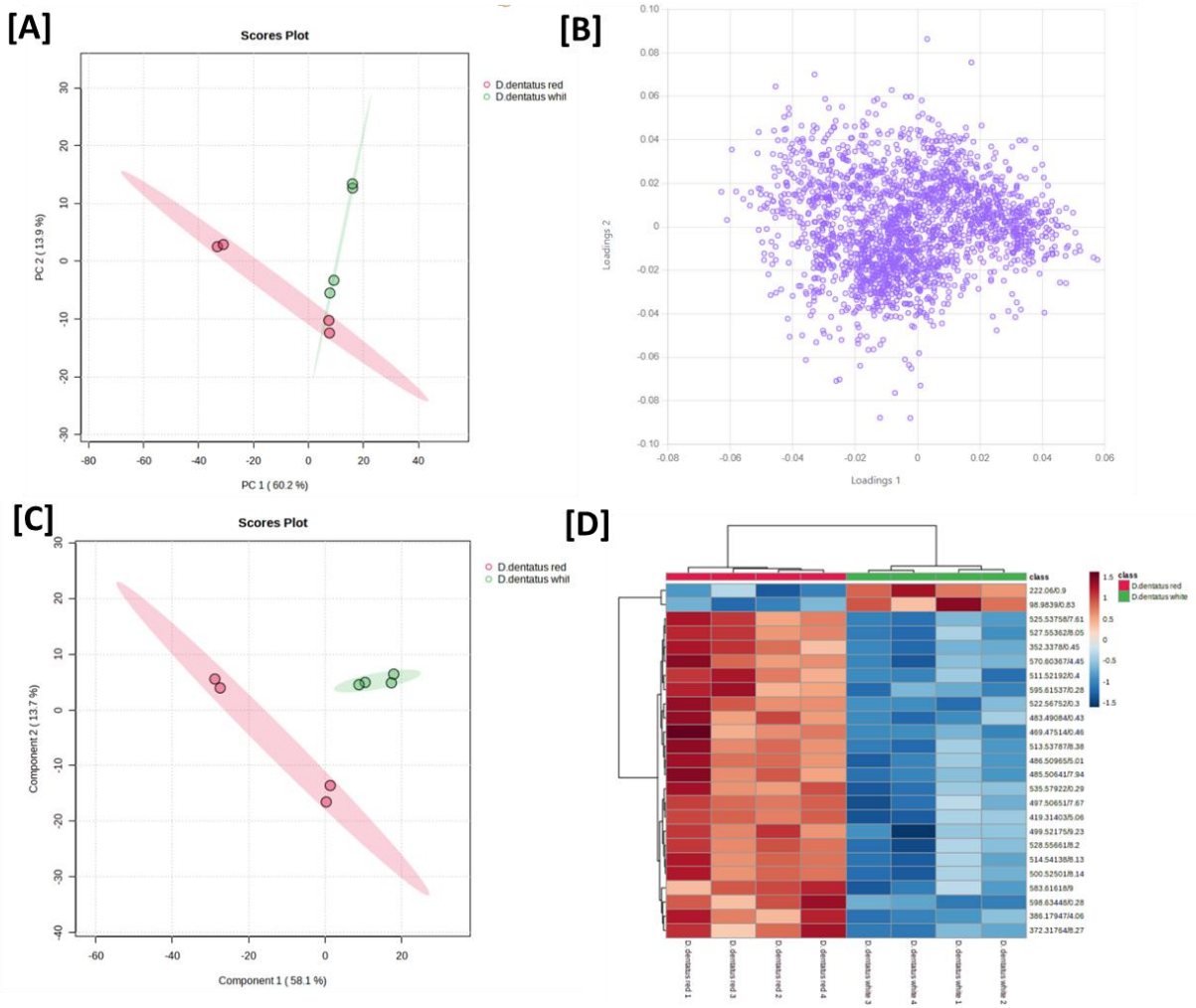

Figure 3. 6: (A) Principal component analysis score plot reflecting the visualization of the relationship among the samples in terms of groupings, trends, or outliers, and showing differences between *D. dentatus* red and white ecotypes along the x−axis (PC1) and y−axis (PC2) from positive ionization data. Principal components 1 and 2 explain 60.2% and 13.9% of the variance, respectively. (B) Loading plot describing the influence of variables on sample segregation. (C) Partial least-squares discriminant analysis (PLS-DA) was applied to differentiate between *D.*

dentatus red and white ecotypes. (D) Hierarchical cluster analysis (HCA), computed based on the top 25 statistically significantly different metabolite features, grouped the samples into two groups and by intensities. The colour scale indicates the relative intensity of each metabolite, and the colour-coded dendrogram on the top of the HCA plot indicates the relationship among the samples.

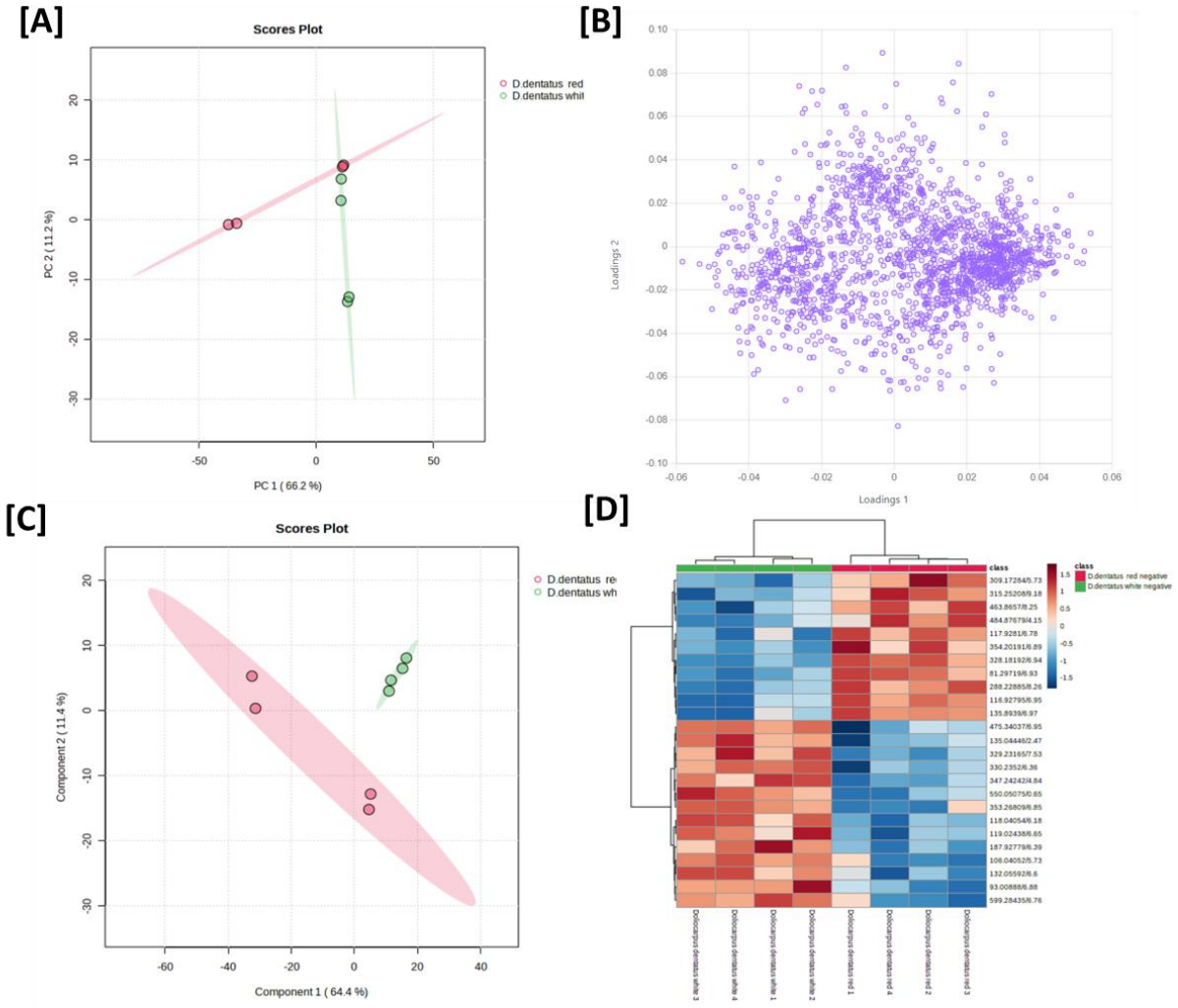

Figure 3. 7: (A) Principal component analysis score plot reflecting visualization of the relationship among the samples in terms of groupings, trends, or outliers, and showing differences between *D. dentatus* red and white ecotypes along the x−axis (PC1) and y−axis (PC2) from negative ionization data. Principal components 1 and 2 explain 66.2% and 11.2% of the variance, respectively. (B) Loading plot describing the influence of variables on sample segregation. (C) Partial least-squares discriminant analysis (PLS-DA) was applied to differentiate between *D. dentatus* red and white ecotypes. (D) Hierarchical cluster analysis (HCA), computed based on the top 25 statistically significantly different metabolite features, grouped the samples into two groups and by intensities.

The colour scale indicates the relative intensity of each metabolite, and the colour-coded dendrogram on the top of the HCA plot indicates the relationship among the samples.

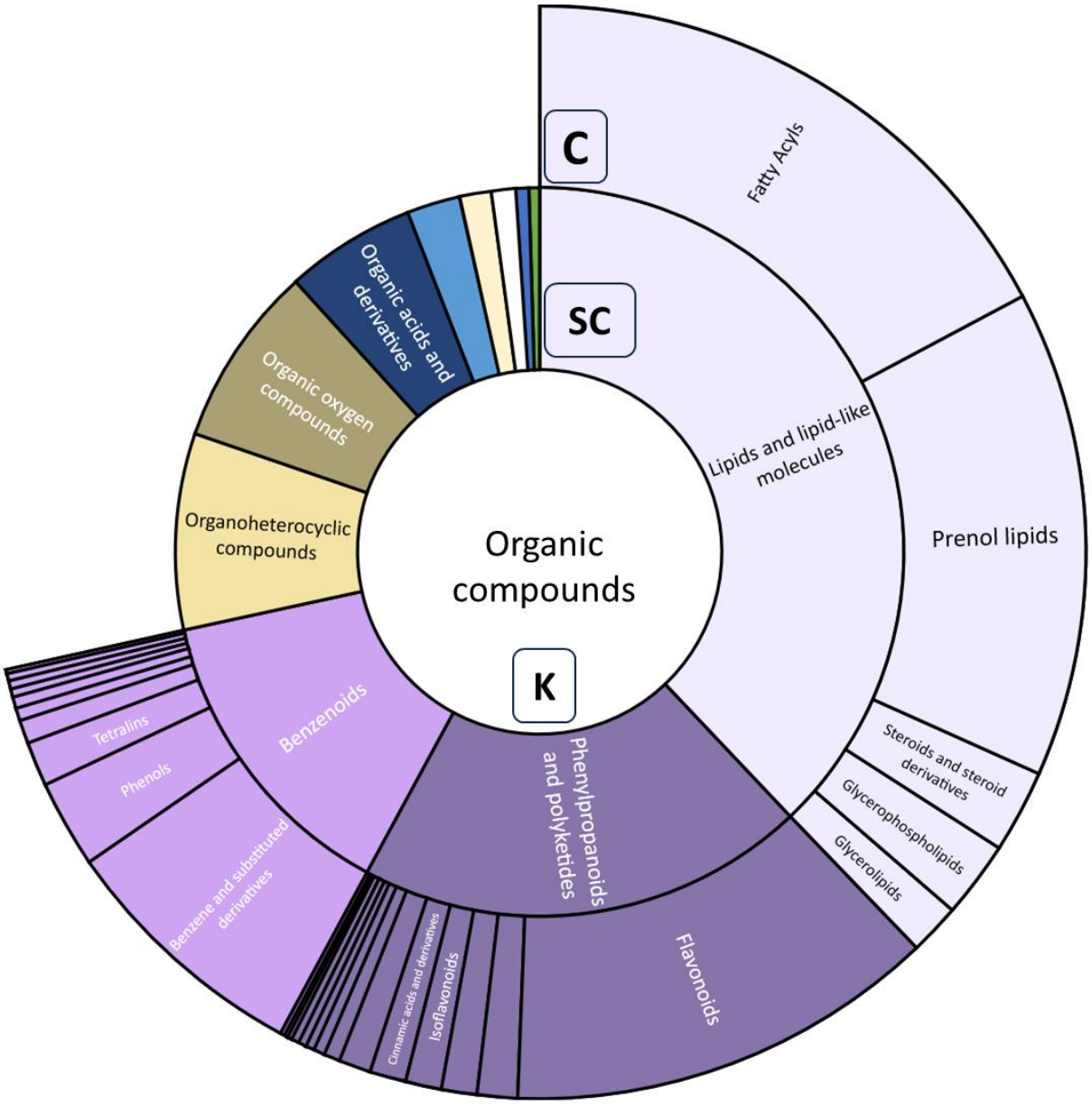

Figure 3. 8: Sunburst plot of the different class levels of the nodes annotated by ClassyFire by compounds from both positive and negative ionization modes from both red and white *D. dentatus* ecotypes. ClassyFire summarizes the compounds according to the kingdom level (K), superclass

level (SC), and class level (C). Benzenoid, phenylpropanoid, polyketide, and lipids and lipid-like molecule superclasses dominate in the contributions of annotated compounds.

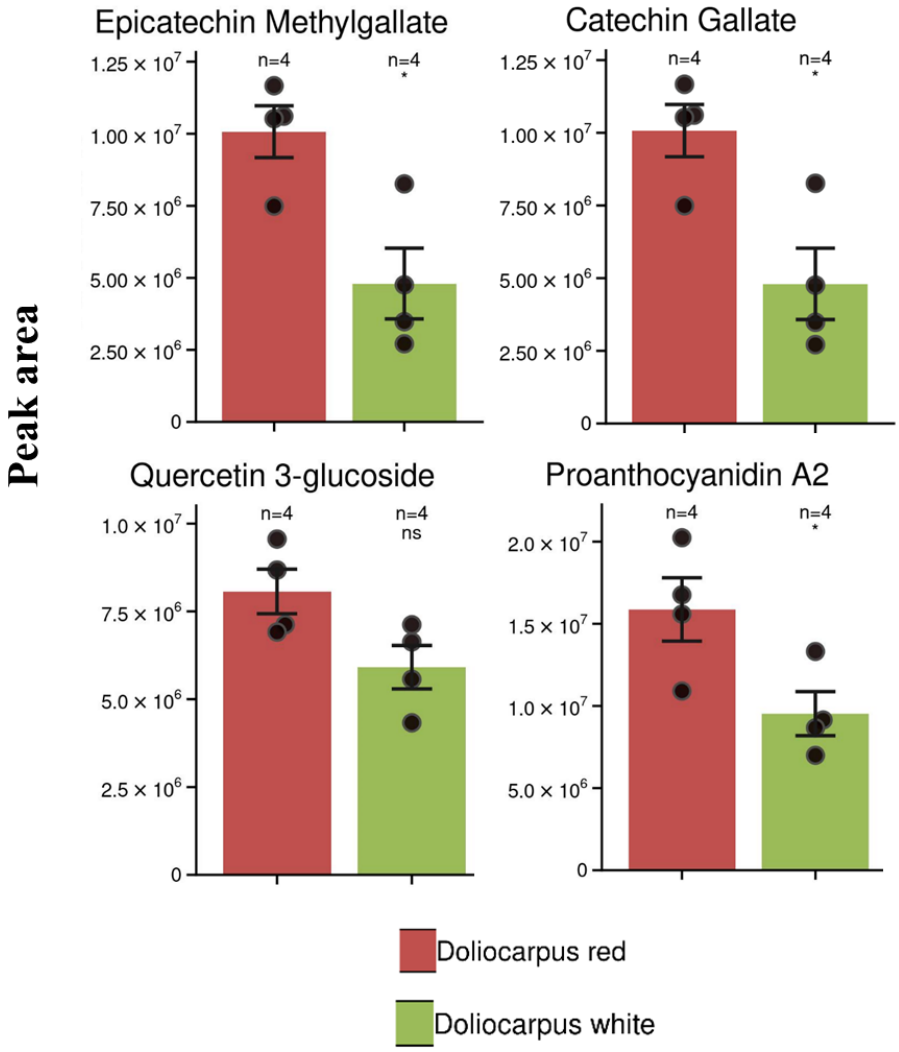

Figure 3. 9: Flavonoid biomarkers of *D. dentatus* red and white ecotypes normalized peak areas (mean ± SE) of the top metabolite features identified by PLS-DA. Within each metabolite, the intensity is dependent on the combination of ecotypes (ANOVA red ecotype × white ecotype (control interaction)): proanthocyanidin A2 $p < 0.04$, epicatechin methyl gallate $p < 0.015$, and catechin gallate $p < 0.015$. "*" and "ns" represent statistical significance and not significant, respectively.

3.3. DISCUSSION

The Orbitrap used in the present work has high resolving power and excellent mass accuracy, precise mass measurements and broad analyte coverage, providing greater confidence in identification, especially for complex matrices (Comtois-Marotte et al., 2017; Jia et al., 2014; Lanekoff et al., 2015; Matysik & Liebisch, 2017; Williamson et al., 2016). Moreover, the full scan mode allows the recording of unlimited compounds, which makes it feasible for the retrospective analysis of any potential compounds of interest. The Orbitrap HRMS can also reduce method cost and development time by not having to purchase multiple standards or in performing manual method set-up. To date, Orbitrap HRMS has been used extensively in mass spectrometry metabolomics base research for targeted and non-targeted analyses. However, LC-MS has some drawbacks, including high instrumentation costs, complex data analysis, time-consuming data processing, and challenges related to sample preparation and matrix effects. Therefore, metabolite annotation was performed by spectral library matching as a first step. Several candidates of *D. dentatus* red and white putative metabolites were then shortlisted. Those that showed identical names from KnapSack (Shinbo et al., 2006), KEGG (Kanehisa et al., 2019), Plant Metabolic Network using the PlantCyc database (https://plantcyc.org) (Hawkins et al., 2021), Metaboquest (Fan et al., 2020), SciFinder (Hounguè et al.) and PubChem (Kim et al., 2022), Global Nature Production Social Molecular Networking (GNPS), SIRIUS and MS Dial were used to query fragments for putative identification (Branquinho, Verdan, Santos, et al., 2021; Li et al., 2016). Afterwards, peak confirmation was done with Xcalibur 4.1 having a mass error of ± 10 ppm to

determine whether these metabolites are present in the methanol extracts of *D. dentatus* red and white ecotypes.

3.3.1. Untargeted Metabolomics Analysis Revealed Metabolites Present in Different Ecotypes of *Doliocarpus Dentatus*

Secondary metabolites comprise organic chemicals that plants, fungi, and microbes synthesize. These compounds play diverse roles in ecological and adaptive processes. Plants provide several ecological functions, including herbivore defence, pollinator attraction, and facilitation of environmental adaptations(Khammassi et al., 2022; Naczk & Shahidi, 2004). The secondary metabolites, including flavonoids, terpenoids, and alkaloids, possess significant value in traditional medicine., pharmaceuticals, perfumery, and flavouring.

The metabolites identified in the different *D. dentatus* ecotypes were diverse, with some reported to have therapeutic benefits due to their varied bioactivities. Using LC-MS/MS analysis, we found polyphenolic, terpenoid, and alkaloid metabolite classes, with polyphenols (flavonoids) being the most statistically significant and relatively abundant between the red and white ecotypes.

There was a statistically significant difference between the polyphenols in the *D. dentatus* red ecotype and the *D. dentatus* white ecotype (Figure 8). Flavonoids such as Epicatechin methyl gallate, Catechin gallate, and Proanthocyanidin A2 significantly differed in the *D. dentatus* red ecotype compared to the *D. dentatus* white ecotype - based on the integrated peak areas. Epicatechin methyl gallate, Catechin gallate, Proanthocyanidin A2 and Proanthocyanidin B2 isomers, Quercetin 3 glycoside, Apigenin, (+)-Catechin, Leucocyanidin, Anthocyanidin 3-O-beta-D-sambubioside, and Resveratrol, are different types of bioactive compounds commonly found in *D.dentatus* (see Tables 1 and 2 , Supplemental Tables 1 – 7). These compounds belong to other

classes of natural products and possess diverse biological activities. Epicatechin methyl gallate, a bioactive compound found in various plant sources, exhibits antioxidant and anti-inflammatory properties that have attracted significant scientific interest due to its potential health-promoting properties (Legeay et al., 2015). One of its notable benefits is its ability to reduce oxidative stress and inflammation in cells.

3.3.2. Flavonoids

Flavonoids are a class of secondary metabolites mainly composed of a benzopyrone ring that contains phenolic or polyphenolic groups at various locations(Cavalcante et al., 2018). The biosynthesis of phenols relies on two pathways: the shikimic acid pathway and the malonic acid pathway (de la Rosa et al., 2019; Mandal et al., 2010). These compounds are predominantly present in various botanical sources such as fruits, herbs, stems, grains, nuts, vegetables, flowers, and seeds (Feliciano et al., 2015; Shan et al., 2017). The therapeutic efficacy and biological activity of these various plant components are attributed to the presence of bioactive phytochemical substances. (Thilakarathna & Rupasinghe, 2013). Flavonoids may offer antioxidant, anti-inflammatory, anticancer, cardiovascular, and neuroprotective benefits (Patel et al., 2018), which may contribute to reducing several sexual dysfunctions such as low sexual desire, erectile dysfunction (ED), inability to achieve orgasm and premature ejaculation, which are relatively common in men even at a young age (Feldman et al., 2000; Gupta et al., 2011; Pallangyo et al., 2016; ROMEO et al., 2000; Selvin et al., 2007; Sipski & Alexander, 1997).

Moreover, research has indicated that incorporating better lifestyle behaviours might enhance erectile function. Specifically, implementing dietary modifications and the augmentation of nutritional antioxidant consumption appears to be the most encouraging and economically

viable strategies for addressing erectile dysfunction (ED) (Barassi et al., 2009; Wing et al., 2010). The consumption of several antioxidant-rich foods, such as pomegranate juice, coffee, wine, nuts, and ginseng, has been associated with lower ED prevalence (Dorrance et al., 2002; Forest et al., 2007; Jang et al., 2008; Lopez et al., 2015; Ramírez et al., 2016).

In general, it has been proposed that incorporating a healthy-style diet, which emphasizes consuming fruits and vegetables while limiting animal protein intake, can potentially improve symptoms of (ED). This dietary approach reduces glucose and lipid metabolism, enhances antioxidant defenses, and elevates arginine levels. Consequently, these effects contribute to increased nitric oxide (NO) activity, ultimately improving erectile function (Di Francesco & Tenaglia, 2017; Estruch et al., 2013; Urpi-Sarda et al., 2012; F. Wang et al., 2013).

The justification for employing antioxidants to mitigate symptoms of erectile dysfunction (ED) is derived from the discovery that ED frequently occurs before the manifestation of cardiovascular (CV) conditions. Antioxidant chemicals have gained recognition for their advantageous impact on mitigating cardiovascular risk, implying their potential to resolve symptoms of erectile dysfunction (Solomon et al., 2003).

Catechin gallate, found in *D.dentatus*, possesses intriguing properties that have attracted scientific attention (see Tables 1 and 2). Similar to other catechins, it exhibits antioxidant activity and potential health benefits. Its antioxidant properties help reduce oxidative stress and prevent chronic diseases associated with free radicals, such as cardiovascular disease (Miller et al., 2019; Y.-Q. Xu et al., 2021). Catechin gallate also exhibits anti-inflammatory effects, mitigating inflammation and potentially reducing the risk of chronic inflammatory diseases. Additionally, it may positively impact cardiovascular health by improving lipid profiles, lowering blood pressure,

and enhancing vascular function (Baranwal et al., 2022; Kim-Park et al., 2016; Oz, 2017). It has antioxidant properties, which help protect cells from damage caused by harmful bodily molecules such as Reactive Oxygen Species (ROS) including superoxide anion, hydroxyl radical, hydrogen peroxide, and peroxynitrite. (+)-Catechin may have several health benefits, including promoting cardiovascular health, reducing inflammation, and potentially aiding in weight management (Isemura, 2019; Kalender et al., 2002; Satoh et al., 2002).

Proanthocyanidin B2 is a specific type of proanthocyanidin, which is a type of flavonoid found in various plants. Proanthocyanidins are known for their antioxidant properties and are commonly found in foods like fruits, vegetables, nuts, seeds, and certain beverages such as red wine and tea (Hornedo-Ortega et al., 2020). Proanthocyanidin B2 has been studied for its potential health benefits. It exhibits antioxidant activity, helping to neutralize harmful free radicals in the body (Barbe et al., 2019). It also has anti-inflammatory properties, which may be beneficial in reducing inflammation-related conditions. Proanthocyanidin B2 may contribute to cardiovascular health by promoting healthy blood vessel function and reducing the risk of blood clot formation.

Additionally, it has been investigated for its potential anticancer properties, as it may help inhibit the growth of cancer cells (Lee et al., 2020). Proanthocyanidin A2 is a flavonoid subclass found in plants recognized for their antioxidant capabilities. It is generated by polymerizing flavan-3-ol monomers and is distinguished by its condensed tannin structure (Hornedo-Ortega et al., 2020). Proanthocyanidins, especially Proanthocyanidin A2, have been linked to various health benefits, including antioxidant activity, cardiovascular health, anti-inflammatory properties, skin health, and dental health (Rauf et al., 2019).

Proanthocyanidins can neutralize dangerous free radicals, promote healthy blood flow, lower blood pressure, and enhance lipid profiles. (Zhang et al., 2018). Quercetin 3-glucoside, also known as isoquercitrin, is a natural plant compound found in fruits, vegetables, and herbs (see Tables 1 and 2). It belongs to the glycoside class and has antioxidant properties that protect cells from free radical damage. Quercetin 3-glucoside also has anti-inflammatory effects, which may help reduce inflammation and manage inflammation-related conditions (Williamson et al., 1996; Zheng et al., 2017). It has been studied for its potential cardiovascular benefits, such as improving blood vessel function, lowering blood pressure, and inhibiting blood clot formation. Quercetin 3-glucoside also modulates the immune system, potentially supporting immune function and defense against infections (Bondonno et al., 2016). Its antioxidant and anti-inflammatory properties may promote healthy skin by protecting against oxidative stress and inflammation (Choi et al., 2012; Lesjak et al., 2018).

Apigenin is a natural flavonoid molecule in many plants with antioxidant, anti-inflammatory, and anticancer activities (Kim et al., 2003). Its prevalence in plant-based meals such as parsley, celery, and chamomile tea contributes to its potential health advantages (Patel et al., 2007). Apigenin is an antioxidant that neutralizes damaging free radicals and lowers oxidative stress associated with chronic illnesses such as cancer, cardiovascular disease, and neurological disorders (Kaur et al., 2008; Kim et al., 2003). It also contains anti-inflammatory qualities, which aid in lessening inflammation and discomfort. Apigenin has been found in studies to cause cell cycle arrest and death in cancer cells, potentially reducing their growth and spread (Kaur et al., 2008; Nicholas et al., 2007). Apigenin has been studied for its potential in cancer prevention and therapy, including applications in breast, colon, prostate, and lung malignancies. It has also been examined

for its potential to improve cardiovascular health, cognitive function, and immune system performance (Madunić et al., 2018; Rossi et al., 2008). Leucocyanidin is a bioactive compound in plants belonging to the flavan-3-ol flavonoids family. It has potent antioxidant capabilities that protect cells from oxidative damage (Tahirovic & Basic, 2017). Moreover, leucocyanidin has anti-inflammatory properties that may help minimize the risk of chronic inflammatory illnesses. It also benefits cardiovascular health by promoting healthy blood vessels and heart function (Augustine, 2019). While further study is needed, leucocyanidin's antioxidant, anti-inflammatory, and cardiovascular effects make it a promising molecule for overall well-being and disease prevention.

Anthocyanidin 3-O-beta-D-sambubioside is a unique anthocyanin pigment that contributes to the vibrant colors of fruits, vegetables, and flowers. Its attachment to beta-D-sambubioside makes it unique, contributing to the vibrant colors in plant-based foods and attracting pollinators for plant reproduction. Anthocyanidin 3-O-beta-D-sambubioside offers potential health benefits due to its antioxidant properties, which neutralize harmful free radicals in the body (Butu et al., 2014; de Pascual-Teresa et al., 2010; Raffa et al., 2017; Santos et al., 2021). These free radicals can cause cellular damage and contribute to chronic diseases like cardiovascular disease and cancer (Butu et al., 2014; Jiang et al., 2020). Additionally, research suggests that anthocyanidin 3-O-beta-D-sambubioside may have anti-inflammatory effects, modulating inflammatory responses and reducing the risk of chronic diseases (de Pascual-Teresa et al., 2010; Peng et al., 2022). The presence of anthocyanidin 3-O-beta-D-sambubioside in fruits and vegetables makes them visually appealing and potentially beneficial for health.

The bioactive compounds discussed previously, such as Epicatechin methyl gallate, Catechin gallate, (+)-Catechin, Proanthocyanidins, Quercetin 3-glucoside and Apigenin, offer various health

benefits, especially for ED due to their antioxidant and anti-inflammatory properties (Şahin et al., 2020). These compounds act as antioxidants, neutralizing harmful free radicals and reducing oxidative stress in cells, which helps protect against cellular damage and supports overall well-being. Additionally, they show potential in promoting cardiovascular health by improving lipid profiles, lowering blood pressure, and enhancing blood vessel function, which may reduce the risk of ED.

3.3.3. Alkaloids

Alkaloids are a class of organic molecules characterized by nitrogen atoms with elemental properties, often found in many organisms, including plants, fungi, and mammals. Alkaloids are a class of organic molecules characterized by the presence of nitrogen atoms, whose specific elemental properties play a crucial role in defining the chemistry and biological activity of these compounds. Nitrogen, as an element, typically forms three covalent bonds and possesses a lone pair of electrons, which imparts basicity to the molecule and allows it to participate in hydrogen bonding and other key interactions. These properties enable alkaloids to exhibit unique chemical reactivity and contribute to their wide range of pharmacological effects. Alkaloids are found in many organisms, including plants, fungi, and mammals, where they often serve important ecological and physiological functions (Bribi, 2018; Roy, 2017). The biosynthesis of alkaloids relies on the Shikimic acid and Malonic acid pathway(Damle et al., 2013; Hsu et al., 2015). These important secondary metabolites have been recognized for their medicinal potential(Ku et al., 2022). These compounds have been categorized into several groups based on their biosynthetic precursor and heterocyclic ring system. These groups include indole, piperidine, tropane, purine, pyrrolizidine, imidazole, quinolozidine, isoquinoline, and alkaloids (Vásquez et al., 2022).

Alkaloids may hinder the initiation of diverse degenerative ailments through their ability to scavenge free radicals or bind with catalysts involved in oxidative reactions (Laines-Hidalgo et al., 2022).

The secondary metabolites, such as Trigonelline, Xanthurenic acid, Thiazole, and Raphanin are all present in *D. dentatus,* of which their relative abundance is higher in the *D. dentatus* white ecotype. At the same time, 4 - Methylelletierine, N – Methylelletierine, Nicotinamide, Stachydrine and Acetylbrowniine were higher in the *D. dentatus* red ecotype (see Table 1 and 2).

Trigonelline exhibits antioxidant and anti-inflammatory properties and may aid blood sugar regulation and metabolic health (Khalili et al., 2018). Xanthurenic Acid is involved in amino acid metabolism and is linked to regulating insulin levels and glucose metabolism (Marie et al., 2016). Thiazole shows diverse biological activities and has garnered interest in medicinal chemistry (Gümüş et al., 2019). Methylelletierine and N-Methylelletierine possess anthelmintic properties, which are beneficial for combating parasitic infections. Nicotinamide and Stachydrine are associated with anti-hypertensive effects and affect blood pressure regulation (X.-R. Wang et al., 2018). Acetylbrowniine offers anti-inflammatory properties (J.-B. Xu et al., 2021), while rapanin, derived from radishes, has potential antioxidant and anticancer effects (Shuveksh et al., 2017). These compounds interact with biological systems in distinct ways, offering a range of potential health benefits, but further research is needed for a comprehensive understanding of their effects.

Secondary metabolites 4-Methylelletrine, N-Methylelletrine, Nicotinamide, Stachydrine, Trigonelline, and Acetylbrowniine have not been subjected to comprehensive investigations as potential therapeutic interventions for erectile dysfunction (ED). Although several compounds may possess features that might potentially impact aspects associated with ED, such as regulating

blood pressure, cardiovascular well-being, and blood sugar control, there is currently insufficient data to substantiate their efficacy as primary therapies for ED.

3.3.4. Terpenoids

Terpenoids are a large and diverse class of structurally secondary metabolites derived from five-carbon isoprene units naturally occurring in many plants (Ludwiczuk et al., 2017). The biosynthesis of the Mevalonic acid pathway relies on the Shikimic acid and Malonic acid pathway(Damle et al., 2013; Dewick, 2002; Hsu et al., 2015). Terpenoids differ due to their functional groups and C10-unit hydrocarbon backbone. These are further categorized based on the number of carbocyclic rings such as monoterpenes (limonene, carvone, (1R)-(-)-Nopol and carveol), diterpenes (the retinoids), and tetraterpenes (α - and β-carotene, lutein, lycopene, zeaxanthine, Betulinic Acid, Betulin and cryptoxanthine) (Christianson, 2017; Welling et al., 2016). These subclasses may have anti-inflammatory, anti-cancer, antioxidant, anti-inflammatory, and antimicrobial properties(Schmitz et al., 2022). Terpenoids are also essential for plant growth and development, impart flavour, aroma, and colour to plants' foliage, flowers, and fruits (Ge et al., 2022; Jafari, 2022) and defend them against insects, herbivores, and fungal diseases (Mithöfer & Boland, 2012).

Secondary metabolites such as alpha-Pinene, Ascaridole, (1R)-(-)-Nopol, 3-(beta-D-glucopyranosyloxy)-2-methyl-4H-Pyran-4-one, 4-(2,6,6-trimethyl-2-cyclohexen-1-yl)- 2-Butanone, Farnesol, Betulinic acid, Betulonic acid, Sumaresinolic acid, Betulin and Saikogenin D are all present in *D. dentatus,* of which their relative abundance is comparable between *D. dentatus* red and white ecotypes (see Tables 1 and 2 and Supplemental tables 1 - 7).

These compounds have diverse bioactive characteristics, from their potential use in medicine to their role as natural antibacterial agents, antioxidants, and enhancers of olfactory and gustatory sensations. Nevertheless, it is imperative to highlight that the precise bioactivities and possible health advantages of these compounds are now being investigated, and their efficacy may differ based on the particular circumstances in which they are utilized, thus requiring additional investigation.

The current body of research on the influence of terpenoids on ED is still constrained. However, it is important to highlight that terpenoids, naturally present in various plants, can indirectly impact aspects related to ED. Terpenoids with anti-inflammatory and antioxidant characteristics have promising potential in enhancing vascular health and mitigating oxidative stress, pertinent factors in (ED). Specific terpenoids have the potential to facilitate vasodilation, which can enhance blood circulation and thus have an indirect impact on improving erectile function(Olabiyi & de Castro Brás, 2023). Moreover, several terpenoids, recognized for their anxiolytic and stress-alleviating properties, can alleviate psychological elements contributing to ED. Additional investigation is necessary to clarify the exact processes and effectiveness of terpenoids in managing ED, considering their significant potential in treating this complex ailment.

3.3.5. Therapeutic Compounds and Possible Synergistic Effects

The compounds discussed in this research demonstrate many synergistic interactions, particularly in the domains of fragrance, possible therapeutic effects, and anti-cancer capabilities(Borges et al., 2019). The combination of Alpha-Pinene and (1R)-(-)-Nopol in essential oils creates pleasant scents that contribute to the overall olfactory attractiveness of these oils. The

potential exists for a synergistic interaction between farnesol and Saikikogenin D, resulting in enhanced anti-inflammatory and antibacterial activities, hence increasing their therapeutic efficacy(Joo & Jetten, 2010). In the context of anticancer activities, it has been shown that compounds such as Betulin, Betulonic Acid, Betulinic Acid, and Sumaresinolic Acid may potentially collaborate to produce favourable outcomes. The degree of synergy between 3-(beta-D-glucopyranosyloxy)-2-methyl-4H-Pyran-4-one and 4-(2,6,6-trimethyl-2-cyclohexen-1-yl)-2-Butanone is contingent upon the specific applications in which they are utilized(Xiao et al., 2022).

In the domain of (ED), secondary metabolites such as flavonoids, alkaloids, terpenoids and other phytochemicals in whole plant extracts have been observed to facilitate favourable interactions, presenting potential advantages(Durak et al., 2014). These interactions may augment blood circulation, mitigate inflammation, and increase vascular and sexual well-being. Research has shown that Green tea polyphenols, particularly epigallocatechin gallate (EGCG), have antioxidant properties that may reduce oxidative stress in the body, which is known to contribute to blood vessel damage and impaired blood flow, factors often linked to ED (Legeay et al., 2015). Yohimbine is an alkaloid found in yohimbe bark, and it's known to have vasodilatory effects, which means it can relax and widen blood vessels, improving blood circulation. In the context of ED, increased blood flow to the penis is essential for achieving and maintaining an erection (Drevin et al., 2020). Ginseng contains various terpenoids that may enhance nitric oxide production. Nitric oxide is a signaling molecule that plays a crucial role in dilating blood vessels and promoting blood flow to the penis, which may improve erectile function (Di Francesco & Tenaglia, 2017; Estruch et al., 2013; Urpi-Sarda et al., 2012; F. Wang et al., 2013).

The synergistic effects of polyphenol-rich extracts derived from sources such as green tea, dark chocolate and berries, alkaloids present in yohimbine and ginseng, and terpenoids sourced from herbs like ginkgo biloba and ginseng may potentially collaborate to enhance blood circulation, induce vasodilation, and augment nitric oxide synthesis, thereby potentially contributing to the amelioration of erectile dysfunction(HemaIswarya & Doble, 2006; Liu, 2003, 2004).

Moreover, the aforementioned phytochemical interactions have the potential to offer antioxidant assistance, hence mitigating the detrimental effects of oxidative stress on blood vessels and the consequential impairment of erectile function. The potential enhancement of sexual health and alleviation of symptoms related to ED can be achieved through the synergistic actions of polyphenols, alkaloids, and terpenoids derived from various sources.

Reactive Oxygen Species (ROS) play important roles in various diseases, including cancer, obesity, and ED (Fernández-Sánchez et al., 2011; Raj et al., 2011; Silva et al., 2014). ROS can negatively impact the function of blood vessels in the penis, leading to vascular dysfunction. Excessive ROS levels can cause oxidative damage to the endothelial cells that line the blood vessels, reducing their ability to produce and release nitric oxide (NO). NO plays a crucial role in vasodilation, essential for achieving and maintaining an erection (Lim & Park, 2014). ROS-induced endothelial dysfunction reduces NO bioavailability, resulting in inadequate blood flow to the penile tissues and erectile dysfunction (Rodriguez-Porcel et al., 2017; Sena et al., 2013).

Moreover, ROS can directly interact with and deactivate NO, further exacerbating the impairment of NO signaling in erectile function (Judkins et al., 2010). NO is a vital signaling molecule that induces smooth muscle relaxation in the penile tissue, facilitating the dilation of

blood vessels and the influx of blood necessary for an erection (Ieda et al., 2020). Increased ROS production can lead to the formation of reactive nitrogen species (RNS), which react with NO to create peroxynitrite, a highly reactive compound that impairs NO-mediated vasodilation (Ieda et al., 2020).

The penile tissue is susceptible to oxidative damage caused by ROS. Excessive ROS levels induce oxidative stress, leading to lipid peroxidation, protein oxidation, and DNA damage within penile cells. These harmful effects disrupt the normal cellular function and integrity of the penile tissue, impairing its ability to achieve and sustain an erection (Chakraborty & Roychoudhury, 2022). Furthermore, ROS-induced oxidative stress can trigger inflammatory responses in the penile tissue. Chronic inflammation can activate fibroblasts and promote the deposition of extracellular matrix proteins, leading to fibrosis (Zhou et al., 2021). Penile fibrosis involves an excessive accumulation of collagen and other fibrous components, resulting in structural changes and stiffness of the erectile tissue, further contributing to erectile dysfunction (Yu et al., 2021).

The detrimental effects of ROS-induced damage on erectile function are multifaceted. Excessive ROS production can impair vascular function, disrupt NO signaling, cause oxidative tissue damage, promote inflammation and fibrosis, and contribute to age-related erectile dysfunction. Understanding the mechanisms through which ROS influence's erectile function can guide the development of therapeutic strategies to mitigate oxidative stress and preserve erectile health. However, further research is needed to understand their effects and specific applications fully.

Plants exhibit an impressive capacity for synthesizing a wide array of organic compounds. Upon conducting LC-MS/MS analysis on Guyana Capadulla ecotypes, we identified a diverse

range of secondary metabolites such as alkaloids, terpenoids, fatty acids, phenylpropanoids, organic acid, polyketides and gallotannins, lignans and flavonoids. These organic compounds are believed to have evolved as a part of plant defense mechanisms against various environmental challenges, including pests, diseases, and droughts (Dixon, 2001). Notably, among the identified metabolites that were found in both ecotypes in more than one sample were, Salsolinol (alkaloid), Lutein (carotenoids), and lyoniside (lignans - iridoid glycosides) (Tables 4 – 6). Salsolinol, found in Guyanese Capadulla, is a natural compound in the isoquinoline alkaloid class that is the combination of dopamine and acetaldehyde (Kurnik-Łucka et al., 2018). Research has focused on its effects on addiction and reward pathways in the brain, particularly its role in reinforcing drug-seeking behavior and addiction to substances like alcohol, nicotine, and opioids (Melis et al., 2015). Salsolinol's interactions with neurotransmitter systems in the brain may contribute to the pleasurable effects of drugs and the development of addictive behaviors. Additionally, it has been studied for potential neurotoxic effects, leading to oxidative stress and damage to neurons, which could be relevant to neurodegenerative diseases (Kurnik-Łucka et al., 2018). However, further research is needed to understand its mechanisms and potential therapeutic applications fully.

In particular, green leafy vegetables like spinach, kale, and broccoli contain lutein, a naturally occurring carotenoid pigment (Wallace et al., 2020). It is an effective antioxidant that protects cells from the damage caused by risky free radicals, which can result in chronic diseases and aging (Alves-Rodrigues & Shao, 2004). Because it is a vital component of the macular pigment, which serves as the macula's protective layer, lutein is also crucial for maintaining eye health. This pigment protects retinal tissues from ultraviolet and high-energy blue light damage, reducing the risk of age-related macular degeneration (AMD) and cataracts. A diet high in lutein

may be linked to better cognitive performance and a lower risk of cognitive decline in older people, according to some research on the possible effects of lutein on cognitive function (Johnson, 2014). To conclusively link lutein intake and cognitive health, additional research is necessary. A diet high in fruits and vegetables, primarily those high in lutein, can support general health and the maintenance of healthy eyes.

Specific plant sources contained a naturally occurring flavonoid glycoside called lyoniside, which has potent anti-inflammatory and antioxidant properties (Chen, 2017) and was putatively identified in Guyanese Capadulla. It functions as an antioxidant to protect cells from the damage of harmful free radicals, which can accelerate aging and lead to chronic diseases. Furthermore, lyoniside has demonstrated potential as a neuroprotective compound, protecting neurons and promoting brain health (Lee et al., 2015). Although lyoniside research is still in its early stages, its novel findings indicate that it has a high potential for therapeutic use, particularly in treating inflammatory and oxidative stress-related diseases.

3.3.6. Several Metabolites Are Ecotype Specific

We described ecotype-specific metabolites as those present in only one ecotype (Supplemental Tables 2- 3).

For instance, (-)-Epigallocatechin, Anthocyanidin 3-O-beta-D-sambubioside and Naringenin (Supplemental Tables 2), which were present only in *D. dentatus* red ecotype, are three bioactive compounds with significant potential in various fields. Epigallocatechin, found in green tea, exhibits antioxidant and anti-inflammatory properties, contributing to its health benefits (Tang et al., 2021). Anthocyanidin 3-O-beta-D-sambubioside, a plant flavonoid, offers antioxidant and

anticancer properties, potentially aiding disease prevention (Wu et al., 2021). Naringenin, commonly found in citrus fruits, has anti-inflammatory and cardiovascular health-promoting effects, making it valuable for overall well-being (Onakpoya et al., 2017; Reshef et al., 2005). These compounds hold promise for further research and applications in medicine, nutrition, and functional foods.

Quercetin and myricetin, present only in *D. dentatus* white ecotype, are two flavonoids renowned for their high bioactive characteristics and multiple health benefits (Flores & Ruiz del Castillo, 2015). Quercetin is present in various fruits and vegetables, including apples, onions, and berries, and is known for its antioxidant, anti-inflammatory, and immune-modulating properties. It has been examined for its ability to lessen the risk of chronic illnesses and improve heart health (Nishimuro et al., 2015). For instance, a comprehensive revealed that quercetin displayed remarkable antioxidant activity in human blood plasma, effectively neutralizing harmful free radicals. Furthermore, a study conducted on rats demonstrated that quercetin had anti-inflammatory properties by inhibiting the production of pro-inflammatory molecules like tumor necrosis factor-alpha (TNF-α) and interleukin-6 (IL-6), leading to a reduction in symptoms associated with inflammatory diseases (Kobori et al., 2016; Mamani-Matsuda et al., 2006). These scientific findings provide compelling evidence supporting the potential health benefits of quercetin and its significance as a valuable dietary component.

Myricetin, on the other hand, is found in foods like berries, grapes, and tea and has comparable antioxidant and anti-inflammatory qualities. Myricetin may have neuroprotective and anticancer properties, according to research. These adaptable flavonoids are gaining attention in scientific studies as vital components of a balanced diet and possible medicinal possibilities

(Maurya et al., 2016). For instance, research has revealed that a diet abundant in berries, grapes, and tea, rich sources of myricetin, can lower the risk of neurodegenerative diseases like Alzheimer's disease (Kimura et al., 2021). Moreover, studies have indicated that myricetin can impede the growth of cancer cells and trigger apoptosis, suggesting its potential as a prospective candidate for upcoming cancer treatments (Agraharam et al., 2022).

Vendors of natural products in Guyana (known as herbalists colloquially) can use this information on ecotype-specific metabolites; by leveraging evidence-based research, herbalists can enhance their practices in selecting, preparing, dosing, and utilizing plant materials for medicinal purposes. Scientific insights aid in proper ecotype selection, ensuring authenticity and quality. Herbalists can adopt standardized preparation methods and understand the mechanisms of action of medicinal plants. Moreover, scientific knowledge guides dosage recommendations, identifies potential interactions, and helps in monitoring treatment effectiveness. By sharing evidence-based information, herbalists can educate patients and contribute to research, leading to safer and more effective herbal medicine practices.

3.4. CONCLUSION

The present study aimed to analyze the phytochemical profiles of *D. dentatus* ecotypes using untargeted and semi-targeted plant metabolomics, employing liquid chromatography in conjunction with electrospray ionization mass spectrometry. Our findings highlight the presence of the diverse bioactive compounds in *D. dentatus* ecotypes, including polyphenolic compounds, such as epicatechin methyl gallate, catechin gallate, proanthocyanidin A2 and proanthocyanidin B2 isomers, quercetin 3 glycoside, apigenin, (+)-Catechin, leucocyanidin, anthocyanidin 3-O-beta-

D-sambubioside, and resveratrol. These compounds exhibited diverse beneficial biological activities. While this study primarily focused on metabolomics, our future investigations will include antioxidant assays. Antioxidant assays and analyses are integral in comprehending the intricate mechanisms that shield organisms from oxidative stress. These assays thoroughly examine compounds and substances, assessing their potential to counteract the harmful impacts of free radicals and reactive oxygen species. By conducting these assays, the researchers can amass the critical data regarding the efficacy of different antioxidants in mitigating oxidative stress. Using other solvents for metabolite extraction, isolating key therapeutic compounds of interest with confirmation using nuclear magnetic resonance, and testing for bioactivity on select cell lines are potential avenues for future research. This research may provide invaluable insights into the potential interventions and treatments for conditions linked to oxidative stress, encompassing cardiovascular disease, erectile dysfunction, and cancer.

Author Contributions: Conceptualization, E.S., S.S.N. and R.N.E.; methodology, E.S.; formal analysis, E.S.; investigation, E.S.; resources, S.S.N. and R.N.E.; data curation, E.S. and A.L.; writing—original draft preparation, E.S.; writing—review and editing, A.L., S.S.N. and R.N.E.; supervision, S.S.N. and R.N.E.; funding acquisition, R.N.E. All authors have read and agreed to the published version of the manuscript.

Funding: Funding was through the Sustainable Guyana Program, a partnership between Trent University and the University of Guyana funded by CGX Energy Inc. and Frontera Energy Corporation.

Institutional Review Board Statement: Not applicable.

3.5. REFERENCE

Agraharam, G., Girigoswami, A., & Girigoswami, K. (2022). Myricetin: a multifunctional flavonol in biomedicine. *Current Pharmacology Reports*, 1-14.

Alves-Rodrigues, A., & Shao, A. (2004). The science behind lutein. *Toxicology Letters*, *150*(1), 57-83. https://doi.org/https://doi.org/10.1016/j.toxlet.2003.10.031

Andel, T. V., & Banki, O. (2003). Commercial Non Timber Forest Products of the Guiana Shields Commercial Non-Timber Forest Products of the Guiana Shield An inventory of commercial NTFP extration and possibilities for. (January 2003), 128-128.

Andel, T. v., MacKinven, A., & Bánki, O. (2003). *Commercial non-timber forest products of the Guiana shield: an inventory of commercial NTFP extraction and possibilities for sustainable harvesting*. Netherlands Committee for IUCN.

Aponte, J. C., Vaisberg, A. J., Rojas, R., Caviedes, L., Lewis, W. H., Lamas, G., Sarasara, C., Gilman, R. H., & Hammond, G. B. (2008). Isolation of cytotoxic metabolites from targeted peruvian amazonian medicinal plants. *Journal of Natural Products*, *71*(1), 102-105. https://doi.org/10.1021/np070560c

Augustine, C. (2019). Unravelling the competence of leucocyanidin in free radical scavenging: a theoretical approach based on electronic structure calculations. *Journal of Structural Chemistry*, *60*, 198-209.

Baranwal, A., Aggarwal, P., Rai, A., & Kumar, N. (2022). Pharmacological actions and underlying mechanisms of catechin: A review. *Mini Reviews in Medicinal Chemistry*, *22*(5), 821-833.

Barassi, A., Colpi, G. M., Piediferro, G., Dogliotti, G., Melzi D'Eril, G. V., & Corsi, M. M. (2009). Oxidative stress and antioxidant status in patients with erectile dysfunction. *The journal of sexual medicine*, *6*(10), 2820-2825.

Barbe, A., Ramé, C., Mellouk, N., Estienne, A., Bongrani, A., Brossaud, A., Riva, A., Guérif, F., Froment, P., & Dupont, J. (2019). Effects of grape seed extract and proanthocyanidin B2 on in vitro proliferation, viability, steroidogenesis, oxidative stress, and cell signaling in human granulosa cells. *International journal of molecular sciences*, *20*(17), 4215.

Bartel, J., Krumsiek, J., & Theis, F. J. (2013). Statistical methods for the analysis of high-throughput metabolomics data. *Computational and structural biotechnology journal*, *4*(5), e201301009.

Bhatia, H., Sharma, Y. P., Manhas, R. K., & Kumar, K. (2014). Ethnomedicinal plants used by the villagers of district Udhampur, J&K, India. *Journal of Ethnopharmacology*, *151*(2), 1005-1018. https://doi.org/10.1016/j.jep.2013.12.017

Blaise, B. J., Correia, G. D., Haggart, G. A., Surowiec, I., Sands, C., Lewis, M. R., Pearce, J. T., Trygg, J., Nicholson, J. K., & Holmes, E. (2021). Statistical analysis in metabolic phenotyping. *Nature Protocols*, *16*(9), 4299-4326.

Blatt-Janmaat, K., Neumann, S., Schmidt, F., Ziegler, J., Qu, Y., & Peters, K. (2023). Impact of in vitro phytohormone treatments on the metabolome of the leafy liverwort Radula complanata (L.) Dumort. *Metabolomics*, *19*(3), 17. https://doi.org/10.1007/s11306-023-01979-y

Blatt-Janmaat, K. L., Neumann, S., Ziegler, J., & Peters, K. (2023). Host Tree and Geography Induce Metabolic Shifts in the Epiphytic Liverwort Radula complanata. *Plants (Basel)*, *12*(3). https://doi.org/10.3390/plants12030571

Böckel, A., Hörisch, J., & Tenner, I. (2021). A systematic literature review of crowdfunding and sustainability: highlighting what really matters. *Management review quarterly*, *71*, 433-453.

Bondonno, N. P., Bondonno, C. P., Rich, L., Mas, E., Shinde, S., Ward, N. C., Hodgson, J. M., & Croft, K. D. (2016). Acute effects of quercetin-3-O-glucoside on endothelial function and blood pressure: a randomized dose-response study. *The American journal of clinical nutrition*, *104*(1), 97-103. https://doi.org/10.3945/ajcn.116.131268

Borges, R. S., Ortiz, B. L. S., Pereira, A. C. M., Keita, H., & Carvalho, J. C. T. (2019). Rosmarinus officinalis essential oil: A review of its phytochemistry, anti-inflammatory activity, and mechanisms of action involved. *Journal of Ethnopharmacology*, *229*, 29-45.

Branquinho, L. S., Verdan, M. H., dos Santos, E., Macorini, L. F. B., Maris, R. S., Kuraoka-Oliveira, A. M., Bacha, F. B., Cardoso, C. A. L., Arena, A. C., Silva-Filho, S. E., & Kassuya, C. A. L. (2021). Toxicological evaluation of ethanolic extract of leaves from Doliocarpus dentatus in Swiss mice. *Drug and Chemical Toxicology*, *0*(0), 1-7. https://doi.org/10.1080/01480545.2021.1982638

Branquinho, L. S., Verdan, M. H., Dos Santos, E., Macorini, L. F. B., Maris, R. S., Kuraoka-Oliveira, A. M., Bacha, F. B., Cardoso, C. A. L., Arena, A. C., Silva-Filho, S. E., & Kassuya, C. A. L. (2021). Toxicological evaluation of ethanolic extract of leaves from Doliocarpus dentatus in Swiss mice. *Drug Chem Toxicol*, 1-7. https://doi.org/10.1080/01480545.2021.1982638

Branquinho, L. S., Verdan, M. H., Santos, E. D., Neves, S. C. D., Oliveira, R. J., Cardoso, C. A. L., & Kassuya, C. A. L. (2021). Aqueous extract from leaves of Doliocarpus dentatus (Aubl.) Standl. relieves pain without genotoxicity activity. *J Ethnopharmacol*, *266*, 113440. https://doi.org/10.1016/j.jep.2020.113440

Branquinho, L. S., Verdan, M. H., Santos, E. d., Neves, S. C. d., Oliveira, R. J., Cardoso, C. A. L., & Kassuya, C. A. L. (2021). Aqueous extract from leaves of Doliocarpus dentatus (Aubl.) Standl. relieves pain without genotoxicity activity. *Journal of Ethnopharmacology*, *266*(September 2020). https://doi.org/10.1016/j.jep.2020.113440

Bribi, N. (2018). Pharmacological activity of alkaloids: a review. *Asian journal of botany*, *1*(1), 1-6.

Butu, M., Rodino, S., Butu, A., & Butnariu, M. (2014). SCREENING OF BIOFLAVONOID AND ANTIOXIDANT ACTIVITY OF LENS CULINARIS MEDIKUS. *Digest Journal of Nanomaterials & Biostructures (DJNB)*, *9*(2).

Cambiaghi, A., Ferrario, M., & Masseroli, M. (2017). Analysis of metabolomic data: tools, current strategies and future challenges for omics data integration. *Briefings in bioinformatics*, *18*(3), 498-510.

Castilla, G., Hall, R. J., Skakun, R., Filiatrault, M., Beaudoin, A., Gartrell, M., Smith, L., Groenewegen, K., Hopkinson, C., & van der Sluijs, J. (2022). The Multisource Vegetation Inventory (MVI): A Satellite-Based Forest Inventory for the Northwest Territories Taiga Plains. *Remote Sensing*, *14*(5), 1108.

Cavalcante, G., da Silva Cabral, A., & Silva, C. (2018). Leishmanicidal Activity of Flavonoids Natural and Synthetic: A Minireview. *Mintage J. Pharm. Med. Sci*, *7*(1), 25-34.

Chakraborty, S., & Roychoudhury, S. (2022). Pathological roles of reactive oxygen species in male reproduction. In *Oxidative Stress and Toxicity in Reproductive Biology and Medicine: A Comprehensive Update on Male Infertility-Volume One* (pp. 41-62). Springer.

Chambers, M. C., Maclean, B., Burke, R., Amodei, D., Ruderman, D. L., Neumann, S., Gatto, L., Fischer, B., Pratt, B., & Egertson, J. (2012). A cross-platform toolkit for mass spectrometry and proteomics. *Nature biotechnology*, *30*(10), 918-920.

Chen, W. (2017). Chemical constituents from Illicium brevistylum and their anti-inflammatory activities. *Chinese Traditional Patent Medicine*, 2081-2085.

Choi, S.-J., Tai, B. H., Cuong, N. M., Kim, Y.-H., & Jang, H.-D. (2012). Antioxidative and anti-inflammatory effect of quercetin and its glycosides isolated from mampat (Cratoxylum formosum). *Food Science and biotechnology*, *21*, 587-595.

Choi, S. Y., Park, J., Kim, J., Lee, J., & Yang, H. (2021). Investigation of Chemical Profiles of Different Parts of Morus alba Using a Combination of Molecular Networking Methods with Mass Spectral Data from Two Ionization Modes of LC/MS. *Plants (Basel)*, *10*(8). https://doi.org/10.3390/plants10081711

Chong, J., Wishart, D. S., & Xia, J. (2019). Using MetaboAnalyst 4.0 for comprehensive and integrative metabolomics data analysis. *Current protocols in bioinformatics*, *68*(1), e86.

Christianson, D. W. (2017). Structural and chemical biology of terpenoid cyclases. *Chemical reviews*, *117*(17), 11570-11648.

Comtois-Marotte, S., Chappuis, T., Duy, S. V., Gilbert, N., Lajeunesse, A., Taktek, S., Desrosiers, M., Veilleux, É., & Sauvé, S. (2017). Analysis of emerging contaminants in water and solid samples using high resolution mass spectrometry with a Q Exactive orbital ion trap and estrogenic activity with YES-assay. *Chemosphere*, *166*, 400-411.

da Silva, R. R., Wang, M., Nothias, L. F., van der Hooft, J. J. J., Caraballo-Rodriguez, A. M., Fox, E., Balunas, M. J., Klassen, J. L., Lopes, N. P., & Dorrestein, P. C. (2018). Propagating annotations of molecular networks using in silico fragmentation. *PLoS Comput Biol*, *14*(4), e1006089. https://doi.org/10.1371/journal.pcbi.1006089

Damle, A. A., Pawar, Y. P., & Narkar, A. A. (2013). Anticancer activity of betulinic acid on MCF-7 tumors in nude mice.

de la Rosa, L. A., Moreno-Escamilla, J. O., Rodrigo-García, J., & Alvarez-Parrilla, E. (2019). Chapter 12 - Phenolic Compounds. In E. M. Yahia (Ed.), *Postharvest Physiology and Biochemistry of Fruits and Vegetables* (pp. 253-271). Woodhead Publishing. https://doi.org/https://doi.org/10.1016/B978-0-12-813278-4.00012-9

de Pascual-Teresa, S., Moreno, D. A., & García-Viguera, C. (2010). Flavanols and anthocyanins in cardiovascular health: a review of current evidence. *International journal of molecular sciences*, *11*(4), 1679-1703.

Dewick, P. M. (2002). *Medicinal natural products: a biosynthetic approach*. John Wiley & Sons.

Di Francesco, S., & Tenaglia, R. L. (2017). Mediterranean diet and erectile dysfunction: a current perspective. *Central European journal of urology*, *70*(2), 185.

Dias, D. A., Urban, S., & Roessner, U. (2012). A historical overview of natural products in drug discovery. *Metabolites*, *2*(2), 303-336.

Dixon, R. A. (2001). Natural products and plant disease resistance. *Nature*, *411*(6839), 843-847.

Djoumbou Feunang, Y., Eisner, R., Knox, C., Chepelev, L., Hastings, J., Owen, G., Fahy, E., Steinbeck, C., Subramanian, S., Bolton, E., Greiner, R., & Wishart, D. S. (2016). ClassyFire: automated chemical classification with a comprehensive, computable taxonomy. *J Cheminform*, *8*, 61. https://doi.org/10.1186/s13321-016-0174-y

Dorrance, A., Lewis, R. W., & Mills, T. (2002). Captopril treatment reverses erectile dysfunction in male stroke prone spontaneously hypertensive rats. *International Journal of Impotence Research*, *14*(6), 494-497.

Drevin, G., Palayer, M., Compagnon, P., Zabet, D., Jousset, N., Briet, M., & Abbara, C. (2020). A fatal case report of acute yohimbine intoxication. *Forensic Toxicology*, *38*, 287-291.

Duhrkop, K., Fleischauer, M., Ludwig, M., Aksenov, A. A., Melnik, A. V., Meusel, M., Dorrestein, P. C., Rousu, J., & Bocker, S. (2019). SIRIUS 4: a rapid tool for turning tandem mass spectra into metabolite structure information. *Nat Methods*, *16*(4), 299-302. https://doi.org/10.1038/s41592-019-0344-8

Duhrkop, K., Nothias, L. F., Fleischauer, M., Reher, R., Ludwig, M., Hoffmann, M. A., Petras, D., Gerwick, W. H., Rousu, J., Dorrestein, P. C., & Bocker, S. (2021). Systematic classification of unknown metabolites using high-resolution fragmentation mass spectra. *Nat Biotechnol*, *39*(4), 462-471. https://doi.org/10.1038/s41587-020-0740-8

Duhrkop, K., Shen, H., Meusel, M., Rousu, J., & Bocker, S. (2015). Searching molecular structure databases with tandem mass spectra using CSI:FingerID. *Proc Natl Acad Sci U S A*, *112*(41), 12580-12585. https://doi.org/10.1073/pnas.1509788112

Durak, A., Gawlik-Dziki, U., & Pecio, Ł. (2014). Coffee with cinnamon–Impact of phytochemicals interactions on antioxidant and anti-inflammatory in vitro activity. *Food Chemistry*, *162*, 81-88.

Ernst, M., Kang, K. B., Caraballo-Rodriguez, A. M., Nothias, L. F., Wandy, J., Chen, C., Wang, M., Rogers, S., Medema, M. H., Dorrestein, P. C., & van der Hooft, J. J. J. (2019). MolNetEnhancer: Enhanced Molecular Networks by Integrating Metabolome Mining and Annotation Tools. *Metabolites*, *9*(7). https://doi.org/10.3390/metabo9070144

Estruch, R., Ros, E., Salas-Salvadó, J., Covas, M.-I., Corella, D., Arós, F., Gómez-Gracia, E., Ruiz-Gutiérrez, V., Fiol, M., & Lapetra, J. (2013). Primary prevention of cardiovascular disease with a Mediterranean diet. *New England Journal of Medicine*, *368*(14), 1279-1290.

Fan, Z., Alley, A., Ghaffari, K., & Ressom, H. W. (2020). MetFID: artificial neural network-based compound fingerprint prediction for metabolite annotation. *Metabolomics*, *16*(10), 1-11.

Feldman, H. A., Johannes, C. B., Derby, C. A., Kleinman, K. P., Mohr, B. A., Araujo, A. B., & McKinlay, J. B. (2000). Erectile dysfunction and coronary risk factors: prospective results from the Massachusetts male aging study. *Preventive medicine*, *30*(4), 328-338.

Feliciano, R. P., Pritzel, S., Heiss, C., & Rodriguez-Mateos, A. (2015). Flavonoid intake and cardiovascular disease risk. *Current Opinion in Food Science*, *2*, 92-99.

Fernández-Sánchez, A., Madrigal-Santillán, E., Bautista, M., Esquivel-Soto, J., Morales-González, Á., Esquivel-Chirino, C., Durante-Montiel, I., Sánchez-Rivera, G., Valadez-Vega, C., & Morales-González, J. A. (2011). Inflammation, oxidative stress, and obesity. *International journal of molecular sciences*, *12*(5), 3117-3132.

Feussner, K., & Feussner, I. (2019). Comprehensive LC-MS-based metabolite fingerprinting approach for plant and fungal-derived samples. *High-throughput metabolomics: Methods and protocols*, 167-185.

Flores, G., & Ruiz del Castillo, M. L. (2015). Variations in ellagic acid, quercetin and myricetin in berry cultivars after preharvest methyl jasmonate treatments. *Journal of Food Composition and Analysis*, *39*, 55-61. https://doi.org/https://doi.org/10.1016/j.jfca.2014.11.007

Fonville, J. M., Richards, S. E., Barton, R. H., Boulange, C. L., Ebbels, T. M., Nicholson, J. K., Holmes, E., & Dumas, M. E. (2010). The evolution of partial least squares models and related chemometric approaches in metabonomics and metabolic phenotyping. *Journal of Chemometrics*, *24*(11-12), 636-649.

Forest, C., Padma-Nathan, H., & Liker, H. (2007). Efficacy and safety of pomegranate juice on improvement of erectile dysfunction in male patients with mild to moderate erectile dysfunction: a randomized, placebo-controlled, double-blind, crossover study. *International Journal of Impotence Research*, *19*(6), 564-567.

Ge, J., Liu, Z., Zhong, Z., Wang, L., Zhuo, X., Li, J., Jiang, X., Ye, X.-Y., Xie, T., & Bai, R. (2022). Natural terpenoids with anti-inflammatory activities: Potential leads for anti-inflammatory drug discovery. *Bioorganic Chemistry*, 105817.

Gorrochategui, E., Jaumot, J., Lacorte, S., & Tauler, R. (2016). Data analysis strategies for targeted and untargeted LC-MS metabolomic studies: Overview and workflow. *TrAC Trends in Analytical Chemistry*, *82*, 425-442.

Granato, D., Santos, J. S., Escher, G. B., Ferreira, B. L., & Maggio, R. M. (2018). Use of principal component analysis (PCA) and hierarchical cluster analysis (HCA) for multivariate association between bioactive compounds and functional properties in foods: A critical perspective. *Trends in Food Science & Technology*, *72*, 83-90.

Gümüş, M., Yakan, M., & Koca, İ. (2019). Recent advances of thiazole hybrids in biological applications. *Future Medicinal Chemistry*, *11*(16), 1979-1998.

Gupta, B. P., Murad, M. H., Clifton, M. M., Prokop, L., Nehra, A., & Kopecky, S. L. (2011). The effect of lifestyle modification and cardiovascular risk factor reduction on erectile dysfunction: a systematic review and meta-analysis. *Archives of internal medicine*, *171*(20), 1797-1803.

Gurni, A. A., König, W. A., & Kubitzki, K. (1981). Flavonoid glycosides and sulphates from the Dilleniaceae. *Phytochemistry*, *20*(5), 1057-1059.

Hammond, D. S. (2005). *Tropical forests of the Guiana Shield: ancient forests in a modern world*. CABI.

Hawkins, C., Ginzburg, D., Zhao, K., Dwyer, W., Xue, B., Xu, A., Rice, S., Cole, B., Paley, S., & Karp, P. (2021). Plant Metabolic Network 15: A resource of genome-wide metabolism databases for 126 plants and algae. *Journal of integrative plant biology*, *63*(11), 1888-1905.

Heberle, H., Meirelles, G. V., da Silva, F. R., Telles, G. P., & Minghim, R. (2015). InteractiVenn: a web-based tool for the analysis of sets through Venn diagrams. *BMC bioinformatics*, *16*, 1-7.

HemaIswarya, S., & Doble, M. (2006). Potential synergism of natural products in the treatment of cancer. *Phytotherapy Research: An International Journal Devoted to Pharmacological and Toxicological Evaluation of Natural Product Derivatives*, *20*(4), 239-249.

Hoffmann, M. A., Nothias, L. F., Ludwig, M., Fleischauer, M., Gentry, E. C., Witting, M., Dorrestein, P. C., Duhrkop, K., & Bocker, S. (2022). High-confidence structural annotation of metabolites absent from spectral libraries. *Nat Biotechnol*, *40*(3), 411-421. https://doi.org/10.1038/s41587-021-01045-9

Horai, H., Arita, M., Kanaya, S., Nihei, Y., Ikeda, T., Suwa, K., Ojima, Y., Tanaka, K., Tanaka, S., Aoshima, K., Oda, Y., Kakazu, Y., Kusano, M., Tohge, T., Matsuda, F., Sawada, Y., Hirai, M. Y., Nakanishi, H., Ikeda, K., Akimoto, N., Maoka, T., Takahashi, H., Ara, T., Sakurai, N., Suzuki, H., Shibata, D., Neumann, S., Iida, T., Tanaka, K., Funatsu, K., Matsuura, F., Soga, T., Taguchi, R., Saito, K., & Nishioka, T. (2010). MassBank: a public repository for sharing mass spectral data for life sciences. *J Mass Spectrom*, *45*(7), 703-714. https://doi.org/10.1002/jms.1777

Hornedo-Ortega, R., González-Centeno, M. R., Chira, K., Jourdes, M., & Teissedre, P.-L. (2020). Phenolic compounds of grapes and wines: Key compounds and implications in sensory perception. *Chemistry and biochemistry of winemaking, wine stabilization and aging*, 1-26.

Hounguè, U. M., Tokoudagba, M., Gbaguidi, A., & Schini-Kerth, B. CARISSA EDULIS PHYTOCHEMICAL AND PHARMACOLOGICAL STUDIES: A REVIEW ARTICLE.

Houriet, J., Vidar, W. S., Manwill, P. K., Todd, D. A., & Cech, N. B. (2022). How Low Can You Go? Selecting Intensity Thresholds for Untargeted Metabolomics Data Preprocessing. *Analytical chemistry*.

Hsu, R.-J., Hsu, Y.-C., Chen, S.-P., Fu, C.-L., Yu, J.-C., Chang, F.-W., Chen, Y.-H., Liu, J.-M., Ho, J.-Y., & Yu, C.-P. (2015). The triterpenoids of Hibiscus syriacus induce apoptosis and inhibit cell migration in breast cancer cells. *BMC complementary and alternative medicine*, *15*(1), 1-9.

Hu, Y., Cai, B., & Huan, T. (2019). Enhancing Metabolome Coverage in Data-Dependent LC-MS/MS Analysis through an Integrated Feature Extraction Strategy. *Anal Chem*, *91*(22), 14433-14441. https://doi.org/10.1021/acs.analchem.9b02980

Huang, D., Dang, F., Huang, Y., Chen, N., & Zhou, D.-M. (2021). Uptake, translocation, and transformation of silver nanoparticles in plants. *Environmental Science: Nano*.

Ieda, N., Hotta, Y., Yamauchi, A., Nishikawa, A., Sasamori, T., Saitoh, D., Kawaguchi, M., Kimura, K., & Nakagawa, H. (2020). Development of a red-light-controllable nitric oxide releaser to control smooth muscle relaxation in vivo. *ACS Chemical Biology*, *15*(11), 2958-2965.

Isemura, M. (2019). Catechin in human health and disease. In (Vol. 24, pp. 528): MDPI.

Ishikawa, R. B., Leitao, M. M., Kassuya, R. M., Macorini, L. F., Moreira, F. M. F., Cardoso, C. A. L., Coelho, R. G., Pott, A., Gelfuso, G. M., Croda, J., Oliveira, R. J., & Kassuya, C. A. L. (2017). Anti-inflammatory, antimycobacterial and genotoxic evaluation of Doliocarpus dentatus. *J Ethnopharmacol*, *204*, 18-25. https://doi.org/10.1016/j.jep.2017.04.004

Ishikawa, R. B., Leitão, M. M., Kassuya, R. M., Macorini, L. F., Moreira, F. M. F., Cardoso, C. A. L., Coelho, R. G., Pott, A., Gelfuso, G. M., Croda, J., Oliveira, R. J., & Kassuya, C. A. L. (2017). Anti-inflammatory, antimycobacterial and genotoxic evaluation of Doliocarpus dentatus. *Journal of Ethnopharmacology*, *204*(February), 18-25. https://doi.org/10.1016/j.jep.2017.04.004

Ishikawa, R. B., Vani, J. M., das Neves, S. C., Rabacow, A. P. M., Kassuya, C. A. L., Croda, J., Cardoso, C. A. L., Monreal, A., Antoniolli, A., Cunha-Laura, A. L., & Oliveira, R. J. (2018). The safe use of Doliocarpus dentatus in the gestational period: Absence of changes in maternal reproductive performance, embryo-fetal development and DNA integrity. *J Ethnopharmacol*, *217*, 1-6. https://doi.org/10.1016/j.jep.2018.01.034

Ishikawa, R. B., Vani, J. M., das Neves, S. C., Rabacow, A. P. M., Kassuya, C. A. L., Croda, J., Cardoso, C. A. L., Monreal, A. C. D. F., Antoniolli, A. C. M. B., Cunha – Laura, A. L., &

Oliveira, R. J. (2018). The safe use of Doliocarpus dentatus in the gestational period: Absence of changes in maternal reproductive performance, embryo-fetal development and DNA integrity. *Journal of Ethnopharmacology*, *217*(January), 1-6. https://doi.org/10.1016/j.jep.2018.01.034

Jafari, S. M. (2022). A Review of Potential Anti-Cancer Effect of Sesquiterpene Lactones in Breast Cancer. *Jorjani Biomedicine Journal*, *10*(4), 48-59.

Jagessar, R. C., Hoolas, G., & Maxwell, A. R. (2013). Journal of Natural Products evaluation of heavy metals ion content of Doliocarpus dentatus. *6*, 5-16.

Jang, D. J., Lee, M. S., Shin, B. C., Lee, Y. C., & Ernst, E. (2008). Red ginseng for treating erectile dysfunction: a systematic review. *British journal of clinical pharmacology*, *66*(4), 444-450.

Jia, W., Ling, Y., Lin, Y., Chang, J., & Chu, X. (2014). Analysis of additives in dairy products by liquid chromatography coupled to quadrupole-orbitrap mass spectrometry. *Journal of Chromatography A*, *1336*, 67-75.

Jiang, B., Song, J., & Jin, Y. (2020). A flavonoid monomer tricin in Gramineous plants: Metabolism, bio/chemosynthesis, biological properties, and toxicology. *Food Chemistry*, *320*, 126617.

Jiang, L., Sullivan, H., & Wang, B. (2022). Principal component analysis (PCA) loading and statistical tests for nuclear magnetic resonance (NMR) metabolomics involving multiple study groups. *Analytical Letters*, *55*(10), 1648-1662.

Johnson, E. J. (2014). Role of lutein and zeaxanthin in visual and cognitive function throughout the lifespan. *Nutrition reviews*, *72*(9), 605-612.

Joo, J. H., & Jetten, A. M. (2010). Molecular mechanisms involved in farnesol-induced apoptosis. *Cancer letters*, *287*(2), 123-135.

Judkins, C. P., Diep, H., Broughton, B. R., Mast, A. E., Hooker, E. U., Miller, A. A., Selemidis, S., Dusting, G. J., Sobey, C. G., & Drummond, G. R. (2010). Direct evidence of a role for Nox2 in superoxide production, reduced nitric oxide bioavailability, and early atherosclerotic plaque formation in ApoE−/− mice. *American Journal of Physiology-Heart and Circulatory Physiology*, *298*(1), H24-H32.

Kalender, S., Kalender, Y., Ates, A., Yel, M., Olcay, E., & Candan, S. (2002). Protective role of antioxidant vitamin E and catechin on idarubicin-induced cardiotoxicity in rats. *Brazilian journal of medical and biological research*, *35*, 1379-1387.

Kanehisa, M., Sato, Y., Furumichi, M., Morishima, K., & Tanabe, M. (2019). New approach for understanding genome variations in KEGG. *Nucleic acids research*, *47*(D1), D590-D595.

Kaur, P., Shukla, S., & Gupta, S. (2008). Plant flavonoid apigenin inactivates Akt to trigger apoptosis in human prostate cancer: an in vitro and in vivo study. *Carcinogenesis*, *29*(11), 2210-2217.

Khalili, M., Alavi, M., Esmaeil-Jamaat, E., Baluchnejadmojarad, T., & Roghani, M. (2018). Trigonelline mitigates lipopolysaccharide-induced learning and memory impairment in the rat due to its anti-oxidative and anti-inflammatory effect. *International Immunopharmacology*, *61*, 355-362.

Khammassi, M., Mighri, H., Mansour, M. B., Amri, I., Jamoussi, B., & Khaldi, A. (2022). Metabolite profiling and potential antioxidant activity of sixteen fennel (Foeniculum vulgare Mill.) populations wild-growing in Tunisia. *South African Journal of Botany*, *148*, 407-414.

Kharazian, N., & Mohammadi, M. (2014). Flavonoid patterns and their diversity in Ten stachys L.(Lamiaceae) species from Iran.

Kim-Park, W. K., Allam, E. S., Palasuk, J., Kowolik, M., Park, K. K., & Windsor, L. J. (2016). Green tea catechin inhibits the activity and neutrophil release of Matrix Metalloproteinase-9. *Journal of traditional and complementary medicine*, *6*(4), 343-346.

Kim, H.-Y., Kim, O.-H., & Sung, M.-K. (2003). Effects of phenol-depleted and phenol-rich diets on blood markers of oxidative stress, and urinary excretion of quercetin and kaempferol in healthy volunteers. *Journal of the American College of Nutrition*, *22*(3), 217-223.

Kim, S., Cheng, T., He, S., Thiessen, P. A., Li, Q., Gindulyte, A., & Bolton, E. E. (2022). PubChem Protein, Gene, Pathway, and Taxonomy Data Collections: Bridging Biology and Chemistry through Target-Centric Views of PubChem Data. *Journal of Molecular Biology*, 167514.

Kimura, A. M., Tsuji, M., Yasumoto, T., Mori, Y., Oguchi, T., Tsuji, Y., Umino, M., Umino, A., Nishikawa, T., & Nakamura, S. (2021). Myricetin prevents high molecular weight Aβ1-42 oligomer-induced neurotoxicity through antioxidant effects in cell membranes and mitochondria. *Free radical biology and medicine*, *171*, 232-244.

Kobori, M., Takahashi, Y., Sakurai, M., Akimoto, Y., Tsushida, T., Oike, H., & Ippoushi, K. (2016). Quercetin suppresses immune cell accumulation and improves mitochondrial gene expression in adipose tissue of diet-induced obese mice. *Molecular nutrition & food research*, *60*(2), 300-312.

Ku, Y.-S., Ng, M.-S., Cheng, S.-S., Luk, C.-Y., Ludidi, N., Chung, G., Chen, S.-P. T., & Lam, H.-M. (2022). Chapter Ten - Soybean secondary metabolites and flavors: The art of

compromise among climate, natural enemies, and human culture. In H.-M. Lam & M.-W. Li (Eds.), *Advances in Botanical Research* (Vol. 102, pp. 295-347). Academic Press. https://doi.org/https://doi.org/10.1016/bs.abr.2022.03.001

Kumar, G., Jayaveera, K., Kumar, C., Sanjay, U. P., Swamy, B., & Kumar, D. (2007). Antimicrobial effects of Indian medicinal plants against acne-inducing bacteria. *Tropical journal of pharmaceutical research*, *6*(2), 717-723.

Kurnik-Łucka, M., Panula, P., Bugajski, A., & Gil, K. (2018). Salsolinol: an unintelligible and double-faced molecule—lessons learned from in vivo and in vitro experiments. *Neurotoxicity Research*, *33*, 485-514.

Laines-Hidalgo, J. I., Muñoz-Sánchez, J. A., Loza-Müller, L., & Vázquez-Flota, F. (2022). An update of the sanguinarine and benzophenanthridine alkaloids' biosynthesis and their applications. *Molecules*, *27*(4), 1378.

Lanekoff, I., Burnum-Johnson, K., Thomas, M., Cha, J., Dey, S. K., Yang, P., Prieto Conaway, M. C., & Laskin, J. (2015). Three-dimensional imaging of lipids and metabolites in tissues by nanospray desorption electrospray ionization mass spectrometry. *Analytical and Bioanalytical Chemistry*, *407*(8), 2063-2071. https://doi.org/10.1007/s00216-014-8174-0

Lee, B., Weon, J. B., Eom, M. R., Jung, Y. S., & Ma, C. J. (2015). Neuroprotective compounds of Tilia amurensis. *Pharmacognosy Magazine*, *11*(Suppl 2), S303.

Lee, K. E., Bharadwaj, S., Yadava, U., & Kang, S. G. (2020). Computational and in vitro investigation of (-)-epicatechin and proanthocyanidin B2 as inhibitors of human matrix metalloproteinase 1. *Biomolecules*, *10*(10), 1379.

Legeay, S., Rodier, M., Fillon, L., Faure, S., & Clere, N. (2015). Epigallocatechin gallate: a review of its beneficial properties to prevent metabolic syndrome. *Nutrients*, *7*(7), 5443-5468.

Lesjak, M., Beara, I., Simin, N., Pintać, D., Majkić, T., Bekvalac, K., Orčić, D., & Mimica-Dukić, N. (2018). Antioxidant and anti-inflammatory activities of quercetin and its derivatives. *Journal of Functional Foods*, *40*, 68-75. https://doi.org/https://doi.org/10.1016/j.jff.2017.10.047

Li, S. S., Zhu, A., Benes, V., Costea, P. I., Hercog, R., Hildebrand, F., Huerta-Cepas, J., Nieuwdorp, M., Salojärvi, J., & Voigt, A. Y. (2016). Durable coexistence of donor and recipient strains after fecal microbiota transplantation. *Science*, *352*(6285), 586-589.

Lim, S., & Park, S. (2014). Role of vascular smooth muscle cell in the inflammation of atherosclerosis. *BMB reports*, *47*(1), 1.

Lima, C. C., Lemos, R. P. L., & Conserva, L. M. (2014). Dilleniaceae family : an overview of its ethnomedicinal uses , biological and phytochemical profile. *3*(2), 181-204.

Liu, R. H. (2003). Health benefits of fruit and vegetables are from additive and synergistic combinations of phytochemicals. *The American journal of clinical nutrition*, *78*(3), 517S-520S.

Liu, R. H. (2004). Potential synergy of phytochemicals in cancer prevention: mechanism of action. *The Journal of nutrition*, *134*(12), 3479S-3485S.

Lopez, D. S., Wang, R., Tsilidis, K. K., Zhu, H., Daniel, C. R., Sinha, A., & Canfield, S. (2015). Role of caffeine intake on erectile dysfunction in US men: results from NHANES 2001-2004. *PloS one*, *10*(4), e0123547.

Ludwiczuk, A., Skalicka-Woźniak, K., & Georgiev, M. I. (2017). Chapter 11 - Terpenoids. In S. Badal & R. Delgoda (Eds.), *Pharmacognosy* (pp. 233-266). Academic Press. https://doi.org/https://doi.org/10.1016/B978-0-12-802104-0.00011-1

Madunić, J., Madunić, I. V., Gajski, G., Popić, J., & Garaj-Vrhovac, V. (2018). Apigenin: A dietary flavonoid with diverse anticancer properties. *Cancer letters*, *413*, 11-22.

Mamani-Matsuda, M., Kauss, T., Al-Kharrat, A., Rambert, J., Fawaz, F., Thiolat, D., Moynet, D., Coves, S., Malvy, D., & Mossalayi, M. D. (2006). Therapeutic and preventive properties of quercetin in experimental arthritis correlate with decreased macrophage inflammatory mediators. *Biochemical pharmacology*, *72*(10), 1304-1310.

Mandal, S. M., Chakraborty, D., & Dey, S. (2010). Phenolic acids act as signaling molecules in plant-microbe symbioses. *Plant Signaling & Behavior*, *5*(4), 359-368. https://doi.org/10.4161/psb.5.4.10871

Mari, A., Montoro, P., D'Urso, G., Macchia, M., Pizza, C., & Piacente, S. (2015). Metabolic profiling of Vitex agnus castus leaves, fruits and sprouts: Analysis by LC/ESI/(QqQ) MS and (HR) LC/ESI/(Orbitrap)/MSn. *Journal of pharmaceutical and biomedical analysis*, *102*, 215-221.

Marie, F., Benjamin, H., Marie, V., Marie, P., Robert, C., Violeta, R., Hélène, V., Audrey, L., Gilles, J. G., Loic, Y., Delphine, A., Philippe, F., François, P., & Odile, P.-G. (2016). Post-Bariatric Surgery Changes in Quinolinic and Xanthurenic Acid Concentrations Are Associated with Glucose Homeostasis. *PloS one*. https://doi.org/10.1371/journal.pone.0158051

Matheny, P. B., Aime, M. C., & Henkel, T. W. (2003). New species of Inocybe from Dicymbe forests of Guyana. *Mycol Res*, *107*(Pt 4), 495-505. https://doi.org/10.1017/s0953756203007627

Matysik, S., & Liebisch, G. (2017). Quantification of steroid hormones in human serum by liquid chromatography-high resolution tandem mass spectrometry. *Journal of Chromatography A*, *1526*, 112-118. https://doi.org/https://doi.org/10.1016/j.chroma.2017.10.042

Maurya, P. K., Kumar, P., Nagotu, S., Chand, S., & Chandra, P. (2016). Multi-target detection of oxidative stress biomarkers in quercetin and myricetin treated human red blood cells. *RSC advances*, *6*(58), 53195-53202.

Melis, M., Carboni, E., Caboni, P., & Acquas, E. (2015). Key role of salsolinol in ethanol actions on dopamine neuronal activity of the posterior ventral tegmental area. *Addiction biology*, *20*(1), 182-193.

Miller, E. D., Dziedzic, A., Saluk-Bijak, J., & Bijak, M. (2019). A review of various antioxidant compounds and their potential utility as complementary therapy in multiple sclerosis. *Nutrients*, *11*(7), 1528.

Mithöfer, A., & Boland, W. (2012). Plant defense against herbivores: chemical aspects. *Annual review of plant biology*, *63*, 431-450.

Mohimani, H., Gurevich, A., Shlemov, A., Mikheenko, A., Korobeynikov, A., Cao, L., Shcherbin, E., Nothias, L. F., Dorrestein, P. C., & Pevzner, P. A. (2018). Dereplication of microbial metabolites through database search of mass spectra. *Nat Commun*, *9*(1), 4035. https://doi.org/10.1038/s41467-018-06082-8

Moon, H., Kim, J., & Hong, S. (2021). Plant-derived polyphenol-based nanomaterials for drug delivery and theranostics. In *Bioinspired and Biomimetic Materials for Drug Delivery* (pp. 39-54). Elsevier.

Naczk, M., & Shahidi, F. (2004). Extraction and analysis of phenolics in food. *Journal of chromatography A*, *1054*(1), 95-111. https://doi.org/https://doi.org/10.1016/j.chroma.2004.08.059

Nguyen, H. N., Butler, C., Palberg, D., Kisiala, A., & Emery, R. J. N. (2023a). The tRNA-degradation pathway impacts the phenotype and metabolome of Arabidopsis thaliana: evidence from atipt2 and atipt9 knockout mutants. *Plant Growth Regulation*. https://doi.org/10.1007/s10725-023-00987-1

Nguyen, H. N., Butler, C., Palberg, D., Kisiala, A., & Emery, R. N. (2023b). The tRNA-degradation pathway impacts the phenotype and metabolome of Arabidopsis thaliana: evidence from atipt2 and atipt9 knockout mutants. *Plant Growth Regulation*, 1-20.

Nicholas, C., Batra, S., Vargo, M. A., Voss, O. H., Gavrilin, M. A., Wewers, M. D., Guttridge, D. C., Grotewold, E., & Doseff, A. I. (2007). Apigenin blocks lipopolysaccharide-induced lethality in vivo and proinflammatory cytokines expression by inactivating NF-κB through the suppression of p65 phosphorylation. *The Journal of Immunology*, *179*(10), 7121-7127.

Nishimuro, H., Ohnishi, H., Sato, M., Ohnishi-Kameyama, M., Matsunaga, I., Naito, S., Ippoushi, K., Oike, H., Nagata, T., & Akasaka, H. (2015). Estimated daily intake and seasonal food sources of quercetin in Japan. *Nutrients*, *7*(4), 2345-2358.

Nothias, L. F., Petras, D., Schmid, R., Duhrkop, K., Rainer, J., Sarvepalli, A., Protsyuk, I., Ernst, M., Tsugawa, H., Fleischauer, M., Aicheler, F., Aksenov, A. A., Alka, O., Allard, P. M., Barsch, A., Cachet, X., Caraballo-Rodriguez, A. M., Da Silva, R. R., Dang, T., Garg, N., Gauglitz, J. M., Gurevich, A., Isaac, G., Jarmusch, A. K., Kamenik, Z., Kang, K. B., Kessler, N., Koester, I., Korf, A., Le Gouellec, A., Ludwig, M., Martin, H. C., McCall, L. I., McSayles, J., Meyer, S. W., Mohimani, H., Morsy, M., Moyne, O., Neumann, S., Neuweger, H., Nguyen, N. H., Nothias-Esposito, M., Paolini, J., Phelan, V. V., Pluskal, T., Quinn, R. A., Rogers, S., Shrestha, B., Tripathi, A., van der Hooft, J. J. J., Vargas, F., Weldon, K. C., Witting, M., Yang, H., Zhang, Z., Zubeil, F., Kohlbacher, O., Bocker, S., Alexandrov, T., Bandeira, N., Wang, M., & Dorrestein, P. C. (2020). Feature-based molecular networking in the GNPS analysis environment. *Nat Methods*, *17*(9), 905-908. https://doi.org/10.1038/s41592-020-0933-6

Olabiyi, A. A., & de Castro Brás, L. E. (2023). Cardiovascular Remodeling Post-Ischemia: Herbs, Diet, and Drug Interventions. *Biomedicines*, *11*(6), 1697.

Oliveros, J. C. (2007). VENNY. An interactive tool for comparing lists with Venn Diagrams. *http://bioinfogp. cnb. csic. es/tools/venny/index. html*.

Olivon, F., Grelier, G., Roussi, F., Litaudon, M., & Touboul, D. (2017). MZmine 2 Data-Preprocessing To Enhance Molecular Networking Reliability. *Anal Chem*, *89*(15), 7836-7840. https://doi.org/10.1021/acs.analchem.7b01563

Ollivier, S., Jehan, P., Olivier-Jimenez, D., Lambert, F., Boustie, J., Lohezic-Le Devehat, F., & Le Yondre, N. (2022). New insights into the Van Krevelen diagram: Automated molecular formula determination from HRMS for a large chemical profiling of lichen extracts. *Phytochem Anal*, *33*(7), 1111-1120. https://doi.org/10.1002/pca.3163

Onakpoya, I., O'Sullivan, J., Heneghan, C., & Thompson, M. (2017). The effect of grapefruits (Citrus paradisi) on body weight and cardiovascular risk factors: A systematic review and meta-analysis of randomized clinical trials. *Critical Reviews in Food Science and Nutrition*, *57*(3), 602-612.

Oz, H. S. (2017). Chronic inflammatory diseases and green tea polyphenols. *Nutrients*, *9*(6), 561.

Pallangyo, P., Nicholaus, P., Kisenge, P., Mayala, H., Swai, N., & Janabi, M. (2016). A community-based study on prevalence and correlates of erectile dysfunction among Kinondoni District Residents, Dar Es Salaam, Tanzania. *Reproductive health*, *13*, 1-6.

Pang, Z., Chong, J., Zhou, G., de Lima Morais, D. A., Chang, L., Barrette, M., Gauthier, C., Jacques, P.-É., Li, S., & Xia, J. (2021). MetaboAnalyst 5.0: narrowing the gap between raw spectra and functional insights. *Nucleic acids research*, *49*(W1), W388-W396. https://doi.org/10.1093/nar/gkab382

Pang, Z., Zhou, G., Ewald, J., Chang, L., Hacariz, O., Basu, N., & Xia, J. (2022). Using MetaboAnalyst 5.0 for LC–HRMS spectra processing, multi-omics integration and covariate adjustment of global metabolomics data. *Nature Protocols*, *17*(8), 1735-1761.

Patel, D., Shukla, S., & Gupta, S. (2007). Apigenin and cancer chemoprevention: progress, potential and promise. *International journal of oncology*, *30*(1), 233-245.

Patel, K., Kumar, V., Rahman, M., Verma, A., & Patel, D. K. (2018). New insights into the medicinal importance, physiological functions and bioanalytical aspects of an important bioactive compound of foods 'Hyperin': Health benefits of the past, the present, the future. *Beni-Suef University Journal of Basic and Applied Sciences*, *7*(1), 31-42.

Peng, F., Yin, H., Du, B., Niu, K., Yang, Y., & Wang, S. (2022). Anti-inflammatory effect of flavonoids from chestnut flowers in lipopolysaccharide-stimulated RAW 264.7 macrophages and acute lung injury in mice. *Journal of Ethnopharmacology*, *290*, 115086. https://doi.org/https://doi.org/10.1016/j.jep.2022.115086

Perez de Souza, L., Alseekh, S., Naake, T., & Fernie, A. (2019). Mass Spectrometry-Based Untargeted Plant Metabolomics. *Curr Protoc Plant Biol*, *4*(4), e20100. https://doi.org/10.1002/cppb.20100

Peris-Díaz, M. D., Sweeney, S. R., Rodak, O., Sentandreu, E., & Tiziani, S. (2019). R-metabolist 2: A flexible tool for metabolite annotation from high-resolution data-independent acquisition mass spectrometry analysis. *Metabolites*, *9*(9), 187.

Peters, K., Blatt-Janmaat, K. L., Tkach, N., van Dam, N. M., & Neumann, S. (2023). Untargeted Metabolomics for Integrative Taxonomy: Metabolomics, DNA Marker-Based Sequencing, and Phenotype Bioimaging. *Plants (Basel)*, *12*(4). https://doi.org/10.3390/plants12040881

Pezzatti, J., Boccard, J., Codesido, S., Gagnebin, Y., Joshi, A., Picard, D., González-Ruiz, V., & Rudaz, S. (2020). Implementation of liquid chromatography–high resolution mass spectrometry methods for untargeted metabolomic analyses of biological samples: A tutorial. *Analytica Chimica Acta*, *1105*, 28-44.

Pietzke, M., & Vazquez, A. (2020). Metabolite AutoPlotter - an application to process and visualise metabolite data in the web browser. *Cancer Metab*, *8*, 15. https://doi.org/10.1186/s40170-020-00220-x

Pluskal, T., Castillo, S., Villar-Briones, A., & Oresic, M. (2010). MZmine 2: modular framework for processing, visualizing, and analyzing mass spectrometry-based molecular profile data. *BMC Bioinformatics*, *11*, 395. https://doi.org/10.1186/1471-2105-11-395

Prabakaran, M., Chung, I.-M., Son, N.-Y., Chi, H.-Y., Kim, S.-Y., Yang, Y.-J., Kwon, C., An, Y.-J., Ahmad, A., & Kim, S.-H. (2018). Analysis of selected phenolic compounds in organic, pesticide-free, conventional rice (Oryza sativa L.) using LC-ESI-MS/MS. *Molecules*, *24*(1), 67.

Raffa, D., Maggio, B., Raimondi, M. V., Plescia, F., & Daidone, G. (2017). Recent discoveries of anticancer flavonoids. *European journal of medicinal chemistry*, *142*, 213-228.

Raj, L., Ide, T., Gurkar, A. U., Foley, M., Schenone, M., Li, X., Tolliday, N. J., Golub, T. R., Carr, S. A., & Shamji, A. F. (2011). Selective killing of cancer cells by a small molecule targeting the stress response to ROS. *Nature*, *475*(7355), 231-234.

Ramírez, R., Pedro-Botet, J., García, M., Corbella, E., Merino, J., Zambón, D., Corbella, X., Pintó, X., & Group, X. d. U. d. L. i. A. I. (2016). Erectile dysfunction and cardiovascular risk factors in a Mediterranean diet cohort. *Internal medicine journal*, *46*(1), 52-56.

Rauf, A., Imran, M., Abu-Izneid, T., Iahtisham Ul, H., Patel, S., Pan, X., Naz, S., Sanches Silva, A., Saeed, F., & Rasul Suleria, H. A. (2019). Proanthocyanidins: A comprehensive review. *Biomedicine & Pharmacotherapy*, *116*, 108999. https://doi.org/https://doi.org/10.1016/j.biopha.2019.108999

Reshef, N., Hayari, Y., Goren, C., Boaz, M., Madar, Z., & Knobler, H. (2005). Antihypertensive effect of sweetie fruit in patients with stage I hypertension. *American journal of hypertension*, *18*(10), 1360-1363.

Reveglia, P., Raimondo, M. L., Masi, M., Cimmino, A., Nuzzo, G., Corso, G., Fontana, A., Carlucci, A., & Evidente, A. (2022). Untargeted and Targeted LC-MS/MS Based Metabolomics Study on In Vitro Culture of Phaeoacremonium Species. *J Fungi (Basel)*, *8*(1). https://doi.org/10.3390/jof8010055

Rodrigues, V. E. G., & de Carvalho, D. A. (2008). Florística de plantas medicinais nativas de remanescentes de floresta estacional semidecidual na região do Alto Rio Grande-Minas Gerais. *Cerne*, *14*(2), 93-112.

Rodriguez-Porcel, M., Chade, A., & Miller, J. (2017). Studies on atherosclerosis. Oxidative stress in applied basic research and clinical practice. *Berlin: Springer*, *10*, 978-971.

Roessner, U., & Dias, D. A. (2013). *Metabolomics tools for natural product discovery*. Springer.

ROMEO, J. H., SEFTEL, A. D., MADHUN, Z. T., & ARON, D. C. (2000). Sexual function in men with diabetes type 2: association with glycemic control. *The Journal of urology*, *163*(3), 788-791.

Rossi, M., Negri, E., Lagiou, P., Talamini, R., Dal Maso, L., Montella, M., Franceschi, S., & La Vecchia, C. (2008). Flavonoids and ovarian cancer risk: a case–control study in Italy. *International journal of cancer*, *123*(4), 895-898.

Roy, A. (2017). A review on the alkaloids an important therapeutic compound from plants. *IJPB*, *3*(2), 1-9.

Şahin, T. D., Gocmez, S. S., Duruksu, G., Yazir, Y., & Utkan, T. (2020). Resveratrol and quercetin attenuate depressive-like behavior and restore impaired contractility of vas deferens in chronic stress-exposed rats: involvement of oxidative stress and inflammation. *Naunyn-Schmiedeberg's Archives of Pharmacology*, *393*, 761-775.

Santos, M. C. B., Barouh, N., Durand, E., Baréa, B., Robert, M., Micard, V., Lullien-Pellerin, V., Villeneuve, P., Cameron, L. C., & Ryan, E. P. (2021). Metabolomics of pigmented rice coproducts applying conventional or deep eutectic extraction solvents reveal a potential antioxidant source for human nutrition. *Metabolites*, *11*(2), 110.

Sasidharan, S., Chen, Y., Saravanan, D., Sundram, K., & Latha, L. Y. (2011). Extraction, isolation and characterization of bioactive compounds from plants' extracts. *African journal of traditional, complementary and alternative medicines*, *8*(1).

Satoh, K., Sakamoto, Y., Ogata, A., Nagai, F., Mikuriya, H., Numazawa, M., Yamada, K., & Aoki, N. (2002). Inhibition of aromatase activity by green tea extract catechins and their endocrinological effects of oral administration in rats. *Food and Chemical Toxicology*, *40*(7), 925-933.

Sauvain, M., Kunesch, N., Poisson, J., Gantier, J. C., Gayral, P., & Dedet, J. P. (1996). Isolation of leishmanicidal triterpenes and lignans from the Amazonian liana Doliocarpus dentatus (Dilleniaceae). *Phytotherapy Research*, *10*(1), 1-4.

Schmitz, G. J. H., Freschi, L., Ferrari, R. C., Peroni-Okita, F. H. G., & Cordenunsi-Lysenko, B. R. (2022). Exploring the significance of photosynthetic activity and carbohydrate metabolism in peel tissues during banana fruit ripening. *Scientia Horticulturae*, *295*, 110811.

Schrimpe-Rutledge, A. C., Codreanu, S. G., Sherrod, S. D., & McLean, J. A. (2016). Untargeted metabolomics strategies—challenges and emerging directions. *Journal of the American Society for Mass Spectrometry*, *27*(12), 1897-1905.

Selvin, E., Burnett, A. L., & Platz, E. A. (2007). Prevalence and risk factors for erectile dysfunction in the US. *The American journal of medicine*, *120*(2), 151-157.

Sena, C. M., Pereira, A. M., & Seiça, R. (2013). Endothelial dysfunction—a major mediator of diabetic vascular disease. *Biochimica et Biophysica Acta (BBA)-Molecular Basis of Disease*, *1832*(12), 2216-2231.

Shan, X., Cheng, J., Chen, K., Liu, Y., & Juan, L. (2017). Comparison of lipoxygenase, cyclooxygenase, xanthine oxidase inhibitory effects and cytotoxic activities of selected flavonoids. *DEStech Trans. Environ. Energy Earth Sci*.

Shannon, P., Markiel, A., Ozier, O., Baliga, N. S., Wang, J. T., Ramage, D., Amin, N., Schwikowski, B., & Ideker, T. (2003). Cytoscape: a software environment for integrated models of biomolecular interaction networks. *Genome Res*, *13*(11), 2498-2504. https://doi.org/10.1101/gr.1239303

Shimizu, T., Watanabe, M., Fernie, A. R., & Tohge, T. (2018). Targeted LC-MS analysis for plant secondary metabolites. *Plant Metabolomics: Methods and Protocols*, 171-181.

Shinbo, Y., Nakamura, Y., Altaf-Ul-Amin, M., Asahi, H., Kurokawa, K., Arita, M., Saito, K., Ohta, D., Shibata, D., & Kanaya, S. (2006). KNApSAcK: a comprehensive species-metabolite relationship database. In *Plant metabolomics* (pp. 165-181). Springer.

Shuveksh, P. S., Ahmed, K., Padhye, S., Schobert, R., & Biersack, B. (2017). Chemical and biological aspects of the natural 1, 4-benzoquinone embelin and its (semi-) synthetic derivatives. *Current medicinal chemistry*, *24*(18), 1998-2009.

Silva, F. H., Leiria, L. O., Alexandre, E. C., Davel, A. P. C., Mónica, F. Z., De Nucci, G., & Antunes, E. (2014). Prolonged therapy with the soluble guanylyl cyclase activator BAY 60-2770 restores the erectile function in obese mice. *The journal of sexual medicine*, *11*(11), 2661-2670.

Singh, R., Ali, A., Jeyabalan, G., & Semwal, A. (2013). An overview of the current methodologies used for evaluation of aphrodisiac agents. *Journal of Acute Disease*, *2*(2), 85-91.

Sipski, M., & Alexander, C. (1997). Sexual function in people with chronic illness: a health professional's guide. In: Aspen Press, Gaithersburg, MD.

Smith, C. A., Want, E. J., O'Maille, G., Abagyan, R., & Siuzdak, G. (2006). XCMS: processing mass spectrometry data for metabolite profiling using nonlinear peak alignment, matching, and identification. *Analytical chemistry*, *78*(3), 779-787.

Solomon, H., Man, J., & Jackson, G. (2003). Erectile dysfunction and the cardiovascular patient: endothelial dysfunction is the common denominator. *Heart*, *89*(3), 251-253.

Sumner. (2007).

Tahirovic, A., & Basic, N. (2017). Determination of phenolic content and antioxidant properties of methanolic extracts from Viscum album ssp. album Beck. *Bulletin of the Chemists and Technologists of Bosnia and Herzegovina*, *49*, 25-30.

Tang, G., Xu, Y., Zhang, C., Wang, N., Li, H., & Feng, Y. (2021). Green tea and epigallocatechin gallate (EGCG) for the management of nonalcoholic fatty liver diseases (NAFLD): Insights into the role of oxidative stress and antioxidant mechanism. *Antioxidants*, *10*(7), 1076.

Thilakarathna, S. H., & Rupasinghe, H. V. (2013). Flavonoid bioavailability and attempts for bioavailability enhancement. *Nutrients*, *5*(9), 3367-3387.

Tsugawa, H., Cajka, T., Kind, T., Ma, Y., Higgins, B., Ikeda, K., Kanazawa, M., VanderGheynst, J., Fiehn, O., & Arita, M. (2015). MS-DIAL: data-independent MS/MS deconvolution for comprehensive metabolome analysis. *Nat Methods*, *12*(6), 523-526. https://doi.org/10.1038/nmeth.3393

Urpi-Sarda, M., Casas, R., Chiva-Blanch, G., Romero-Mamani, E. S., Valderas-Martínez, P., Arranz, S., Andres-Lacueva, C., Llorach, R., Medina-Remón, A., & Lamuela-Raventos, R. M. (2012). Virgin olive oil and nuts as key foods of the Mediterranean diet effects on inflammatory biomarkers related to atherosclerosis. *Pharmacological research*, *65*(6), 577-583.

Vacek, Z., Vacek, S., Bílek, L., Remeš, J., & Štefančík, I. (2015). Changes in horizontal structure of natural beech forests on an altitudinal gradient in the Sudetes. *Dendrobiology*, *73*, 33-45. https://doi.org/10.12657/denbio.073.004

Van Andel, T. (2001). Floristic composition and diversity of mixed primary and secondary forests in northwest Guyana. *Biodiversity and Conservation*, *10*(10), 1645-1682. https://doi.org/10.1023/A:1012069717077

Van Andel T, T. R. (2003). Floristic composition and diversity of three swamp forests in northwest Guyana. *Plant Ecology*, *167*(2), 293-317. https://doi.org/10.1023/A:1023935326706

van Andel, T. R. (2000). *Non-timber forest products of the North-West District of Guyana*. Utrecht University.

Vásquez, S. M., Abascal, G. G. W., Leal, C. E., Cardineau, G. A., & Lara, S. G. (2022). Application of metabolic engineering to enhance the content of alkaloids in medicinal plants. *Metabolic Engineering Communications*, e00194.

Wallace, T. C., Bailey, R. L., Blumberg, J. B., Burton-Freeman, B., Chen, C. O., Crowe-White, K. M., Drewnowski, A., Hooshmand, S., Johnson, E., & Lewis, R. (2020). Fruits, vegetables, and health: A comprehensive narrative, umbrella review of the science and recommendations for enhanced public policy to improve intake. *Critical Reviews in Food Science and Nutrition*, *60*(13), 2174-2211.

Wang, F., Dai, S., Wang, M., & Morrison, H. (2013). Erectile dysfunction and fruit/vegetable consumption among diabetic Canadian men. *Urology*, *82*(6), 1330-1335.

Wang, H., Fan, W., Li, H., Yang, J., Huang, J., & Zhang, P. (2013). Functional characterization of dihydroflavonol-4-reductase in anthocyanin biosynthesis of purple sweet potato underlies the direct evidence of anthocyanins function against abiotic stresses. *PloS one*, *8*(11), e78484.

Wang, L., Xing, X., Chen, L., Yang, L., Su, X., Rabitz, H., Lu, W., & Rabinowitz, J. D. (2018). Peak annotation and verification engine for untargeted LC–MS metabolomics. *Analytical chemistry*, *91*(3), 1838-1846.

Wang, M., Carver, J. J., Phelan, V. V., Sanchez, L. M., Garg, N., Peng, Y., Nguyen, D. D., Watrous, J., Kapono, C. A., Luzzatto-Knaan, T., Porto, C., Bouslimani, A., Melnik, A. V., Meehan, M. J., Liu, W. T., Crusemann, M., Boudreau, P. D., Esquenazi, E., Sandoval-Calderon, M., Kersten, R. D., Pace, L. A., Quinn, R. A., Duncan, K. R., Hsu, C. C., Floros, D. J., Gavilan, R. G., Kleigrewe, K., Northen, T., Dutton, R. J., Parrot, D., Carlson, E. E., Aigle, B., Michelsen, C. F., Jelsbak, L., Sohlenkamp, C., Pevzner, P., Edlund, A., McLean, J., Piel, J., Murphy, B. T., Gerwick, L., Liaw, C. C., Yang, Y. L., Humpf, H. U., Maansson, M., Keyzers, R. A., Sims, A. C., Johnson, A. R., Sidebottom, A. M., Sedio, B. E., Klitgaard, A., Larson, C. B., P, C. A. B., Torres-Mendoza, D., Gonzalez, D. J., Silva, D. B., Marques, L. M., Demarque, D. P., Pociute, E., O'Neill, E. C., Briand, E., Helfrich, E. J. N., Granatosky, E. A., Glukhov, E., Ryffel, F., Houson, H., Mohimani, H., Kharbush, J. J., Zeng, Y., Vorholt, J. A., Kurita, K. L., Charusanti, P., McPhail, K. L., Nielsen, K. F., Vuong, L., Elfeki, M., Traxler, M. F., Engene, N., Koyama, N., Vining, O. B., Baric, R., Silva, R. R., Mascuch, S. J., Tomasi, S., Jenkins, S., Macherla, V., Hoffman, T., Agarwal, V., Williams, P. G., Dai, J., Neupane, R., Gurr, J., Rodriguez, A. M. C., Lamsa, A., Zhang, C., Dorrestein, K., Duggan, B. M., Almaliti, J., Allard, P. M., Phapale, P., Nothias, L. F., Alexandrov, T., Litaudon, M., Wolfender, J. L., Kyle, J. E., Metz, T. O., Peryea, T., Nguyen, D. T., VanLeer, D., Shinn, P., Jadhav, A., Muller, R., Waters, K. M., Shi, W., Liu, X., Zhang, L., Knight, R., Jensen, P. R., Palsson, B. O., Pogliano, K., Linington, R. G., Gutierrez, M., Lopes, N. P., Gerwick, W. H., Moore, B. S., Dorrestein, P. C., & Bandeira, N. (2016). Sharing and community curation of mass spectrometry data with Global Natural Products Social Molecular Networking. *Nat Biotechnol*, *34*(8), 828-837. https://doi.org/10.1038/nbt.3597

Wang, X.-R., Yang, J.-W., Ji, C.-S., Zeng, X.-H., Shi, G.-X., Fisher, M., & Liu, C.-Z. (2018). Inhibition of NADPH oxidase–dependent oxidative stress in the rostral ventrolateral medulla mediates the antihypertensive effects of acupuncture in spontaneously hypertensive rats. *Hypertension*, *71*(2), 356-365.

Welling, M. T., Liu, L., Rose, T. J., Waters, D. L., & Benkendorff, K. (2016). Arbuscular mycorrhizal fungi: effects on plant terpenoid accumulation. *Plant Biology*, *18*(4), 552-562.

Williamson, G., Plumb, G. W., Uda, Y., Price, K. R., & Rhodes, M. J. C. (1996). Dietary quercetin glycosides: antioxidant activity and induction of the anticarcinogenic phase II marker enzyme quinone reductase in Hepalclc7 cells. *Carcinogenesis*, *17*(11), 2385-2387. https://doi.org/10.1093/carcin/17.11.2385

Williamson, J. C., Edwards, A. V., Verano-Braga, T., Schwämmle, V., Kjeldsen, F., Jensen, O. N., & Larsen, M. R. (2016). High-performance hybrid Orbitrap mass spectrometers for quantitative proteome analysis: Observations and implications. *Proteomics*, *16*(6), 907-914.

Wing, R. R., Rosen, R. C., Fava, J. L., Bahnson, J., Brancati, F., Gendrano III, I. N. C., Kitabchi, A., Schneider, S. H., & Wadden, T. A. (2010). Effects of weight loss intervention on erectile function in older men with type 2 diabetes in the Look AHEAD trial. *The journal of sexual medicine*, *7*(1_Part_1), 156-165.

Wu, Y., Zhang, C., Huang, Z., Lyu, L., Li, J., Li, W., & Wu, W. (2021). The color difference of rubus fruits is closely related to the composition of flavonoids including anthocyanins. *LWT*, *149*, 111825. https://doi.org/https://doi.org/10.1016/j.lwt.2021.111825

Xiao, Y., Huang, Y., Chen, Y., Xiao, L., Zhang, X., Yang, C., Li, Z., Zhu, M., Liu, Z., & Wang, Y. (2022). Discrimination and characterization of the volatile profiles of five Fu brick teas from different manufacturing regions by using HS–SPME/GC–MS and HS–GC–IMS. *Current Research in Food Science*, *5*, 1788-1807.

Xu, J.-B., Li, Y.-Z., Huang, S., Chen, L., Luo, Y.-Y., Gao, F., & Zhou, X.-L. (2021). Diterpenoid alkaloids from the whole herb of Delphinium grandiflorum L. *Phytochemistry*, *190*, 112866.

Xu, Y.-Q., Gao, Y., & Granato, D. (2021). Effects of epigallocatechin gallate, epigallocatechin and epicatechin gallate on the chemical and cell-based antioxidant activity, sensory properties, and cytotoxicity of a catechin-free model beverage. *Food Chemistry*, *339*, 128060.

Yu, Y., Yan, Y., Niu, F., Wang, Y., Chen, X., Su, G., Liu, Y., Zhao, X., Qian, L., & Liu, P. (2021). Ferroptosis: A cell death connecting oxidative stress, inflammation and cardiovascular diseases. *Cell Death Discovery*, *7*(1), 193.

Zhang, M., Wu, Q., Chen, Y., Duan, M., Tian, G., Deng, X., Sun, Y., Zhou, T., Zhang, G., & Chen, W. (2018). Inhibition of proanthocyanidin A2 on porcine reproductive and respiratory syndrome virus replication in vitro. *PloS one*, *13*(2), e0193309.

Zheng, Y.-Z., Deng, G., Liang, Q., Chen, D.-F., Guo, R., & Lai, R.-C. (2017). Antioxidant Activity of Quercetin and Its Glucosides from Propolis: A Theoretical Study. *Scientific reports*, *7*(1), 7543. https://doi.org/10.1038/s41598-017-08024-8

Zhou, B., Chen, Y., Yuan, H., Wang, T., Feng, J., Li, M., & Liu, J. (2021). NOX1/4 inhibitor GKT-137831 improves erectile function in diabetic rats by ROS reduction and endothelial nitric oxide synthase reconstitution. *The journal of sexual medicine*, *18*(12), 1970-1983.

PREFACE

CHAPTER 4

Title: Exploring The Cytokinin Profiles of *Doliocarpus Dentatus* (Capadulla) and its Relationship with Secondary Metabolites: Insights to its Potential Therapeutic Benefits.

Authors: Ewart Smith, Erin Morrison, Ainsely Lewis, Kimberly Molina-Bean, Suresh S Narine and RJ Neil Emery

Reference: To be published in Phyton – International Journal of Experimental Botany 2024 / 2025

Contributions: EAS assembled phytohormones and metabolomics data, created figures and wrote the manuscript. AL worked on the modification of the workflow and experimental design. SN and RJNE conceived, directed and obtained funding for research present in the study. EAS, AL, RJNE and SN edited the manuscript prior to submission.

4. CHAPTER 4

Exploring The Cytokinin Profiles of *Doliocarpus Dentatus* and its Relationship with Secondary Metabolites: Insights to its Potential Therapeutic Benefits.

ABSTRACT

Doliocarpus dentatus, a plant traditionally used in Guyanese medicine known as "Capadulla" or "Guyanese natural Viagra," is renowned for its alleged therapeutic benefits, including treating erectile dysfunction, cystitis, malaria, and other conditions, as well as possessing anticancer properties. There are two known ecotypes of *D. dentatus* in Guyana: the red and white ecotypes, both utilized for therapeutic benefits, particularly for erectile dysfunction. While both ecotypes are used in Guyanese traditional medicine, the red ecotype appears to be preferred for its potentially higher therapeutic efficacy, particularly for treating Erectile Dysfunction (ED). The preference for the red ecotype may stem from a higher concentration of therapeutic compounds, particularly polyphenols. These compounds may be enhanced by signaling molecules such as cytokinins, which could contribute to higher antioxidant properties, potentially enhancing the production of nitric oxide or improving blood vessel formation and providing better synergistic effects with other compounds present in the red ecotype, such as betulin, which has demonstrated protective effects against cardiovascular diseases and oxidative stress.

CKs in *D. dentatus*, such as tZ, cZ, and iPR, have shown promise in reducing oxidative stress, a factor in chronic diseases such as cancer and neurodegenerative disorders. Emerging evidence indicates that complex interrelationships exist between cytokinins (CKs) and secondary metabolites in plants, mediated by intricate signalling pathways and biochemical processes. These relationships may directly regulate the production of specific secondary metabolites, such as

flavonoids and alkaloids, by modulating the activity of key enzymes involved in the biosynthetic pathways of these compounds. This study investigates the phytohormone profiles, particularly CKs, and their interaction with secondary metabolites in the red and white ecotypes of *D. dentatus* for its alleged therapeutic benefits in treating erectile dysfunction. The research employed liquid chromatography-tandem mass spectrometry (LC-MS/MS) to analyze and compare the CK composition and metabolomes of the two ecotypes collected from Eagle Mountain Forest in Guyana. A targeted approach was used for CK analysis, while a semi-untargeted approach was implemented for metabolomic data analysis. The study detected 20 forms of CKs in both ecotypes, with the red ecotype showing higher concentrations of active CKs, particularly trans-zeatin (*t*Z) and cis-zeatin (*c*Z), along with their glucoside forms, which accounted for 98.38% of the total CKs content (9135.49 ± 3174.72 pmol/g FW). Untargeted metabolomic analysis revealed 20,382 potential metabolite features in the red ecotype and 11,021 in the white ecotype. Further analysis identified 5,275 tentative metabolite features, with 159 upregulated and 110 downregulated in the red ecotype. Polyphenols accounted for 63.9% of identified compounds in both ecotypes.

Pathway analysis showed that the red ecotype demonstrated a higher occurrence of flavonoids, flavone, flavonols, and anthocyanin biosynthesis, while the white ecotype was more associated with monoterpenoid biosynthesis. Correlation network analysis highlighted positive associations between specific CKs and alkaloids, as well as between *t*Z and iPR with phenolic compounds. These findings suggest that the enhanced bioactivity of the red ecotype, evidenced by elevated levels of CKs and increased enrichment in flavonoid biosynthesis, may support its preferential application in traditional therapy. The study highlights the intricate interplay between CKs and secondary metabolites in *D. dentatus*, providing critical insights into the regulatory

mechanisms governing biochemical processes and signalling pathways involved in secondary metabolite production.

Future research should focus on further elucidating the antioxidant potential of *D. dentatus*. This could involve a comprehensive comparative analysis of antioxidant activities between the red and white ecotypes using multiple assays, such as DPPH (2,2-diphenyl-1-picrylhydrazyl), ABTS (2,2'-azino-bis (3-ethylbenzothiazoline-6-sulphonic acid)), and ORAC (Oxygen Radical Absorbance Capacity). Additionally, isolating and characterizing specific compounds responsible for antioxidant activity, particularly polyphenols, would be beneficial. Furthermore, developing standardized extracts based on antioxidant compounds, studying environmental factors impacting antioxidant content, conducting comparative ethnobotanical studies of traditional uses in different regions of Guyana and assessing antioxidant stability under various storage and processing conditions would contribute to a more comprehensive understanding of *D. dentatus's* antioxidant potential and its possible therapeutic applications.

KEYWORDS: mass spectrometry, Capadulla, Cytokinins, Secondary metabolites, Metabolomics,Therapeutic potential,

4.1. INTRODUCTION

Doliocarpus dentatus, commonly referred to as Guyanese natural viagra, is a woody vine belonging to the Dilleniaceae family. Its native habitat spans from Mexico to Southern Brazil covering areas in Central to South America and exhibits the highest density in the Amazon (Branquinho, Verdan, dos Santos, et al., 2021). The *D. dentatus* vine, variously referred to as Capadulla, Kabuduli, and Kapadula, flourishes in both mixed and evergreen lowland forests in Guyana (Bhatia et al., 2014; Huang et al., 2022; Kumar et al., 2007; Sasidharan et al., 2011) (Fig 4.1). This species occupies a significant role in the traditional medicinal practices of Guyana (Gurni et al., 1981; Lima et al., 2014). Within the Doliocarpus genus, *D. dentatus* is regarded as one of the most important species due to its relatively high abundance of phenylpropanoids and polyketides (Ewart smith, 2023). Notably, the flavonoid class constitutes the predominant component, representing 63.9% of the total identified compounds in both ecotypes, followed by macrolides and monologues at 5.9% (Ewart smith, 2023; Raissa Borges Ishikawa et al., 2017; Raissa Borges Ishikawa et al., 2018). Cinnamic acids and their derivatives, as well as isoflavonoids, contribute equally to the overall composition. This species is known for its purported aphrodisiac properties. It is believed that consuming it as a tea or cold drink can enhance libido and treat male impotence (Ewart smith, 2023; Van Andel T, 2003; Van Andel T et al., 2003). In Guyana, the *D. dentatus* species has distinct red and white ecotypes (Fig 4.1) and these ecotypes can be distinguished by their morphological and physical characteristics (Fig 4.1), such as the texture of the vine's outer bark and the colour of the xylem and phloem that can be seen during harvesting (van Andel, 2000).

Other genera (Acrotrema, Davilla, and Dillenia) of the Dilleniaceae family have been researched extensively due to their unique ethnobotanical uses and recognized for their extensive therapeutic potential, characterized by a diverse array of secondary metabolites, including flavonoids, terpenoids, lignans, and phenolic derivatives (Alexandre-Moreira et al., 1999; Branquinho, Verdan, et al., 2021a; Bruniera & Groppo, 2010; De Oliveira et al., 2002; Killeen et al., 1993; Kumari et al., 2009; Lima et al., 2014; Lopes et al., 2007; Sharma et al., 2001; Soares et al., 2005). These metabolites are classified into various structural classes that are utilized in the treatment of numerous health conditions, such as arthritis, diabetes, gastrointestinal disorders, and inflammation (Lima et al., 2014). The biological activities exhibited by the Dilleniaceae family are varied, encompassing anti-inflammatory, antioxidant, antimicrobial, and anti-ulcer properties, which can be primarily attributed to the presence of flavonoids and terpenoids (Branquinho, Verdan, dos Santos, et al., 2021; Branquinho, Verdan, Silva-Filho, et al., 2021; Raissa Borges Ishikawa et al., 2017; Lima et al., 2014).

We now have evidence that *D. dentatus* ecotypes contain several forms of phytohormones with distinct effects that might be able to influence its wider phytochemical profiles (Ewart smith, 2023). Phytohormones, organic signalling molecules derived from plants, play crucial roles in regulating all plant processes including growth, development, source/sink transitions, and nutrient distribution; moreover, they function as key mediators in plant response to various biotic and abiotic stresses, thereby enabling plants to adapt to their dynamic environment (Kamada-Nobusada et al., 2013). These compounds are typically synthesized in small amounts ($<10^{-8}$M) within the plant and are produced both in root and aerial organs (Hirose et al., 2008; Kamada-Nobusada et al., 2013; Kuroha et al., 2009; Takei et al., 2004).

***Doliocarpus dentatus* red ecotype (A)**

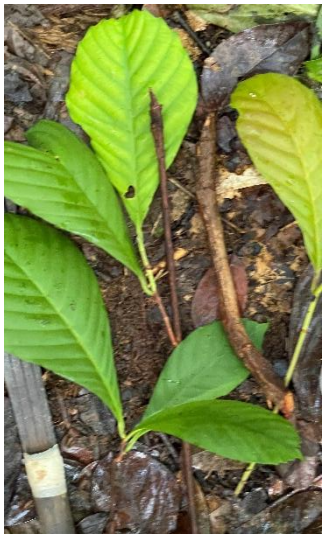

***Doliocarpus dentatus* leaves (both ecotypes) (B)**

***Doliocarpus dentatus* white ecotype (C)**

***Doliocarpus dentatus* red ecotype (D)**

***Doliocarpus dentatus* Fruit (both ecotypes) (E)**

***Doliocarpus dentatus* white ecotype (F)**

Figure 4.1. *D. dentatus* red and white ecotypes morphological features. (1A). *D. dentatus* red outer bark, (1B) mature leaves of both ecotypes, (1C) *D. dentatus* white outer bark, (1D) D. dentatus red inner bark, (1E), *D. dentatus* young leaves of both ecotypes and (1F) *D. dentatus* white inner bark. Photos by Ewart Smith (21N0261909 – 0578704 - Potaro Siparuni, August 2021, Guyana).

Extensive research has been carried out on phytohormones, including Auxins (IAA), cytokinins (CK), gibberellins (GA), abscisic acid (ABA), and ethylene (ET) (Aoki et al., 2024; Bean et al., 2022; Gibb et al., 2020; Kisiala et al., 2019; Kisiala et al., 2013; Morrison & Woldemariam, 2022; Peres et al., 2019; Valleser, 2022). These plant hormones are well known for their roles in controlling plant growth, development, and reactions to environmental stimuli across disciplines such as biotechnology, agriculture, and horticulture (Bychkov et al., 2024; Jogawat et al., 2021). Recently, there has been an increasing emphasis on researching CKs, their related conjugates, and how they interact with plant secondary metabolites such as polyphenols, flavonoids, terpenoids, and alkaloids (A Urra et al., 2013; Abbey et al., 2024; Gautam, 2023; Jenča et al., 2024; Qiu et al., 2018; Zhang et al., 2025). Emerging evidence suggests there are intricate relationships between CKs and secondary metabolites in plants, through complex signaling pathways and biochemical processes. Understanding these interactions will help in developing new strategies to enhance crop yield, improve stress tolerance, understand therapeutic benefits and manage plant growth in various environmental conditions (Skalak et al., 2021).

CKs are phytohormones that play pivotal and significant roles in virtually all aspects of plant growth. They regulate processes such as cell division, differentiation, photosynthesis, and distribution of nutrients to actively growing sites (Jogawat et al., 2021; Kambhampati et al., 2017; Kieber & Schaller, 2018). Additionally, CKs are instrumental in flower and seed development, seed filling, the regulation of leaf senescence and anthocyanin production (Hutchison & Kieber, 2002). These hormones are vital for the production of crops or other plant products that are valuable to humans and enable plants to respond to both biotic and abiotic environmental factors (Fahad et al., 2015; Goh et al., 2019; Mok & Mok, 2001). Moreover, CKs act as signalling

molecules in beneficial interactions with plant growth-promoting microbes and are essential regulators of plant defence mechanisms against pathogenic species (Chanclud et al., 2016; Jorge et al., 2019). CKs have been discovered in a broad range of organisms beyond plants, including bacteria, fungi, algae, nematodes, insects, and even mammals (Jiskrová et al., 2016; Wareing et al., 1977; N. Zhang et al., 2016).

Chemically, CKs are small molecules that are derivatives of an adenine structure with an isoprenoid or aromatic side chain attached to the N^6 position, (Fig 2) (Goh et al., 2019; Kieber & Schaller, 2018; Márquez-López et al., 2019). Four primary types of naturally occurring CKs include: isopentenyladenine (iP), zeatin—which includes both *trans*- and *cis*-isomers (*t*Z, *c*Z) and dihydrozeatin (DZ) (Fig 2). Other CKs can have aromatic side chains, such as ortho-topolin (oT), benzyladenine (BA), and kinetin (KIN). These aromatic CKs are often used in bioassays because of their increased biological activity, although they are less prevalent in nature than the isoprenoid CK forms (Márquez-López et al., 2019). Further modifications to CK structures result in different forms including riboside and nucleotide derivatives as well as downstream sugar conjugates. CK conjugates can result from glycosylation, xylosylation, or amino acid attachment. Glycosylation, facilitated by the enzyme UGT, occurring at the *O*- or *N*-position of the CK molecule is thought to deactivate CKs (Fig 2). Irreversible *N*-glucosides, form especially when CK levels are high due to gene overexpression or external CK application. *O*-glucosides, on the other hand, can be de-glycosylated and act as a storage form of free-CKs. Large amounts of *N*-glucosides of isopentenyl adenine (iP) and *trans*-zeatin (tZ) are found outside plant cells, particularly in the xylem. This modification of CKs helps regulate their levels and activity within plants (Fox et al., 1973; Galichet

et al., 2008; Hošek et al., 2020; Jiskrová et al., 2016; Parker et al., 1972; Wareing et al., 1977; D. Zhang et al., 2016).

This differential metabolism of *N*-glucosides represents a novel mechanism for regulating bioactive cytokinin levels, with *tZ N*-glucosides functioning as a readily accessible storage form rather than merely an irreversible inactivation product (Hošek et al., 2020; Hoyerová & Hošek, 2020). Additionally, a thiol group (-SH) can be added to position 2 of the adenine ring to create methylthiolated CKs (Gibb et al., 2020). The biological activity of these modifications to the chemical structure remains largely unknown (Goh et al., 2019).

Phytohormones, which are naturally occurring compounds in plants that regulate growth and development, present potential therapeutic benefits for humans (Del Mondo et al., 2023). Specific phytohormones, such as salicylic acid (SA), abscisic acid (ABA), and jasmonic acid (JA), exhibit antioxidant properties that protect cells from damage caused by free radicals (Baltazar et al., 2011; Randjelović et al., 2015). Others possess anti-inflammatory effects, which may assist in the management of inflammatory conditions (Randjelović et al., 2015; Thrash-Williams et al., 2016; Zheng et al., 2018). Certain phytohormones have been associated with improvements in cardiovascular health by reducing blood pressure and enhancing cholesterol levels, while additional compounds demonstrate neuroprotective effects that could safeguard brain cells. Research suggests that some phytohormones exhibit anticancer properties, inhibiting the growth and spread of cancer cells (Fausto de Souza et al., 2020). Furthermore, phytohormones may promote skin health by stimulating collagen production, reducing wrinkles, and enhancing skin elasticity; contribute to bone health by facilitating bone formation and preventing bone loss; and

modulate the immune system, thereby enhancing its capacity to combat infections and diseases (Del Mondo et al., 2023; Egamberdieva et al., 2017).

In both humans and animals, cytokinins and their derivatives demonstrate a range of effects at both the cellular and organismal levels, indicating potential therapeutic applications, including efficacy in the treatment of proliferative diseases such as cancer (Casati et al., 2011). Cytokinin ribosides have shown anticancer activity in both in vitro and in vivo studies (Voller et al., 2010). Kinetin, a specific type of cytokinin, has been observed to protect cells against oxidative stress at low doses by reducing apoptosis (Othman et al., 2016). Additionally, cytokinins may exhibit antioxidant properties, thereby providing protection against oxidative damage and enhancing cellular viability(M. Fathy et al., 2022; Naseem et al., 2020).

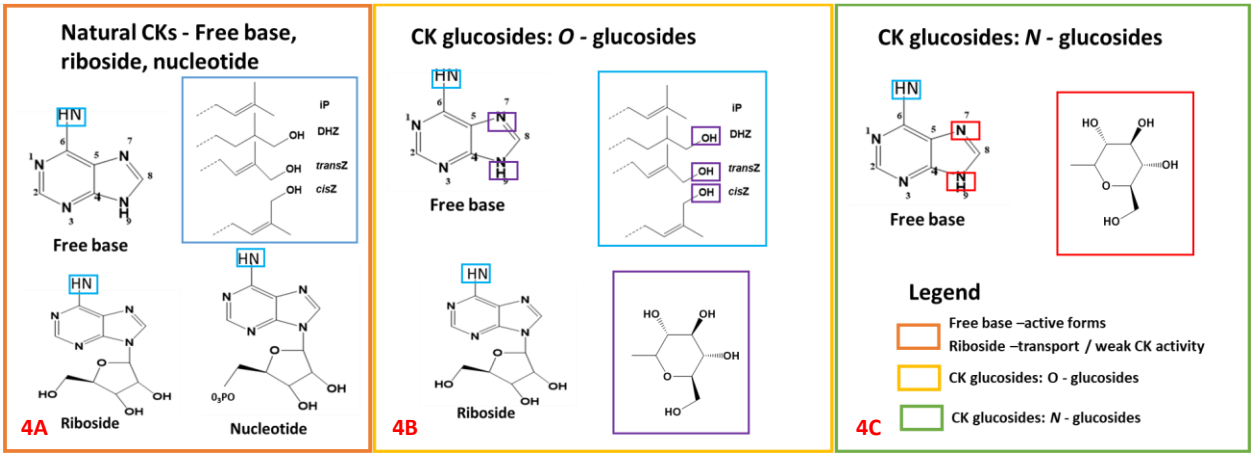

Figure 4. 2. Chemical structure of cytokinins (CKs), adapted and modified from (Márquez-López et al., 2019; Morrison, Emery, et al., 2015). Panel (4A) exhibits the adenine structure, and the numbering system utilized for CK nomenclature, encompassing free base, riboside, and nucleotide CKs. Panel (4B) outlines CK O-glucosides, and (4C) demonstrates N-glucosides. Blue boxes highlight the incorporation of side chains, with larger blue boxes indicating the various side chains. For O-glucosides, blue boxes indicate the glucose structure and glycosylation sites. Similarly, purple and red boxes indicate the glucose structure and glycosylation sites for N-glucosides.

CK interaction with secondary metabolites is an area of growing interest in plant biology, as these interactions can influence both the biosynthesis of secondary metabolites and the overall metabolic profile of plants (Kabera et al., 2014). CKs have been shown to influence the biosynthesis of various secondary metabolites, including flavonoids, phenolic compounds, and alkaloids (Jogawat et al., 2021; Kabera et al., 2014; Kumari et al., 2023). Research has shown that CKs have significant effects on many genes involved in secondary metabolism, especially those in flavonoid biosynthesis which are important for plant defence and pigmentation (Costa-Pérez et al., 2023; Dobrev et al., 2017; Lebedev et al., 2022). In the carob study, the combination of 6-benzyladenine (BA) (a synthetic cytokinin) and UV-C irradiation resulted in increased levels of soluble flavonoids, flavonols, and hydroxycinnamic acids. This enhancement is often mediated through the upregulation of genes involved in the flavonoid biosynthetic pathway (Bhargava et al., 2013) and their critical role linked to redox states in cells, particularly glutaredoxin genes, which suggested a protective function against oxidative stress (Dobrev et al., 2017; Lebedev et al., 2022). Research has revealed that CKs such as BA play a critical role in boosting the biosynthesis and accumulation of secondary metabolites in *Santalum album* heartwood (Celedon et al., 2016; Meng et al., 2024). BA application significantly enhanced the production of essential oil (EO), flavonoids, and phenolics. BA treatment also upregulated genes involved in terpenoid and flavonoid biosynthesis, showcasing its regulatory effect on metabolic pathways. Additionally, BA synergized with other phytohormones such as auxins, gibberellins, and jasmonic acid to promote essential oils (EO) biosynthesis. Transcriptomic and metabolomic analyses revealed that BA

activates a complex regulatory network, inducing heartwood formation and improving metabolite production (Li et al., 2021; Zhang et al., 2025; Zhang et al., 2021).

The biosynthesis of phenolic compounds, which serve various functions including UV protection and pathogen resistance, can also be influenced by CK levels (Aremu et al., 2015; García-Pérez et al., 2021; Marchica et al., 2020; Ray, 1986). Studies have indicated that CKs can stimulate the production of phenolic acids in certain plant species, thereby enhancing their antioxidant capacity and overall stress tolerance (Åstot et al., 2000; Costa-Pérez et al., 2023; Kytidou et al., 2020; Lv et al., 2021b). As an example, CKs have the remarkable ability to stimulate development and trigger the production of secondary metabolites called phytoalexins found in legumes, potato, (*Solanum tuberosum*) banana (*Musa species*), Tomato (*Solanum lycopersicum*) and Rice (*Oryza sativa*). These phytoalexins serve as protective mechanisms that help plants defend against diseases (Jogawat et al., 2021; Lee et al., 2024). This interaction is particularly relevant in the context of plant responses to biotic and abiotic stresses, where phenolic compounds play a crucial role in defence mechanisms (Dobrev et al., 2017; Khetsha et al., 2021).

CKs have been reported to affect the accumulation of alkaloids in certain plant species, which can enhance a plant's defence mechanisms against herbivores and pathogens (Kadi et al., 2013; Tariq et al., 2019). *Catharanthus roseus* and *Amaryllidaceae species* are prominent sources of alkaloids. The application of CKs has been shown to enhance their alkaloid production, potentially through the modulation of specific biosynthetic pathways. (Allen et al., 2002; Correa et al., 2022). This observation indicates that CKs may function as signalling molecules, promoting metabolic

flux toward alkaloid biosynthesis (Aoki et al., 2024; Aremu et al., 2015; López-Vázquez et al., 2024).

CKs exhibit a variety of physiological functions, involving subtle changes in structure that allow for fine-tuning of various physiological processes in plants (Ahmad et al., 2023). CKs, like other phytohormones, are found in living tissues at extremely low concentrations, (fmol to pmol concentrations) (Kisiala et al., 2019; Márquez-López et al., 2019). Because of this, very accurate and sensitive analytical tools are needed to find and measure CKs in biological samples, which usually have complex chemical matrices. Liquid Chromatography-Electrospray Ionization-Mass Spectrometry (LC-ESI-MS) can accurately detect and measure many different chemical compounds (Smith, 2006; Stuckey, 2014; Wingfield & Wilson, 2016). Documenting potential interactions between phytohormones and secondary metabolites would offer valuable insights into the biochemical pathways in plants that may contribute to their medicinal properties. (Jogawat et al., 2021; Santino et al., 2013). Moreover, understanding any interactions between phytohormones and secondary metabolites would offer a chance to improve the therapeutic efficacy of medicinal plants.

In Guyana, the *D. dentatus* red ecotype is the preferred choice for traditional applications to treat illnesses, including the after-effects of malaria, cystitis, erectile dysfunction and leishmanial ulcers. It is also used as a contraceptive and disinfectant (Aponte et al., 2008; Hamuel, 2012; Lima et al., 2014; van Andel, 2000). However, there is a significant lack of understanding regarding the phytohormone profiles between *D. dentatus* red and white ecotypes and any associations with secondary metabolites. The metabolic network involving CKs and secondary metabolites can be complex, as CKs may influence the biosynthesis of secondary metabolites and they are subject to regulation (Motyka et al., 2003; Nester & Ditchenko, 2020; M. Zhang et al., 2024).

Our previous work on *D. dentatus* red and white ecotypes shows that the red ecotype has a relatively higher abundance of flavonoids (epicatechin methyl gallate and catechin gallate), phenolic compounds (gallic acid, catechol and protocatechuic acid) and alkaloids (Ewart smith, 2023). This may be the reason why the red ecotype is preferred and more commonly used in contrast to the white ecotype.

Given the importance of understanding these complex interactions, our research aims to expand our knowledge of CKs and their relationships with secondary metabolites in medicinal plants, focusing specifically on *D. dentatus* ecotypes. The primary objective was to analyze the CK composition of *D. dentatus* ecotypes and investigate any associations with various secondary metabolites, including alkaloids, flavonoids, and other phenolic compounds. By highlighting these relationships, we hope to gain insight into the regulation of complex biochemical processes and signalling pathways involved in secondary metabolite production. Ultimately, this study aims to

deepen our understanding of the medicinal properties of the specific ecotypes of *D. dentatus* and contribute to ongoing efforts to develop treatments using medicinal plants.

4.2. MATERIAL AND METHODS

4.2.1. Collection sites for *D. dentatus* red and white ecotypes - Eagle Mountain Forest Potaro – Siparuni, Guyana.

The Eagle Mountain Forest is located approximately 200 km south-southwest of Georgetown, the capital city of Guyana (21N0261909 - 0578704). The forest features steep sandstone ridges ranging in elevation from 100 m to 724.8 m above sea level. The annual rainfall in this area is exceptionally high, ranging from 3500-4000 mm, with a peak in May and June (Fig 3). In July 2022 and December 2024, a total of three biological samples of the red and white ecotypes were collected at random from the *D. dentatus* liana population found in the Eagle Mountain study location (Fig 4.3). A biological sample refers to plant material collected from the same wood vine (Mei et al., 2019). *D. dentatus* red was collected in plot A 200 meters from plot B where *D. dentatus* white ecotype was collected. These collections included both red and white *D. dentatus* , ranging in diameter classes from 4 cm to 20 cm (Ewart smith, 2023). The differences between *D. dentatus* red and white are recognized by their wood colour (Fig 4.1) instead of their botanical features such as leaves outer and inner barks and fertile organs (van Andel, 2000).

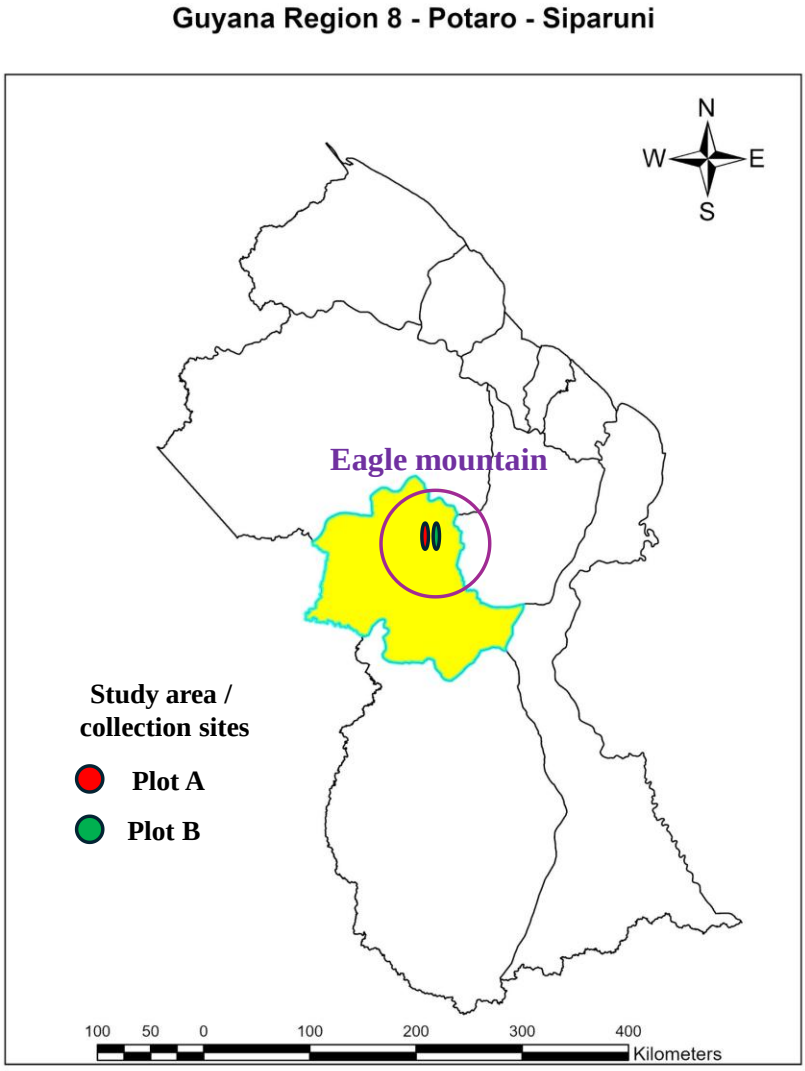

Figure 4. 3. Map of the Study area on the Eagle Mountain Forest located in Potaro Siparuni (21N0261909 - 0578704) Region 8. The yellow area highlights Potaro Siparuni Region 8 of which the study area is a part encompasses. Plot A the collection of the *D. dentatus* red ecotype represented by a red circle. Plot B collection of *D. dentatus* white ecotype represented by the green circle.

4.2.2. Extraction and purification of phytohormone and metabolites

The extraction of multiple phytohormones from *D. dentatus* red and white ecotypes was performed with slight modifications to previously published methods (Aoki et al., 2019; Castilla et al., 2022; Kojima et al., 2009; P. Brandon Matheny et al., 2003; Stirk et al., 2018; Stirk et al., 2013). The Guyana Capadulla extracts (GCE) samples, (Fig 4.1, panel A-D) were pulverized using a Thomas Wiley Mill (Model ED-5; Greater Minneapolis, USA). The grounded samples were sieved and immediately stored at -80°C for later extraction. Tissue 30 gm ± 0.03 was ground using a ball mill grinder and zirconium oxide grinding beads (Comeau Technique Ltd., Vaudreuil-Dorion, Canada; 25 mZ, 5 minutes, 4℃). Stainless steel grinding cylinders were used for tissue (xylem and phloem) greater than ~ 0.25 g (25 mZ, 30 seconds, 4 ℃, Retsch MM300). In each sample, 1 mL of 80 % methanol (MeOH), 1M of formic acid (HCOOH) 0.5 mL of chloroform ($CHCI_3$), and 0.2 mL of water (ddH_2O) were added with 10 nanograms (ng) of each internal standard (IS) (Fig 4.1, Table 1 and 2 contains a list of all of the CKs and phytohormones scanned that were detected with their internal standards and other analytes scanned that were not detected (Tables 4.1, 4.2).

Table 4. 1**.** Cytokinins (CKs) and congregates that were scanned and detected in either or both of *D. dentatus* red and white ecotypes.

Endogenous CKs	Abbreviation	^{2}H-labelled Internal Standards	Concentration (ng)
Free bases (CKFB)			
N^6-isopentenyladenine	iP	$^{2}H_6$iP	10
trans-zeatin	*t*Z	$^{2}H_3$DZ	10
cis-zeatin	cZ	$^{2}H_3$DZ	10
Dihydrozeatin	DZ	$^{2}H_3$DZ	10
Ribosides (CKRB)			
N^6-isopentyadenosine	iPR	$^{2}H_6$[9R]iP	10
trans-zeatin riboside	*t*ZR	$^{2}H_5$[9R]*t*Z	10
cis-zeatin riboside	cZR	$^{2}H_5$[9R]*t*Z	10
Dihydrozeatin riboside	DZR	$^{2}H_3$[9R]DZ	10
Glucosides (CKGLUC)			
isopentenyladenine-7-glucoside	iP7G	$^{2}H_6$iP	10
isopentenyladenine-9-glucoside	iP9G	$^{2}H_6$iP	10
trans-zeatin-O-glucoside	*t*ZOG	$^{2}H_5$tZOG	10
cis-zeatin-O-glucoside	cZOG	$^{2}H_5$tZOG	10
Dihydrozeatin-O-glucoside	DZOG	$^{2}H_7$DZOG	10
Dihydrozeatin-O-glucoside riboside	DZROG	$^{2}H_7$DZROG	10
trans-zeatin-9-glucoside	*t*Z9G	$^{2}H_5$tZ9G	10
cis-zeatin-9-glucoside	cZ9G	$^{2}H_5$tZ9G	10
Dihydrozeatin-9-glucoside	DZ9G	$^{2}H_3$DZ9G	10

Homogenized GCE samples were sonicated, vortexed and centrifuged at 8400 x g for 20 minutes (Sorvall ST 16 Centrifuge or Fisher Scientific Centrifuge at maximum speed). The extraction used MeOH, $CHCl_3$ and DI H_2O which resulted in the separation into polar and nonpolar fractions. The polar fraction on the top layer was decanted into another vial (Fig 4). A second round of extractions for the polar fraction was performed in the same way, except residues were reconstituted in 1 mL of 1 M formic acid to completely protonate all CKs (Kisiala et al. 2019; Persaud et al. 2025). The polar fraction was subdivided into phytohormones and metabolites fractions. The solvent fractions of MeOH and $CHCl_3$ were combined to calculate total CKs within

both *D. dentatus* ecotypes. A second round of extractions was performed in the same way except residues were reconstituted in 1 mL of 1 M formic acid to ensure the complete protonation of all CKs.

Table 4.2. Cytokinins (CKs) and phytohormones were scanned but not detected in either of *D. dentatus* red or white ecotypes

Endogenous CKs	Abbreviation	^{2}H-labelled Internal Standards	Concentration (ng)
Glucosides (CKGLUC)			
trans-zeatin-O-glucoside riboside	*t*ZROG	$^2H_5$tZROG	10
cis-zeatin-O-glucoside riboside	cZROG	$^2H_5$tZROG	10
Methylthiols (2MeS-CK)			
2-Methylthio- N^6-isopentayladenine	2MeSiP	$^2H_6$2MeSiP	10
2-Methylthio-N^6-isopentenyladenosine	2MeSiPR	$^2H_6$2MeSiPR	10
2-Methylthio-zeatin	2MeSZ	$^2H_5$2MeStZ	10
2-Methylthio-zeatin riboside	2MeSZR	$^2H_5$2MeStZR	10
Aromatics			
Kinetin	KIN	$^2H_7$BA	10
N^6-benzyladenine	BA	$^2H_7$BA	10
N^6-benzyladenosine	BAR	$^2H_7$[9R]BA	10
Acidic Phytohormones			
Abscisic acid	ABA	[$^2H_4$] ABA	60
Indole-3-Acetic Acid	IAA	[$^2H_5$] IAA	10
Jasmonic acid	JA	[$^2H_6$] JA (not added)	
Salicylic acid	SA	[$^2H_4$]SA	10
Gibberellin A_1	GA_1	[$^2H_4$]GA_1	20
Gibberellin A_4	GA_4	[$^2H_2$]GA_4	20
Gibberellin A_7	GA_7	[$^2H_2$]GA_7	20
Gibberellin A_9	GA_9	[$^2H_2$]GA_9	20
Gibberellin A_{20}	GA_{20}	[$^2H_2$]GA_{20}	20

HLB cartridges (VIOLET™ 200mg/6 mL, 40 mL; Canadian Life Sciences; Peterborough, Canada) were pre-conditioned with methanol, DI H2O, and 50% ACN before loading supernatants. 2 mL of 30% aqueous ACN was then added. Each extract was divided into two fractions: one for CK analysis, the other was subjected to derivatization of acidic phytohormones

and other metabolites. The derivatization process was carried out using a modified method based on Kojima et al. All samples were evaporated to dryness at ambient temperature in a speed vacuum centrifuge concentrator (Thermo Savant UVS 400a; Thermo Fisher Scientific, Berlin, Germany).

4.2.3. Derivatization of acidic phytohormones

The dried samples were reconstituted with 75 µL of 1-propanol (Fisher Scientific; Ottawa, Canada), 20 µL of DIH_2O water, 5 µL of 500 mM bromocholine (Fisher Scientific; Ottawa, Canada) in 70% ACN, and 1 µL of triethylamine (Fisher Scientific; Ottawa, Canada). These mixed samples were vortexed and incubated at 80 °C for 130 minutes. Following incubation samples were transferred to ice and dried using a speed vacuum concentrator (Thermo Savant UVS 400a; ThermoFisher Scientific, Berlin, Germany) as above for 3 hours (A Urra et al., 2013; Fahad et al., 2015; Goh et al., 2019; Hutchison & Kieber, 2002; Kambhampati et al., 2017; Kieber & Schaller, 2018; Mok & Mok, 2001; Skalak et al., 2021; Zhang et al., 2025) .

4.2.4. Solid phase extraction - sequential elution of CK fractions: free base, riboside, methyl-thiolated and nucleotide forms.

The sequential extraction of free base, riboside, methylthiolated, and nucleotide forms of CK was performed following Kisiala et al.(Kisiala et al., 2019) and Morrison et al. (Morrison, Emery, et al., 2015). The CK isolation procedure used MCX cartridges (Oasis MCX 6 cc; Waters, Mississauga, Canada) specifically designed for simple, polar compounds. Dried supernatant residues were reconstituted in 1 mL of 1 M formic acid (HCOOH) to facilitate the complete protonation of CKs. The reconstituted samples were subjected to MCX SPE. Solid-phase

extraction (SPE) using a mixed-mode, reverse-phase/cation exchange cartridge. The cartridges were activated with 5 mL of methanol and equilibrated with 5 mL of 1 M formic acid. Following the equilibration process, the sample was loaded onto the cartridge and subsequently washed with 5 mL of 1 M formic acid (Morrison, Emery, et al., 2015). Samples were resuspended in 300 µL of AcOH: ACN: DIH_2O in a volumetric ratio of 0.08:5:94.92 (v: v: v) respectively. Samples were then centrifuged at 8400 x g for 10 min and transferred to 2 mL clear vials fitted with 350 µL glass inserts and stored at -20°C until mass spectrometry analysis.

The gradient elution and acquisition mode for mass spectrometry analysis was followed as previously published (Bean et al., 2022; Ewart smith, 2023; Kisiala et al., 2019). A Thermo Q-Exactive™ Orbitrap mass spectrometer, coupled to a Thermo Dionex Ultimate 3000 Liquid Chromatograph System, was used to obtain data in full scan (FS) mode (Thermo Scientific, San Jose, CA, USA). CKs were measured in positive ionization mode. Acidic phytohormones were monitored using a full scan in positive ionization mode for 10 minutes. The experiment encompassed a mass range from m/z 80 to 900. The analysis was conducted at a resolution of 140,000 at m/z 200, employing a full width at half maximum (FWHM) configuration.

The categorization of phytohormones in different sample types based on CK groups, including aromatics, free bases, ribosides, nucleotides, glucosides, and methylthiols are specified in (Table 1 and 2). Furthermore, the classification by Bean et al. (Bean et al., 2022) was employed to determine the CK types, namely iP, *t*Z, *c*Z-, and DZ-types, and glucosides.

Isotope dilution analyses were used to determine the quantities of plant phytohormones. quantifying the peak areas of the endogenous analytes relative to those of internal standards (IS). (Kisiala et al., 2019). following formula, phytohormone concentration [pmol/gFW] = (((peak area

of analyte/peak area of IS) × mass of IS)/MW × 1000)/mass of sample; where FW − mass of the tissue, mass of IS = (10 ng, 20 ng or 60.1ng for CKs, GAs and ABA respectively) as per used in method, MW −molecular mass of CK [g].(Kisiala et al., 2019). Three replicates of each type of plant sample were analyzed. All recorded phytohormones met the level 1 annotation requirements set by the Metabolomics Standards Initiative (Ewart smith, 2023; Schrimpe-Rutledge et al., 2016; Sumner et al., 2007).

4.2.5. Liquid chromatography-mass spectrometry analysis of phytohormones and metabolites

A parallel set of samples was split off from the CK profiling samples described above for red and white ecotypes and those underwent untargeted metabolomics analysis (Fig 4.4) (Kojima et al., 2009). The Thermo Q-Exactive™ Orbitrap mass spectrometer, coupled to a Thermo Dionex Ultimate 3000 Liquid Chromatograph System, was used to obtain mass spectrometry data in full scan (FS) mode (Thermo Scientific, San Jose, CA, USA). Metabolites in the (MeOH) and ($CHCl_3$) fractions were analyzed using both positive and negative modes of electrospray ionization (ESI). The initial mass range was from 80 to 900 m/z, and the resolution was 140,000 at 200 m/z full width at half maximum (FWHM). The automatic gain control (AGC) target was set to 3×10^6, and the maximum injection time (IT) was 524 ms. For the heated electrospray ionization (HESI) probe, the capillary temperature was set to 250 °C, the sheath gas was 30 arbitrary units, and the auxiliary gas was 8 units. The probe heater temperature was set to 450 °C, the S-Lens RF level was 60%, and the capillary voltage was 3.9 kV.

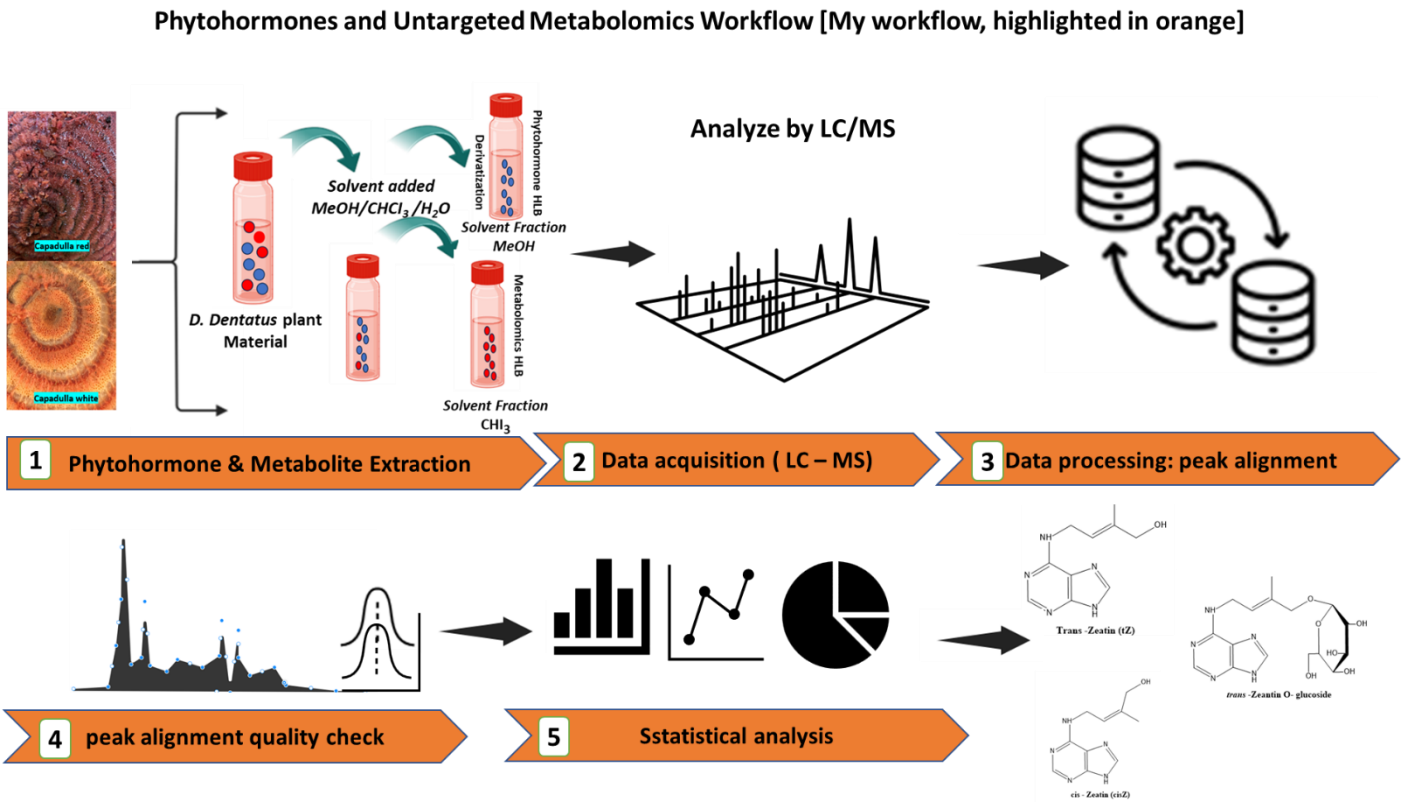

Figure 4.4. The workflow diagram outlines a detailed analysis process for phytohormones and untargeted metabolites in *D. dentatus* plant material. The orange arrows present the different steps in the analysis. (1) the extraction using a MeOH/$CHCl_3$/H_2O solvent mixture, resulting in separated fractions. (2-3) LC-MS analysis follows, with data processing focused on peak alignment and quality control through chromatographic profiles. (4) statistical analysis and visualization using bar charts, line graphs, and pie charts. (5) the final output identifies specific phytohormones and secondary metabolites compounds. The icons used are a combination of Noun Project and BioRender.com.

4.2.6. Metabolomic Analysis of *D. dentatus* ecotypes

The study used the MS transform function of ProteoWizard to convert raw mass spectrometric data into mzXML format (Fig 4.4) (Chambers et al., 2012). LC-MS collection was performed in full scan ionization mode, with negative and positive ions extracted separately. XCMS Online was used for peak identification, retention duration adjustment, and grouping. Statistical analysis was performed using MetaboAnalyst 6.0, with normalization, log transformation, PCA, and PLS-DA

for visualization (Chong et al., 2019). Compound comparisons were made against databases containing physiologically active substances, and potential medicinal chemical families were inputted into XCalibur 4.1 for peak quantification based on protonated and deprotonated masses (Ewart smith, 2023; Morrison & Woldemariam, 2022).

The chemical composition of red and white ecotypes of *D. dentatus* was analysed using various databases and analytical tools (Bartel et al., 2013; Cambiaghi et al., 2017; Ewart smith, 2023; Jiang et al., 2020; Jiang et al., 2022; Morrison & Woldemariam, 2022; Pang et al., 2022; Schrimpe-Rutledge et al., 2016). Key secondary metabolite families such as flavonoids, terpenoids, and alkaloids were identified. The study ensured accurate monitoring of sample peaks and categorized substances based on their relative intensity. This was done using XCMS Online, MetaboAnalyst 6.0 and XCalibur 4.1. software (Ewart smith, 2023).

4.2.7. Statistical Analysis and Bioinformatics tools

Data normalization was executed using sum normalization, $\log^2$ transformation, and Pareto scaling via the Metabo Analyst 6.0 platform (Pang et al., 2022) (www.metaboanalyst.ca, accessed between April 14, 2024, and November 10, 2024). These preprocessing steps were critical for calibrating the data to a common scale for equitable comparison and robust statistical evaluation. After rescaling and normalizing, ANOVA and volcano plot analyses were used to identify any differences between red and white ecotypes and to identify m/z features that had changed significantly, ($P< 0.005$).

XCMS Online was used for LC-MS dataset annotation before utilizing MetaboAnalyst 6.0. A standard volcano plot was used to identify different metabolites using t-tests and fold-change

methods (Cambiaghi et al., 2017). This plot depicted log-transformed fold-change values against negative log-transformed p-values from t-tests. Analysis of Variance (ANOVA) and comparison of Least Significant Difference (LSD) were applied to compare associations between CKs and alkaloids, flavonoids, terpenoids and other compounds present in *D. dentatus* ecotypes.

4.2.8. Tandem mass spectrometry (MS^2) data processing

4.2.8.1. Data pre-processing: feature alignment using mzMine 2.5.3

Data pre-processing for feature alignment utilizing MZmine 2.5.3 is critical for the analysis of mass spectrometry data, especially in the context of data-dependent tandem mass spectrometry (DDA; $ddMS^2$). The workflow commences with the conversion of raw $ddMS^2$ data into mzXML or mzML formats, achieved through the use of the MSConvert tool within ProteoWizard (Bhamber et al., 2021; Ewart smith, 2023). Subsequently, these files undergo processing through the MZmine 2.5.3 pipeline to identify MS^1 features that correspond to MS^2 fragments from various samples (Heuckeroth et al., 2024). The pipeline incorporates parameters including mass detection, chromatogram building, smoothing, deconvolution, deisotoping, alignment, and gap filling, all grounded in established methodologies to ensure consistency (Guo & Huan, 2023; Heuckeroth et al., 2024). The processed data, which is saved in .mgf format, facilitates further analysis with bioinformatics tools (Petras et al., 2022). Particularly proficient in untargeted metabolomics, MZmine 2.5.3 effectively manages large datasets, thereby assisting in the alignment and characterization of compounds within complex biological samples (Heuckeroth et al., 2024; Stincone et al., 2023; Tronel et al., 2024). This robust methodology establishes a foundation for enhancing the understanding of metabolomic profiles.

4.2.9. Metabolite annotation using Global Natural Products Social Molecular Networking (GNPS) and Metabolite annotation using MS-DIAL (v. 5.1)

Metabolite identification was conducted utilizing the GNPS platform through the Classical Molecular Networking workflow (Ewart smith, 2023; Phelan, 2020; Zuo et al., 2024). Mass spectrometry data were processed in MZmine (version 3.0) and subsequently exported for GNPS analysis. A molecular network for both negative and positive ionization data was created using the online workflow (https://ccms-ucsd.github.io/GNPSDocumentation/, accessed on 14 September 2024) on the GNPS website (http://gnps.ucsd.edu, accessed on 14 September 2024). The data were filtered to removed MS/MS fragment ions within ±17 Da of the precursor m/z while retaining the top six fragment ions within a ±50 Da window (Petras et al., 2022; Zuo et al., 2024). Tolerances for precursor and fragment ions were established at 0.02 Da and 0.05 Da, respectively. Molecular networks were constructed with edges necessitating a cosine score exceeding 0.6 and a minimum of three matched peaks, while nodes were interconnected if they ranked among each other's top ten most similar nodes (Zuo et al., 2024). Matches to GNPS spectral libraries were required to adhere to similar thresholds, with DEREPLICATOR employed for additional MS/MS spectrum annotation (Zuo et al., 2024). Cytoscape software was utilized for network visualization (Doncheva et al., 2023; Lima et al., 2021).

Concurrently, LC-MS/MS data were processed using MS-DIAL (version 5.1), concentrating on retention times between 0 and 10 minutes and a mass range of 0 to 700 Da in positive ionization mode (Takeda et al., 2024). MS1 and MS2 tolerances were set at 0.01 and 0.025 Da, respectively, with alignment parameters configured for a 0.015 Da mass tolerance and 0.5 minutes retention

time tolerance (Takeda et al., 2024). Compound confirmation was supported by various public databases, including MassBank, GNPS, ReSpect, and RIKEN PlaSMA, encompassing multiple levels of metabolite identification (MSI) classification (Takeda et al., 2024) Key adducts such as $[M+H]^+$ and $[M+H]^-$ were incorporated into the analysis (Ewart smith, 2023; Takeda et al., 2024). This integrated approach, which amalgamates FBMN and MS-DIAL, facilitated comprehensive metabolite annotation and network visualization, thereby providing deeper insights into the metabolomic profiles of the studied samples (Phelan, 2020; Takeda et al., 2024).

4.2.10. Correlation Analysis

Metabolite AutoPlotter v2.6 represents an advanced analytical tool designed for the analysis and visualization of metabolomic data, encompassing correlation analysis (Matthias Pietzke & Alexei Vazquez, 2020). The data preparation involved organizing the information into Excel files formatted appropriately, specifically with designated columns for phytohormones and metabolites. Upon loading the data, specific variables were analyzed to assess correlations. The Pearson correlation coefficients served as the statistical measure for evaluating the associations between cytokinins (CKs) and various classes of secondary metabolites. For visualization purposes, heatmaps and network diagrams were utilized. These visualizations are customizable, allowing for the accentuation of strong correlations or the highlighting of specific patterns. The default settings were employed to identify significant correlations based on coefficient values and p-values. Ultimately, the correlation matrix and accompanying visualizations were exported for subsequent analysis. Further analysis was conducted on the data processed using Metabolite AutoPlotter v2.6 (https://mpietzke.shinyapps.io/autoplotter) in conjunction with R Studio 12.0.

4.3. RESULTS

4.3.1. Metabolomic and phytohormone profiling of red and white ecotypes of *D. dentatus* using LC-MS/MS and bioinformatics

Liquid chromatography-tandem mass spectrometry (LC-MS/MS) was employed to analyze the phytohormone profiles and metabolomes of the red and white ecotypes of *D. dentatus*. The analysis of CKs was conducted with a targeted approach, while a semi-targeted approach was adopted for the metabolomic analysis. Putative mass-to-charge (m/z) features identified in the metabolomics study were compared against databases containing physiologically active compounds documented in the scientific literature. Public bioinformatics servers were employed to distinguish metabolite features, including GNPS, MS-DIAL, and SIRIUS for untargeted metabolomics studies (Ewart smith, 2023; Pluskal et al., 2020).

Tissue samples were scanned for over 35 different forms of CKs. Of these, 18 forms of CK were detected (Fig 4.5, APX 3, Table 1) and they were classified into three groups based on their function or structure: CK glucosides, active/freebase CKs, and riboside/nucleotide CKs. (Fig 4.5). Among these, CK glucosides, which are considered mostly inactive forms (Cortleven et al., 2019; Kieber & Schaller, 2018; Kleczkowski et al., 1995; Lomin et al., 2015; Šmehilová et al., 2016; Spíchal et al., 2004), were identified in the *D. dentatus* ecotypes, including: DHZOG, DHZROG, DHZ9G, *t*ZOG, *t*ZROG, *t*Z9G, *c*ZOG, *c*ZROG, and *c*Z9G. In addition, active CK forms and their immediate ribose conjugates were detected: iP, iPR, DHZ, DHZR, *t*Z, *t*ZR, *c*Z, and *c*ZR. The concentrations of these analytes are detailed in (Fig 4. 5, APX 3, Table 1).

The red ecotype of *D. dentatus* typically exhibited elevated concentrations of various cytokinins (CKs) compared to the white ecotypes, especially in the glucoside form, which constituted 98.38% of the total CKs (Fig 4.5, S1Table 1). The most notable exceptions were iP7G and iP9G, for which the white, ecotype had higher levels. The red ecotype had higher levels of free base CK (1.83% of what?).

*t*Z and iPR cytokinins exhibited significant interrelationships with various secondary metabolites, including: alkaloids, phenolics, and flavonoids. Notably, *t*Z and iPR had strong positive correlations with phenolic compounds, particularly 1-O-sinapoyl-beta-D-glucose. Additionally, tropine had a strong positive correlation with *c*Z and its derivatives within the alkaloid category. Furthermore, the analysis of flavonoids indicates that leucocyanidin is strongly associated with several types of cytokinins, especially *t*Z derivatives (Fig 4.7). The red ecotype was also enriched in the flavonoid biosynthesis pathway (Fig 4.8).

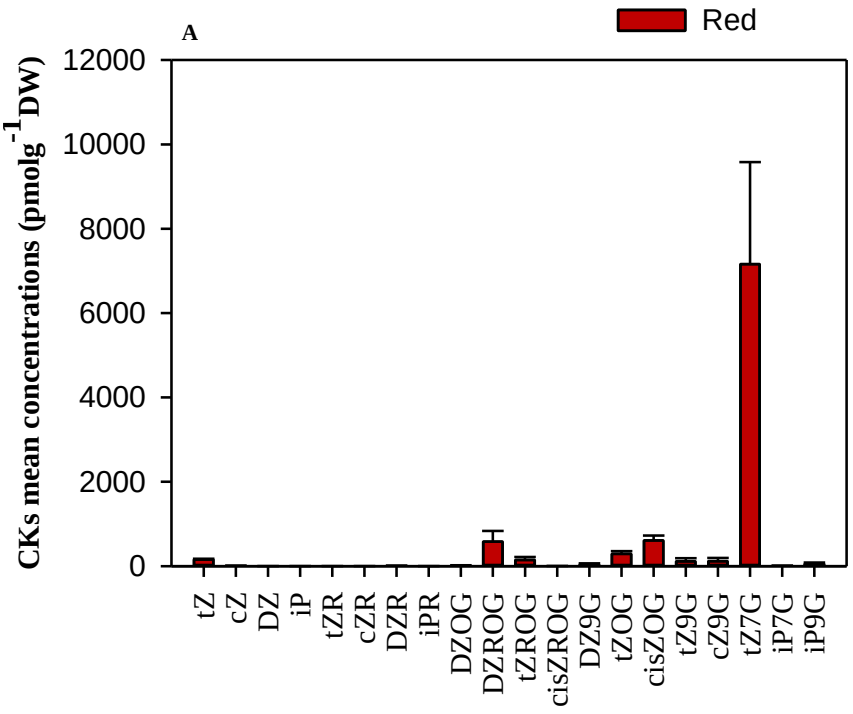
A
Red
CKs mean concentrations (pmolg-1DW)
12000
10000
8000
6000
4000
2000
0
tZ
cZ
DZ
iP
tZR
cZR
DZR
iPR
DZOG
DZROG
tZROG
cisZROG
DZ9G
tZOG
cisZOG
tZ9G
cZ9G
tZ7G
iP7G
iP9G

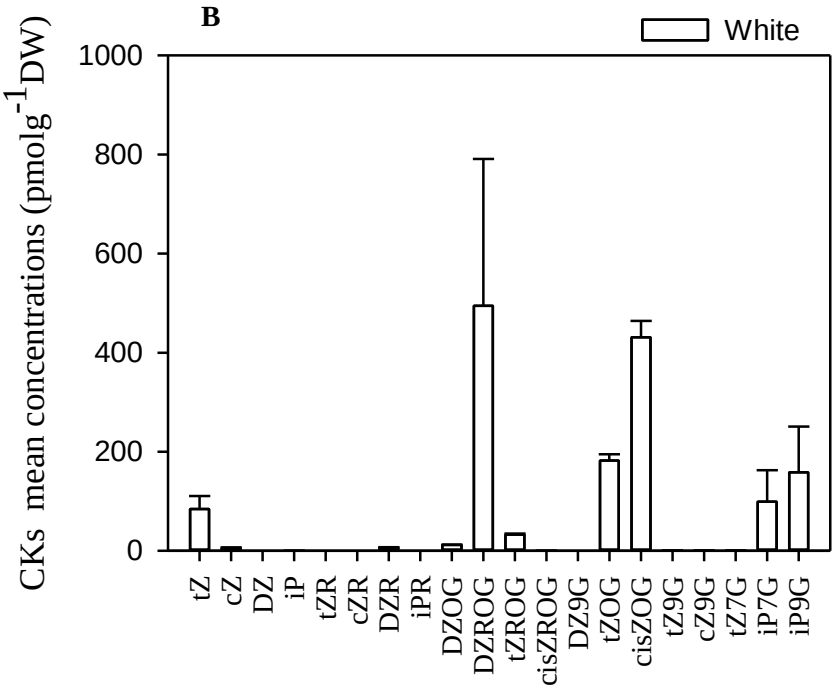
B
White
CKs mean concentrations (pmolg-1DW)
1000
800
600
400
200
0
tZ
cZ
DZ
iP
tZR
cZR
DZR
iPR
DZOG
DZROG
tZROG
cisZROG
DZ9G
tZOG
cisZOG
tZ9G
cZ9G
tZ7G
iP7G
iP9G

Figure 4. 5. The mean CK concentrations and forms (glucosides, freebase and ribosides) (pmol g^{-1} DW) in D. dentatus ecotypes. (A) distribution of CK concentrations in D. dentatus red. (B), distribution of CK concentrations in D. dentatus white ecotypes. The red ecotype exhibits a substantially higher total cytokinin content (9135.49 ± 3174.72 pmol/g FW) compared to the white ecotype (1478.53 ± 527.209 pmol/g FW), indicating a marked difference in cytokinin accumulation between these two ecotypes.

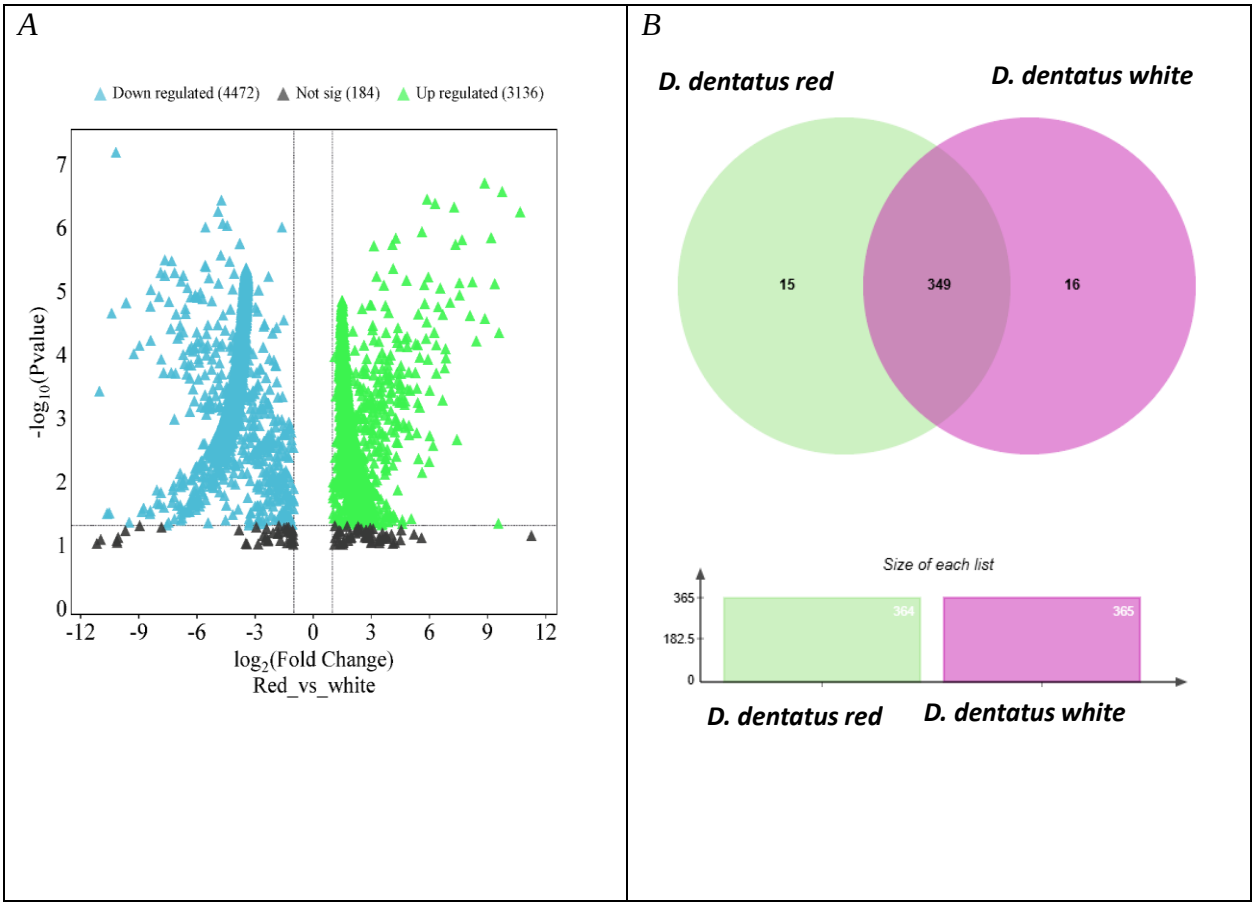

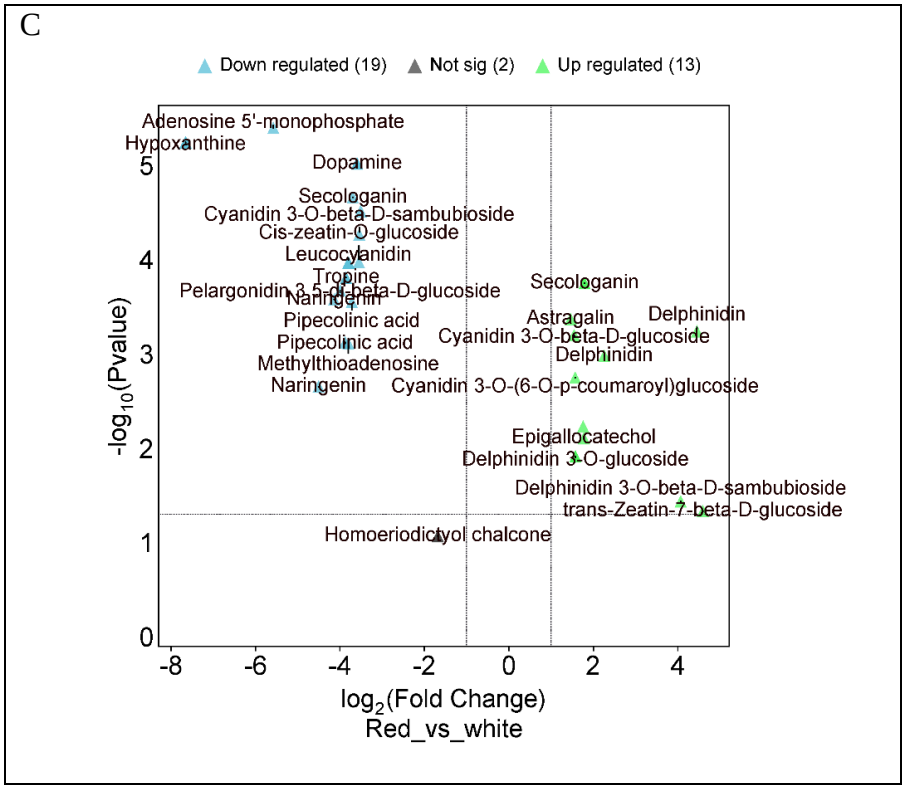

Figure 4. 6. Comparative analysis of phytochemical profiles between *D. dentatus* red and white ecotypes. (A) volcano plot displaying differential tentative metabolites between red and white ecotypes, where green indicates upregulated metabolites in red, blue indicates downregulated metabolites, and black represents non-significant changes. The x-axis corresponds to the logarithmic fold change, which indicates the extent and direction of tentative metabolite expression changes. The y-axis provides the -logarithmic p-values, which indicate the statistical significance of these changes. (B) Venn diagram highlighting shared and unique metabolites in red and white ecotypes, accompanied by bar plots showing the total number of metabolites identified in each ecotype. (C) Highlighted metabolites with significant fold changes, showing key bioactive compounds such as secondary metabolites and phytohormones with differential abundance between the two ecotypes.

The analysis the *D. dentatus* extracts revealed significant differences in metabolite profiles. The white ecotype showed 11,021 potential metabolite features across three samples (N=3), with the *D. dentatus* red ecotype exhibiting 20,382 putative m/z features in both positive and negative ionization modes. The *D. dentatus* white ecotype contained 9,696 potential metabolite features in both positive ionization $[M+H]^+$ and negative ionization $[M-H]^-$ mode (Fig 6).

Further analysis of the metabolomic data using analysis of variance (ANOVA) depicted in the volcano plots (Fig 6 and Fig S1), showed 5,275 mz tentative metabolite features were identified, with 2,829 mz in the positive ionization mode. In the *D. dentatus* red ecotype, 159 mz features were upregulated, and 110 mz features were downregulated, using the white ecotype as a control to identify differences in metabolite profiles. These findings align with previous research, which reported higher upregulation of polyphenols and flavonoids (including flavones, flavanones, flavanonols, and flavone-3-ols) in the red ecotype compared to the white ecotype (Ewart smith, 2023).

In the negative ionization mode, 2,446 mz tentative features were analyzed, resulting in 98 mz features being upregulated and 88 mz features downregulated in the *D. dentatus* red ecotype compared to the white ecotype as the control. To further our understanding of the metabolic differences between the two ecotypes, we utilized the "Functional Analysis" module and the Gene Set Enrichment Assay (GSEA) tool in MetaboAnalyst 6.0 (Fig 6). We compared the 5,275 potential metabolite characteristics acquired from examining the two ecotypes in combined fractions. Utilizing the GSEA program, we searched the annotated *A. thaliana* metabolite database to find metabolite characteristics that closely corresponded to our (m/z) features. This allowed us to recognize resemblances with the Kyoto Encyclopedia of Genes and Genomes (KEGG) database

and GNPS, MS-DIAL, and SIRIUS (Ewart smith, 2023; Pluskal et al., 2020) services in untargeted metabolomics at annotation levels 4 and 3 (Schrimpe-Rutledge et al., 2016).

Upon completion of the global metabolomic analysis, we found 349 putative metabolite features with annotation between levels 2, 3 and 4 (Schrimpe-Rutledge et al., 2016) based on matching reference databases. Among these, 16 features (0.9 %) were exclusive to the *D. dentatus* red ecotype (e.g. kaempferol and luteolin), while 17 putative features (e.g. dihydromyricetin, eriodyctiol and eriodyctiol chalcone) belong to the *D. dentatus* white ecotype (4.2 %). Notably, approximately 91.5 % of these putative metabolite features, were common to the *D. dentatus* red and? white ecotypes (Fig 4.6).

To confirm our matches of the putative m/z from the previous search (Fig 6), the Omics Craft database (http://tools.omicscraft.com/MetaboQuest/, was accessed from September 2024 to November 2024). Putative features were searched within a ± 5 ppm error range with level 3 identification using MetaboAnalyst 6.0 and associated with KEGG pathways. XCalibur Software (version 4.1) verified the masses in sample duplicates (Ewart smith, 2023; Tsugawa et al., 2019). The search revealed the presence of compounds such as naringenin, delphinidin, delphinidin 3 -O-glucoside, *trans* – Zeatin – beta – D-sambubioside, epigallocatechol, and cyanidin – 3 – O – beta D – sambubioside, among others (Fig 7, S, Table 3). The detected *D. dentatus* ecotypes are dominated by polyphenols (63.9%). Polyphenols are essential bioactive phytochemicals present in many plant species, renowned for their powerful antioxidant activities. In light of these benefits, we undertook a more comprehensive investigation of polyphenols, within the *D. dentatus* red ecotype.

4.3.2. Integration of Correlation network analysis with CKs and Alkaloids, Flavonoids and Phenolic compounds

The study utilized correlation network analysis to find possible associations between CKs and secondary metabolites such as alkaloids flavonoids and other phenolic compounds in different ecotypes of *D. dentatus.* The correlation matrix reveals relationships between zeatin variants and other compounds, where orange indicates positive correlations and teal indicates negative correlations (Fig 4.7)

cZ derivatives (cZ9G, cZOG, cZR, cZROG) show positive correlations with coniferin and dopamine, while cZ, cZ9G, cZR, and cZROG exhibit negative correlations with pipecolinic acid. dihydrozeatin (DZ) derivatives (DZ, DZ9G, DZOG, DZR, DZROG) are positively correlated with hypoxanthine and coniferin and negatively correlated with pipecolinic acid. iP derivatives (iP, iP7G, iP9G, iPR) are positively correlated with hypoxanthine and dopamine. Finally, trans-zeatin (tZ) derivatives (tZ, tZ7G, tZ9G, tZOG, tZR, tZROG) tend to have positive correlations with tropine and negative correlations with coniferin (Fig 4.7 A)

Proanthocyanidin_B2, pelargonidin_3,5-di-beta-D-glucoside, naringenin, and leucocyanidin show strong positive correlations among themselves, but negative correlations with trans-zeatin derivatives (tZ, tZ7G, tZ9G, tZOG, tZR, and tZROG). kaempferol_3-O-glucoside, kaempferin, and homoeriodictyol_chalcone are positively correlated but negatively correlated with (cZ, cZ9G, cZOG, cZR, and cZROG). genistein is positively correlated with delphinidin_3-O-glucoside, which in turn shows positive correlations with delphinidin_3-O-beta-D-sambubioside and delphinidin. Further positive correlations are observed within the cyanidin series (cyanidin_3-O-glucoside, cyanidin_3-O-beta-D-sambubioside, cyanidin_3-O-beta-D-glucoside, and cyanidin_3-

O-(6-O-p-coumaroyl)glucoside1), as well as between cyanidin, chalconaringenin, apiforol, 4-coumaroylshikimate, and (-)-cpigallocatechin. Notably, (-)-epigallocatechin exhibits a positive correlation with cis-zeatin derivatives (cZ, cZ9G, cZOG, cZR, and cZROG), while dihydrozeatin derivatives (DZ, DZ9G, DZOG, DZR, DZROG) show some correlations with other compounds, and trans-zeatin derivatives are negatively correlated with proanthocyanidin_B2, pelargonidin_3,5-di-beta-D-glucoside, paringenin, and leucocyanidin (Fig 4.7 B).

The correlation matrix displays relationships between zeatin variants and other compounds, with orange indicating positive and teal indicating negative correlations. Cis-zeatin derivatives like cZ, cZ9G, cZOG, cZR, and cZROG show positive correlations with 3-O-methyl gallate, with cZOG also positively correlated with sinapyl alcohol, while they generally exhibit negative correlations with Vanillic acid; dihydrozeatin derivatives (DZ, DZ9G, DZOG, DZR, and DZROG) are positively correlated with coniferyl alcohol and 3-O-methyl gallate, with DZOG also showing a positive correlation with Sinapyl alcohol, and these forms also show negative correlations with vanillic acid; in contrast, trans-zeatin derivatives (tZ, tZ7G, tZ9G, tZOG, tZR, and tZROG) tend to have positive correlations with sinapyl alcohol, and a negative correlation with 5-O-caffeoyl-shikimic acid, with tZ7G and tZ9G showing weak correlations overall (Fig 4.7 C).

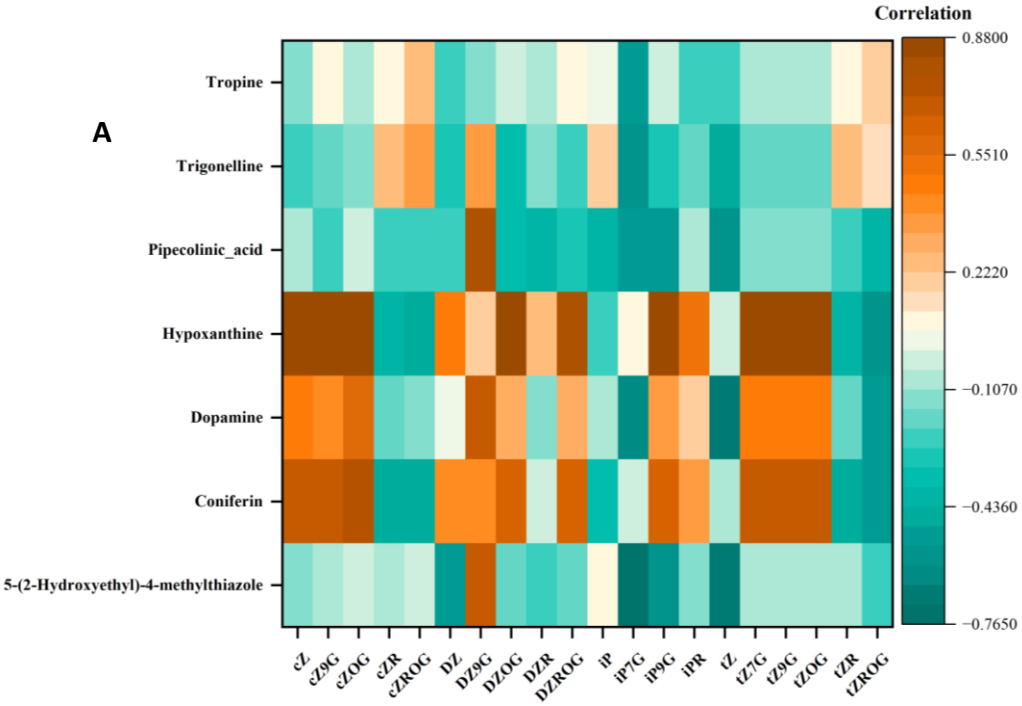
A
Correlation
0.8800
0.5510
0.2220
−0.1070
−0.4360
−0.7650
Tropine
Trigonelline
Pipecolinic_acid
Hypoxanthine
Dopamine
Coniferin
5-(2-Hydroxyethyl)-4-methylthiazole
cZ
cZ9G
cZOG
cZR
cZROG
DZ
DZ9G
DZOG
DZR
DZROG
iP
iP7G
iP9G
iPR
tZ
tZ7G
tZ9G
tZOG
tZR
tZROG

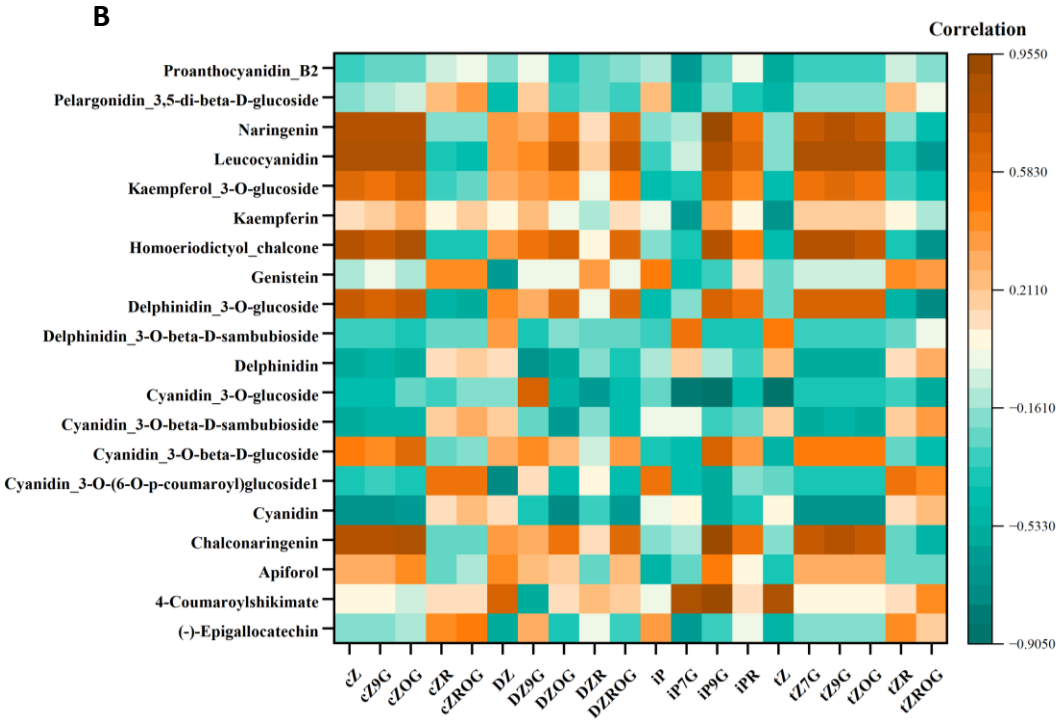
B
Correlation
0.9550
0.5830
0.2110
−0.1610
−0.5330
−0.9050
Proanthocyanidin_B2
Pelargonidin_3,5-di-beta-D-glucoside
Naringenin
Leucocyanidin
Kaempferol_3-O-glucoside
Kaempferin
Homoeriodictyol_chalcone
Genistein
Delphinidin_3-O-glucoside
Delphinidin_3-O-beta-D-sambubioside
Delphinidin
Cyanidin_3-O-glucoside
Cyanidin_3-O-beta-D-sambubioside
Cyanidin_3-O-beta-D-glucoside
Cyanidin_3-O-(6-O-p-coumaroyl)glucoside1
Cyanidin
Chalconaringenin
Apiforol
4-Coumaroylshikimate
(-)-Epigallocatechin
cZ
cZ9G
cZOG
cZR
cZROG
DZ
DZ9G
DZOG
DZR
DZROG
iP
iP7G
iP9G
iPR
tZ
tZ7G
tZ9G
tZOG
tZR
tZROG

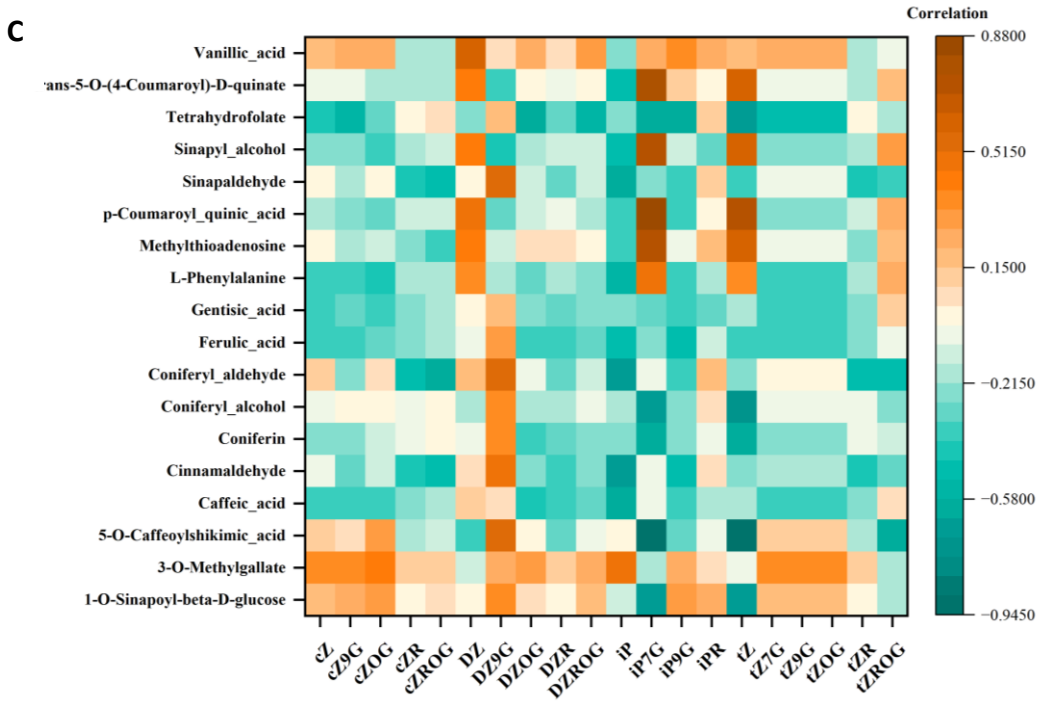

Figure 4. 7. Correlation heatmaps showing the relationships between CKs and three classes of secondary metabolites in *D.dentatus* ecotypes. Panel (A): alkaloid correlations with CKs, displaying values from -0.875 to 0.985. Panel (B): flavonoid correlations with CKs, revealing diverse interaction patterns across different compounds. Brown colors indicate positive correlations while teal colors represent negative correlations. Panel (C): phenolic compounds showing correlations with various CKs, with colour intensity ranging from -0.945 (dark green) to 0.880 (dark brown).

4.4. Visualizing metabolic diversity: biosynthetic signatures in red and white *D. dentatus* ecotypes.

The analysis combines p-values from pathway enrichment analysis with pathway impact values from topology analysis using KEGG pathways in MetaboAnalyst 6.0. The data in the scatter plots reveal the impacts and significance of various biosynthesis pathways in *D. dentatus* ecotypes (Fig 8). In the red ecotype, key pathways such as flavonoid biosynthesis, monoterpenoid biosynthesis, and flavone and flavonol biosynthesis show high impact and significance, as

evidenced by large, dark red dots. These pathways are closely associated with secondary metabolites involved in pigmentation and aroma, reflecting the red ecotype's distinct colouration. Additionally, anthocyanin biosynthesis, another pathway related to pigmentation, displays significance ($p = 0.02 < 0.05$) , further highlighting the metabolic emphasis on colouration in the red ecotype.

In contrast, the white ecotype was enriched in pathways such as phenylpropanoid biosynthesis and flavonoid biosynthesis, but these showed lower pathway impact and significance compared to the red ecotype. Flavone and flavonol biosynthesis were less prominent, reflecting reduced metabolic activity in pigmentation-related pathways. Furthermore, monoterpenoid biosynthesis, significant in the red ecotype, was minimally impactful in the white ecotype. These differences indicate that the red ecotype is metabolically geared towards pigmentation and aroma biosynthesis, while the white ecotype demonstrates lower activity in these pathways, consistent with its lack of pigmentation.

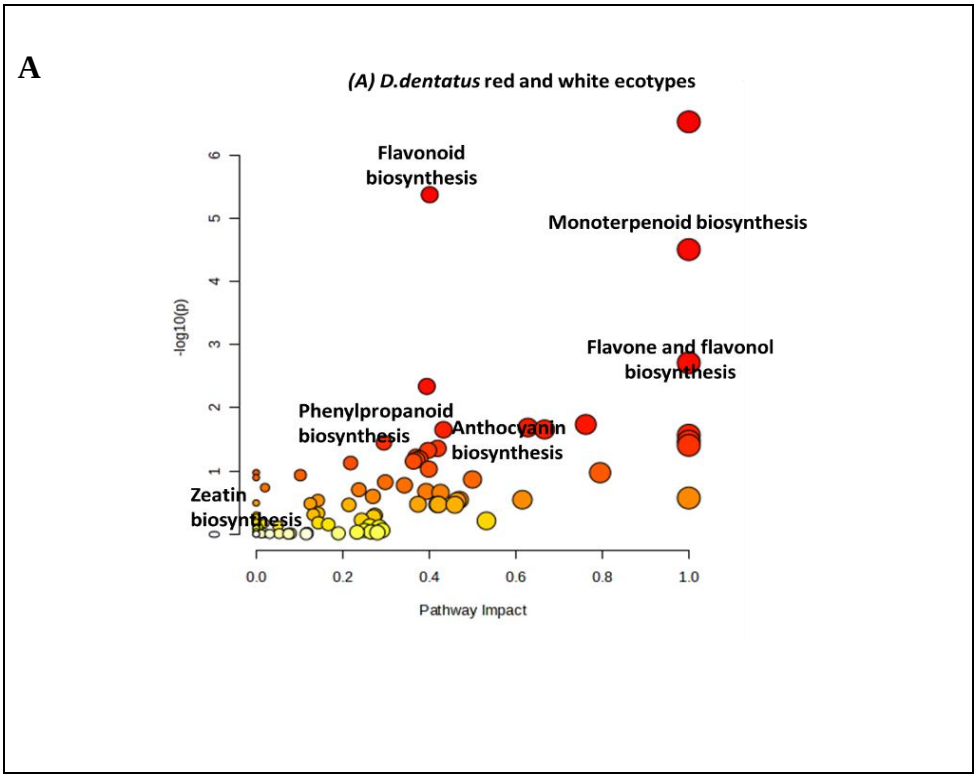
A
(A) D.dentatus red and white ecotypes
Flavonoid biosynthesis
Monoterpenoid biosynthesis
Flavone and flavonol biosynthesis
Phenylpropanoid biosynthesis
Anthocyanin biosynthesis
Zeatin biosynthesis
-log10(p)
Pathway Impact

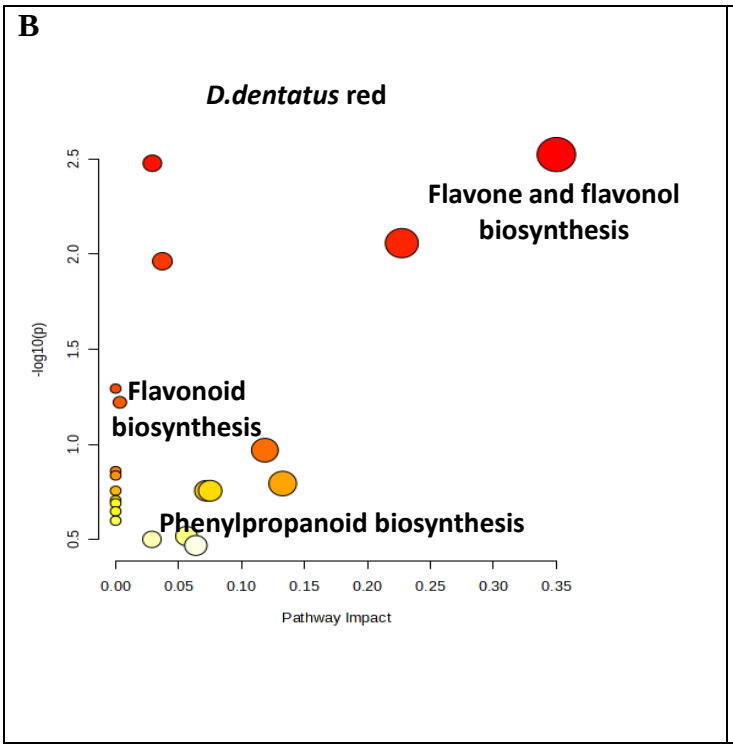
B
D.dentatus red
Flavone and flavonol biosynthesis
Flavonoid biosynthesis
Phenylpropanoid biosynthesis
-log10(p)
Pathway Impact

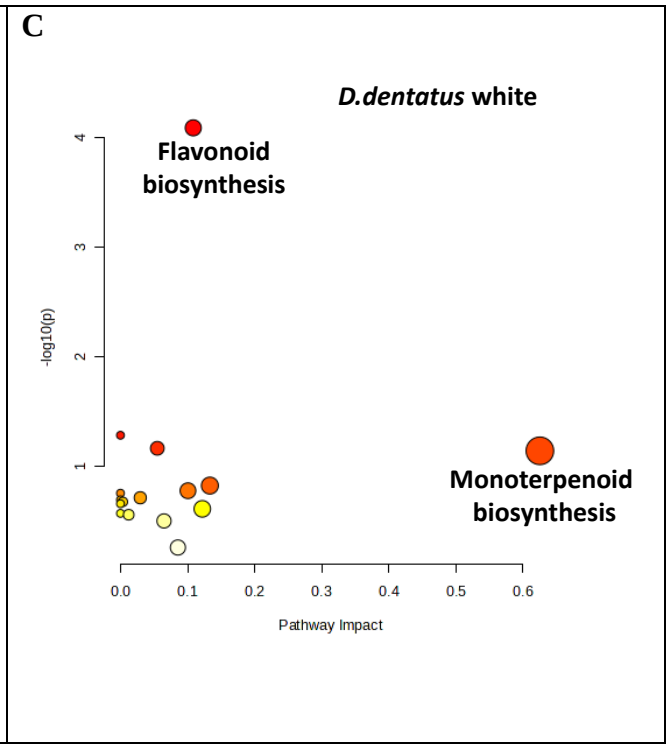
C
D.dentatus white
Flavonoid biosynthesis
Monoterpenoid biosynthesis
-log10(p)
Pathway Impact

Figure 4. 8. Presents a summary of pathway analysis, including selected metabolic pathways obtained from the KEGG and HMDB databases for (A) *D. dentatus* red and white, (B) *D. dentatus* red, and (C) *D. dentatus* white. The pathways that have been found are arranged according to their corresponding p-values, which are shown on the y-axis. These p-values are obtained from the functional analysis pathway enrichment. Furthermore, the x-axis presents pathway effect values obtained from pathway topology analysis. The magnitude of each node in the overview correlates to its effect value, while different node colours reflect variable p-values. The integrated pathway activity profile identifies metabolite properties that are significantly related to biosynthetic pathways, with a statistical significance threshold of $p < 0.05$. The analysis was performed using MetaboAnalyst 6.0, employing the GSEA method with default settings. The Arabidopsis thaliana pathway was used as the reference library.

4.5. DISCUSSION

4.5.1. Guyanese Capadulla *D. dentatus* red and white ecotypes reveal contrasting phytohormone (Cytokinins) profiles.

D. dentaus red and white ecotypes are widely recognized in Guyanese traditional medicine for their application in treating various underlying conditions, including erectile dysfunction (Ewart smith, 2023; van Andel, 2000). However, the interactions between its phytochemistry (phytohormones and phytochemical) remain largely unexplored and poorly understood.

The red and white ecotypes of *D. dentatus* demonstrate substantial medicinal potential due to their distinct phytochemical profiles, particularly in their CKs and secondary metabolite composition. Extracts from *D. dentatus* are rich in bioactive compounds such as alkaloids, phenolics, flavonoids, and triterpenes (Fig 4.7, Table 3) which contribute to its pharmacological properties, including anti-inflammatory, antioxidant, antimicrobial, antitumor and antidiabetic effects (De Toledo et al., 2011; Divekar et al., 2022; Ewart smith, 2023; Kleczkowski et al., 1995; Lomin et al., 2015; Šmehilová et al., 2016; Spíchal et al., 2004). CKs in *D. dentatus*, such as *t*Z *c*Z and iPR have shown promise in reducing oxidative stress, a factor in chronic diseases such as

cancer and neurodegenerative disorders (Allen et al., 2002; Correa et al., 2022; López-Vázquez et al., 2024). Traditional use of *D. dentatus* for conditions such as arthritis, diabetes, and gastrointestinal disorders may support its therapeutic potential, with the red ecotype showing higher CK concentrations and enhanced bioactivity compared to the white ecotype (Branquinho, Verdan, dos Santos, et al., 2021; Costa et al., 2008; De Toledo et al., 2011; Divekar et al., 2022; R. Jagessar et al., 2013; Sauvain et al.).

Cytokinins, particularly those in the red ecotype, may offer potential therapeutic benefits, including antioxidant, anti-ageing, and neuroprotective effects (Choudhary & Kumari, 2021; Daudu et al., 2017; Raiola et al., 2018; Thanapairoje et al., 2023) . Elevated levels of CKs such as *t*Z and its derivatives (DHZOG, DHZROG, DHZ9G, *t*ZOG, *t*ZROG, *t*Z9G, *c*ZOG, *c*ZROG, and *c*Z9G) in the red ecotype suggest improved storage, transport, and activation mechanisms (Santino et al., 2013; Stuckey, 2014; Wingfield & Wilson, 2016). Ribosides such as DZR (Fig 5, S1 Table 1) play crucial roles in CK metabolism and could contribute to prolonged therapeutic efficacy when extracted for human applications. Controlled activation of CK conjugates, such as *t*Z7G and *t*Z9G, may enable sustained-release systems of secondary metabolites, reducing side effects and enhancing stability in targeted treatments (Ewart smith, 2023; M Fathy et al., 2022; M. Fathy et al., 2022; Raissa Borges Ishikawa et al., 2018; Jacob et al., 2022; Prajapat et al., 2022; Rafael et al., 2023). This could be particularly useful in areas such as cancer therapy, immune modulation, and wound healing (Jacob et al., 2022; R. Jagessar et al., 2013; Rattan & Clark, 1994), where the red ecotype's enhanced CK profile could provide distinct advantages.

The presence of *O*-glucosides and *N*-glucosides in *D. dentatus* further emphasizes the adaptability and pharmacological relevance of this species. *O*-glucosides, linked to antioxidant and

anti-inflammatory properties, and *N*-glucosides, associated with nitrogen storage and herbivore defence, may offer additional therapeutic benefits (Rattan & Clark, 1994; Zadeh Hashem & Eslami, 2018; Zwack & Rashotte, 2013). Studies have shown that CK forms such as *t*Z7G and *t*Z9G act as storage reservoirs, releasing active cytokinins under specific conditions, which could be harnessed for sustainable therapeutic applications (Rattan & Sodagam, 2005; Vedenicheva et al., 2021). The higher CK concentrations and diverse metabolite profiles of the red ecotype provide insights into its enhanced bioactivity, offering a foundation for applications in natural medicine, dietary supplements, and pharmaceutical developments (Mboene Noah et al., 2021; A Mukherjee et al., 2022; Nambara & Van Wees, 2021; Rattan & Clark, 1994; Rattan & Sodagam, 2005). These findings underscore the need for further research to explore its full potential in human health and sustainable practices.

The correlation network analysis revealed positive associations among CKs including *t*Z, cZ, cZ9G, and *t*Z9G, which exhibited strong positive correlations with alkaloids such as tropine and hypoxanthine (Fig 7). Alkaloids are a large class of plant secondary metabolites that possess antimicrobial, analgesics, antimalarials and anticancer activity (Hesse, 2002; Mohammed et al., 2024; Shao et al., 2024). These findings suggest that these CKs may play a significant role in promoting the biosynthesis or accumulation of these compounds, which are frequently associated with the plant's adaptive mechanisms, including defence and stress tolerance. CKs have been shown to influence the production of tropane alkaloids in the Solanaceae family. The biosynthesis of tropane alkaloids, including tropine, involves complex pathways that can be regulated by plant hormones such as CKs (Spíchal, 2012).

Großkinsky et al.,(2013) demonstrated that *t*Z pre-treatment in *Nicotiana tabacum* significantly elevated salicylic acid (SA) levels by 30%, enhancing systemic acquired resistance (SAR) against Pseudomonas syringae and reducing bacterial proliferation (Großkinsky et al., 2013). In contrast, cZ exhibited weaker effects on SA accumulation but still suppressed pathogen symptoms, suggesting alternative signaling pathways. These differences were attributed to tZ's preferential binding to cytokinin receptors (e.g., AHK3/4) and its higher bioactivity compared to cZ (Großkinsky et al., 2013).

Rasi & Arash, et al., (2024) further highlighted the role of methyl jasmonate (MJ) in modulating tropane alkaloid (TA) biosynthesis, with MJ treatment (150–300 μM) upregulating genes such as TR1 (tropinone reductase I) and HYOS (hyoscyamine synthase), leading to increased scopolamine and atropine production (Rasi et al., 2024). This aligns with the broader role of cytokinins in regulating secondary metabolism, as *c*Z and *t*Z derivatives (e.g., *t*Z9G) delay senescence and stabilize chloroplast function, indirectly supporting alkaloid synthesis (Hallmark et al., 2020). Gajdošová et al., (2013), emphasized cZ's role as a stress-response marker, correlating its accumulation with defense alkaloid production under herbivory or pathogen attack (Schäfer et al., 2015).

Notably, CKs such as *c*ZR, *t*ZR, and iP show significant negative correlations with dopamine (Fig 7). This trend indicates that these CKs might suppress dopamine biosynthesis or redirect metabolic resources toward other pathways. Such regulatory trade-offs emphasize the balancing act between different secondary metabolite pathways, reflecting the plant's dynamic response to environmental or physiological factors (Shao et al., 2024).

Correlations between CKs and secondary metabolites particularly flavonoids and anthocyanins, have been investigated (Fang et al., 1998; Solekha et al., 2024). Among the key findings, cZ9G demonstrates a strong positive association with chalconaringenin (Fig 5), suggesting its role in promoting the biosynthesis of flavonoid precursors that are essential for plant defence mechanisms and pigmentation (Kumar et al., 2020). Similarly, *t*ZR exhibits a strong positive correlation with delphinidin glucosides and cyanidin derivatives, emphasizing its role in enhancing anthocyanin production, crucial for antioxidant activity and stress tolerance (Hsiao et al., 2003; Mielcarek & Isalan, 2021; Qamar et al., 2020; Vedenicheva et al., 2021; Zadeh Hashem & Eslami, 2018). Chalcones, including chalconaringenin, are pivotal intermediates in the flavonoid biosynthetic pathway, leading to the production of various flavonoids and anthocyanins. The promotion of chalconaringenin biosynthesis by *c*Z9G indicates a potential mechanism through which CKs can modulate secondary metabolite profiles in plants, enhancing their ability to cope with environmental stresses and attract pollinators through pigmentation (Zhang et al., 2022; Zhu et al., 2024).

Gong et al. (Gong et al., 2022) investigated the effects of varying nitrogen (N) conditions on the accumulation of flavonoids and phytohormones in (*Camellia sinensis*) tea plants. The results indicated complex correlation patterns. Certain flavonoid compounds (taxifolin, myricetin, and apigenin) were positively correlated with CKs, such as iP, cZ and *t*ZR. Furthermore, the interaction between CKs and flavonoid biosynthesis has been linked to improved antioxidant activity in plants, which is essential for mitigating oxidative stress. This highlights the broader implications of CKs in enhancing plant resilience and adaptability through the regulation of secondary metabolites (Gong et al., 2022; Zhang et al., 2022).

Several notable correlations between phenolic and CKs. Among the most significant relationships, vanillic acid (Fig 4.7, Table 3) had strong positive correlations with multiple CKs, (Fig 7). 5-O-(4-Coumaroyl)-D-quinate also shows distinct positive correlations across several CKs (Fig 7). Tetrahydrofolate exhibits a mixed pattern of correlations, with some strong positive associations indicated by orange colours and some negative correlations shown in turquoise. Sinapyl alcohol and sinapaldehyde display moderate to strong positive correlations with specific CKs, while p-coumaroyl quinic acid shows a more varied correlation pattern across different CK compounds (Fig 4.7).

The correlations between phenolic compounds and cytokinins (CKs) highlight significant regulatory interactions in plant secondary metabolism. Among these, vanillic acid shows strong positive correlations with multiple CKs, (Grzegorczyk-Karolak et al., 2020) such as *t*Z, *t*ZR and *t*ZROG (Fig 7, Table 3). This suggests that CKs may play a key role in modulating the biosynthesis of vanillic acid, which is a phenolic compound with well-known antioxidant properties (Aimvijarn et al., 2023; Ismail & Wright, 2018). Such interactions could imply a broader regulatory network where CKs influence phenolic pathways to enhance plant stress responses or metabolic activity (Barakate et al., 2011; Hoffmann et al., 2004; Lv et al., 2024).

Additionally, 5-O-(4-Coumaroyl)-D-quinate, a precursor in the biosynthesis of lignin and other phenylpropanoids, also demonstrates consistent positive correlations with several CKs (Fig 4.7). This points to CKs as potential regulators of lignin biosynthesis and structural phenolics critical for plant integrity and defence mechanisms. Tetrahydrofolate exhibits a more mixed correlation profile, with both strong positive (orange) and negative (turquoise) associations, indicating a nuanced role of CKs in its metabolic pathways. Compounds such as sinapyl alcohol and

sinapaldehyde show moderate to strong positive correlations with specific CKs, suggesting their biosynthesis might be selectively regulated by certain CK derivatives. In contrast, p-coumaroyl quinic acid displays a varied pattern of correlations across different CKs, suggesting there is a complex interplay that may involve context-specific regulation or competing metabolic priorities. These findings emphasize the multifaceted role of CKs in fine-tuning the production of phenolics, with implications for plant stress tolerance, structural adaptation, and metabolic optimization.

3.1. Metabolic diversity and therapeutic potential of *D. dentatus* ecotypes

The study of *D. dentatus* reveals metabolic differences between its red and white ecotypes, particularly in the biosynthesis of secondary metabolites, some of which have potential health benefits (Fig 4.8). The red ecotype demonstrated 20 metabolic pathways, while the white ecotype showed 16 pathways, highlighting the plant's complex biochemical capabilities and ecological adaptations. Key pathways such as flavonoid, flavone, flavonol, anthocyanin, and monoterpenoid biosynthesis were found to be highly significant. The red ecotype demonstrated higher activity in flavone, flavonol and anthocyanin biosynthesis ($p = 0.002$ – $0.060 < 0.05$) compounds known for their antioxidant and anti-inflammatory properties; meanwhile the white ecotype was more associated with monoterpenoid and flavonoid biosynthesis. Flavonoids, such as quercetin, have been extensively studied for their ability to combat oxidative stress, reduce inflammation, exhibit anti-cancer properties, and prevent cell ageing (Hönig et al., 2018; Naseem et al., 2020; Simioni et al., 2018). Anthocyanins, pigments responsible for the red and purple hues in plants, were particularly abundant in the red ecotype and are linked to anti-inflammatory, anticancer, and neuroprotective effects (Noodén & Letham, 1986; Noodén et al.; Simioni et al., 2018). Meanwhile,

monoterpenoids in the white ecotype, recognized for their antimicrobial, anti-inflammatory, and analgesic properties, further highlight the plant's therapeutic potential (Hu & Shani, 2023). The categorization of metabolites into nitrogen-containing compounds (e.g., alkaloids) and nitrogen-deficient compounds (e.g., terpenoids and phenolics) underscores the plant's broad chemodiversity. Alkaloids have been used for centuries in medicine for their diverse pharmacological activities, including analgesic, antimalarial, and anticancer properties, while phenolics have been associated with anti-inflammatory, antidiabetic, and cardioprotective benefits (Durán-Medina et al., 2017).

The red ecotype had phytohormone profiles with higher concentrations of active cytokinins, such as *t*Z and *c*Z, alongside glucoside forms such as *t*Z7G, which may serve as CK reserves for activation under specific conditions. The untargeted metabolomics analysis further revealed a greater number of upregulated metabolites in the red ecotype, with polyphenols accounting for 63.9% of identified compounds in both ecotypes. This abundance of polyphenols, particularly in the red ecotype, underscores the potential therapeutic value of *D. dentatus*, given their well-documented antioxidant and anti-inflammatory properties (Hönig et al., 2018; Naseem et al., 2020). Together, these metabolic and phytochemistry differences between the ecotypes illustrate their unique adaptations and underscore *D. dentatus* as a promising source of bioactive compounds for medicinal applications.

Future research on *D. dentatus* should prioritize the quantification of phenolic compounds in both red and white ecotypes while also considering the ecological and environmental factors that contribute to the metabolic variations between them. By doing so, valuable insights can be gained regarding the adaptive mechanisms of these ecotypes and their potential resilience in the face of climate change. Additionally, by focusing on the biosynthesis pathways of key metabolites such

as flavonoids, anthocyanins, and monoterpenoids, we can uncover the regulatory genes and enzymes involved, potentially paving the way for biotechnological applications. Further investigation into the bioavailability and therapeutic effectiveness of these metabolites in clinical settings would also substantiate their potential benefit to human health. Furthermore, it is important to delve deeper into the physiological relevance of CK glucosides, specifically *t*Z7G, as reservoirs for active cytokinins under stressful conditions. Lastly, broadening the scope of metabolomic and genomic analyses to encompass related species would enhance our understanding of both the conserved and distinctive characteristics of secondary metabolites in *D. dentatus*, thereby contributing to our understanding of the evolutionary importance of these compounds.

Author Contributions: Conceptualization, Ewart Smith, RJ Neil Emery and Suresh Narine; methodology, Ewart Smith and Kimberly Molina; formal analysis, Ewart Smith; investigation, Ewart Smith; resources, Suresh Narine and RJ Neil Emery; data curation, Ewart Smith Erin, N. Morrison, and Ainsely Lewis; writing—original draft preparation, Ewart Smith; writing—review and editing, Ainsely Lewis, Suresh Narine and RJ Neil Emery; supervision, Suresh Narine and RJ Neil Emery; funding acquisition, RJ Neil Emery. All authors have read and agreed to the published version of the manuscript.

Funding: Funding was through the Sustainable Guyana Program, a partnership between Trent University and the University of Guyana funded by CGX Energy Inc. and Frontera Energy Corporation.

Institutional Review Board Statement: Not applicable

Informed Consent Statement: Not applicable

Data Availability Statement: All relevant data generated or analyzed during this study are included in this published article and supplemental information. Other raw data will be available upon request.

Acknowledgements: Funding was through the Sustainable Guyana Program, a partnership between Trent University and the University of Guyana funded by CGX Energy Inc. and Frontera Energy Corporation. The authors recognize The Ontario Research Fund and the Canadian Foundation for Innovation provided funding to purchase mass spectrometers and other instrumentation in the Water Quality Centre at Trent University.

Conflicts of Interest: The authors declare no conflict of interest.

4.6. REFERENCES

A Urra, F., Córdova-Delgado, M., Pessoa-Mahana, H., Ramírez-Rodríguez, O., Weiss-López, B., Ferreira, J., & Araya-Maturana, R. (2013). Mitochondria: A promising target for anticancer alkaloids. Current Topics in Medicinal Chemistry, 13(17), 2171-2183.

Abbey, L., Asiedu, S. K., Chada, S., Ofoe, R., Amoako, P. O., Owusu-Nketia, S., Ajeethan, N., Kumar, A. P., & Nutsukpo, E. B. (2024). Photosynthetic Activities, Phytohormones, and Secondary Metabolites Induction in Plants by Prevailing Compost Residue. Metabolites, 14(8). https://doi.org/10.3390/metabo14080400

Ahmad, N., Jiang, Z., Zhang, L., Hussain, I., & Yang, X. (2023). Insights on Phytohormonal Crosstalk in Plant Response to Nitrogen Stress: A Focus on Plant Root Growth and Development. Int J Mol Sci, 24(4). https://doi.org/10.3390/ijms24043631

Aimvijarn, P., Payuhakrit, W., Charoenchon, N., Okada, S., & Suwannalert, P. (2023). Riceberry Rice Germination and UVB Radiation Enhance Protocatechuic Acid and Vanillic Acid to Reduce Cellular Oxidative Stress and Suppress B16F10 Melanogenesis Relating to F-Actin Rearrangement. Plants (Basel), 12(3). https://doi.org/10.3390/plants12030484

Alexandre-Moreira, M., Piuvezam, M., Araújo, C., & Thomas, G. (1999). Studies on the anti-inflammatory and analgesic activity of Curatella americana L. Journal of Ethnopharmacology, 67(2), 171-177.

Allen, M., Qin, W., Moreau, F., & Moffatt, B. (2002). Adenine phosphoribosyltransferase isoforms of Arabidopsis and their potential contributions to adenine and cytokinin metabolism. Physiologia Plantarum, 115(1), 56-68.

Aoki, M. M., Kisiala, A. B., Li, S., Stock, N. L., Brunetti, C. R., Huber, R. J., & Emery, R. (2019). Cytokinin detection during the Dictyostelium discoideum life cycle: profiles are dynamic and affect cell growth and spore germination. Biomolecules, 9(11), 702.

Aoki, M. M., Kisiala, A. B., Mathavarajah, S., Schincaglia, A., Treverton, J., Habib, E., Dellaire, G., Emery, R. J. N., Brunetti, C. R., & Huber, R. J. (2024). From biosynthesis and beyond-Loss or overexpression of the cytokinin synthesis gene, iptA, alters cytokinesis and mitochondrial and amino acid metabolism in Dictyostelium discoideum. Faseb j, 38(1), e23366. https://doi.org/10.1096/fj.202301936RR

Aponte, J. C., Vaisberg, A. J., Rojas, R., Caviedes, L., Lewis, W. H., Lamas, G., Sarasara, C., Gilman, R. H., & Hammond, G. B. (2008). Isolation of cytotoxic metabolites from targeted peruvian amazonian medicinal plants. Journal of Natural Products, 71(1), 102-105. https://doi.org/10.1021/np070560c

Aremu, A. O., Plačková, L., Gruz, J., Bíba, O., Šubrtová, M., Novák, O., Doležal, K., & Van Staden, J. (2015). Accumulation pattern of endogenous cytokinins and phenolics in different organs of 1-year-old cytokinin pre-incubated plants: implications for conservation. Plant Biol (Stuttg), 17(6), 1146-1155. https://doi.org/10.1111/plb.12367

Åstot, C., Dolezal, K., Nordström, A., Wang, Q., Kunkel, T., Moritz, T., Chua, N.-H., & Sandberg, G. (2000). An alternative cytokinin biosynthesis pathway. Proceedings of the National Academy of Sciences, 97(26), 14778-14783. https://doi.org/10.1073/pnas.260504097

Baltazar, M. T., Dinis-Oliveira, R. J., Duarte, J. A., Bastos, M. L., & Carvalho, F. (2011). Antioxidant properties and associated mechanisms of salicylates. *Curr Med Chem*, *18*(21), 3252-3264. https://doi.org/10.2174/092986711796391552

Barakate, A., Stephens, J., Goldie, A., Hunter, W. N., Marshall, D., Hancock, R. D., Lapierre, C., Morreel, K., Boerjan, W., & Halpin, C. (2011). Syringyl lignin is unaltered by severe sinapyl alcohol dehydrogenase suppression in tobacco. Plant Cell, 23(12), 4492-4506. https://doi.org/10.1105/tpc.111.089037

Bartel, J., Krumsiek, J., & Theis, F. J. (2013). Statistical methods for the analysis of high-throughput metabolomics data. Computational and structural biotechnology journal, 4(5), e201301009. htts://doi.org/10.5936/csbj.201301009

Bean, K. M., Kisiala, A. B., Morrison, E. N., & Emery, R. N. (2022). Trichoderma synthesizes cytokinins and alters cytokinin dynamics of inoculated Arabidopsis seedlings. Journal of plant growth regulation, 41(7), 2678-2694.

Bhamber, R. S., Jankevics, A., Deutsch, E. W., Jones, A. R., & Dowsey, A. W. (2021). mzMLb: A Future-Proof Raw Mass Spectrometry Data Format Based on Standards-Compliant mzML and Optimized for Speed and Storage Requirements. J Proteome Res, 20(1), 172-183. https://doi.org/10.1021/acs.jproteome.0c00192

Bhargava, A., Clabaugh, I., To, J. P., Maxwell, B. B., Chiang, Y.-H., Schaller, G. E., Loraine, A., & Kieber, J. J. (2013). Identification of cytokinin-responsive genes using microarray meta-analysis and RNA-Seq in Arabidopsis. Plant physiology, 162(1), 272-294. htts://doi.org/10.1104/pp.112.208707

Bhatia, H., Sharma, Y. P., Manhas, R. K., & Kumar, K. (2014). Ethnomedicinal plants used by the villagers of district Udhampur, J&K, India. Journal of Ethnopharmacology, 151(2), 1005-1018. https://doi.org/10.1016/j.jep.2013.12.017

Branquinho, L. S., Verdan, M. H., dos Santos, E., Macorini, L. F. B., Maris, R. S., Kuraoka-Oliveira, A. M., Bacha, F. B., Cardoso, C. A. L., Arena, A. C., Silva-Filho, S. E., & Kassuya, C. A. L. (2021). Toxicological evaluation of ethanolic extract of leaves from Doliocarpus dentatus in Swiss mice. Drug and Chemical Toxicology, 0(0), 1-7. https://doi.org/10.1080/01480545.2021.1982638

Branquinho, L. S., Verdan, M. H., Santos, E. d., Neves, S. C. d., Oliveira, R. J., Cardoso, C. A. L., & Kassuya, C. A. L. (2021). Aqueous extract from leaves of Doliocarpus dentatus (Aubl.) Standl. relieves pain without genotoxicity activity. Journal of Ethnopharmacology, 266(October 2020).https://doi.org/10.1016/B978-0-12-822800-5.00011-1

Branquinho, L. S., Verdan, M. H., Silva-Filho, S. E., Oliveira, R. J., Cardoso, C. A. L., Arena, A. C., & Kassuya, C. A. L. (2021). Antiarthritic and antinociceptive potential of ethanolic extract from leaves of Doliocarpus dentatus (aubl.) standl. in mouse model. Pharmacognosy Research, 13(1). https://doi.org/10.4103/pr.pr_79_20

Bruniera, C. P., & Groppo, M. (2010). Flora da Serra do Cipó, Minas Gerais: Dilleniaceae. Boletim de Botânica da Universidade de São Paulo, 59-67.

Bychkov, I. A., Andreeva, A. A., Vankova, R., Lacek, J., Kudryakova, N. V., & Kusnetsov, V. V. (2024). Modified Crosstalk between Phytohormones in Arabidopsis Mutants for PEP-Associated Proteins. International journal of molecular sciences, 25(3), 1586. https://doi.org/10.3390/ijms25031586

Cambiaghi, A., Ferrario, M., & Masseroli, M. (2017). Analysis of metabolomic data: tools, current strategies and future challenges for omics data integration. Briefings in bioinformatics, 18(3), 498-510. https://doi.org/10.1093/bib/bbw031

Casati, S., Ottria, R., Baldoli, E., Lopez, E., Maier, J. A., & Ciuffreda, P. (2011). Effects of cytokinins, cytokinin ribosides and their analogs on the viability of normal and neoplastic human cells. *Anticancer Research*, *31*(10), 3401-3406.

Castilla, G., Hall, R. J., Skakun, R., Filiatrault, M., Beaudoin, A., Gartrell, M., Smith, L., Groenewegen, K., Hopkinson, C., & van der Sluijs, J. (2022). The Multisource Vegetation Inventory (MVI): A Satellite-Based Forest Inventory for the Northwest Territories Taiga Plains. Remote Sensing, 14(5), 1108. https://doi.org/10.3390/rs14051108

Cedzich, A., Stransky, H., Schulz, B., & Frommer, W. B. (2008). Characterization of cytokinin and adenine transport in Arabidopsis cell cultures. Plant Physiol, 148(4), 1857-1867. https://doi.org/10.1104/pp.108.128454

Celedon, J. M., Chiang, A., Yuen, M. M., Diaz-Chavez, M. L., Madilao, L. L., Finnegan, P. M., Barbour, E. L., & Bohlmann, J. (2016). Heartwood-specific transcriptome and metabolite signatures of tropical sandalwood (Santalum album) reveal the final step of (Z)-santalol fragrance biosynthesis. Plant J, 86(4), 289-299. https://doi.org/10.1111/tpj.13162

Chambers, M. C., Maclean, B., Burke, R., Amodei, D., Ruderman, D. L., Neumann, S., Gatto, L., Fischer, B., Pratt, B., & Egertson, J. (2012). A cross-platform toolkit for mass spectrometry and proteomics. Nature biotechnology, 30(10), 918-920. https://doi.org/10.1038/nbt.2377

Chanclud, E., Kisiala, A., Emery, N. R. J., Chalvon, V., Ducasse, A., Romiti-Michel, C., Gravot, A., Kroj, T., & Morel, J.-B. (2016). Cytokinin production by the rice blast fungus is a pivotal requirement for full virulence. PLoS Pathogens, 12(2), e1005457. Htts://doi.org/ 10.1371/journal.ppat.1005457

Chong, J., Wishart, D. S., & Xia, J. (2019). Using MetaboAnalyst 4.0 for comprehensive and integrative metabolomics data analysis. Current protocols in bioinformatics, 68(1), e86. htts://doi.org/10.1002/cpbi.86

Choudhary, M., & Kumari, A. (2021). Understanding Plant Hormones: Mechanisms and Functions in Growth and Development. Plant Science Archives.

Correa, D. I., Pastene-Navarrete, E., Baeza, M., Bustamante, L., & Alarcón-Enos, J. (2022). Effect of plant growth regulators on alkaloid the production in cell cultures of Chilean Amaryllidaceae: Rhodophiala pratensis, Rhodophiala splendens, Rhodophiala advena, and Rhodolirium speciosum. Plant Cell, Tissue and Organ Culture (PCTOC), 151(3), 521-534. htts://doi.org/ 10.1007/s11240-022-02356-5

Cortleven, A., Leuendorf, J. E., Frank, M., Pezzetta, D., Bolt, S., & Schmülling, T. (2019). Cytokinin action in response to abiotic and biotic stresses in plants. Plant, cell & environment, 42(3), 998-1018.

Costa-Pérez, A., Ferrer, M. A., & Calderón, A. A. (2023). Combined effects of cytokinin and UV-C light on phenolic pattern in Ceratonia siliqua shoot cultures. Agronomy, 13(3), 621. Htts://doi.org/10.3390/agronomy13030621

Costa, E., Hiruma-Lima, C. A., Lima, E., Sucupira, G., Bertolin, A., Lolis, S., Andrade, F., Vilegas, W., & Souza-Brito, A. (2008). Antimicrobial activity of some medicinal plants of the Cerrado, Brazil. Phytotherapy Research: An International Journal Devoted to Pharmacological and Toxicological Evaluation of Natural Product Derivatives, 22(5), 705-707.

Daudu, D., Allion, E., Liesecke, F., Papon, N., Courdavault, V., Dugé de Bernonville, T., Mélin, C., Oudin, A., Clastre, M., Lanoue, A., Courtois, M., Pichon, O., Giron, D., Carpin, S., Giglioli-Guivarc'h, N., Crèche, J., Besseau, S., & Glévarec, G. (2017). CHASE-Containing Histidine Kinase Receptors in Apple Tree: From a Common Receptor Structure to Divergent Cytokinin Binding Properties and Specific Functions. Front Plant Sci, 8, 1614. https://doi.org/10.3389/fpls.2017.01614

Del Mondo, A., Vinaccia, A., Pistelli, L., Brunet, C., & Sansone, C. (2023). On the human health benefits of microalgal phytohormones: An explorative in silico analysis. *Computational and structural biotechnology journal*, *21*, 1092-1101.

De Oliveira, B. H., Santos, C. A. M., & Espíndola, A. P. D. M. (2002). Determination of the triterpenoid, betulinic acid, in Doliocarpus schottianus by HPLC. Phytochemical analysis, 13(2), 95-98. https://doi.org/10.1002/pca.628

De Toledo, C. E., Britta, E. A., Ceole, L. F., Silva, E. R., De Mello, J. C., Dias Filho, B. P., Nakamura, C. V., & Ueda-Nakamura, T. (2011). Antimicrobial and cytotoxic activities of medicinal plants of the Brazilian cerrado, using Brazilian cachaça as extractor liquid.

Journal of Ethnopharmacology, 133(2), 420-425. Htts:doi.org/ 10.1016/j.jep.2010.10.006

Divekar, P. A., Narayana, S., Divekar, B. A., Kumar, R., Gadratagi, B. G., Ray, A., Singh, A. K., Rani, V., Singh, V., & Singh, A. K. (2022). Plant secondary metabolites as defense tools against herbivores for sustainable crop protection. International journal of molecular sciences, 23(5), 2690. htts:doi.org/10.3390/ijms23052690

Dobrev, P. I., Hoyerová, K., & Petrášek, J. (2017). Analytical determination of auxins and cytokinins. Auxins and cytokinins in plant biology: Methods and protocols, 31-39. Springer.

Doncheva, N. T., Morris, J. H., Holze, H., Kirsch, R., Nastou, K. C., Cuesta-Astroz, Y., Rattei, T., Szklarczyk, D., von Mering, C., & Jensen, L. J. (2023). Cytoscape stringApp 2.0: Analysis and Visualization of Heterogeneous Biological Networks. J Proteome Res, 22(2), 637-646. https://doi.org/10.1021/acs.jproteome.2c00651

Durán-Medina, Y., Díaz-Ramírez, D., & Marsch-Martínez, N. (2017). Cytokinins on the move. Frontiers in Plant Science, 8, 146.

Egamberdieva, D., Wirth, S. J., Alqarawi, A. A., Abd_Allah, E. F., & Hashem, A. (2017). Phytohormones and beneficial microbes: essential components for plants to balance stress and fitness. *Frontiers in Microbiology*, *8*, 2104.

Ewart smith, A. L., Suresh S. Narine and R.J Neil Emery (2023). Unlocking Potentially Therapeutic Phytochemicals in Capadulla (Doliocarpus dentatus) from Guyana Using Untargeted Mass Spectrometry-Based Metabolomics. Metabolites. htts://doi.org/10.3390/metabo13101050

Fathy, M., Saad Eldin, S. M., Naseem, M., Dandekar, T., & Othman, E. M. (2022). Cytokinins: Wide-Spread Signaling Hormones from Plants to Humans with High Medical Potential. *Nutrients*, *14*(7). https://doi.org/10.3390/nu14071495

Fahad, S., Hussain, S., Matloob, A., Khan, F. A., Khaliq, A., Saud, S., Hassan, S., Shan, D., Khan, F., & Ullah, N. (2015). Phytohormones and plant responses to salinity stress: a review. Plant growth regulation, 75(2), 391-404.htts://doi.org/ 10.1007/s10725-015-0013-6

Fang, Y., Smith, M. A. L., & Pépin, M. F. (1998). Benzyl adenine restores anthocyanin pigmentation in suspension cultures of wild Vaccinium pahalae. Plant Cell, Tissue and Organ Culture, 54, 113-122. htts://doi.org/10.1007/s10725-015-0013-6

Fathy, M., Saad Eldin, S. M., Naseem, M., Dandekar, T., & Othman, E. M. (2022). Cytokinins: Wide-Spread Signaling Hormones from Plants to Humans with High Medical Potential. Nutrients, 14(7). https://doi.org/10.3390/nu14071495

Fausto de Souza, D., Tsering, T., Burnier, M. N., Bravo-Filho, V., Dias, A. B. T., Abdouh, M., Goyeneche, A., & Burnier, J. V. (2020). Acetylsalicylic acid exerts potent antitumor and antiangiogenic effects in cutaneous and uveal melanoma cell lines. *Ocular Oncology and Pathology*, *6*(6), 442-455.

Fox, J. E., Cornette, J., Deleuze, G., Dyson, W., Giersak, C., Niu, P., Zapata, J., & McChesney, J. (1973). The formation, isolation, and biological activity of a cytokinin 7-glucoside. Plant physiology, 52(6), 627-632.

Galichet, A., Hoyerová, K., Kamínek, M., & Gruissem, W. (2008). Farnesylation directs AtIPT3 subcellular localization and modulates cytokinin biosynthesis in Arabidopsis. Plant physiology, 146(3), 1155-1164. Htts://doi.org/ 10.1104/pp.107.112326

García-Pérez, P., Zhang, L., Miras-Moreno, B., Lozano-Milo, E., Landin, M., Lucini, L., & Gallego, P. P. (2021). The Combination of Untargeted Metabolomics and Machine Learning Predicts the Biosynthesis of Phenolic Compounds in Bryophyllum Medicinal Plants (Genus Kalanchoe). Plants (Basel), 10(11). https://doi.org/10.3390/plants10112430

Gautam, G. (2023). Advancement of Network Pharmacology in Multi-targeted Therapeutic Evaluation of Medicinal Plants. Journal of CAM Research Progress.

Gibb, M., Kisiala, A. B., Morrison, E. N., & Emery, R. N. (2020). The origins and roles of methylthiolated cytokinins: Evidence from among life kingdoms. Frontiers in Cell and Developmental Biology, 8, 605672. htts://doi.org/ 10.3389/fcell.2020.605672

Goh, D. M., Cosme, M., Kisiala, A. B., Mulholland, S., Said, Z. M., Spíchal, L., Emery, R., Declerck, S., & Guinel, F. C. (2019). A stimulatory role for cytokinin in the arbuscular mycorrhizal symbiosis of pea. Frontiers in Plant Science, 10, 433683. htts://doi.org/10.3389/fpls.2019.00262

Gong, X., Li, L., Qin, L., Huang, Y., Ye, Y., Wang, M., Wang, Y., Xu, Y., Luo, F., & Mei, H. (2022). Targeted metabolomics reveals impact of N application on accumulation of amino acids, flavonoids and phytohormones in tea shoots under soil nutrition deficiency stress. Forests, 13(10), 1629. htts://doi.org/ 10.3390/f13101629

Großkinsky, D. K., Edelsbrunner, K., Pfeifhofer, H., van der Graaff, E., & Roitsch, T. (2013). Cis- and trans-zeatin differentially modulate plant immunity. *Plant Signal Behav*, *8*(7), e24798. https://doi.org/10.4161/psb.24798

Grzegorczyk-Karolak, I., Hnatuszko-Konka, K., Zarzycka, M., & Kuźma, Ł. (2020). The Stimulatory Effect of Purine-Type Cytokinins on Proliferation and Polyphenolic Compound Accumulation in Shoot Culture of Salvia Viridis. Biomolecules, 10(2). https://doi.org/10.3390/biom10020178

Guo, J., & Huan, T. (2023). Mechanistic Understanding of the Discrepancies between Common Peak Picking Algorithms in Liquid Chromatography-Mass Spectrometry-Based Metabolomics. Anal Chem, 95(14), 5894-5902. https://doi.org/10.1021/acs.analchem.2c04887

Gurni, A. A., König, W. A., & Kubitzki, K. (1981). Flavonoid glycosides and sulphates from the Dilleniaceae. Phytochemistry, 20(5), 1057-1059. Htts://doi.org/10.1016/0031-9422(81)83026-3

Hallmark, H. T., Černý, M., Brzobohatý, B., & Rashotte, A. M. (2020). trans-Zeatin-N-glucosides have biological activity in Arabidopsis thaliana. PloS one, 15(5), e0232762.

Hamuel, J. (2012). Phytochemicals: Extraction Methods, Basic Structures and Mode of Action as Potential Chemotherapeutic Agents. Phytochemicals - A Global Perspective of Their Role in Nutrition and Health. https://doi.org/10.5772/26052

Hesse, M. (2002). Alkaloids: Nature's Curse or Blessing? John Wiley & Sons. ISBN: 3906390241

Heuckeroth, S., Damiani, T., Smirnov, A., Mokshyna, O., Brungs, C., Korf, A., Smith, J. D., Stincone, P., Dreolin, N., Nothias, L. F., Hyötyläinen, T., Orešič, M., Karst, U., Dorrestein, P. C., Petras, D., Du, X., van der Hooft, J. J. J., Schmid, R., & Pluskal, T. (2024). Reproducible mass spectrometry data processing and compound annotation in MZmine 3. Nat Protoc, 19(9), 2597-2641. https://doi.org/10.1038/s41596-024-00996-y

Hirose, N., Takei, K., Kuroha, T., Kamada-Nobusada, T., Hayashi, H., & Sakakibara, H. (2008). Regulation of cytokinin biosynthesis, compartmentalization and translocation. Journal of experimental botany, 59(1), 75-83. https://doi.org/10.1093/jxb/erm298

Hoffmann, L., Besseau, S., Geoffroy, P., Ritzenthaler, C., Meyer, D., Lapierre, C., Pollet, B., & Legrand, M. (2004). Silencing of hydroxycinnamoyl-coenzyme A shikimate/quinate

hydroxycinnamoyltransferase affects phenylpropanoid biosynthesis. Plant Cell, 16(6), 1446-1465. https://doi.org/10.1105/tpc.020297

Hönig, M., Plíhalová, L., Husičková, A., Nisler, J., & Doležal, K. (2018). Role of cytokinins in senescence, antioxidant defence and photosynthesis. International journal of molecular sciences, 19(12), 4045. https://doi.org/10.3390/ijms19124045

Hošek, P., Hoyerová, K., Kiran, N. S., Dobrev, P. I., Zahajská, L., Filepová, R., Motyka, V., Müller, K., & Kamínek, M. (2020). Distinct metabolism of N-glucosides of isopentenyladenine and trans-zeatin determines cytokinin metabolic spectrum in Arabidopsis. New Phytologist, 225(6), 2423-2438. https://doi.org/10.1111/nph.16310

Hoyerová, K., & Hošek, P. (2020). New Insights Into the Metabolism and Role of Cytokinin N-Glucosides in Plants. Front Plant Sci, 11, 741. https://doi.org/10.3389/fpls.2020.00741

Hsiao, G., Shen, M.-Y., Lin, K.-H., Chou, C.-Y., Tzu, N.-H., Lin, C.-H., Chou, D.-S., Chen, T.-F., & Sheu, J.-R. (2003). Inhibitory activity of kinetin on free radical formation of activated platelets in vitro and on thrombus formation in vivo. European journal of pharmacology, 465(3), 281-287. https://doi.org/10.1016/S0014-2999(03)01344-4

Hu, Y., & Shani, E. (2023). Cytokinin activity - transport and homeostasis at the whole plant, cell, and subcellular levels. New Phytol, 239(5), 1603-1608. https://doi.org/10.1111/nph.19001

Huang, D., Dang, F., Huang, Y., Chen, N., & Zhou, D. (2022). Uptake, translocation, and transformation of silver nanoparticles in plants. Environmental Science: Nano, 9(1), 12-39.htts://doi.org/ 10.1039/d1en00870f

Hutchison, C. E., & Kieber, J. J. (2002). Cytokinin signaling in Arabidopsis. Plant Cell, 14 Suppl(Suppl), S47-59. https://doi.org/10.1105/tpc.010444

Ishikawa, R. B., Leitão, M. M., Kassuya, R. M., Macorini, L. F., Moreira, F. M. F., Cardoso, C. A. L., Coelho, R. G., Pott, A., Gelfuso, G. M., Croda, J., Oliveira, R. J., & Kassuya, C. A. L. (2017). Anti-inflammatory, antimycobacterial and genotoxic evaluation of Doliocarpus dentatus. Journal of Ethnopharmacology, 204(February), 18-25. https://doi.org/10.1016/j.jep.2017.04.004

Ishikawa, R. B., Vani, J. M., das Neves, S. C., Rabacow, A. P. M., Kassuya, C. A. L., Croda, J., Cardoso, C. A. L., Monreal, A. C. D. F., Antoniolli, A. C. M. B., Cunha – Laura, A. L., & Oliveira, R. J. (2018). The safe use of Doliocarpus dentatus in the gestational period: Absence of changes in maternal reproductive performance, embryo-fetal development

and DNA integrity. Journal of Ethnopharmacology, 217(January), 1-6. https://doi.org/10.1016/j.jep.2018.01.034

Ismail, N., & Wright, L. J. (2018). FORMATION OF VANILLIN AND VANILLIC ACID FROM KRAFT LIGNIN THROUGH GREEN CHEMICAL OXIDATION (Pembentukan Vanillin dan Asid Vanillik dari Kraft Lignin melalui Proses Pengoksidaan Kimia Hijau). https://doi.org/10.17576/mjas-2018-2206-03

Jacob, S., Nair, A. B., Shah, J., Gupta, S., Boddu, S. H. S., Sreeharsha, N., Joseph, A., Shinu, P., & Morsy, M. A. (2022). Lipid Nanoparticles as a Promising Drug Delivery Carrier for Topical Ocular Therapy-An Overview on Recent Advances. Pharmaceutics, 14(3). https://doi.org/10.3390/pharmaceutics14030533

Jagessar, R., Hoolas, G., & Maxwell, A. (2013). Phytochemical screening, isolation of betulinic acid, trigonelline and evaluation of heavy metals ion content of Doliocarpus dentatus. Journal of Natural Products (India), 6, 5-16.

Jenča, A., Mills, D. K., Ghasemi, H., Saberian, E., Jenča, A., Karimi Forood, A. M., Petrášová, A., Jenčová, J., Jabbari Velisdeh, Z., Zare-Zardini, H., & Ebrahimifar, M. (2024). Herbal Therapies for Cancer Treatment: A Review of Phytotherapeutic Efficacy. Biologics, 18, 229-255. https://doi.org/10.2147/btt.S484068

Jiang, B., Song, J., & Jin, Y. (2020). A flavonoid monomer tricin in Gramineous plants: Metabolism, bio/chemosynthesis, biological properties, and toxicology. Food Chemistry, 320, 126617. htts://doi.org/ 10.1016/j.foodchem.2020.126617

Jiang, L., Sullivan, H., & Wang, B. (2022). Principal component analysis (PCA) loading and statistical tests for nuclear magnetic resonance (NMR) metabolomics involving multiple study groups. Analytical Letters, 55(10), 1648-1662.

Jiskrová, E., Novák, O., Pospíšilová, H., Holubová, K., Karády, M., Galuszka, P., Robert, S., & Frébort, I. (2016). Extra-and intracellular distribution of cytokinins in the leaves of monocots and dicots. New Biotechnology, 33(5), 735-742.htts://doi.org/ 10.1016/j.nbt.2015.12.010

Jogawat, A., Yadav, B., Chhaya, Lakra, N., Singh, A. K., & Narayan, O. P. (2021). Crosstalk between phytohormones and secondary metabolites in the drought stress tolerance of crop plants: a review. Physiologia Plantarum, 172(2), 1106-1132. htts://doi.org/ 10.1111/ppl.13328

Jorge, G. L., Kisiala, A., Morrison, E., Aoki, M., Nogueira, A. P. O., & Emery, R. N. (2019). Endosymbiotic Methylobacterium oryzae mitigates the impact of limited water availability in lentil (Lens culinaris Medik.) by increasing plant cytokinin levels. Environmental and Experimental Botany, 162, 525-540.htts://doi.org/ 10.1016/j.envexpbot.2019.03.015

Kabera, J. N., Semana, E., Mussa, A. R., & He, X. (2014). Plant secondary metabolites: biosynthesis, classification, function and pharmacological properties. J. Pharm. Pharmacol, 2(7), 377-392. htts://doi.org/ 10.1111/jphp.12234

Kadi, K., Yahia, A., Hamli, S., Auidane, L., Khabthane, H., & Ali, W. K. (2013). In vitro antibacterial activity and phytochemical analysis of White henbane treated by phytohormones. Pak J Biol Sci, 16(19), 984-990. https://doi.org/10.3923/pjbs.2013.984.990

Kamada-Nobusada, T., Makita, N., Kojima, M., & Sakakibara, H. (2013). Nitrogen-dependent regulation of de novo cytokinin biosynthesis in rice: the role of glutamine metabolism as an additional signal. Plant and Cell Physiology, 54(11), 1881-1893.htts://doi.org/10.1093/pcp/pct130

Kambhampati, S., Kurepin, L. V., Kisiala, A. B., Bruce, K. E., Cober, E. R., Morrison, M. J., & Emery, R. N. (2017). Yield associated traits correlate with cytokinin profiles in developing pods and seeds of field-grown soybean cultivars. Field Crops Research, 214, 175-184. htts://doi.org/ 10.1016/j.fcr.2017.09.012

Khetsha, Z., Sedibe, M., Pretorius, R., & Van Der Watt, E. (2021). Plant growth regulators and simulated hail-damage improve rose-geranium (Pelargonium graveolens L'Hér.) leaf mineral status and phenolic composition. Applied Ecology and Environmental Research(4), 3083-3095. htts://doi.org/ 10.15666/aeer/2021/v20i4/3083-3095

Kieber, J. J., & Schaller, G. E. (2018). Cytokinin signaling in plant development. Development, 145(4), dev149344. htts://doi.org/ 10.1242/dev.149344

Killeen, T. J., García, E., & Beck, S. G. (1993). Guía de árboles de Bolivia. Herbario Nacional de Bolivia; Missouri Botanical Garden.

Kisiala, A., Kambhampati, S., Stock, N. L., Aoki, M., & Emery, R. N. (2019). Quantification of cytokinins using high-resolution accurate-mass orbitrap mass spectrometry and parallel reaction monitoring (PRM). Analytical chemistry, 91(23), 15049-15056.htts://doi.org/ 10.1021/acs.analchem.9b03038

Kisiala, A., Laffont, C., Emery, R. N., & Frugier, F. (2013). Bioactive cytokinins are selectively secreted by Sinorhizobium meliloti nodulating and nonnodulating strains. Molecular plant-microbe Interactions, 26(10), 1225-1231. htts://doi.org/ 10.1094/MPMI-05-13-0134-R

Kleczkowski, K., Schell, J., & Bandur, R. (1995). Phytohormone conjugates: nature and function. Critical Reviews in Plant Sciences, 14(4), 283-298.htts://doi.org/ 10.1080/07352689509701945

Kojima, M., Kamada-Nobusada, T., Komatsu, H., Takei, K., Kuroha, T., Mizutani, M., Ashikari, M., Ueguchi-Tanaka, M., Matsuoka, M., & Suzuki, K. (2009). Highly sensitive and high-throughput analysis of plant hormones using MS-probe modification and liquid chromatography–tandem mass spectrometry: an application for hormone profiling in Oryza sativa. Plant and Cell Physiology, 50(7), 1201-1214.

Kumar, G., Jayaveera, K., Kumar, C., Sanjay, U. P., Swamy, B., & Kumar, D. (2007). Antimicrobial effects of Indian medicinal plants against acne-inducing bacteria. Tropical journal of pharmaceutical research, 6(2), 717-723.

Kumar, K., Gambhir, G., Dass, A., Tripathi, A. K., Singh, A., Jha, A. K., Yadava, P., Choudhary, M., & Rakshit, S. (2020). Genetically modified crops: current status and future prospects. Planta, 251(4), 91.

Kumari, J., Navas, M., Dan, M., & Rajasekharan, S. n. (2009). Pharmacognostic studies on Acrotrema arnottianum Wight — A promising ethnomedicinal plant. Indian Journal of Traditional Knowledge, 8, 334-337.

Kumari, S., Nazir, F., Maheshwari, C., Kaur, H., Gupta, R., Siddique, K. H., & Khan, M. I. R. (2023). Plant hormones and secondary metabolites under environmental stresses: Shedding light on defense molecules. Plant Physiology and Biochemistry, 108238.htts://doi.org/ 10.1016/j.plaphy.2023.108238

Kuroha, T., Tokunaga, H., Kojima, M., Ueda, N., Ishida, T., Nagawa, S., Fukuda, H., Sugimoto, K., & Sakakibara, H. (2009). Functional analyses of LONELY GUY cytokinin-activating enzymes reveal the importance of the direct activation pathway in Arabidopsis. The Plant Cell, 21(10), 3152-3169.

Kytidou, K., Artola, M., Overkleeft, H. S., & Aerts, J. M. (2020). Plant glycosides and glycosidases: a treasure-trove for therapeutics. Frontiers in Plant Science, 11, 521948.htts://doi.org/ 10.3389/fpls.2020.00357

Lebedev, V. G., Lebedeva, T. N., Vidyagina, E. O., Sorokopudov, V. N., Popova, A. A., & Shestibratov, K. A. (2022). Relationship between phenolic compounds and antioxidant activity in berries and leaves of raspberry genotypes and their genotyping by SSR markers. Antioxidants, 11(10), 1961. https://doi.org/10.3390/antiox11101961

Lee, K. Y., Nam, D.-H., Jeon, Y., Park, S. U., Cho, J., Gulandaz, M. A., Chung, S.-O., & Lee, G.-J. (2024). Exploring the Production of Secondary Metabolites from a Halophyte Tetragonia tetragonoides through Callus Culture. Horticulturae, 10(3), 244. https://doi.org/10.3390/horticulturae10030244

Li, Y., Zhang, X., Cheng, Q., Teixeira da Silva, J. A., Fang, L., & Ma, G. (2021). Elicitors Modulate Young Sandalwood (Santalum album L.) Growth, Heartwood Formation, and Concrete Oil Synthesis. Plants (Basel), 10(2). https://doi.org/10.3390/plants10020339

Lima, C. C., Lemos, R. P. L., & Conserva, L. M. (2014). Dilleniaceae family : an overview of its ethnomedicinal uses , biological and phytochemical profile. 3(2), 181-204.

Lima, D. B., Zhu, Y., & Liu, F. (2021). XlinkCyNET: A Cytoscape Application for Visualization of Protein Interaction Networks Based on Cross-Linking Mass Spectrometry Identifications. J Proteome Res, 20(4), 1943-1950. https://doi.org/10.1021/acs.jproteome.0c00957

Lomin, S. N., Krivosheev, D. M., Steklov, M. Y., Arkhipov, D. V., Osolodkin, D. I., Schmülling, T., & Romanov, G. A. (2015). Plant membrane assays with cytokinin receptors underpin the unique role of free cytokinin bases as biologically active ligands. Journal of experimental botany, 66(7), 1851-1863.htts://doi.org/ 10.1093/jxb/erv047

Lopes, F. C. M., Placeres, M. C. P., Jordão Junior, C. M., Higuchi, C. T., Rinaldo, D., Vilegas, W., Leite, C. Q. F., & Carlos, I. Z. (2007). Immunological and microbiological activity of Davilla elliptica St. Hill.(Dilleniaceae) against Mycobacterium tuberculosis. Memórias do Instituto Oswaldo Cruz, 102, 769-772.

López-Vázquez, A. L., Sepúlveda-García, E. B., Rubio-Rodríguez, E., Ponce-Noyola, T., Trejo-Tapia, G., Barrera-Cortés, J., Cerda-García-Rojas, C. M., & Ramos-Valdivia, A. C. (2024). Induction of Monoterpenoid Oxindole Alkaloids Production and Related Biosynthetic Gene Expression in Response to Signaling Molecules in Hamelia patens Plant Cultures. Plants (Basel), 13(7). https://doi.org/10.3390/plants13070966

Lv, T., Xue, D., Wang, P., Gong, W., & Wang, K. (2024). Vanillic Acid Protects PC12 Cells from Corticosterone-Induced Neurotoxicity via Regulating Immune and Metabolic Dysregulation Based on Computational Metabolomics. ACS Omega, 9(39), 40456-40467. https://doi.org/10.1021/acsomega.4c03050

Lv, Z.-Y., Sun, W.-J., Jiang, R., Chen, J.-F., Ying, X., Zhang, L., & Chen, W.-S. (2021). Phytohormones jasmonic acid, salicylic acid, gibberellins, and abscisic acid are key mediators of plant secondary metabolites. World Journal of Traditional Chinese Medicine, 7(3), 307-325. https://doi.org/10.4103/wjtcm.wjtcm_20_21

Marcelo, C. L., & Dunham, W. R. (1993). Fatty acid metabolism studies of human epidermal cell cultures. J Lipid Res, 34(12), 2077-2090.

Marchica, A., Cotrozzi, L., Detti, R., Lorenzini, G., Pellegrini, E., Petersen, M., & Nali, C. (2020). The Biosynthesis of Phenolic Compounds is an Integrated Defence Mechanism to Prevent Ozone Injury in Salvia officinalis. Antioxidants (Basel), 9(12). https://doi.org/10.3390/antiox9121274

Márquez-López, R. E., Quintana-Escobar, A. O., & Loyola-Vargas, V. M. (2019). Cytokinins, the Cinderella of plant growth regulators. Phytochemistry Reviews, 18(6), 1387-1408. https://doi.org/10.1016/S0022-2275(20)39964-6

Matheny, P. B., Aime, M. C., & Henkel, T. W. (2003). New species of Inocybe from Dicymbe forests of Guyana. Mycological Research, 107(4), 495-505. https://doi.org/10.1017/S0953756203007627

Mboene Noah, A., Casanova-Sáez, R., Makondy Ango, R. E., Antoniadi, I., Karady, M., Novák, O., Niemenak, N., & Ljung, K. (2021). Dynamics of auxin and cytokinin metabolism during early root and hypocotyl growth in Theobroma cacao. Plants, 10(5), 967. https://doi.org/10.3390/plants10050967

Mei, Y., Wei, L., Chai, C., Zou, L., Liu, X., Chen, J., Tan, M., Wang, C., Cai, Z., & Zhang, F. (2019). A method to study the distribution patterns for metabolites in xylem and phloem of Spatholobi Caulis. Molecules, 25(1), 167. https://doi.org/10.3390/molecules25010167

Meng, S., Lian, N., Qin, F., Yang, S., Meng, D., Bian, Z., Xiang, L., & Lu, J. (2024). The AREB transcription factor SaAREB6 promotes drought stress-induced santalol biosynthesis in sandalwood. Horticulture Research.

Mielcarek, M., & Isalan, M. (2021). Kinetin stimulates differentiation of C2C12 myoblasts. PloS one, 16(10), e0258419. https://doi.org/10.1371/journal.pone.0258419

Mohammed, N. J., Al-Behadili, W. A. A., & Al-fahham, A. A. (2024). The Chemical Structure, Classification and Clinical Significance of Alkaloids. International Journal of Health & Medical Research.

Mok, D. W., & Mok, M. C. (2001). Cytokinin metabolism and action. Annual review of plant biology, 52(1), 89-118. https://doi.org/10.1146/annurev.arplant.52.1.89

Morrison, E. N., Emery, R. N., & Saville, B. J. (2015). Phytohormone involvement in the Ustilago maydis–Zea mays pathosystem: relationships between abscisic acid and cytokinin levels and strain virulence in infected cob tissue. PloS one, 10(6), e0130945. https://doi.org/10.1371/journal.pone.0130945

Morrison, J. A., & Woldemariam, M. (2022). Ecological and metabolomic responses of plants to deer exclosure in a suburban forest. Ecology and Evolution, 12(11), e9475. https://doi.org/10.1002/ece3.9475

Motyka, V., Vaňková, R., Čapková, V., Petrášek, J., Kamínek, M., & Schmülling, T. (2003). Cytokinin-induced upregulation of cytokinin oxidase activity in tobacco includes changes in enzyme glycosylation and secretion. Physiologia Plantarum, 117(1), 11-21. https://doi.org/10.1034/j.1399-3054.2003.1170102.x

Mukherjee, A., Gaurav, A., Singh, S., Yadav, S., Bhowmick, S., Abeysinghe, S., & Verma, J. (2022). The bioactive potential of phytohormones: a review. Biotechnol Rep 35: e00748. In.

Nambara, E., & Van Wees, S. C. (2021). Plant hormone functions and interactions in biological systems. In (Vol. 105, pp. 287-289): Wiley Online Library.

Naseem, M., Othman, E. M., Fathy, M., Iqbal, J., Howari, F. M., AlRemeithi, F. A., Kodandaraman, G., Stopper, H., Bencurova, E., & Vlachakis, D. (2020). Integrated structural and functional analysis of the protective effects of kinetin against oxidative stress in mammalian cellular systems. Scientific reports, 10(1), 13330.

Naseem, M., Othman, E. M., Fathy, M., Iqbal, J., Howari, F. M., AlRemeithi, F. A., Kodandaraman, G., Stopper, H., Bencurova, E., & Vlachakis, D. (2020). Integrated structural and functional analysis of the protective effects of kinetin against oxidative stress in mammalian cellular systems. *Scientific reports*, *10*(1), 13330.

Nester, G. V., & Ditchenko, T. I. (2020). Stimulation of phenolic nature secondary metabolites biosynthesis in Echinacea purpurea L. Moench suspension cell cultures under influence yeast extract elisitors.

Noodén, L., & Letham, D. (1986). Cytokinin control of monocarpic senescence in soybean. Plant Growth Substances 1985: Proceedings of the 12th International Conference on Plant Growth Substances, Held at Heidelberg, August 26–31, 1985,

Noodén, L. D., Singh, S., & Letham, D. S. Senescence in Soybean1.

Othman, E. M., Naseem, M., Awad, E., Dandekar, T., & Stopper, H. (2016). The plant hormone cytokinin confers protection against oxidative stress in mammalian cells. *PloS one*, *11*(12), e0168386.

Pang, Z., Zhou, G., Ewald, J., Chang, L., Hacariz, O., Basu, N., & Xia, J. (2022). Using MetaboAnalyst 5.0 for LC–HRMS spectra processing, multi-omics integration and covariate adjustment of global metabolomics data. Nature Protocols, 17(8), 1735-1761. https://doi.org/10.1038/s41596-022-00710-w

Parker, C., Letham, D., Cowley, D., & MacLeod, J. (1972). Raphanatin, an unusual purine derivative and a metabolite of zeatin. Biochemical and biophysical research communications, 49(2), 460-466. https://doi.org/10.1016/0006-291x(72)90433-0

Peres, A., Soares, J. S., Tavares, R. G., Righetto, G., Zullo, M. A. T., Mandava, N. B., & Menossi, M. (2019). Brassinosteroids, the Sixth Class of Phytohormones: A Molecular View from the Discovery to Hormonal Interactions in Plant Development and Stress Adaptation. Int J Mol Sci, 20(2). https://doi.org/10.3390/ijms20020331

Petras, D., Phelan, V. V., Acharya, D., Allen, A. E., Aron, A. T., Bandeira, N., Bowen, B. P., Belle-Oudry, D., Boecker, S., Cummings, D. A., Jr., Deutsch, J. M., Fahy, E., Garg, N., Gregor, R., Handelsman, J., Navarro-Hoyos, M., Jarmusch, A. K., Jarmusch, S. A., Louie, K., Maloney, K. N., Marty, M. T., Meijler, M. M., Mizrahi, I., Neve, R. L., Northen, T. R., Molina-Santiago, C., Panitchpakdi, M., Pullman, B., Puri, A. W., Schmid, R., Subramaniam, S., Thukral, M., Vasquez-Castro, F., Dorrestein, P. C., & Wang, M. (2022). GNPS Dashboard: collaborative exploration of mass spectrometry data in the web browser. Nat Methods, 19(2), 134-136. https://doi.org/10.1038/s41592-021-01339-5

Phelan, V. V. (2020). Feature-Based Molecular Networking for Metabolite Annotation. Methods Mol Biol, 2104, 227-243. https://doi.org/10.1007/978-1-0716-0239-3_13

Pietzke, M., & Vazquez, A. (2020). Metabolite AutoPlotter-an application to process and visualise metabolite data in the web browser. Cancer & Metabolism, 8, 1-11.

Pluskal, T., Korf, A., Smirnov, A., Schmid, R., Fallon, T. R., Du, X., & Weng, J.-K. (2020). CHAPTER 7. Metabolomics Data Analysis Using MZmine.htts://doi.org/ 10.1039/9781788019880-00232

Prajapat, P., Agrawal, D., & Bhaduka, G. (2022). A brief overview of sustained released drug delivery system. Journal of Applied Pharmaceutical Research.

Qamar, A. Y., Fang, X., Bang, S., Kim, M. J., & Cho, J. (2020). Effects of kinetin supplementation on the post-thaw motility, viability, and structural integrity of dog sperm. Cryobiology, 95, 90-96.

Qiu, T., Wu, D., Yang, L., Ye, H., Wang, Q., Cao, Z., & Tang, K. (2018). Exploring the mechanism of flavonoids through systematic bioinformatics analysis. Frontiers in pharmacology, 9, 918. htts://doi.org/ 10.3389/fphar.2018.00918

Rafael, D., Guerrero, M., Marican, A., Arango, D., Sarmento, B., Ferrer, R., Durán-Lara, E. F., Clark, S. J., & Schwartz, S., Jr. (2023). Delivery Systems in Ocular Retinopathies: The Promising Future of Intravitreal Hydrogels as Sustained-Release Scaffolds. Pharmaceutics, 15(5). https://doi.org/10.3390/pharmaceutics15051484

Raiola, A., Pizzolongo, F., Manzo, N., Montefusco, I., Spigno, P., Romano, R., & Barone, A. (2018). A comparative study of the physico-chemical properties affecting the organoleptic quality of fresh and thermally treated yellow tomato ecotype fruit. International Journal of Food Science & Technology, 53, 1219–1226.

Randjelović, P., Veljković, S., Stojiljković, N., Sokolović, D., Ilić, I., Laketić, D., Randjelović, D., & Randjelović, N. (2015). The beneficial biological properties of salicylic acid. *Acta facultatis medicae Naissensis*, *32*(4), 259-265.

Rasi, A., Sabokdast, M., Naghavi, M. R., Jariani, P., & Dedičová, B. (2024). Modulation of Tropane Alkaloids' Biosynthesis and Gene Expression by Methyl Jasmonate in Datura stramonium L.: A Comparative Analysis of Scopolamine, Atropine, and Hyoscyamine Accumulation. Life (Basel), 14(5). https://doi.org/10.3390/life14050618

Rattan, S. I., & Clark, B. F. (1994). Kinetin delays the onset of aging characteristics in human fibroblasts. Biochemical and biophysical research communications, 201(2), 665-672.

Rattan, S. I., & Sodagam, L. (2005). Gerontomodulatory and youth-preserving effects of zeatin on human skin fibroblasts undergoing aging in vitro. Rejuvenation research, 8(1), 46-57.

Ray, S. D. (1986). GA, ABA, phenol interaction in the control of growth: Phenolic compounds as effective modulators of GA-ABA interaction in radish seedlings. Biologia Plantarum, 28, 361-369.

Santino, A., Taurino, M., De Domenico, S., Bonsegna, S., Poltronieri, P., Pastor, V., & Flors, V. (2013). Jasmonate signaling in plant development and defense response to multiple (a) biotic stresses. Plant cell reports, 32, 1085-1098.htts://doi.org/ 10.1007/s00299-013-1434-4

Sasidharan, S., Chen, Y., Saravanan, D., Sundram, K., & Latha, L. Y. (2011). Extraction, isolation and characterization of bioactive compounds from plants' extracts. African journal of traditional, complementary and alternative medicines, 8(1).

Sauvain, M., Gantier, J.-C., & Gayral, P. Isolation of Leishmanicidal Triterpenes and Lignans frorn the Amazonian Liana Doliocarpus.

Schäfer, M., Brütting, C., Meza-Canales, I. D., Großkinsky, D. K., Vankova, R., Baldwin, I. T., & Meldau, S. (2015). The role of cis-zeatin-type cytokinins in plant growth regulation and mediating responses to environmental interactions. Journal of experimental botany, 66(16), 4873-4884.

Schmidt, C. S., Mrnka, L., Frantík, T., Motyka, V., Dobrev, P. I., & Vosátka, M. (2017). Combined effects of fungal inoculants and the cytokinin-like growth regulator thidiazuron on growth, phytohormone contents and endophytic root fungi in Miscanthus× giganteus. Plant Physiology and Biochemistry, 120, 120-131. Htts://doi.org/ 10.1016/j.plaphy.2017.09.012

Schrimpe-Rutledge, A. C., Codreanu, S. G., Sherrod, S. D., & McLean, J. A. (2016). Untargeted metabolomics strategies—challenges and emerging directions. Journal of the American Society for Mass Spectrometry, 27(12), 1897-1905.htts://doi.org/ 10.1007/s13361-016-1503-4

Shao, Q., Ran, Q., Li, X., Dong, C., Zhang, Y., & Han, Y. (2024). Differential responses of the phyllosphere abundant and rare microbes of Eucommia ulmoides to phytohormones. Microbiological Research, 286, 127798.htts://doi.org/ 10.1016/j.micres.2023.127798

Sharma, H. K., Chhangte, L., & Dolui, A. K. (2001). Traditional medicinal plants in Mizoram, India. Fitoterapia, 72(2), 146-161.

Simioni, C., Zauli, G., Martelli, A. M., Vitale, M., Sacchetti, G., Gonelli, A., & Neri, L. M. (2018). Oxidative stress: role of physical exercise and antioxidant nutraceuticals in adulthood and aging. Oncotarget, 9(24), 17181. htts://doi.org/ 10.18632/oncotarget.24729

Skalak, J., Nicolas, K. L., Vankova, R., & Hejatko, J. (2021). Signal integration in plant abiotic stress responses via multistep phosphorelay signaling. Frontiers in Plant Science, 12, 644823.htts://doi.org/10.3389/fpls.2021.644823

Šmehilová, M., Dobrůšková, J., Novák, O., Takáč, T., & Galuszka, P. (2016). Cytokinin-specific glycosyltransferases possess different roles in cytokinin homeostasis maintenance. Frontiers in Plant Science, 7, 197810.

Smith, R. D. (2006). Future directions for electrospray ionization for biological analysis using mass spectrometry. Biotechniques, 41(2), 147-148. https://doi.org/10.2144/000112217

Soares, M., Rezende, M., Ferreira, H., Figueiredo, A., Bustamante, K., Bara, M., & Paula, J. (2005). Pharmacognostic characterization of the leaves of Davilla elliptica St.-Hil.(Dilleniaceae). Revista Brasileira de Farmacognosia, 15, 352-360.

Solekha, R., Purnobasuki, H., Puspaningsih, N. N. T., & Setiyowati, P. A. I. (2024). Secondary Metabolites and Antioxidants Activity from Citronella Grass Extract (Cymbopogon nardus L.). Indian Journal of Pharmaceutical Education and Research. https://doi.org/10.5530/ijper.58.1s.32

Spíchal, L. (2012). Cytokinins–recent news and views of evolutionally old molecules. Functional Plant Biology, 39(4), 267-284. htts://doi.org/ https://doi.org/10.1071/FP11234

Spíchal, L., Rakova, N. Y., Riefler, M., Mizuno, T., Romanov, G. A., Strnad, M., & Schmülling, T. (2004). Two Cytokinin Receptors of Arabidopsis thaliana, CRE1/AHK4 and AHK3, Differ in their Ligand Specificity in a Bacterial Assay. Plant and Cell Physiology, 45(9), 1299-1305. https://doi.org/10.1093/pcp/pch132

Stincone, P., Pakkir Shah, A. K., Schmid, R., Graves, L. G., Lambidis, S. P., Torres, R. R., Xia, S. N., Minda, V., Aron, A. T., Wang, M., Hughes, C. C., & Petras, D. (2023). Evaluation of Data-Dependent MS/MS Acquisition Parameters for Non-Targeted Metabolomics and Molecular Networking of Environmental Samples: Focus on the Q Exactive Platform. Anal Chem, 95(34), 12673-12682. https://doi.org/10.1021/acs.analchem.3c01202

Stirk, W. A., Bálint, P., Tarkowská, D., Strnad, M., van Staden, J., & Ördög, V. (2018). Endogenous brassinosteroids in microalgae exposed to salt and low temperature stress. European Journal of Phycology, 53(3), 273-279. https://doi.org/10.1080/09670262.2018.1441447

Stirk, W. A., Ördög, V., Novák, O., Rolčík, J., Strnad, M., Bálint, P., & van Staden, J. (2013). Auxin and cytokinin relationships in 24 microalgal strains1. Journal of phycology, 49(3), 459-467.

Stuckey, M. E. (2014). Using SPE and HPLC-MS to Quantify and Identify Pharmaceutical Compounds in St. John's University Wastewater.

Sumner, L. W., Amberg, A., Barrett, D., Beale, M. H., Beger, R., Daykin, C. A., Fan, T. W.-M., Fiehn, O., Goodacre, R., & Griffin, J. L. (2007). Proposed minimum reporting standards for chemical analysis: chemical analysis working group (CAWG)

metabolomics standards initiative (MSI). Metabolomics, 3, 211-221. https://doi.org/10.1007/s11306-007-0082-2

Takeda, H., Matsuzawa, Y., Takeuchi, M., Takahashi, M., Nishida, K., Harayama, T., Todoroki, Y., Shimizu, K., Sakamoto, N., Oka, T., Maekawa, M., Chung, M. H., Kurizaki, Y., Kiuchi, S., Tokiyoshi, K., Buyantogtokh, B., Kurata, M., Kvasnička, A., Takeda, U., Uchino, H., Hasegawa, M., Miyamoto, J., Tanabe, K., Takeda, S., Mori, T., Kumakubo, R., Tanaka, T., Yoshino, T., Arita, M., & Tsugawa, H. (2024). MS-DIAL 5 multimodal mass spectrometry data mining unveils lipidome complexities. bioRxiv.

Takei, K., Ueda, N., Aoki, K., Kuromori, T., Hirayama, T., Shinozaki, K., Yamaya, T., & Sakakibara, H. (2004). AtIPT3 is a key determinant of nitrate-dependent cytokinin biosynthesis in Arabidopsis. Plant and Cell Physiology, 45(8), 1053-1062.htts://doi.org/ 10.1093/pcp/pch115

Tariq, S., Wani, S., Rasool, W., Shafi, K., Bhat, M. A., Prabhakar, A., Shalla, A. H., & Rather, M. A. (2019). A comprehensive review of the antibacterial, antifungal and antiviral potential of essential oils and their chemical constituents against drug-resistant microbial pathogens. Microbial pathogenesis, 134, 103580. htts://doi.org/ 10.1016/j.micpath.2019.103580

Thanapairoje, K., Junsiritrakhoon, S., Wichaiyo, S., Osman, M. A., & Supharattanasitthi, W. (2023). Anti-ageing effects of FDA-approved medicines: a focused review. J Basic Clin Physiol Pharmacol, 34(3), 277-289. https://doi.org/10.1515/jbcpp-2022-0242. https://doi.org/10.1515/jbcpp-2022-0242

Thrash-Williams, B., Karuppagounder, S. S., Bhattacharya, D., Ahuja, M., Suppiramaniam, V., & Dhanasekaran, M. (2016). Methamphetamine-induced dopaminergic toxicity prevented owing to the neuroprotective effects of salicylic acid. *Life sciences*, *154*, 24-29.

Tronel, A., Roger-Margueritat, M., Plazy, C., Cunin, V., Mohanty, I., Dorrestein, P., Soranzo, T., & Le Gouellec, A. (2024). Untargeted and Semi-Targeted Metabolomics Approach for Profiling Small Intestinal and Fecal Metabolome Using High-Resolution Mass Spectrometry. bioRxiv.

Tsugawa, H., Nakabayashi, R., Mori, T., Yamada, Y., Takahashi, M., Rai, A., Sugiyama, R., Yamamoto, H., Nakaya, T., Yamazaki, M., Kooke, R., Bac-Molenaar, J. A., Oztolan-Erol, N., Keurentjes, J. J. B., Arita, M., & Saito, K. (2019). A cheminformatics approach to characterize metabolomes in stable-isotope-labeled organisms. Nature Methods, 16(4), 295-298. https://doi.org/10.1038/s41592-019-0358-2

Valleser, V. C. (2022). Applications and Effects of Phytohormones on the Flower and Fruit Development of Pineapple (Ananas comosus L.).

Van Andel T, T. R. (2003). Floristic composition and diversity of three swamp forests in northwest Guyana. Plant Ecology, 167(2), 293-317. https://doi.org/10.1023/A:1023935326706

Van Andel T, T. R., MacKinven, A., & Bánki, O. (2003). Commercial non-timber forest products of the Guiana shield: an inventory of commercial NTFP extraction and possibilities for sustainable harvesting. Netherlands Committee for IUCN.

van Andel, T. R. (2000). Non-timber forest products of the North-West District of Guyana. Utrecht University.

Vedenicheva, N. P., Al-Maali, G. A., Bisko, N. A., Kosakivska, I. V., Ostrovska, G. V., Khranovska, N. M., Gorbach, O. I., Garmanchuk, L. V., & Ostapchenko, L. I. (2021). Effect of cytokinin-containing extracts from some medicinal mushroom mycelia on HepG2 cells in vitro. International Journal of Medicinal Mushrooms, 23(3).

Voller, J., Zatloukal, M., Lenobel, R., Dolezal, K., Béres, T., Krystof, V., Spíchal, L., Niemann, P., Dzubák, P., Hajdúch, M., & Strnad, M. (2010). Anticancer activity of natural cytokinins: a structure-activity relationship study. *Phytochemistry*, *71*(11-12), 1350-1359. https://doi.org/10.1016/j.phytochem.2010.04.018

Wareing, P., Horgan, R., Henson, I., & Davis, W. (1977). Cytokinin relations in the whole plant. Plant Growth Regulation: Proceedings of the 9th International Conference on Plant Growth Substances Lausanne, August 30–September 4, 1976,

Wingfield, J., & Wilson, I. D. (2016). Advances in Mass Spectrometry Within Drug Discovery. J Biomol Screen, 21(2), 109-110. https://doi.org/10.1177/1087057115623454

Zadeh Hashem, E., & Eslami, M. (2018). Kinetin improves motility, viability and antioxidative parameters of ram semen during storage at refrigerator temperature. Cell and tissue banking, 19, 97-111.htts://doi.org/ 10.1007/s10561-017-9655-6

Zhang, D., Tong, J., Xu, Z., Wei, P., Xu, L., Wan, Q., Huang, Y., He, X., Yang, J., & Shao, H. (2016). Soybean C2H2-type zinc finger protein GmZFP3 with conserved QALGGH motif negatively regulates drought responses in transgenic Arabidopsis. Frontiers in Plant Science, 7, 325. Htts://doi.org/10.3389/fpls.2016.00325

Zhang, M., Deng, Y., Xie, G., Deng, B., Zhao, T., & Yan, Y. (2024). Regulation of exogenous sugars on the biosynthesis of key secondary metabolites in Cyclocarya paliurus. Physiol Plant, 176(5), e14552. https://doi.org/10.1111/ppl.14552

Zhang, N., Xie, Y.-D., Guo, H.-J., Zhao, L.-S., Xiong, H.-C., Gu, J.-Y., Li, J.-H., Kong, F.-Q., Sui, L., & Zhao, Z.-W. (2016). Gibberellins regulate the stem elongation rate without affecting the mature plant height of a quick development mutant of winter wheat (Triticum aestivum L.). Plant Physiology and Biochemistry, 107, 228-236. https://doi.org/10.1016/j.plaphy.2016.06.011

Zhang, X., Xiong, Y., Wang, Y., Wu, C., da Silva, J. A. T., & Ma, G. (2025). 6-benzyladenine, a cytokinin, promotes the accumulation of essential oil, flavonoids, and phenolics in Santalum album heartwood by interacting with other hormones. Industrial Crops and Products, 223, 120285. https://doi.org/10.1016/j.indcrop.2024.120285

Zhang, Y., Guo, W., Chen, L., Shen, X., Yang, H., Fang, Y., Ouyang, W., Mai, S., Chen, H., & Chen, S. (2022). CRISPR/Cas9-mediated targeted mutagenesis of GmUGT enhanced soybean resistance against leaf-chewing insects through flavonoids biosynthesis. Frontiers in Plant Science, 13, 802716. https://doi.org/10.3389/fpls.2022.802716

Zhang, Y., Yan, H., Li, Y., Xiong, Y., Niu, M., Zhang, X., Teixeira da Silva, J. A., & Ma, G. (2021). Molecular Cloning and Functional Analysis of 1-Deoxy-D-Xylulose 5-Phosphate Reductoisomerase from Santalum album. Genes (Basel), 12(5). https://doi.org/10.3390/genes12050626

Zheng, J.-X., Han, Y.-S., Wang, J.-C., Yang, H., Kong, H., Liu, K.-J., Chen, S.-Y., Chen, Y.-R., Chang, Y.-Q., & Chen, W.-M. (2018). Strigolactones: A plant phytohormone as novel anti-inflammatory agents. *MedChemComm*, *9*(1), 181-188.

Zhu, L., Liao, Y., Lin, K., Wu, W., Duan, L., Wang, P., Xiao, X., Zhang, T., Chen, X., & Wang, J. (2024). Cytokinin promotes anthocyanin biosynthesis via regulating sugar accumulation and MYB113 expression in Eucalyptus. Tree Physiology, 44(1), tpad154.

Zuo, Y., Gong, S., Zhang, L., Zhou, J., Wu, J. L., & Li, N. (2024). A Deep Mining Strategy for Peptide Rapid Identification in Lactobacillus reuteri Based on LC-MS/MS Integrated with FBMN and De Novo Sequencing. Metabolites, 14(9). https://doi.org/10.3390/metabo14090467

Zwack, P. J., & Rashotte, A. M. (2013). Cytokinin inhibition of leaf senescence. Plant Signaling & Behavior, 8(7), e24737.

CHAPTER 5

PREFACE

Title: The total Phenolic Content and Antioxidant Capacity of Guyanese Wood vine *Doliocarpus dentatus* (Capadulla)

Authors: Ewart Smith[1*], Dev Seneviratne[2], Faith Shadipo[2], Ainsley Lewis[2], Suresh S Narine[3], RJ Neil Emery[2] and Sanela Martic[2]

Reference: To be published in International Journal Ethnobotany Research and Applications or Journal of Phytochemical Analysis 2024 / 2025

Contributions: EAS assembled data on phenolic, flavonoid contents and metabolomics data, created figures and wrote the manuscript. DS and EAS worked on the chemical assays to determine the quchening and antioxidant activities of the exreacts. FS worked on spectroscopic evaluation of ROS data. AL worked on the modification of the workflow and experimental design. SN and RJNE conceived, directed and obtained funding for research present in the study. EAS, AL, RJNE and SN edited the manuscript prior to submission.

5. CHAPTER 5

The Total Phenolic Content and Antioxidant Capacity of Guyanese Wood vine *Doliocarpus dentatus* (Capadulla)

ABSTRACT

Doliocarpus dentatus, a plant traditionally utilized in Guyanese medicine and referred to as "Capadulla" or "Guyanese natural Viagra," is recognized for its purported therapeutic benefits, particularly in the treatment of erectile dysfunction. Within Guyana, two distinct ecotypes of *D. dentatus*, namely the red and white varieties, are employed for their therapeutic properties. The phytochemical analyses of these ecotypes reveal a prevalence of secondary metabolites, including phenolic and flavonoid compounds. The mechanisms of action of these secondary metabolites are understood to support antioxidant and anti-inflammatory properties, which may enhance overall health, promote blood circulation, and exhibit adaptogenic effects that can mitigate oxidative stress. Despite its prominent use in Guyanese traditional medicine, the red ecotype is preferred for the treatment of erectile dysfunction, likely due to its higher concentration of therapeutic compounds, particularly polyphenols. However, there is a paucity of information concerning the total phenolic content, total flavonoid content, and antioxidant capacity of both the red and white ecotypes of *D. dentatus*.

This study investigates the total phenolic and flavonoid content, as well as the antioxidant capacity, of two ecotypes (red and white) of the Guyanese wood species *D. dentatus*. The aqueous extracts of both ecotypes were subjected to analysis using spectrophotometric methods, including

Folin-Ciocalteu assays for total phenolic content, aluminum chloride assays for flavonoid content, and 2,2-Diphenyl-1-picrylhydrazyl (DPPH) and hydrogen peroxide (H_2O_2) assays to assess antioxidant activity. The red ecotype demonstrates considerable potential as a natural product, primarily attributable to its elevated phenolic content (119.70 mg GAE/g) and flavonoid content (4.146 mg QE/g) when compared to the white ecotype (61.08 mg GAE/g and 1.584 mg QE/g, respectively). This ecotype also exhibits a higher level of antioxidant activity, as evidenced by the DPPH and H_2O_2 scavenging assays, which indicate its capacity to neutralize reactive oxygen species (ROS) and mitigate oxidative stress. The chemical assays suggest that the red ecotype possesses the potential to protect cells from damage, which is critical in preventing or alleviating various physiological conditions, including cellular damage, ageing, cancer, and disorders impacting vital organs. Compounds such as apigenin and cyanidin 3-O-beta-D-glucoside, which are found in higher concentrations in the red ecotype, are linked with cardiovascular health, anti-inflammatory effects, and metabolic benefits. Fourier-transform infrared (FTIR) analysis reveals an increased concentration of hydroxyl and amine functional groups in the red ecotype, further substantiating the presence of secondary metabolites such as flavonoids, tannins, and alkaloids. These compounds may interact with various free radicals and biological processes to promote overall health. The red ecotype's enhanced capacity to quench ROS in comparison to the white ecotype suggests a protective role against oxidative stress-related diseases, thus supporting its traditional use in herbal medicine for the management of conditions associated with oxidative stress and inflammation. Further research is warranted to identify the specific bioactive compounds responsible for the observed antioxidant properties and to explore their potential health benefits in vivo.

keywords: Antioxidant, scavenging, ecotypes, phenolic, flavonoid, fluorescence spectroscopy, DPPH, Capadulla

5.1. INTRODUCTION

Reactive Oxygen Species (ROS) are highly reactive molecules or ions that contain oxygen and have unpaired electrons. These include the superoxide anion (O2•-), hydroxyl radical (•OH), and hydrogen peroxide (H_2O_2) (Baliyan et al., 2022; Lewis et al., 2022). An excessive production of ROS can lead to oxidative stress, which is a key factor in the development of various physiological conditions such as cellular damage, aging, cancer, and disorders affecting the liver, brain, heart, and kidneys (Aryal et al., 2019). This condition occurs when there is an imbalance between the production of ROS and the cell's ability to detoxify or repair them. As a result, there is potential damage to lipids, proteins, DNA, and other critical cellular components. Such damage can interfere with cell function and lead to disease (Sera Kim et al., 2021). Environmental factors such as pollutants, UV radiation, and certain chemicals can increase ROS levels. This underscores the importance of antioxidants in neutralizing these agents to maintain cellular balance and protect against oxidative damage (Aryal et al., 2019; Raj Rai et al., 2021). However, the body's natural antioxidants may be insufficient under elevated oxidative stress, highlighting the necessity of incorporating dietary antioxidants into our diet (Aryal et al., 2019).

Recently, there has been a lot of attention on the benefits of naturally occurring antioxidants due to their safe properties and their ability to interact with different free radicals found in living cells (Mardani-Ghahfarokhi & Farhoosh, 2020). Numerous epidemiological studies have demonstrated that consuming leafy vegetables rich in phenolic and flavonoid compounds, known for their strong antioxidant properties, is linked to a reduced occurrence of cardiovascular diseases, cancer, diabetes, and neurodegenerative disorders. These natural antioxidants, mainly phenolic compounds, help eliminate harmful reactive oxygen and nitrogen species/radicals that are

generated by various biological processes, such as ionizing radiation, photosensitization, enzymatic activity, and biochemical reactions (Aryal et al., 2019; Nkwocha et al., 2023).

Although synthetic phenolic antioxidants such as butylated hydroxyanisole and butylated hydroxytoluene are widely employed to reduce oxidative stress, their usage can potentially lead to adverse health effects. As a result, the use of phenolic antioxidants derived from food and herbal medicine is gaining widespread acceptance. These antioxidants are valued for their natural origins, affordability, and ability to protect against radiation (Aryal et al., 2019).

Doliocarpus dentatus (Capadulla) stands as a amazing woody vine in the *Dilleniaceae* family thriving, within the vibrant lush rainforests of South and Central America and has captured the curiosity of researchers due to its diverse phytochemical and phytohormone profiles (De Oliveira et al., 2002; Ewart smith, 2023; Mihalik, 1978). The woody vine is known for its various biological properties including anti-hemorrhagic (Nishijima et al., 2009; Sauvain et al.), anti-inflammatory, antioxidant, antimicrobial (Costa et al., 2008; De Toledo et al., 2011), antitumoral (Camila et al., 2009), anti-ulcer, immunological (Kushima et al., 2009), and cancer chemoprevention properties (Endringer et al., 2010). The phytochemical constituents of this species included polyphenols, flavonoids, lignans and many others (Ewart smith, 2023; Raissa Borges Ishikawa et al., 2017; R. Jagessar et al., 2013; Jahangeer et al., 2021). The woody vine of *D. dentatus* is extensively employed in traditional Eastern medicine for the treatment of leishmanial ulcers utilizing its bark. It is also known for its aphrodisiac properties used to manage diabetes mellitus, hypertension, and various eye conditions and used as a treatment for malaria (Andel et al., 2003; Cinthia et al., 2013; Ewart smith, 2023).

While some studies on *D. dentatus* woody vine in Guyana have focused on its traditional applications (Van Andel T et al., 2003; van Andel, 2000), we now have evidence that *D. dentatus* red and white ecotypes contain secondary metabolites that may contain antioxidant, anti inflammatory, antimicrobial and cancer chemoprevention properties.

To our best knowledge there is limited information available on its total phenolic, total flavonoid content and antioxidant capacity. This study aims to analyze the total phenolic content, total flavonoid content, and antioxidant activity of aqueous extracts of *D. dentatus* red and white ecotypes.

5.2. MATERIALS AND EXPERIMENTAL METHOD

5.2.1. Sample Collection

5.2.2. Study site and plots – Eagle Mountain Forest Potaro - Siparuni, Guyana

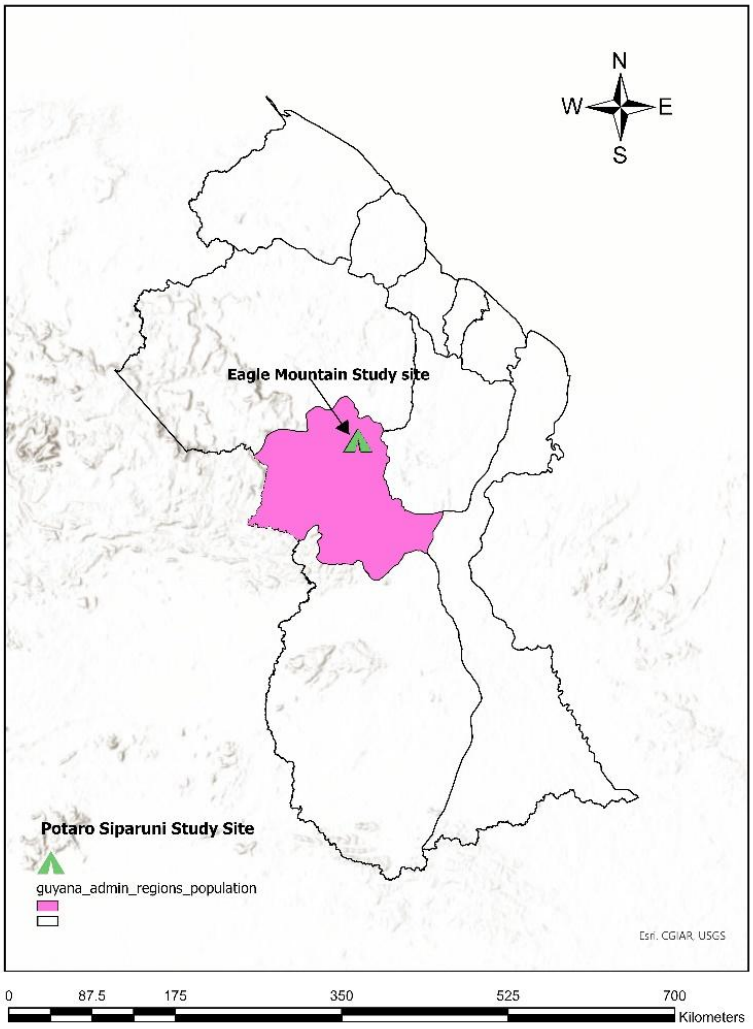

Figure 5. 1Eagle Mountain Forest located in mining district of Potaro Siparuni Region 8 (21N0261909 - 0578704) Guyana South America located in the pink.

The *D.dentatus* red and white ecotypes were collected from the Eagle Mountain Forest located approximately 200 km south-southwest of Georgetown, the capital city of Guyana (21N0261909 - 0578704) and further identified by Officers (Dendrologist) of the Guyana Forestry Commission and members of the University of Guyana Faculty of Agriculture and Forestry.

For every individual D. dentatus liana selected, a disc ranging in diameter (50 mm– 200 mm) was carefully extracted from various points along the woody vine, encompassing the ground level, an intermediate position, and an emergent point.

In July 2023, a total of three biological replicates for each ecotype of D. dentatus red and white were collected. The processed samples of the same ecotypes with similar diameter formed 3 composite samples, 3 biological replicates for each ecotype and 9 technical replicates for each ecotype.

Following sample preparation protocol , these samples were promptly placed in dry ice to maintain their metabolic integrity during transit. Subsequently, they were transported to the University of Guyana (Greater Georgetown, Guyana). Here, the samples underwent further processing to prepare them for in-depth analysis. Finally, the samples were sent to Trent University (Peterborough, Canada), where advanced metabolomic analysis was conducted. The samples were grounded with a Thomas Wiley ED-5. The samples were them sieved (0.0029 mesh opening).

5.2.3. Sample Preparation

The sample preparation for the total phenolic content and antioxidant capacity of Guyanese *D. dentatus* (Capadulla) red and white ecotypes with slight modifications to the previously published methods (Cicco et al., 2009; Raissa Borges Ishikawa et al., 2017; Tahirovic & Basic,

2017; Tan et al., 2014). One gram (1g) of each dried *D.dentatus* grounded sample was soaked in 100 ml of boiling, high-purity water (DI H_2O). The mixture was then left to stand for 20 minutes. The extracts were filtered using a Buckner funnel and Fisher brand filter paper with coarse porosity with a fast flow rate. Each filtrate was concentrated to dryness using a speed vacuum concentrator under reduced pressure and controlled temperature (40-50 ℃) to give final extracts, which was stored at - 80 ℃ until further use.

5.2.4. Chemicals

Gallic acid, Sodium carbonate (Na_2CO_3), Folin-Ciocalteu's reagent (FC) reagent and 2,2-iphenyl-2-picrylhydrazyl (DPPH), Hydrogen peroxide H_2O_2 and the reference standards L-ascorbic acid, were purchased from Sigma Chemical Co. (St. Louis, MO, USA). HPLC-grade methanol was purchased from Thermo Fisher scientific (Ontario, Canada). Fresh stock solutions were prepared before each analysis. The absorbance measurements were performed using a Bioteck Cytation800 spectrophotometer (Fullerton, CA, USA).

5.2.5. UV-Vis Spectrophotometer Analyses

The Agilent BioTek Cytation 5 Cell Imaging Multi-Mode Reader combines automated digital microscopy and conventional microplate detection in a configurable, upgradable platform was used to measure absorbance and fluorescence were measured from 200 to 760 nm (Rees et al., 2025) using the default settings. It offers fluorescence, brightfield, high contrast brightfield, color brightfield, and phase contrast imaging with magnification options ranging from 1.25x to 60x (Little et al., 2020). The multi-mode detection modules include filter- and monochromator-based fluorescence detection, luminescence, and UV-Vis absorbance detection (Dong et al., 2025;

Queiroz et al., 2019). The system supports a wide range of microplate types, from 6- to 1536-well plates, as well as other labware such as microscope slides and cell culture dishes (Queiroz et al., 2019). Environmental controls include temperature regulation up to 65°C, with optional CO_2/O_2 control and Peltier cooling (Zein-Sabatto et al., 2025). Data acquisition and analysis are managed through Gen5 software, which provides complete control over imaging and detection functions (Zein-Sabatto et al., 2025).

5.2.6. Fourier-Transform Infrared Spectroscopy (FTIR)

Attenuated total reflectance Fourier-transform infrared spectroscopy (FTIR-ATR) spectra was collected using a Thermo Scientific Nicolet 380 FTIR spectrometer (Thermo Electron Scientific Instruments LLC, Swedesboro, NJ, USA) equipped with a single reflection diamond ATR accessory. Samples were mounted on the diamond ATR crystal and measurements were performed at room temperature. A total of 46 scans were collected for each sample over a range of 400 to 4000 cm−1 at a spectral resolution of 4 cm−1. ATR correction was performed after each data acquisition. OMNIC software (Thermo Scientific Inc., Waltham, MA, USA) (https://www.thermofisher.com/order/catalog/product/INQSOF0 18) was used for all spectral manipulations.

5.2.7. Standard preparation for Total Phenolic Content (TPC)

The detailed procedure for preparing gallic acid standard solutions was previously described and with slight modification (Cicco et al., 2009; Kupina et al., 2018). Experiments were conducted using Folin-Ciocalteu's reagent (FC) reagent from Merck (1.09001), Sodium carbonate (S6139), and pure Gallic acid (C0626) from Sigma. Gallic acid was selected as the standard to

measure the phenol due to its presence in our *D. dentatus* extracts was as follows: 1 g of gallic acid standard, measured using an analytical scale, were dissolved in 100 MeOH and DI H_2O respectively in a 1000 ml volumetric flask. Then, 1, 2, 3, 4, 5 and 6 ml of the above stock solution were diluted to 10 ml with DI H_2O to obtain different concentrations of gallic acid standard in methanol at 5, 10, 15, 20 25 and 30 respectively. To prepare the calibration standard solutions, refer to table 5.1 (approximately 10–90 mg/L gallic acid). A measured volume of the stock standard solution was transferred to a 250 mL flask and diluted to the mark with deionized water. These solutions were stored at 4 °C for up to one week. Fresh 100 mg/L gallic acid solutions were then prepared for each methanol and distilled water concentration by further diluting the stored solutions with methanol and water as needed to achieve the desired concentrations.

Table 5.1. The preparation of the calibration standard for gallic acid (mg/L).

Calibration standard solution	Volume of stock standard solution (mL)	Volume of flask(mL)	concentration of gallic acid (mg/L)
1	0.25	50	5
2	0.5	50	10
3	0.75	50	15
4	1	50	20
5	1.25	50	25
6	1.5	50	30

Briefly, 1 g of extract (100-500 µg/mL) solution was mixed with 2.5 mL of 10 % (w/v) Folin-Ciocalteu reagent. After 5 min, 2.0 mL of Na_2CO_3 (75%) was subsequently added to the *D. dentatus* extracts and incubated at 50 °C for 10 min with intermittent agitation. Afterwards, the sample was cooled, and the absorbance was measured using a UV Spectrophotometer (Shimadzu,

UV-1800) at 743 nm against a blank without extract. The outcome data was expressed as mg/g of gallic acid equivalents in milligrams per gram (mg GAE/g) of dry extract.

The Guyanese traditional *D.dentatus* tea extraction procedure was carried out using a grounded method with modifications (Cheng et al., 2023). 25 grams of *D.dentatus* tea soaked in 400 mL DI H_2O at a temperature of 90°C and set for 10,20,30,04,50 and 60 minutes and stirred using a magnetic stirrer with a speed of 300 rpm. The grounding *D.dentatus* tea results filtered using a speed vacuum concentrator under reduced pressure and controlled temperature (40-50 ℃). The second filtering process was carried out using the yellow hydrophilic syringe filter (45mm) to give final extracts, which was stored at - 80 ℃ until further use.

5.2.8. Determination of Total Phenolic Content

The total phenolic content (TPC) was determined using the spectrophotometric method on a PerkinElmer UV/Vis spectrometer Lambda 25. Folin-Ciocalteu's reagent was used in this method to lower Mo (VI) ions with phenolics from *D. dentatus* ecotypes extracts. This creates blue Me(V)-oxides that absorb light best at 743 nm (Aryal et al., 2019; Noreen et al., 2017; Singleton & Rossi, 1965; Slinkard & Singleton, 1977). To do the test, 1 mL of the supernatant from diluted *D. dentatus* ecotypes was mixed with 1 mL of Folin-Ciocalteu reagent that had been diluted 1/10. The mixture was then allowed to stand for 10 minutes. Next, 0.8 mL of 7.5% Na_2CO_3 was added to the Folin-Ciocalteu reagent. After 30 minutes of incubation at room temperature, the absorbance of the solutions was measured at 743 nm. The TPC was expressed as gallic acid (GA) equivalents (mg) per volume of tea infusion (100 mL).

5.2.9. Determination of Flavonoid Contents

The flavonoid contents of *D. dentatus* extracts were measured as per the Dowd method (Arvouet-Grand et al., 1994; Aryal et al., 2019). An aliquot of 1 mL of extract solution (25–200 µg/mL) or quercetin (25–200 µg/mL) was mixed with 0.2 mL of 10% (w/v) $AlCl_3$ solution in methanol, 0.2 mL (1 M) potassium acetate and 5.6 mL distilled water. The mixture was incubated for 30 min at room temperature followed by the measurement of absorbance at 415 nm against the blank. The outcome data were expressed as mg/g of quercetin equivalents in milligrams per gram (mg QE/g) of dry extract.

5.2.10. DPPH Radical Scavenging Activity

The DPPH radical scavenging activity of the sample was analyzed using the DPPH method (Ahmed et al., 2019; Aryal et al., 2019) with slight modification. The DPPH• radical had a maximum absorbance at 520 nm, and the DPPH radical scavenging activity of the sample was evaluated as a decrease in the absorbance. Briefly, the sample (50µL), methanol (4.4 mL), and DPPH• radical methanol solution (0.5 mL, 1 mM) were mixed and reacted at room temperature for 30 min. The absorbance of the mixture was measured at 520 nm using a spectrophotometer. A standard curve for the concentration of the standard compound and DPPH radical scavenging rate was plotted using ascorbic acid. Radical scavenging capacity was expressed as a percentage RSA (RSA%) and calculated using the following equation:

Pencentage of Radical Scavenging Activity (H_2O_2) = $\left[(A_0 - A_1)/A_0\right] X 100$, where A_0 = absorbance of the control (phosphate buffer with H_2O_2) and A_1 = absorbance of the *D.dentatus* red and white ecotypes extracts.

5.2.11. Hydrogen Peroxide Scavenging Activity

The radical scavenging activity of *D.dentatus* ecotype extracts was determined using the H_2O_2 method (Aryal et al., 2019) with slight modification. Briefly, 2 mL of extract solution (0.5–1 μg/mL) was added to 4.0 mL of H_2O_2 (20 mM) solution in phosphate buffer (pH 7.4). After 10 min, the absorbance was measured at λ max 270 nm against the phosphate buffer blank solution. The percentage scavenging of H_2O_2 was calculated using the equation:

Pencentage of Radical Scavenging Activity (H_2O_2) = $\left[(A_0 - A_1)/A_0\right] X 100$, where A_0 = absorbance of the control (phosphate buffer with H_2O_2) and A_1 = absorbance of the *D.dentatus* red and white ecotypes extracts.

5.2.12. Phytochemical preparation of the *D. dentatus* tea extracts

The phytochemical preparation was done using (Zhang et al., 2012) with modifications. The *D. dentatus* woody vines were ground to 0.508 mesh, and 22,500 mg of each sample (red and white ecotype) the sample were put into 1000 mL round bottle flasks were soaked in 400 ml of boiling, high-purity water. The mixture was then left to stand for 20 minutes. The extracts were filtered using a Buckner funnel and Fisher brand filter paper with coarse porosity with a fast flow rate. 400 mL of the mixture was added into the separate flasks. The extraction was carried out in a water bath (Fisher Scientific Isotemp 3006D) at 40 ° which was connected to a 2L solventvap rotary evaporator and speed vacuum concentrator (BUCH- Switzerland vacuum pump). Each

filtrate was concentrated to dryness using a speed vacuum concentrator under reduced pressure and controlled temperature (40-50 ℃) to give final extracts. The extracts were weighed to give the yield of the *D. dentatus* extract.

The Metabolomics profiles of *D. dentatus* tea extracts were determined using the method by Smith, Ewart, et al., (Ewart smith, 2023) with slight modification. Tea extracts from both *D. dentatus* ecotypes (i.e., red and white) were analyzed by LC-MS (Nguyen et al., 2023b) with slight modifications. In the processing module of XCalibur 4.1 (ThermoScientific, Waltham, MA, USA), we inputted the putative identities of key therapeutic compound family of interest (Polyphenols) and extracted the exact masses of protonated or deprotonated compounds. This semi-targeted approach was performed to determine peak quality and to monitor the peaks within the samples for therapeutic compounds. The relative quantification of peak areas was conducted to determine up- or downregulated compounds by calculating the ratio of the averages of *D.dentatus* Red to *D.dentatus* white. If the ratio (fold change; FC) was greater than 1, the samples were considered upregulated. The semi targeted approach foces on the polyphenols (phenolics and flavonoids) compounds. These secondary metabolities classes were selected due to the high relative aboundance in the both *D.dentaus* red and white ecotypes. Polyphenols are structurally diverse (e.g., flavonoids, phenolic acids, lignans) and exhibit strong antioxidant properties due to hydroxyl groups and conjugated double bonds (Aryal et al., 2019; Qi et al., 2025).. Their ability to scavenge free radicals, chelate metals, and modulate oxidative stress makes them critical targets for health-related studies (Pandey & Rizvi, 2009; Quesada-Vázquez et al., 2024)

5.2.13. Statistical analysis

The experimental results were expressed as mean ± standard error of the mean (SEM) of three replicates. Where applicable, the data were subjected to one-way analysis of variance (ANOVA) and the differences between samples were determined by Duncan's Multiple Range tests using Origin Pro student version 2024. P Values ≤ 0.05 were regarded as significant.

5.3. RESULTS

5.3.1. The FTIR spectrum comparing the red and white ecotypes of *D. dentatus* reveals several key quantitative differences and similarities across 4000 – 500 cm $^{-1}$ wavenumber

The image presents FTIR (Fourier Transform Infrared Spectroscopy) spectra comparing red and white ecotypes, with absorbance plotted against wavenumber (Fig 5.2). The red ecotype demonstrates a higher absorbance peak around 3300 cm^{-1}. Graphs (B) and (C) offer a more detailed examination of the individual spectra for the red and white ecotypes, respectively, highlighting specific peaks that correspond to various functional groups or molecular vibrations within the samples (Fig 5.2).

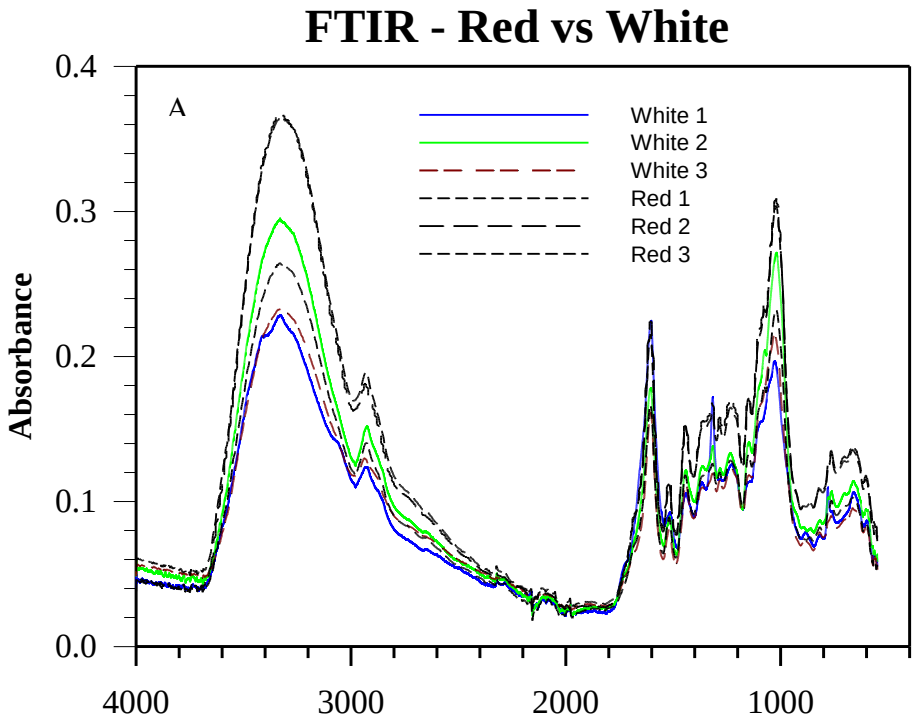
FTIR - Red vs White
A
White 1
White 2
White 3
Red 1
Red 2
Red 3
Absorbance
0.4
0.3
0.2
0.1
0.0
4000
3000
2000
1000

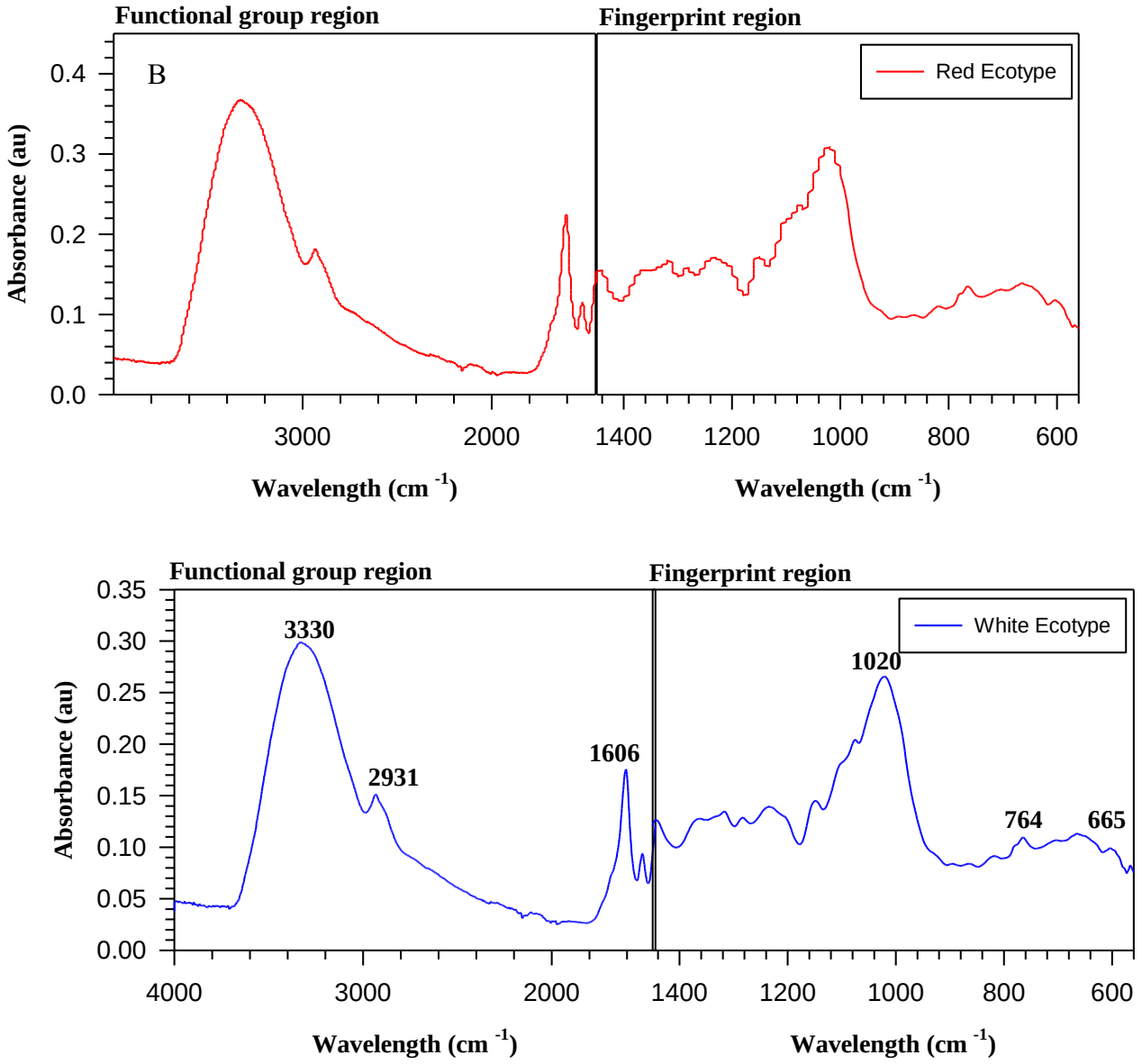

Figure 5. 2. A. FTIR spectra comparing the red and white ecotypes of D. dentatus, with three biological replicates for each ecotype (N = 3). The x-axis represents the wavenumber in cm^{-1}, spanning from 4000 to approximately 500 cm^{-1}, whereas the y-axis indicates absorbance values ranging from 0 to 0.4. B. Illustrates the distinct chemical groups observed in the (3375.4 - 2936.0) cm^{-1} and (1600 - 600) cm^{-1} wave band regions.

Table (5.2) provides a detailed comparison of the infrared (IR) spectral data for *D. dentatus* ecotypes, highlighting the differences in peak intensities and assignments of functional groups. At a wavenumber of 3400 cm^{-1}, both ecotypes exhibited broad peaks attributed to O-H or N-H stretching vibrations, with the red ecotype showing a strong broad peak (0.35–0.37) compared to a medium broad peak (0.22–0.29) in in the white ecotype (Fig 5.2). At 3000 cm^{-1}, medium shoulder peaks (0.15–0.18) are observed in the white ecotype, while the second sample shows weaker shoulder peaks (0.12–0.15), corresponding to C-H stretching in aliphatic compounds. Both ecotypes displayed very weak absorption (0.03–0.04) at 2000 cm^{-1}, which is associated with combination bands. At 1600 cm^{-1}, sharp peaks are noted in both ecotypes—slightly stronger in the red ecotype (0.20–0.22) compared to the white ecotype (0.18–0.20)—indicating C=O stretching or C=C aromatic vibrations. Strong, well defined peaks are present at 1000 cm^{-1} for ecotypes, with similar intensities (0.25–0.31 for the red ecotype and 0.25–0.30 for the white ecotype), corresponding to C-O-C stretching and single C-O bonds.

The fingerprint region between 800 and 500 cm^{-1}, multiple weak peaks are observed, with slightly higher intensities (0.08–0.15) in the red ecotype compared to the white ecotype (0.07–0.12), representing C-C and C-H bending vibrations characteristic of this region.

Table 5.2. Characteristic FTIR absorption bands, relative intensities, and functional region assignments for *D.dentatus* red and white ecotypes in the spectral range of 4000-400 cm^{-1}. The absorbance values show distinct variations between Red and White samples, particularly in the O-H/N-H stretching region (~3400 cm^{-1}), while maintaining similar peak patterns across the fingerprint region.

Wavenumber (cm^{-1})	***D.dentatus***	***D.dentatus***	**Assignment group**
3400	Strong broad peak (0.35-0.37)	Medium broad peak (0.22-0.29)	O-H/N-H stretching vibrations
3000	Medium shoulder peaks (0.15-0.18)	Weak shoulder peaks (0.12-0.15)	C-H stretching (aliphatic)
2000	Very weak absorption (0.03-0.04)	Very weak absorption (0.03-0.04)	Combination bands
1600	Sharp peak (0.20-0.22)	Sharp peak (0.18-0.20)	C=O stretching/C=C aromatic vibrations
1000	Strong complex peaks (0.25-0.31)	Strong complex peaks (0.25-0.30)	C-O-C stretching, C-O single bonds
800 - 500	Multiple weak peaks (0.08-0.15)	Multiple weak peaks (0.07-0.12)	Fingerprint region (C-C, C-H bending)

5.3.2. Total Phenolic and Flavonoid content

5.3.3. Standard curve for Gallic acid showing the Linear relationship between absorbance and gallic acid concentration (mg/L, N = 3, X ± SEM).

The graph showing the relationship between the concentration of Gallic acid (measured in mg/L) and its absorbance (Fig 5.2). The data points, represented by circular markers accompanied by error bars, demonstrate an upward trend, indicating a positive correlation between Gallic acid concentration and absorbance. A regression line, labeled "Plot 1 Reg" is fitted to the data points, providing a visual summary of the linear relationship.

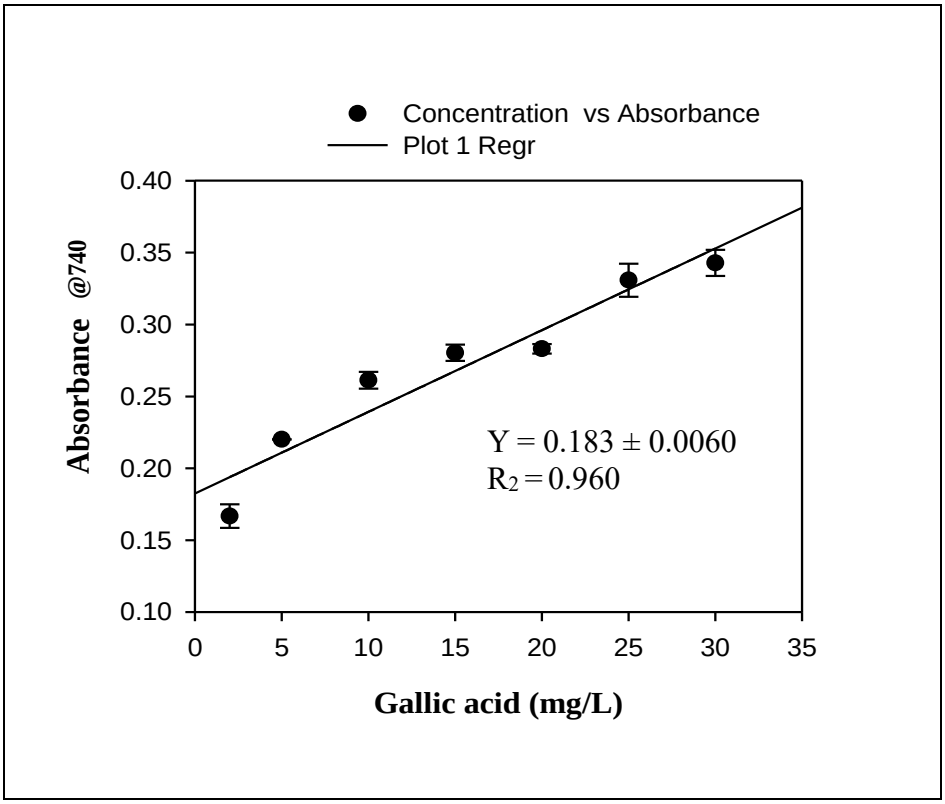

Figure 5. 3: Standard curve for Gallic acid showing the Linear relationship between absorbance and gallic acid concentration (mg/L) N=3. The equation of the line is y = 0.183 + 0.0060x, with a high correlation coefficient (r = 0.96) and an R-Square value of 0.960, indicating a strong fit.

Table 5.3.total phenol content estimation 743 nm in different concentrations of *D. dentatus* ecotypes (N = 3, X ± SEM).

Items	Ecotypes	Absorbance	Concentration	Corrected Conc.GA (mg/L)	mg/g	Average	SE
1	*D. dentatus* red	0.3158	26.1042	104416.6667	104.4167	119.70	8.27
2	*D. dentatus* red	0.3075	24.3750	121875.0000	121.875		
3	*D. dentatus* red	0.3180	26.5625	132812.5000	132.8125		
4	*D. dentatus* white	0.2499	12.3750	61875.0000	61.875	61.08	0.26
5	*D. dentatus* white	0.2485	12.0833	60416.6667	60.41667		
6	*D. dentatus* white	0.2490	12.1875	60937.5000	60.9375		

The table highlights a significant difference in total phenol content between the red and white ecotypes of *D. dentatus*. The red ecotype exhibits a markedly higher phenol content, averaging 119.70 mg/g, compared to the white ecotype's average of 61.08 mg/g.

In terms of corrected concentration, the red ecotype values significantly exceed those of the white ecotype, ranging from 104.4167 mg/L to 132.8125 mg/L for the red ecotype, while the white ecotype's corrected concentrations fall between 60.4167 mg/L and 61.875 mg/L. Also, the standard deviation (SD) shows that the phenol content is less variable in the white ecotype samples (0.26) than it is in the red ecotype samples (8.27).

5.3.4. Linear relationship between absorbance at 429 nm and quercetin equivalents per 5g of dry weight (DW).

The total Flavonoid Content (TFC) was measured using the Dowd's Method.

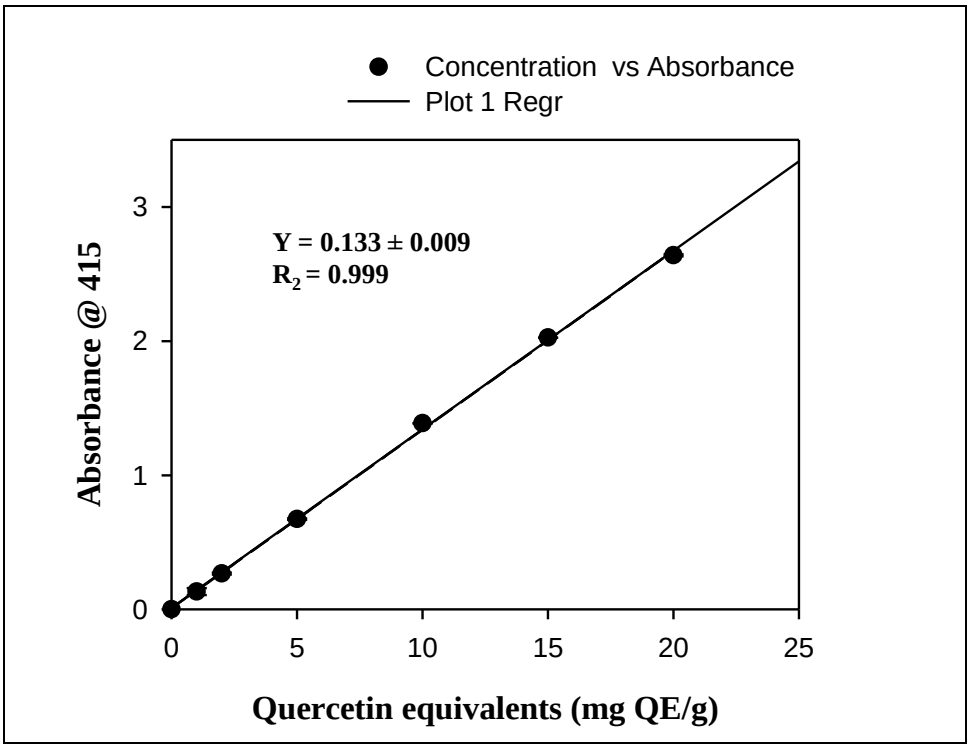

Figure 5. 3. calibration curve showing linear relationship between absorbance at 429 nm and quercetin equivalents per 5g of dry weight (DW) N = 3. The equation is y= 0.133 ± 0.0009x with a Pearson's r of 0.99, indicating an excellent fit.

Table 5.4.total Flavonoid content estimation @ 415 nm in different concentrations of *D. dentatus* ecotypes (N = 3, X ± standard error of the mean (SEM).

Items	Ecotypes	Absorbance	Concentration	Corrected Conc. (mg/L)	mg/g	Average	SE
1	*D. dentatu*s red	0.2191	1.6148	3229.6185	3.230	4.146	0.55
2	*D. dentatu*s red	0.2533	1.8706	3741.2117	3.741		
3	*D. dentatu*s red	0.3416	2.5310	5062.0793	5.062		
4	*D. dentatus* white	0.1076	0.7809	1561.7053	1.562	1.584	0.03
5	*D. dentatus* white	0.1044	0.7569	1513.8369	1.514		
6	*D. dentatus* white	0.1106	0.8033	1606.5819	1.607		

Table 5.4 highlights a significant difference in total flavonoid content between the red and white ecotypes of *D. dentatus*. The red ecotype exhibits a higher average flavonoid content of 4.146 mg/g, compared to the white ecotype, which averages only 1.584 mg/g.

The standard error (SE) underscores this difference: the red ecotype shows greater variability (0.55) in its flavonoid content, whereas the white ecotype has a much lower SE of 0.03, indicating more consistency in its flavonoid content.

5.3.5. Total Phenolic Content (TPC) measured in mg GAE/g over time for two variants of *D. dentatus* - red and white.

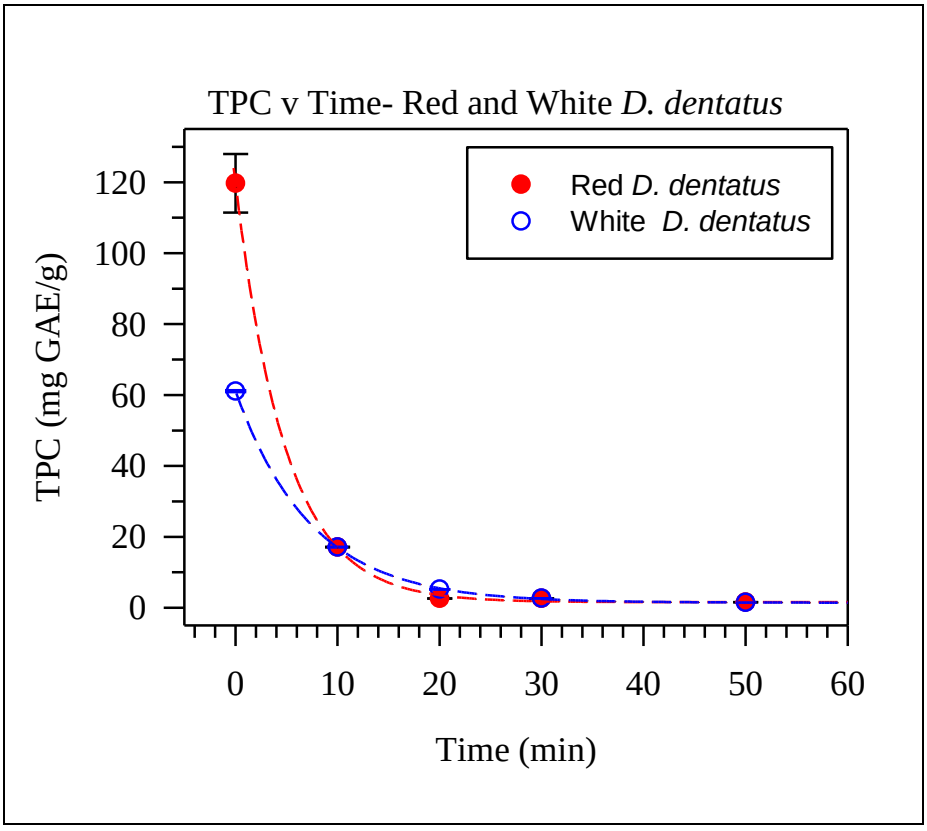

Figure 5.4.Graph showing the concentration of *D. dentatus* red and white ecotypes over time (N=3). Both ecotypes exhibit a rapid decrease in concentration from 10 to 20 minutes, stabilizing at low levels by 30 minutes.

The graph presents a significant comparison of Total Phenolic Content (TPC) degradation between red and white ecotypes of *D. dentatus* over time. A notable aspect of the data is the pronounced difference in initial TPC concentrations, with the red variant commencing at approximately 120 mg GAE/g, while the white *D. dentatus* initiates at a considerably lower concentration of around 60 mg GAE/g. These initial differences rapidly diminish as both ecotypes exhibit significant exponential decay during the first 10 minutes of the experiment. By the 10-minute mark, both

ecotypes converge to comparable TPC levels of approximately 20 mg GAE/g, effectively negating the initial concentration difference (Fig 5.4). The degradation process continues at a reduced rate between 10 and 30 minutes, after which both variants stabilize at near-zero TPC levels. This trend persists throughout the remainder of the 60-minute observation period. Furthermore, Error bars will always be present in the measurements however, the degree (size) of error may be important to note.

5.3.6. Comparison of total flavonoid content in two ecotypes of *D. dentatus* over time

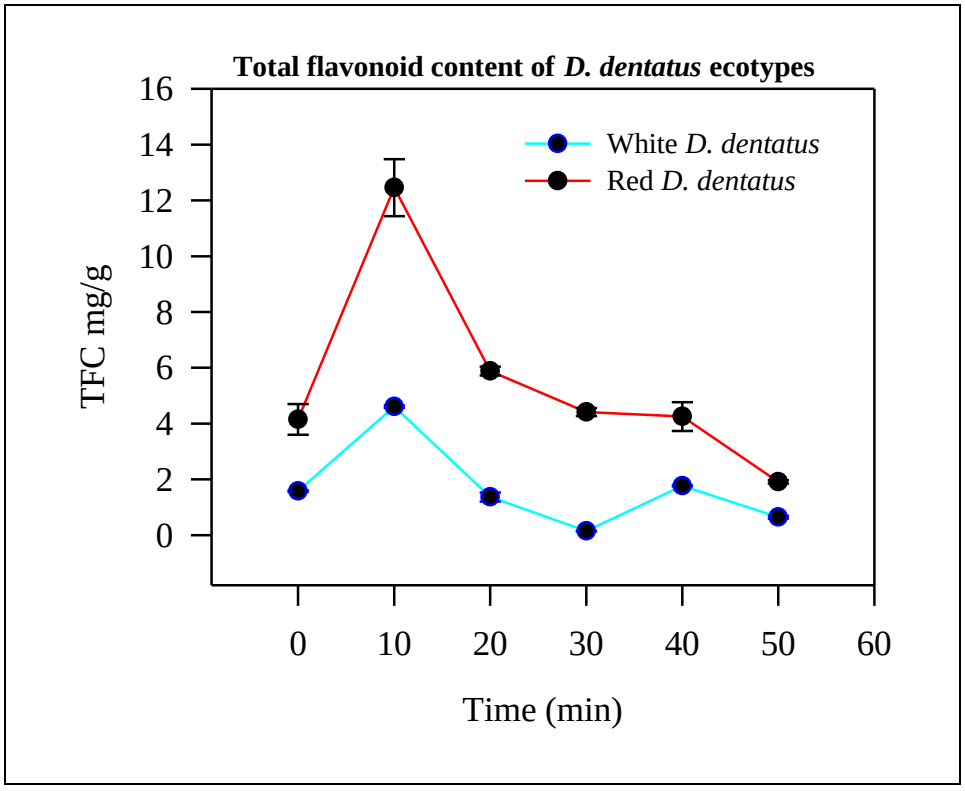

Figure 5. 5: Comparison of total flavonoid content in two ecotypes of *D. dentatus* over time (N=3). The red line represents the red ecotype while the blue line represents the white ecotype

The figure 5.6 illustrates distinct patterns in flavonoid content between red and white ecotypes of *D. dentatus* over a 50-minute interval. The red ecotype consistently exhibits higher flavonoid levels, reaching a peak of 12 mg/g at the 10-minute mark, while the white ecotype attains a lower maximum of 4 mg/g at the same time point. Following this peak, both ecotypes demonstrate a decline in flavonoid content; however, the red ecotype experiences a steeper initial decrease, followed by a more gradual reduction, whereas the white ecotype maintains lower levels throughout the measurement period. The two ecotypes converge near the 50-minute time point, with the red ecotype sustaining slightly elevated levels (2 mg/g) compared to the white ecotype (1 mg/g). The error bars in the measurements reflect natural biological variation, particularly notable at peak concentrations.

5.3.7. UV – Vis Absorbance and Fluorescence spectra of *D. dentatus* ecotypes

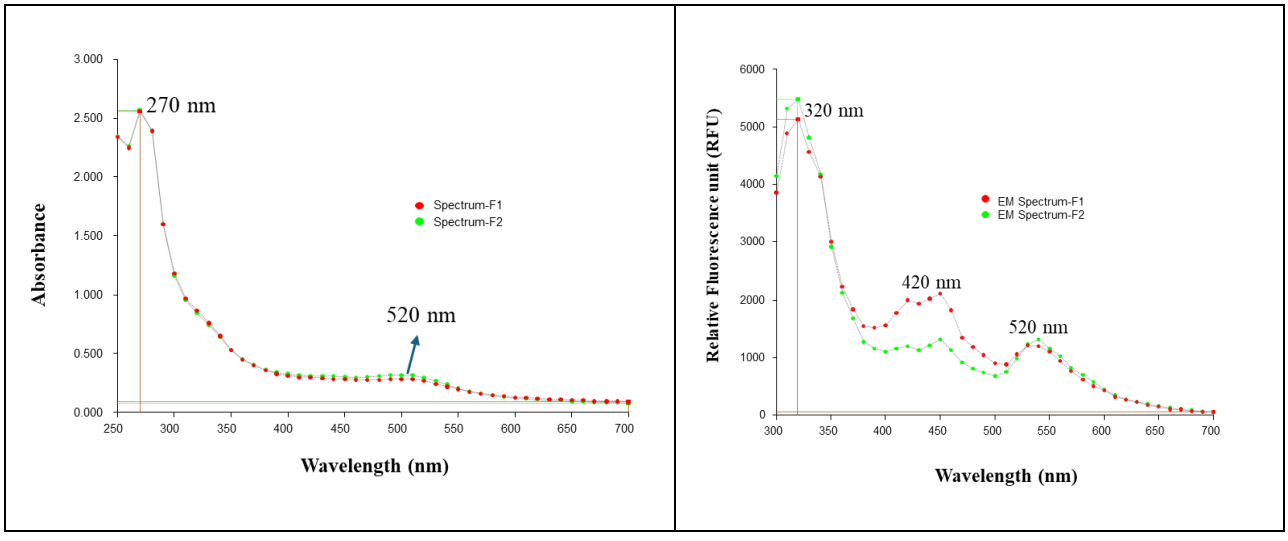

Figure 5. 6. showing the Uv – vis spectra of *D. dentatus* ecotypes. *(A)* absorbance spectra of two *ecotypes*, Spectrum-F1 (red) and Spectrum-F2 (white), plotted as absorbance against wavelength (nm). *(*B*)* fluorescence emission spectra of the same samples, with relative fluorescence units (RFU) plotted against wavelength (nm).

In spectra A, the absportion spectrum is depicted, showing fluorescence intensity as a function of wavelength for two different spectra, labeled Spectrum-F1 (red) and Spectrum-F2 (green). The graph reveals a prominent peak at 270 nm, indicating strong fluorescence intensity at this wavelength. A smaller peak or feature is noted around 520 nm, suggesting another point of interest in the emission profile.

Graph B presents the excitation spectrum for the same ecotypes, with fluorescence intensity measured at 270 nm and 520 nm. Here, three distinct peaks are observed: a major peak at 320 nm and two additional peaks at 420 nm and 520 nm. These peaks indicate the wavelengths at which the ecotypes exhibit significant excitation. These wavelengths correspond to potential energy absorption points that induce fluorescence.

5.3.8. The absorbance and emission measurements at two different wavelengths of *D. dentatus* red and white ecotypes

The two figures illustrate absorbance measurements of *D. dentatus* red and white ecotypes at two wavelengths, 270 nm (graph a) and 520 nm (graph b), over two time points: 0 hours (black bars) and 12 hours (white bars). In Graph (a), which represents absorbance at 270 nm, both samples display high absorbance values, ranging from approximately 2.5 to 3.0. The absorbance increases slightly after 12 hours for both red and white ecotypes with minimal differences between the two ecotypes, low variability in the measurements. *D. dentatus* red exhibited a 4% gain in signal, while *D.dentatus* white showed an 8% gain. This indicates that, relative to their starting values,

D.dentatus white ecotype experienced a greater increase in absorbance compared to *D.dentatus* red ecotype during the observed timeframe

In contrast, figure (b), which illustrates absorbance at 520 nm, reveals significantly lower absorbance values, ranging from approximately 0.10 to 0.15. At 520 nm, *D.dentatus* red ecotype showed a 40% gain in signal, whereas *D.dentatus* white had a 20% gain, meaning *D.dentatus* red ecotype experienced a substantially larger relative increase in absorbance at this wavelength compared to *D.dentatus* white. These percentage changes highlight that, over the observed timeframe, *D.dentatus* white had the greatest relative gain at 270 nm, while *D.dentatus* red ecotype had the greatest relative gain at 520 nm.

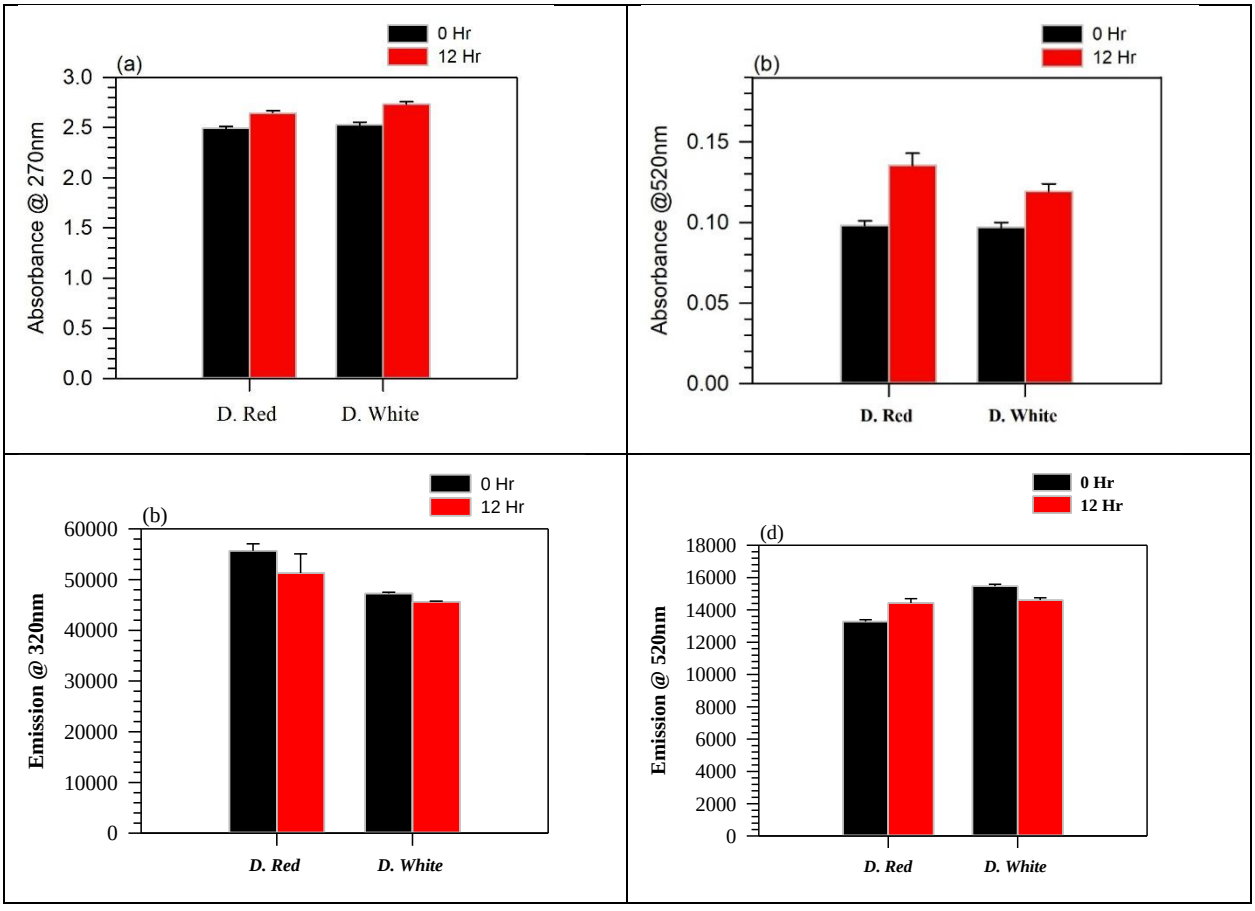

Figure 5.7. showing the absorbance and fluorescence emission measurements of *D. dentatus* red and *D. dentatus* White ecotypes at 0 hours (black bars) and after 12 hours (red bars). (a) Absorbance at 270 nm, (b) absorbance at 520 nm, (c) fluorescence emission at 320 nm, and (d) fluorescence emission at 520 nm. Data are presented as mean ± standard deviation.

Graph (a), the emission intensity at 320 nm is slightly higher for red ecotype compared to the white ecotype at both time points. *D. dentatus* red ecotype showed a signal loss of approximately 7% at 320 nm, while the *D. dentatus* white ecotype had a smaller signal loss of about 2% at the same wavelength

In graph (b), the emission intensity at 520 nm shows a different trend. Both *D. dentatus* red and white ecotypes exhibit an increase in emission intensity after 12 hours, as seen by the taller red bars compared to the black bars. At 520 nm, both *D. dentatus* red ecotype and *D. dentatus* white ecotype exhibited signal gains, with *D. dentatus* red ecotype increasing by around 15% and D. White by about 5%. These results indicate that *D. dentatus* red ecotype experienced a greater decrease in emission at 320 nm and a larger increase in emission at 520 nm compared to *D. dentatus* white ecotype over the observed timeframe.

5.3.9. Comparative UV-vis absorbance and emission spectra reveal oxidative stability differences in red and white *D. dentatus** ecotypes under varying H_2O_2 concentrations.

The UV-vis absorbance and fluorescence spectra of two different extracts red ecotype and white ecotype, after titration with varying concentrations of hydrogen peroxide (H_2O_2). The top two graphs (a and b) show the UV-vis absorbance spectra for both extracts, while the bottom two graphs (c and d) show their fluorescence spectra (Fig 5.8). The concentrations of H_2O_2 range from 0% to 20%, and each spectrum is color-coded accordingly. In both extracts, increasing

concentrations of H_2O_2 lead to a general decrease in absorbance and fluorescence intensity. This suggests that H_2O_2 causes degradation or oxidation of the compounds responsible for the absorbance and fluorescence signals.

In the UV-Vis spectra, distinct peaks are observed around 235-244 nm for both extracts, which shift slightly as H_2O_2 concentration increases. The reduction in peak intensity with higher H_2O_2 concentrations indicates that the chromophores in the extracts are being altered or degraded. Similarly, in the fluorescence spectra, a strong peak at 335 nm is seen for both extracts at 0% H_2O_2, which diminishes as more H_2O_2 is added (Fig 5.8).

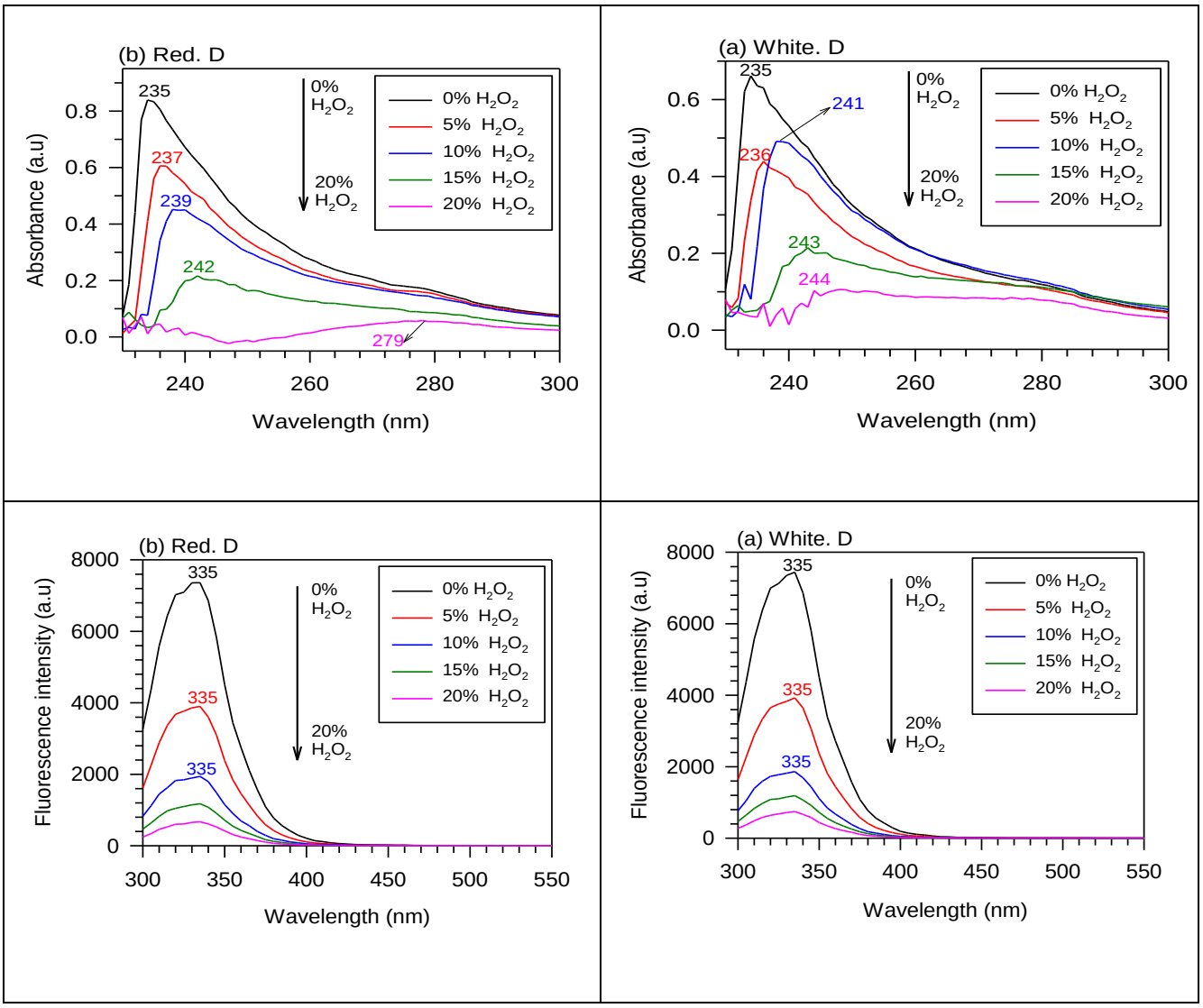

Figure 5. 8. The graphs display the UV-vis emission spectra of *D. dentatus* extracts from red (left panel) and white (right panel) ecotypes (N=3) with varying concentrations of hydrogen peroxide (H_2O_2) ranging from 0% to 20%.

5.3.10. Comparison of Reactive Oxygen Species (ROS) quenching activity in *D. dentatus* ecotypes: 'red' ecotupe shows higher absorbance, florescence emissioin and potential activity than 'white' ecotype.

Figure 5.10. showing the relationship between the concentration of hydrogen peroxide (H_2O_2) and its absorbance at 270 nm. The graph displays a positive linear correlation between H_2O_2 concentration and absorbance values as the concentration increases from 0 to 6 μM, the absorbance correspondingly increases from approximately 0.07 to 0.20. The vertical error bars indicate the standard deviation for each measurement. Standard deviation reflects the variability or spread of absorbance values obtained from repeated measurements at each concentration, providing an indication of the precision and reliability of the data.

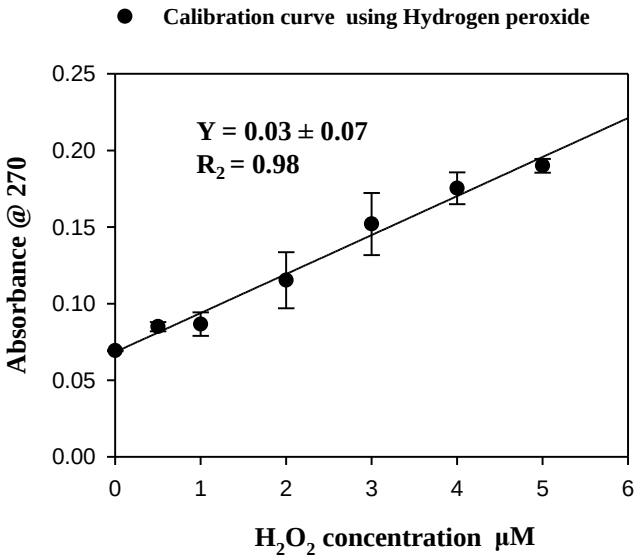

Figure 5.9. Calibration curve for hydrogen peroxide showing the relationship between concentration and obsorbance (N = 3) .

The figure 5.11 shows the absorbance at 270 nm for both ecotypes of *D. dentatus* under two different conditions (Initial and Quench). The Initial condition is represented by the dark red (for Red) and gray (for White) bars, while the Quench condition is shown by the light pink (for *D.dentatus* red ecotypes) and white (for *D.dentatus* white ecotypes) bars (Fig 5.11).

For both ecotypes, the absorbance is higher in the Initial condition, with the *D.dentatus* red ecotypes starting at about 0.37 and the *D.dentatus* white ecotypes at about 0.27. After the quenching process, absorbance decreases to approximately 0.20 for *D.dentatus* red ecotypes and 0.17 for *D.dentatus* white ecotypes. The percentages above each pair of bars indicate the reduction in absorbance due to quenching 47% for Red and 37% for White.

This pattern suggests that the quenching process significantly reduces the concentration of the compound absorbing at 270 nm in both samples, with a more pronounced effect in the *D.dentatus* red ecotypes. The standard variation reflect variability in the measurements.

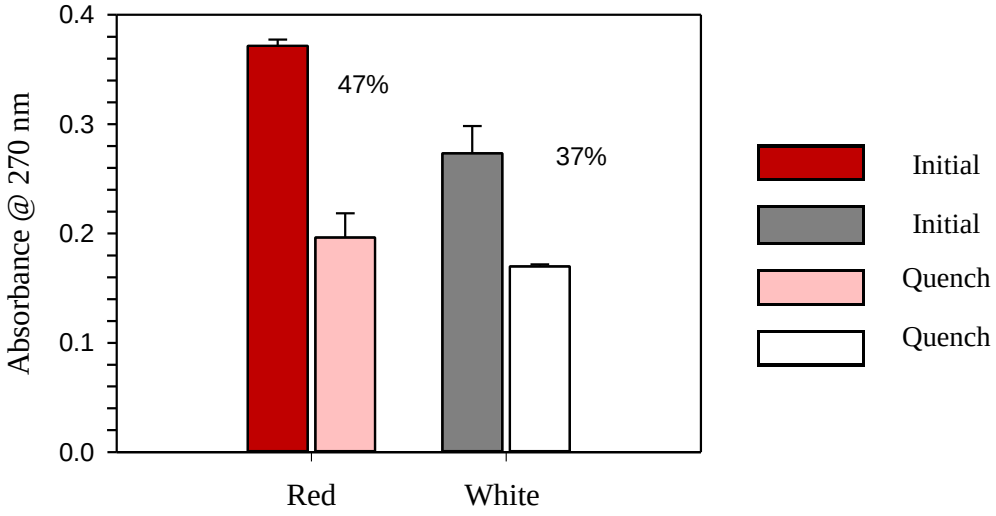

Figure 5. 10. Absorbance at 270 nm for *D. dentatus* red and white ecotypes (N=3), showing initial and quenched absorbance values. The red ecotype exhibits higher quenching (47% reduction) compared to the white ecotype (37% reduction).

The red ecotype (shown by darker bars) and white ecotype (shown by lighter bars) have the strongest fluorescence at 320 nm, with the *D. dentatus* red ecotype nearly reaching 340 a.u. and showing 29% quenching activity, while the *D. dentatus* white ecotype reaches 330 a.u. with 34% quenching activity. The percentages above each bar pair represent the ROS quenching efficiency at that wavelength, calculated as [(A0-A1)/A0] × 100%, where A0 is the absorbance of the control (phosphate buffer with H_2O_2) and A1 is the absorbance of the extract of *D. dentatus*.

A noticeable drop in fluorescence is seen at longer wavelengths, where both extracts show similar patterns but much lower values, dropping below 100 a.u. at 420, 450, and 550 nm. A noticeable drop in fluorescence intensity happens at longer wavelengths, where both extracts show similar trends but much lower values, dropping below 100 a.u. at 420, 450, and 550 nm. The percentage of quenching at these longer wavelengths is between 7% and 20%, with the D. dentatus white ecotype usually showing more quenching activity than the *D. dentatus* red ecotype at 420 nm (20% compared to 13%) and 450 nm (19% compared to 12%). Conversely, the *D. dentatus* red ecotype demonstrates marginally superior performance at 550 nm (10% vs. 7%). The standard deviation reflects measurement variability across replicate samples, indicating that the experimental results possess a degree of reliability.

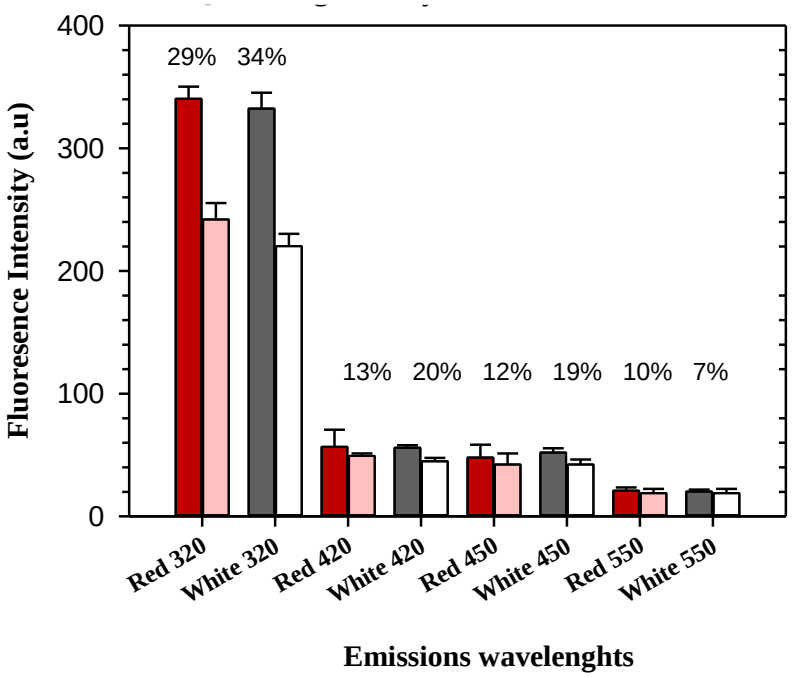

Figure 5. 12. Fluorescence intensity of *D. dentatus* red and white ecotypes at different emission wavelengths (320, 420, 450, and 550 nm). Bars represent mean fluorescence intensity (a.u.) with error bars indicating standard deviation. Percentages above each bar pair indicate the ROS quenching efficiency at each wavelength for the respective extract, calculated as [(A0-A1)/A0] × 100%, where A0 = absorbance of the control (phosphate buffer with H2O2) and A1 = absorbance of the *D.dentatus* red and white ecotypes extracts.

5.3.11. Antioxidant activity assessment of *D. dentatus* red and white ecotypes using ascorbic acid as a reference standard

Figure 5.12 illustrates the reversible redox reaction between L-ascorbic acid (vitamin C) and L-dehydroascorbic acid. L-ascorbic acid, shown on the left, acts as an antioxidant by donating two hydrogen atoms (as $2H^+$ and $2e^-$) during oxidation, which converts it into L-dehydroascorbic acid, depicted on the right. This process is central to the antioxidant activity of vitamin C, as it allows L-ascorbic acid to neutralize reactive oxygen species and other oxidants. The reaction is reversible; L-dehydroascorbic acid can be reduced back to L-ascorbic acid in the presence of suitable cellular reductants. This redox cycling enables vitamin C to continuously protect cells from oxidative damage by alternating between its reduced and oxidized forms.

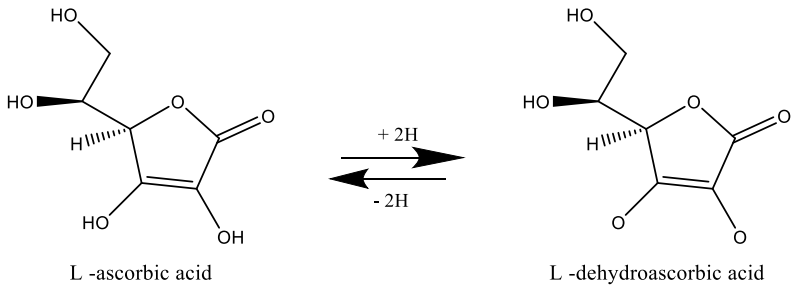

Figure 5.13. The oxidation-reduction (redox) reaction of vitamin C, molecular forms in equilibrium. L-dehydroascorbic acid also possesses biological activity, due to that in the body it is reduced to form ascorbic acid. Strucutes were drawn with the ChemDraw Professional 15.0

Figure 5.13a shows plots of ascorbic acid concentration (in μM) on the x-axis against radical scavenging activity (RSA, %) on the y-axis. As the concentration of ascorbic acid increases, the RSA percentage also increases in a linear fashion, as shown by the regression equation (Y =

57.18x + 8.043, R^2 = 0.98). This indicates that higher concentrations of ascorbic acid are more effective at neutralizing free radicals, which is consistent with its known antioxidant properties.

Figure 5.13b shows the calibration curve showing the relationship between ascorbic acid concentration (x-axis) and absorbance at 520nm (y-axis). Here, as the concentration of ascorbic acid increases, the absorbance decreases linearly (Y = –3.66x + 4.45, R^2 = 0.98). This negative correlation occurs because ascorbic acid reduces the colored DPPH radical to a colourless form, resulting in lower absorbance readings at higher ascorbic acid concentrations. The calibration curve allows for the quantification of antioxidant activity in unknown samples by comparing their absorbance values to this standard curve.

Together, these figures confirm that ascorbic acid is a potent antioxidant: increasing its concentration leads to greater radical scavenging activity and a corresponding decrease in absorbance due to reduction of the DPPH radical. The high R^2 values in both graphs indicate strong linear relationships and reliable data fits. Error bars represent the standard deviation, reflecting good precision and reproducibility of the measurements

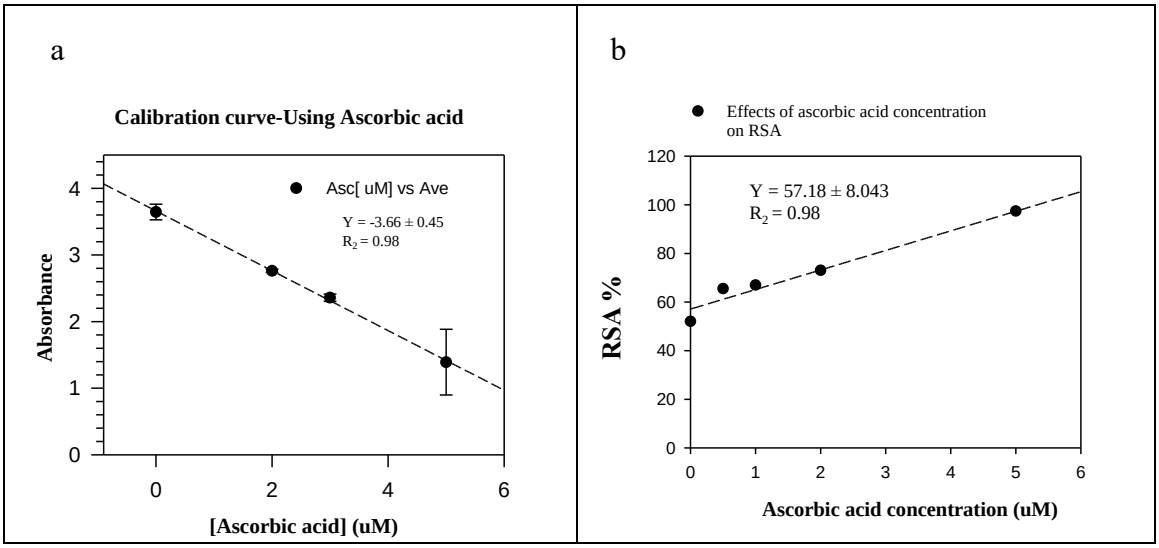

Figure 5. 11. Correlation of Ascorbic acid concentration with Absorbance at 520 nm and RSA. Ascorbic acid concentration exhibits a strong correlation with absorbance (left panel; $R^2 = 0.98$) and RSA (right panel; $R_2 = 0.98$). The equations for the lines of best fit are displayed on each graph.

Figure 5.15 provide insights into the antioxidant properties of *D. dentatus* ecotypes, specifically examining absorbance over time and antioxidant activity percentage. Graph A shows the average absorbance at 520 nm over time for two ecotypes of *D. dentatus* red and white ecotypes. The absorbance values decrease over time for both ecotypes. The *D.dentatus* red ecotype (black circles) has a trend line with the equation ($y = 1.384 - 0.002x$) and an R^2 value of 0.996, while the white ecotype (white circles) has a trend line with the equation ($y = 1.384 - 0.001x$) and an R^2 value of 0.982 (Fig 5.15).

Graph B displays the antioxidant activity of the red and white ecotypes of *D. dentatus* in percentage form, with values presented as bars. The red ecotype has an average antioxidant activity of 48.5%, while the white ecotype has an average of 47.5%.

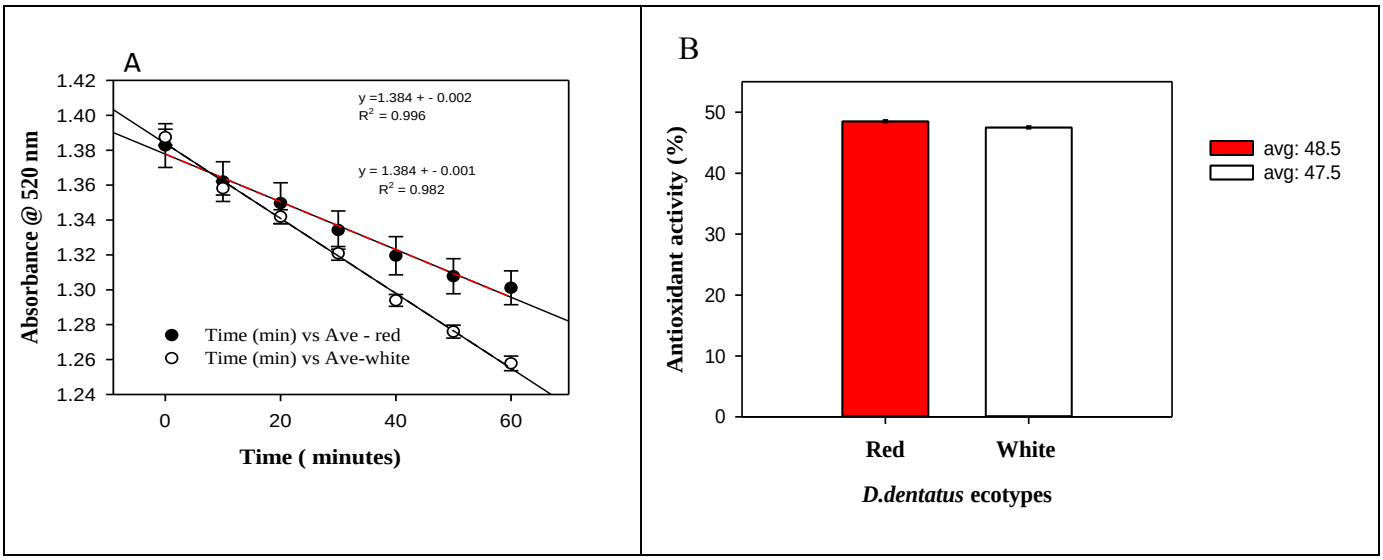

Figure 5. 12: presents data (N=3) on the absorbance and antioxidant activity of *D. dentatus* ecotypes. Panel (A) shows the decline in absorbance at 520 nm over time for both red and white ecotypes, (B) compares the antioxidant activity between the two ecotypes.

5.3.12. Comparative Analysis of MS - Derived Peak Areas for Various Flavonoids and Phenolic Compounds Between *D. dentatus* red and white ecotypes

The relative peak areas of various flavonoid compounds, as illustrated in the bar plots, indicate notable differences in their abundance between *D.dentatus* red and white ecotypes represented by the red and green bars (Fig 5.16) For chalconaringenin, the *D.dentatus* red ecotype demonstrates a higher peak area compared to the *D.dentatus* white ecotype, ($p = 0.081$). Similarly, naringenin displays a comparable trend, with the *D.dentatus* red ecotype exhibiting a higher peak area than the *D.dentatus* white ecotype ($p = 0.081$).

In the cases of cyanidin 3-O-beta-D-glucoside, cyanidin 3-O-glucoside, and cyanidin 3-O-beta-D-sambubiside, the red group consistently shows higher peak areas than the green group; however, none of these differences reach statistical significance (p-values of 0.73, 0.33, and 0.41, respectively). A comparable pattern is observed for delphinidin 3-O-glucoside ($p = 0.15$) and delphinidin 3-O-beta-D-sambubios (p-value not clearly labeled), wherein the red group also has a slightly higher peak area (Fig 5. 16)

In the instances of genistein and apiforol, the red ecotypes continues to exhibit higher peak areas than the white ecotype (green bars), although these differences are not statistically significant ($p = 0.2$ and $p = 0.26$) respectively. For kaempferin, leucocyanidin, and kaempferol 3-O-glucoside, the red ecotypes again presents slightly higher peak areas than the green group, with p-values of 0.57, 0.33, and 0.89, respectively. Finally, for homoeriodictyol, there is minimal difference between the two ecotypes ($p = 0.92$), indicating similar levels of this compound across both conditions.

Overall, while trends suggest higher relative peak areas for most flavonoids in the red ecotype compared to the white ecotype (green bars), none of these differences attain statistical significance based on the provided p-values. This observation implies that, although variations in flavonoid abundance exist between the ecotypes, they are not pronounced enough to be considered statistically meaningful under these conditions.

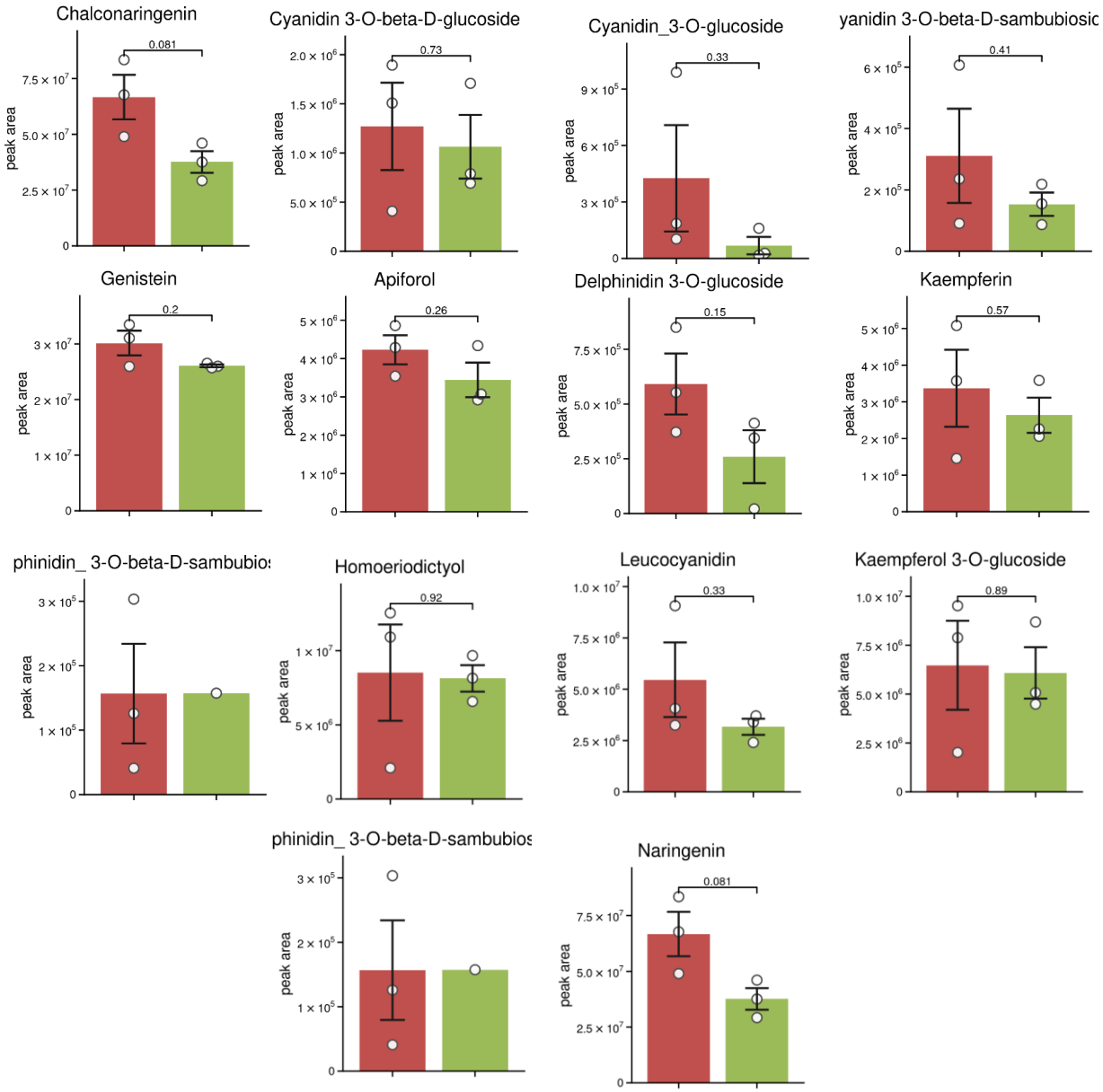

Figure 5. 13: The bar graph compares the relative peak area of various flavonoid compounds in the red (red bars) and white (green bars) ecotypes tea extract of *D. dentatus* (N=3). It highlights the differences in peak areas for each compound, indicating distinct phytochemical profiles between the two ecotypes

5.4. DISCUSSION

The study on *D. dentatus* (Capadulla) reveals differences in the phytochemical profiles and antioxidant activity between its red and white ecotypes. The woody vine of the red ecotype of *D. dentatus* exhibited a much higher total phenolic (119.70 mg/g) and flavonoid contents (4.146 mg/g) compared to the white ecotype (61.08 mg/g) and (1.584 mg/g) respectively (Table 2 & 3). The red ecotype demonstrated higher spectroscopic responses compared to the *D. dentatus* white ecotype. FTIR analysis revealed higher concentrations of compounds containing hydroxyl (OH) and amine (NH) functional groups in the red ecotype (Fig 5.2 and appendix 3). IR spectra detect a broad range of compounds, including amino acids, proteins, DNA/RNA, and secondary metabolites such as flavonoids, tannins, and alkaloids (Appendix 2). The fingerprint region (1600–1000 cm^{1}) showed increased intensity, indicating elevated levels of anthocyanins and flavonoid glycosides. Additionally, enhanced signals in the CH stretching region (~3000 cm^{1}) may suggested greater abundance of complex organic structures, particularly terpenoids, monoterpenes, and sesquiterpenes (Lu et al., 2017; Nandiyanto et al., 2019; Park et al., 2018). This difference may suggest that the red ecotype likely offers higher antioxidant potential, similar to what researchers have observed in other medicinal plant species (Mattera et al., 2024; Mihaylova et al., 2024).

The variations between the ecotypes highlight the red ecotype's potential as a more potent antioxidant source, essential for combating oxidative stress in the body (Kurutas, 2015; Sultana et al., 2023).

Total phenolic content serves as a strong indicator of the antioxidant capacity of medicinal plants. Antioxidants, commonly found in medicinal plants, are crucial for reducing oxidative stress

by neutralizing reactive oxygen species (ROS) and protecting cells from damage, thus promoting overall health and wellness (Sejin Kim et al., 2021; Kim et al., 2020; La, 2022).

The semi-targeted MS analysis of *D. dentatus* red and white ecotypes revealed distinct flavonoid and phenolic profiles. Notable differences in peak area between the *D. dentatus* red and white ecotypes as illustrated in Figure 5.15. Chalconaringenin and naringenin both display higher relative peak areas in the *D. dentatus* ecotype compared to the *D. dentatus* with ecotype, p-values of 0.081, indicating a clear trend toward greater abundance in the *D. dentatus* red ecotype. Delphinidin 3-O-glucoside also exhibits a higher peak area in the red ecotype ($p = 0.15$), suggesting a greater presence of this anthocyanin, which may contribute to the red colouration and enhanced antioxidant properties. Similarly, cyanidin 3-O-beta-D-sambubioside is more abundant in the *D. dentatus* ecotype ($p = 0.41$), further supporting the pattern of elevated anthocyanin content in this ecotype. Other compounds, such as genistein, apiforol, and kaempferin, show less pronounced differences, with p-values above 0.2, while most remaining flavonoids and phenolic compounds demonstrate similar levels between the *D. dentatus* red and white ecotypes.

The compounds identified in the results, including chalconaringenin, naringenin, cyanidin 3-O-beta-D-glucoside, cyanidin 3-O-glucoside, cyanidin 3-O-beta-D-sambubioside, delphinidin 3-O-glucoside, genistein, apiforol, kaempferin, homoeriodictyol, leucocyanidin, and kaempferol 3-O-glucoside, are well-known for their diverse biological activities (Fig. 5.15). Chalconaringenin and related chalcones serve as precursors in flavonoid biosynthesis and exhibit a broad spectrum of bioactivities, such as antioxidant, antimicrobial, anti-inflammatory, and anticancer effects, largely due to their α,β-unsaturated carbonyl system and ability to modulate cellular signalling pathways (Elkanzi et al., 2022; Goyal et al., 2021; Rudrapal et al., 2022; Rudrapal et al., 2021;

Yerragunta et al., 2013). Naringenin, a prominent flavanone, is recognised for its strong antioxidant and anti-inflammatory properties, as well as antidiabetic, anticancer, antimicrobial, cardioprotective, and neuroprotective actions. Its health benefits are attributed to its capacity to scavenge free radicals, prevent lipid peroxidation, and modulate inflammatory responses(Uçar & Göktaş, 2023).

The anthocyanins, including cyanidin and delphinidin derivatives, are potent antioxidants with additional bioactivities such as anti-inflammatory, anti-angiogenic, antiviral, and even enzyme inhibitory effects. For example, cyanidin 3-O-beta-D-sambubioside not only acts as a strong antioxidant but also inhibits nitric oxide production, angiotensin-converting enzyme (ACE) activity, and influenza neuraminidase, highlighting its potential in cardiovascular and antiviral therapies[4]. Delphinidin 3-O-glucoside is noted for its free radical scavenging ability, antitumor, antiatherosclerotic, hypoglycemic, and antiallergic effects, and can modulate key inflammatory pathways such as TNF-α signalling (Sari et al., 2019).

Other flavonoids, such as genistein and kaempferol derivatives, are also widely studied for their antioxidant, anti-inflammatory, and anticancer activities, contributing to cellular protection and modulation of metabolic and immune pathways. Collectively, these compounds contribute to the health-promoting properties of *D. dentatus*, and their varying abundance between ecotypes may influence the plant's overall antioxidant capacity and therapeutic potential.

Consuming plant-based foods rich in dietary antioxidants such as polyphenols, flavonoids, carotenoids, and tocopherols can help scavenge free radicals and decrease the risk of oxidative stress-related diseases (Sejin Kim et al., 2021). Antioxidants from medicinal plants help maintain

cellular balance, protect against damage induced by oxidative stress, and contribute to better health outcomes (Da Silva et al., 2018).

Mehnaz et al. (Pervin et al., 2013) reported that the *Vaccinium corymbosum* (blueberry) leaf extract contained significant levels of phenolic compounds (9.25 mg GAE/100g) and flavonoids (12.66 mg CE/100g), demonstrating notable antioxidant activity through free radical scavenging and lipid peroxidation inhibition. This study's findings align with those of (Mehnaz et al.,2013) and broader literature, which suggest a correlation between higher phenolic content and increased antioxidant potential (Pervin et al., 2013). While the red ecotype stems show higher phenolic and flavonoid levels, Ishikawa et al. (Raissa Borges Ishikawa et al., 2017), reported that the leaves of *D. dentatus* contained phytochemicals, including 204.04 mg/g of phenols, 89.17 mg/g of flavonoids, and 12.05 mg/g tannin (Raissa Borges Ishikawa et al., 2017). Variations in phenolic and flavonoid levels among plants can result from factors such as genotype, seasonal changes, variety, and extraction methods (Sun et al., 2018; Yavorska et al., 2023).

The study found that the red ecotype contained a higher total flavonoid content (4.146 mg/g) than the white ecotype (1.584 mg/g). Research on onions, red varieties have been shown to possess significantly higher levels of flavonoids and polyphenols than their white varieties. For example, the red onion variety Karmen contains approximately 108,300 mg/kg dry matter of total polyphenols, including key flavonoids like spiraeoside and quercetin, whereas white varieties contain only about 26,445 mg/kg dry matter. This mirrors the results of your study, where the red ecotype exhibited roughly 2.6 times more flavonoids than the white ecotype (Chernukha et al., 2022; Lachman et al., 2003; Vijayalakshmi et al., 2021) the red ecotype of *D. dentatus* may provide greater health benefits.

Several factors contribute to this disparity. First, the biosynthesis of flavonoids is often linked to pigment production in plants. Red ecotypes typically overexpress genes involved in the flavonoid pathway, such as F3'H, DFR, and UFGT, leading to higher production of anthocyanins and related compounds. Enzymes like flavonoid 3'-hydroxylase (F3'H) and dihydroflavonol 4-reductase (DFR) drive anthocyanin synthesis (Falcone Ferreyra et al., 2012). These enzymes modify the flavonoid skeleton, enabling hydroxylation and glycosylation steps critical for red pigmentation. For example, F3'H adds hydroxyl groups to dihydrokaempferol, forming a dihydroquercetin precursor for cyanidin-based anthocyanins (Falcone Ferreyra et al., 2012).

These compounds not only provide red pigmentation but also enhance the plant's antioxidant capacity and offer protection against ultraviolet (UV) radiation. Additionally, higher flavonoid content in red ecotypes may be an adaptive response to environmental stress, as these compounds can improve the plant's resilience to abiotic factors like intense sunlight or drought. For instance, red pitahaya (*Hylocereus monacanthus*) accumulates more polyphenols in both its peel and pulp compared to white or yellow varieties, likely as a defence mechanism (Bai et al., 2022; Gould, 2004).

Structurally, red cultivars often accumulate specific flavonoids, such as cyanidin-3-glucoside in onions or delphinidin derivatives in other species, which are either absent or present in much lower concentrations in white varieties (Gould, 2004). This metabolic divergence is thought to reflect evolutionary optimisation, where red pigmentation and associated flavonoids provide multiple ecological advantages, including photoprotection and increased resistance to pathogens. Overall, the higher flavonoid content observed in red ecotypes is a well-documented

phenomenon across plant species and is driven by both genetic and environmental factors (Bai et al., 2022; Gould, 2004).

The antioxidant activity of *D dentatus* ecotypes, as measured by DPPH and H_2O_2 quenching, shows competitive potential compared to well-known antioxidant-rich plants, though with nuanced differences. The red ecotype (48.5% activity) and white ecotype (47.5%) exhibit similar DPPH scavenging capacities, aligning with plants like *Centella asiatica* (IC_{50} ~50 mg/mL) but underperforming compared to Rumex dentatus (IC_{50} 0.012 mg/mL) (Ewart smith, 2023; Pandey & Murugan, 2023). The red ecotype's faster absorbance decline (slope: -0.002 vs. -0.001 for white) suggests marginally superior radical-neutralising kinetics, likely due to its higher polyphenol diversity, e.g., epicatechin methyl gallate, proanthocyanidin A2 (Ewart smith, 2023).

While specific H_2O_2 IC_{50} values for *D. dentatus* ecotypes are not provided, its methanolic extracts show activity comparable to *Pittosporum undulatum* (IC_{50} <50 µg/mL), indicating strong hydroxyl radical inhibition (Rets'epile et al., 2021).

D. dentatus's antioxidant profile is enriched with flavonoids and phenolic acids akin to Camellia sinensis (green tea) and Vaccinium spp. (blueberries) (Ewart smith, 2023; Koa et al., 2015). However, its activity percentages (48–49%) lag behind extracts like *Justicia procumbens* (68.83 µg/mL DPPH IC_{50}) (Agrawal et al., 2021) or Bacopa monnieri (66.85% inhibition) (Meena et al., 2012).

The *D. dentatus* red ecotype's elevated polyphenol content and unique compounds (e.g., catechin gallate) position it as a moderately potent antioxidant source, particularly for niche applications like combating oxidative stress in erectile dysfunction (Ewart smith, 2023). While not

surpassing top-tier plants (e.g., rosemary or turmeric), its chemodiversity and stress-adaptive traits suggest untapped therapeutic potential.

Fluorescence spectroscopy showed clear emission peaks in *D. dentatus* extracts, which suggests that they contain bioactive compounds that may make them more useful as a medicine (Ewart smith, 2023). This finding is significant as it suggests that the plant contains various phytochemicals that could contribute to its medicinal properties (Sandhu et al., 2023). Modern analytical methods, such as mass spectrometry-based metabolomics, have helped scientists find many compounds in *D. dentatus* that could be used as medicine. These include polyphenols and other bioactive molecules (Ewart smith, 2023). The antioxidant properties and potential therapeutic applications of *D. dentatus* can be compared to other well-studied medicinal plants, such as pomegranate, which has been extensively researched for its antioxidant, antimicrobial, and potential cosmetic applications (Savali et al., 2023; Uysal & Efe Arslan, 2024). Finding these bioactive compounds and their antioxidant properties in *D. dentatus* supports the idea that they could be used to treat conditions related to oxidative stress such as ED (Ewart smith, 2023).

5.5. CONCLUSION

In conclusion, this study reveals significant phytochemical and antioxidant differences between the red and white ecotypes of *D. dentatus* (Capadulla). The red ecotype demonstrates notably higher phenolic and flavonoid contents, indicating a stronger antioxidant potential, which aligns with findings from other medicinal plants known for their high antioxidant activity.

These results enhance our understanding of *D. dentatus'* chemical diversity and open avenues for future research into its potential therapeutic applications. The marked differences between ecotypes underscore the importance of considering genetic and environmental factors in phytochemical studies. Further investigations into the specific compounds responsible for these variations and their biological activities could lead to the development of novel natural antioxidants or other bioactive agents.

This research also highlights the value of preserving and studying different ecotypes of medicinal plants, as they may possess unique and potentially beneficial properties. The findings support the traditional use of the *D. dentatus* red ecotype in folk medicine and emphasize its potential as a valuable source of natural antioxidants for health and therapeutic applications. To validate these benefits and explore practical uses of *D. dentatus* extracts in health and medicine, further research, particularly clinical studies, is essential.

5.6. REFERENCE

Agrawal, M., Agrawal, Y., Arora, S., Lahange, P., & Kshirsagar, N. (2021). Phytochemical screening and evaluation of antioxidant activity of hydroalcoholic extract of Justicia procumbans leaf. Journal of Ayurvedic and Herbal Medicine, 7(1), 41-45.

Ahmed, A. F., Attia, F. A., Liu, Z., Li, C., Wei, J., & Kang, W. (2019). Antioxidant activity and total phenolic content of essential oils and extracts of sweet basil (Ocimum basilicum L.) plants. Food Science and Human Wellness, 8(3), 299-305. https://doi.org/10.1016/j.fshw.2019.07.004

Andel, T. v., MacKinven, A., & Bánki, O. (2003). Commercial non-timber forest products of the Guiana shield: an inventory of commercial NTFP extraction and possibilities for sustainable harvesting. Netherlands Committee for IUCN.

Arvouet-Grand, A., Vennat, B., Pourrat, A., & Legret, P. (1994). Standardization of propolis extract and identification of principal constituents. Journal de Pharmacie de Belgique, 49(6), 462-468.

Aryal, S., Baniya, M. K., Danekhu, K., Kunwar, P., Gurung, R., & Koirala, N. (2019). Total phenolic content, flavonoid content and antioxidant potential of wild vegetables from Western Nepal. Plants, 8(4), 96. https://doi.org/10.3390/plants8040096

Bai, Y., Gu, Y., Liu, S., Jiang, L., Han, M., & Geng, D. (2022). Flavonoids metabolism and physiological response to ultraviolet treatments in Tetrastigma hemsleyanum Diels et Gilg. Front Plant Sci, 13, 926197. https://doi.org/10.3389/fpls.2022.926197

Baliyan, S., Mukherjee, R., Priyadarshini, A., Vibhuti, A., Gupta, A., Pandey, R. P., & Chang, C.-M. (2022). Determination of antioxidants by DPPH radical scavenging activity and quantitative phytochemical analysis of Ficus religiosa. Molecules, 27(4), 1326. https://doi.org/10.3390/molecules27041326

Boussaa, F., Zaouay, F., Burló-Carbonell, F., Noguera-Artiaga, L., Carbonell-Barrachina, Á. A., Melgarejo, P., Hernández, F., & Mars, M. (2020). Growing location affects physical properties, bioactive compounds, and antioxidant activity of pomegranate fruit (Punica granatum L. var. Gabsi). International Journal of Fruit Science, 20(3), 508-523. https://doi.org/10.1080/15538362.2020.1746730

Camila, B. d. A., De Matos, D. C., Lopes, F. C., Maia, D. C., Dias, M. B., Sannomiya, M., Rodrigues, C. M., Andreo, M. A., Vilegas, W., & Colombo, L. L. (2009). Isolated flavonoids against mammary tumour cells LM2. Zeitschrift für Naturforschung C, 64(1-2), 32-36.

Chen, J., Zhong, H., Huang, Z., Chen, X., You, J., & Zou, T. (2023). A critical review of kaempferol in intestinal health and diseases. Antioxidants, 12(8), 1642. https://doi.org/10.3390/antiox12081642

Chen, S., Wang, X., Cheng, Y., Gao, H., & Chen, X. (2023). A review of classification, biosynthesis, biological activities and potential applications of flavonoids. Molecules, 28(13), 4982. https://doi.org/10.3390/molecules28134982

Cheng, Y., Xue, F., & Yang, Y. (2023). Hot Water Extraction of Antioxidants from Tea Leaves-Optimization of Brewing Conditions for Preparing Antioxidant-Rich Tea Drinks. Molecules, 28(7). https://doi.org/10.3390/molecules28073030

Chernukha, I., Kupaeva, N., Kotenkova, E., & Khvostov, D. (2022). Differences in Antioxidant Potential of Allium cepa Husk of Red, Yellow, and White Varieties. Antioxidants (Basel), 11(7). https://doi.org/10.3390/antiox11071243

Cicco, N., Lanorte, M. T., Paraggio, M., Viggiano, M., & Lattanzio, V. (2009). A reproducible, rapid and inexpensive Folin–Ciocalteu micro-method in determining phenolics of plant methanol extracts. Microchemical Journal, 91(1), 107-110. https://doi.org/10.1016/j.microc.2008.08.011

Cinthia, C. d., Lemos, R. P. L., & Conserva, L. M. (2013). Chemical constituents, larvicidal effects and radical scavenging activity of Tetracera breyniana Schltdl.(Dilleniaceae). Journal of Applied pharmaceutical science, 3(9), 14.

Costa, E., Hiruma-Lima, C. A., Lima, E., Sucupira, G., Bertolin, A., Lolis, S., Andrade, F., Vilegas, W., & Souza-Brito, A. (2008). Antimicrobial activity of some medicinal plants of the Cerrado, Brazil. Phytotherapy Research: An International Journal Devoted to Pharmacological and Toxicological Evaluation of Natural Product Derivatives, 22(5), 705-707. https://doi.org/10.1002/ptr.2397705-707.

de Almeida Camila, B., De Matos, D. C., Lopes, F. C., Maia, D. C., Dias, M. B., Sannomiya, M., Rodrigues, C. M., Andreo, M. A., Vilegas, W., & Colombo, L. L. (2009). Isolated flavonoids against mammary tumour cells LM2. Zeitschrift für Naturforschung C, 64(1-2), 32-36. https://doi.org/10.1515/znc-2009-1-206

De Cinthia, C., Lemos, R. P. L., & Conserva, L. M. (2013). Chemical constituents, larvicidal effects and radical scavenging activity of Tetracera breyniana Schltdl. (Dilleniaceae). Journal of Applied Pharmaceutical Science, 3(9), 14-18. https://doi.org/10.7324/JAPS.2013.3903

Da Silva, I. B., Sá, R. D., Macêdo, D. P. C., & Randau, K. P. (2018). Use of medicinal plants in the treatment of erysipelas: A review. Pharmacognosy Reviews, 12(24), 200-207. https://doi.org/10.4103/phrev.phrev_11_18

De Oliveira, B. H., Santos, C. A. M., & Espíndola, A. P. D. M. (2002). Determination of the triterpenoid, betulinic acid, in Doliocarpus schottianus by HPLC. Phytochemical Analysis, 13(2), 95-98. https://doi.org/10.1002/pca.628

De Toledo, C. E., Britta, E. A., Ceole, L. F., Silva, E. R., de Mello, J. C., Dias Filho, B. P., Nakamura, C. V., & Ueda-Nakamura, T. (2011). Antimicrobial and cytotoxic activities of medicinal plants of the Brazilian cerrado, using Brazilian cachaça as extractor liquid. Journal of Ethnopharmacology, 133(2), 420-425. https://doi.org/10.1016/j.jep.2010.10.019

Deepika, Dakal, T. C., Sharma, N. K., Ranga, V., & Maurya, P. K. (2024). Naringenin orchestrates and regulates the reactive oxygen species-mediated pathways and proinflammatory signaling: Targeting hallmarks of aging-associated disorders. Rejuvenation Research, 27(1), 3-16. https://doi.org/10.1089/rej.2023.0065

Dong, J., Croslow, S. W., Lane, S. T., Castro, D. C., Blanford, J., Zhou, S., Park, K., Burgess, S., Root, M., & Cahoon, E. B. (2025). Enhancing lipid production in plant cells through automated high-throughput genome engineering and phenotyping. The Plant Cell, 37(2).

Elkanzi, N. A., Hrichi, H., Alolayan, R. A., Derafa, W., Zahou, F. M., & Bakr, R. B. (2022). Synthesis of chalcones derivatives and their biological activities: a review. *ACS Omega*, *7*(32), 27769-27786.

Endringer, D. C., Valadares, Y. M., Campana, P. R., Campos, J. J., Guimarães, K. G., Pezzuto, J. M., & Braga, F. C. (2010). Evaluation of Brazilian plants on cancer chemoprevention targets in vitro. Phytotherapy Research, 24(6), 928-933. https://doi.org/10.1002/ptr.3050

Falcone Ferreyra, M. L., Rius, S. P., & Casati, P. (2012). Flavonoids: biosynthesis, biological functions, and biotechnological applications. Frontiers in Plant Science, 3, 222.

Goyal, K., Kaur, R., Goyal, A., & Awasthi, R. (2021). Chalcones: A review on synthesis and pharmacological activities. *Journal of Applied pharmaceutical science, 11*(1), 001-014.

Gould, K. S. (2004). Nature's Swiss Army Knife: The Diverse Protective Roles of Anthocyanins in Leaves. J Biomed Biotechnol, 2004(5), 314-320. https://doi.org/10.1155/s1110724304406147

Ishikawa, R. B., Leitão, M. M., Kassuya, R. M., Macorini, L. F., Moreira, F. M. F., Cardoso, C. A. L., Coelho, R. G., Pott, A., Gelfuso, G. M., Croda, J., Oliveira, R. J., & Kassuya, C. A. L. (2017). Anti-inflammatory, antimycobacterial and genotoxic evaluation of Doliocarpus dentatus. Journal of Ethnopharmacology, 204, 18-25. https://doi.org/10.1016/j.jep.2017.04.004

Jagessar, R., Hoolas, G., & Maxwell, A. (2013). Phytochemical screening, isolation of betulinic acid, trigonelline and evaluation of heavy metals ion content of Doliocarpus dentatus. Journal of Natural Products, 6, 5-16.

Jahangeer, M., Fatima, R., & Ashiq, M. (2021). Therapeutic and biomedical potentialities of terpenoids–A review. Journal of Pure and Applied Microbiology, 15(2), 531-547. https://doi.org/10.22207/JPAM.15.2.10

Khoo, H. E., Azlan, A., Tang, S. T., & Lim, S. M. (2017). Anthocyanidins and anthocyanins: Colored pigments as food, pharmaceutical ingredients, and the potential health benefits. Food & Nutrition Research, 61(1), 1361779. https://doi.org/10.1080/16546628.2017.1361779

Khoo, N. K., White, C. R., Pozzo-Miller, L., Zhou, F., Constance, C., Inoue, T., Patel, R. P., & Parks, D. A. (2010). Dietary flavonoid quercetin stimulates vasorelaxation in aortic vessels. Free Radical Biology and Medicine, 49(3), 339-347. https://doi.org/10.1016/j.freeradbiomed.2010.04.022

Kim, S., Kim, M., Kang, M.-C., Lee, H. H. L., Cho, C. H., Choi, I., Park, Y., & Lee, S.-H. (2021). Antioxidant effects of turmeric leaf extract against hydrogen peroxide-induced oxidative stress in vitro in vero cells and in vivo in zebrafish. Antioxidants, 10(1), 112. https://doi.org/10.3390/antiox10010112

Kim, S., Kim, N., Jeong, J., Lee, S., Kim, W., Ko, S.-G., & Kim, B. (2021). Anti-cancer effect of Panax ginseng and its metabolites: From traditional medicine to modern drug discovery. Processes, 9(8), 1344. https://doi.org/10.3390/pr9081344

Kim, S. W., Goossens, A., Libert, C., Van Immerseel, F., Staal, J., & Beyaert, R. (2020). Phytohormones: Multifunctional nutraceuticals against metabolic syndrome and comorbid diseases. Biochemical Pharmacology, 175, 113866. https://doi.org/10.1016/j.bcp.2020.113866

Koa, E. Y., Kim, D., Roh, S. W., Yoonc, W. J., Jeon, Y. J., Ahn, G., & Kim, K. N. (2015). Evaluation on antioxidant properties of sixteen plant species from Jeju Island in Korea. Excli j, 14, 133-145. https://doi.org/10.17179/excli2014-589

Kupina, S., Fields, C., Roman, M. C., & Brunelle, S. L. (2018). Determination of total phenolic content using the Folin-C assay: Single-laboratory validation, first action 2017.13. Journal of AOAC International, 101(5), 1466-1472. https://doi.org/10.5740/jaoacint.18-0031

Kurutas, E. B. (2015). The importance of antioxidants which play the role in cellular response against oxidative/nitrosative stress: current state. Nutrition Journal, 15, 1-22. https://doi.org/10.1186/s12937-016-0180-y

Kushima, H., Nishijima, C. M., Rodrigues, C. M., Rinaldo, D., Sassá, M. F., Bauab, T. M., Di Stasi, L. C., Carlos, I. Z., Brito, A. R. M. S., & Vilegas, W. (2009). Davilla elliptica and Davilla nitida: gastroprotective, anti-inflammatory immunomodulatory and anti-Helicobacter pylori action. Journal of Ethnopharmacology, 123(3), 430-438. https://doi.org/10.1016/j.jep.2009.03.004

La, E. H. (2022). Modulating photochromism of acylated anthocyanins by ultraviolet-visible excitation and acylation patterns for the expansion of color diversification [Doctoral dissertation, The Ohio State University]. OhioLINK Electronic Theses and Dissertations Center. http://rave.ohiolink.edu/etdc/view?acc_num=osu1650898779405222

Lachman, J., Pronek, D., Hejtmánková, A., Dudjak, J., Pivec, V., & Faitová, K. (2003). Total polyphenol and main flavonoid antioxidants in different onion (Allium cepa L.) varieties. Horticultural Science, 30(4), 142-147. https://doi.org/10.17221/3876-HORTSCI

Lewis, T., Wallace, W., Peterson, F. D., Rafferty, S., & Martic, S. (2022). Reactivities of quercetin and metallo-quercetin with superoxide anion radical and molecular oxygen. Electrochemical Science Advances, 2(4), e2100054. https://doi.org/10.1002/elsa.202100054

Little, A. C., Kovalenko, I., Goo, L. E., Hong, H. S., Kerk, S. A., Yates, J. A., Purohit, V., Lombard, D. B., Merajver, S. D., & Lyssiotis, C. A. (2020). High-content fluorescence imaging with the metabolic flux assay reveals insights into mitochondrial properties and functions. Communications biology, 3(1), 271.

Lu, N., Bernardo, E. L., Tippayadarapanich, C., Takagaki, M., Kagawa, N., & Yamori, W. (2017). Growth and accumulation of secondary metabolites in perilla as affected by photosynthetic photon flux density and electrical conductivity of the nutrient solution. Frontiers in Plant Science, 8, 708. https://doi.org/10.3389/fpls.2017.00708

Mardani-Ghahfarokhi, A., & Farhoosh, R. (2020). Antioxidant activity and mechanism of inhibitory action of gentisic and α-resorcylic acids. Scientific Reports, 10(1), 19487. https://doi.org/10.1038/s41598-020-76622-0

Masuku, N. P., Unuofin, J. O., & Lebelo, S. L. (2020). Promising role of medicinal plants in the regulation and management of male erectile dysfunction. Biomedicine & Pharmacotherapy, 130, 110555. https://doi.org/10.1016/j.biopha.2020.110555

Mattera, M. G., Gonzalez-Polo, M., Peri, P. L., & Moreno, D. A. (2024). Intraspecific variation in leaf (poly) phenolic content of a southern hemisphere beech (Nothofagus antarctica) growing under different environmental conditions. Scientific Reports, 14(1), 20050. https://doi.org/10.1038/s41598-023-47579-7\

Mattioli, R., Francioso, A., Mosca, L., & Silva, P. (2020). Anthocyanins: A comprehensive review of their chemical properties and health effects on cardiovascular and neurodegenerative diseases. Molecules, 25(17), 3809. https://doi.org/10.3390/molecules25173809

Meena, H., Pandey, H. K., Pandey, P., Arya, M. C., & Ahmed, Z. (2012). Evaluation of antioxidant activity of two important memory enhancing medicinal plants Baccopa monnieri and Centella asiatica. Indian J Pharmacol, 44(1), 114-117. https://doi.org/10.4103/0253-7613.91880

Mihalik, G. J. (1978). Guyanese ethnomedical botany: A folk pharmacopoeia. Ethnomedicine, 5(1-2), 83-96. https://doi.org/10.1515/ethn.1978.5.1-2.83

Mihaylova, D., Dimitrova-Dimova, M., & Popova, A. (2024). Dietary phenolic compounds—Wellbeing and perspective applications. International Journal of Molecular Sciences, 25(9), 4769. https://doi.org/10.3390/ijms25094769

Nandiyanto, A. B. D., Oktiani, R., & Ragadhita, R. (2019). How to read and interpret FTIR spectroscope of organic material. Indonesian Journal of Science and Technology, 4(1), 97-118. https://doi.org/10.17509/ijost.v4i1.15806

Nguyen, H. N., Butler, C., Palberg, D., Kisiala, A., & Emery, R. N. (2023). The tRNA-degradation pathway impacts the phenotype and metabolome of Arabidopsis thaliana: evidence from atipt2 and atipt9 knockout mutants. Plant Growth Regulation, 1-20. https://doi.org/10.1007/s10725-023-00987-1

Nishijima, C. M., Rodrigues, C. M., Silva, M. A., Lopes-Ferreira, M., Vilegas, W., & Hiruma-Lima, C. A. (2009). Anti-hemorrhagic activity of four Brazilian vegetable species against Bothrops jararaca venom. Molecules, 14(3), 1072-1080. https://doi.org/10.3390/molecules14031072

Nkwocha, C. C., Felix, O. J., & Idoko, N. R. (2023). GC-FID spectroscopic analysis and antioxidant activities of methanolic fraction of Cassia tora leaves. Pharmacological Research-Modern Chinese Medicine, 9, 100338. https://doi.org/10.1016/j.prmcm.2023.100338

Noreen, H., Semmar, N., Farman, M., & McCullagh, J. S. (2017). Measurement of total phenolic content and antioxidant activity of aerial parts of medicinal plant Coronopus didymus. Asian Pacific Journal of Tropical Medicine, 10(8), 792-801. https://doi.org/10.1016/j.apjtm.2017.07.024

Pandey, K. B., & Rizvi, S. I. (2009). Plant polyphenols as dietary antioxidants in human health and disease. Oxidative medicine and cellular longevity, 2, 270-278.

Pandey, K. B., & Rizvi, S. I. (2009). Plant polyphenols as dietary antioxidants in human health and disease. Oxidative medicine and cellular longevity, 2, 270-278.

Parhiz, H., Roohbakhsh, A., Soltani, F., Rezaee, R., & Iranshahi, M. (2015). Antioxidant and anti-inflammatory properties of the citrus flavonoids hesperidin and hesperetin: An updated review of their molecular mechanisms and experimental models. Phytotherapy Research, 29(3), 323-331. https://doi.org/10.1002/ptr.5256

Park, C. H., Yeo, H. J., Kim, N. S., Park, Y. E., Park, S. Y., Kim, J. K., & Park, S. U. (2018). Metabolomic profiling of the white, violet, and red flowers of Rhododendron schlippenbachii Maxim. Molecules, 23(4), 827. https://doi.org/10.3390/molecules23040827

Pervin, M., Hasnat, M. A., & Lim, B. O. (2013). Antibacterial and antioxidant activities of Vaccinium corymbosum L. leaf extract. Asian Pacific Journal of Tropical Disease, 3(6), 444-453. https://doi.org/10.1016/S2222-1808(13)60099-7

Qi, N., Zhao, W., Xue, C., Zhang, L., Hu, H., Jin, Y., Xue, X., Chen, R., & Zhang, J. (2025). Phenolic Acid and Flavonoid Content Analysis with Antioxidant Activity Assessment in Chinese C. pi. Shen Honey. Molecules, 30(2), 370.

Quesada-Vázquez, S., Eseberri, I., Les, F., Pérez-Matute, P., Herranz-López, M., Atgié, C., Lopez-Yus, M., Aranaz, P., Oteo, J. A., Escoté, X., Lorente-Cebrian, S., Roche, E., Courtois, A., López, V., Portillo, M. P., Milagro, F. I., & Carpéné, C. (2024). Polyphenols and metabolism: from present knowledge to future challenges. J Physiol Biochem, 80(3), 603-625. https://doi.org/10.1007/s13105-024-01046-7

Raj Rai, S., Bhattacharyya, C., Sarkar, A., Chakraborty, S., Sircar, E., Dutta, S., & Sengupta, R. (2021). Glutathione: Role in oxidative/nitrosative stress, antioxidant defense, and treatments. ChemistrySelect, 6(18), 4566-4590. https://doi.org/10.1002/slct.202100773

Rees, A., Villamor, E., Evans, D., Gooz, M., Fallon, C., Mina-Abouda, M., Disharoon, A., Eblen, S. T., & Delaney, J. R. (2025). Screening Methods to Discover the FDA-Approved Cancer Drug Encorafenib as Optimally Selective for Metallothionein Gene Loss Ovarian Cancer. Genes, 16(1), 42.

Rets'epile, P. M., Polile, R., & Hlokoane, O. (2021). Analysis of phytochemical profile, ferric reducing power, H2O2 scavenging activity and 2, 2-diphenyl-1-picrylhydrazyl (DPPH) radical scavenging activity of extracts from aerial parts of Pseudognaphalium undulatum.

Rudrapal, M., Khairnar, S. J., Khan, J., Dukhyil, A. B., Ansari, M. A., Alomary, M. N., Alshabrmi, F. M., Palai, S., Deb, P. K., & Devi, R. (2022). Dietary Polyphenols and Their Role in Oxidative Stress-Induced Human Diseases: Insights Into Protective Effects, Antioxidant

Potentials and Mechanism(s) of Action. Front Pharmacol, 13, 806470. https://doi.org/10.3389/fphar.2022.806470

Rudrapal, M., Khan, J., Dukhyil, A. A. B., Alarousy, R., Attah, E. I., Sharma, T., Khairnar, S. J., & Bendale, A. R. (2021). Chalcone Scaffolds, Bioprecursors of Flavonoids: Chemistry, Bioactivities, and Pharmacokinetics. Molecules, 26(23). https://doi.org/10.3390/molecules26237177

Sandhu, A. K., Islam, M., Edirisinghe, I., & Burton-Freeman, B. (2023). Phytochemical composition and health benefits of figs (fresh and dried): A review of literature from 2000 to 2022. Nutrients, 15(11), 2623. https://doi.org/10.3390/nu15112623

Sari, D. R. T., Cairns, J. R. K., Safitri, A., & Fatchiyah, F. (2019). Virtual Prediction of the Delphinidin-3-O-glucoside and Peonidin-3-O-glucoside as Anti-inflammatory of TNF-α Signaling. Acta Inform Med, 27(3), 152-157. https://doi.org/10.5455/aim.2019.27.152-157

Sauvain, M., Kunesch, N., Poisson, J., Gantier, J. C., Gayral, P., & Dedet, J. P. (1996). Isolation of leishmanicidal triterpenes and lignans from the Amazonian liana Doliocarpus dentatus (Dilleniaceae). Phytotherapy Research, 10(1), 1-4. https://doi.org/10.1002/(SICI)1099-1573(199602)10:1<1::AID-PTR757>3.0.CO;2-A

Savali, A., Shende, M., & Chandrasekhar, S. B. (2023). Antioxidant, antistress, nootropic activity and its correlation studies of aqueous extract of Punica granatum fruit estimated by noninvasive biomarkers and Y-maze test in rodents. Research Journal of Pharmacy and Technology, 16(10), 5125-5130. https://doi.org/10.52711/0974-360X.2023.00855

Silva dos Santos, J., Gonçalves Cirino, J. P., de Oliveira Carvalho, P., & Ortega, M. M. (2021). The pharmacological action of kaempferol in central nervous system diseases: A review. Frontiers in Pharmacology, 11, 565700. https://doi.org/10.3389/fphar.2020.565700

Singleton, V. L., & Rossi, J. A. (1965). Colorimetry of total phenolics with phosphomolybdic-phosphotungstic acid reagents. American Journal of Enology and Viticulture, 16(3), 144-158. https://doi.org/10.5344/ajev.1965.16.3.144

Slinkard, K., & Singleton, V. L. (1977). Total phenol analysis: Automation and comparison with manual methods. American Journal of Enology and Viticulture, 28(1), 49-55. https://doi.org/10.5344/ajev.1977.28.1.49

Smith, E., Lewis, A., Narine, S. S., & Emery, R. J. N. (2023). Unlocking potentially therapeutic phytochemicals in Capadulla (Doliocarpus dentatus) from Guyana using untargeted mass spectrometry-based metabolomics. Metabolites, 13(10), 1050. https://doi.org/10.3390/metabo13101050

Sultana, N., Saini, P. K., Kiran, S. R., & Kanaka, S. (2023). Exploring the antioxidant potential of medicinal plant species: A comprehensive review. Journal of Plant Biota, 1(1), 1-14. https://doi.org/10.1234/jpb.2023.1.1.1

Sun, X., Yao, C., Xiong, D., Zhang, B., Sun, J., Liao, S., Wang, A., Lan, Y., & Li, Y. (2018). Simultaneous quantification of seven caffeoylquinic acids in ecotypes of Blumea balsamifera at various life stages by high-performance liquid chromatography. Analytical Letters, 51(11), 1642-1653. https://doi.org/10.1080/00032719.2017.1384920

Tahirović, A., & Bašić, N. (2017). Determination of phenolic content and antioxidant properties of methanolic extracts from Viscum album ssp. album Beck. Bulletin of the Chemists and Technologists of Bosnia and Herzegovina, 49, 25-30. https://doi.org/10.5555/20193142415

Tan, S. P., Stathopoulos, C., Parks, S., & Roach, P. (2014). An optimised aqueous extract of phenolic compounds from bitter melon with high antioxidant capacity. Antioxidants, 3(4), 814-829. https://doi.org/10.3390/antiox3040814

Uçar, K., & Göktaş, Z. (2023). Biological activities of naringenin: A narrative review based on in vitro and in vivo studies. Nutr Res, 119, 43-55. https://doi.org/10.1016/j.nutres.2023.08.006

Ullah, A., Munir, S., Badshah, S. L., Khan, N., Ghani, L., Poulson, B. G., Emwas, A. H., & Jaremko, M. (2020). Important flavonoids and their role as a therapeutic agent. Molecules, 25(22), 5243. https://doi.org/10.3390/molecules25225243

Uysal, S., & Efe Arslan, D. (2024). Impact of drying methods on the bioactive compounds and antioxidant capacity of pomegranate (Punica granatum L.) peel. Selçuk Üniversitesi Fen Fakültesi Fen Dergisi, 50, 55-64. https://doi.org/10.15317/scitech.2024.1460047

Van Andel, T. R., MacKinven, A., & Bánki, O. (2003). Commercial non-timber forest products of the Guiana shield: An inventory of commercial NTFP extraction and possibilities for sustainable harvesting. Netherlands Committee for IUCN.

van Andel, T. R. (2000). Non-timber forest products of the North-West District of Guyana [Doctoral dissertation, Utrecht University]. Utrecht University Repository. https://dspace.library.uu.nl/handle/1874/1168

Yavorska, H. V., Vorobets, N. M., Yavorska, N. Y., & Fafula, R. V. (2023). Screening of anticandidal activity of Vaccinium corymbosum shoots' extracts and content of polyphenolic compounds during seasonal variation. Studia Biologica, 17(2), 3-14. https://doi.org/10.30970/sbi.1702.703

Yerragunta, V., Suman, D., Anusha, V., Patil, P., & Samhitha, T. (2013). A review on chalcones and its importance. PharmaTutor, 1(2), 54-59.

Zafar, F., Asif, H. M., Shaheen, G., Ghauri, A. O., Rajpoot, S. R., Tasleem, M. W., Shamim, T., Hadi, F., Noor, R., Ali, T., Gulzar, M. N., & Nazar, H. (2023). A comprehensive review on medicinal plants possessing antioxidant potential. Clinical and Experimental Pharmacology and Physiology, 50(3), 205-217. https://doi.org/10.1111/1440-1681.13743

Zargar, S., Altwaijry, N., Wani, T. A., & Alkahtani, H. M. (2023). Evaluation of the possible pathways involved in the protective effects of quercetin, naringenin, and rutin at the gene, protein and miRNA levels using in-silico multidimensional data analysis. Molecules, 28(13), 4904. https://doi.org/10.3390/molecules28134904

Zhang, X., Gao, H., Zhang, L., Liu, D., & Ye, X. (2012). Extraction of essential oil from discarded tobacco leaves by solvent extraction and steam distillation, and identification of its chemical composition. Industrial Crops and Products, 39, 162-169. https://doi.org/10.1016/j.indcrop.2012.02.029

6. - GENERAL DISCUSSION

6.1.INTRODUCTION

The findings of this thesis on *D. dentatus* (Capadulla) provide new insights into the plant's chemical diversity and therapeutic potential, particularly through the comparative study of its red and white ecotypes. *D. dentatus*, a plant species indigenous to Guyana and its surrounding regions, has been historically valued in traditional medicinal practices for its varied therapeutic applications. This traditional botanical remedy has been utilized to address a range of health concerns including inflammatory conditions and dermatological disorders. Furthermore, it has been employed as a natural adjunct for the enhancement of sexual well-being in men. However, the underlaying chemistry including the specific class of secondary metabolites and associated pathways of these effects had not been attempted until this study. The analysis uncovers a wide range of bioactive compounds in both ecotypes, with notable differences in polyphenol and flavonoid concentrations. These compounds are known for their strong antioxidant and anti-inflammatory properties, which are linked to disease prevention and health enhancement. By revealing the metabolomic profiles of the red and white ecotypes, this research not only validates the traditional uses of *D. dentatus* but also identifies specific bioactive compounds that could be harnessed in developing targeted natural therapies.

The main objectives were:

1. To examine international and national policy frameworks governing natural product research in Guyana.
2. To determine the general profile and target bioactive compounds of taxonomic origin *of D. dentatus* ecotypes in response to erectile dysfunction (ED) therapy.
3. To determine the phytohormone profiles in *D. dentatus* red and white ecotypes.
4. To assess the phenolic, flavonoid content and antioxidant capacities of *D. dentatus* red and white ecotypes

In Chapters 1 and 2, a comprehensive literature review was conducted to examine Guyana's ethical and legal framework regarding natural product research. This review highlighted Guyana's commitment to traditional knowledge and biodiversity preservation, aligning with international agreements such as the CBD and Nagoya Protocol, while advocating for community-based forest management and sustainable practices. Additionally, to address the limited scientific evidence supporting the traditional medicinal uses of *D. dentatus* as a treatment for ED, a second literature review was conducted to examine the phytochemical and phytohormone profiles of *D. dentatus*. These foundational reviews set the stage for data collection in Guyana, South America.

Building on this groundwork, the thesis aims to provide an in-depth, untargeted screening approach for bioactive compounds from secondary metabolite classes such as polyphenols, alkaloids, and terpenoids for the treatment of ED (Chapter 3). This broad approach was followed by a more targeted investigation into the phytohormone profiles and their interactions with secondary metabolites like polyphenols, alkaloids, and terpenoids of *D. dentatus* ecotypes

(Chapter 4). Furthermore, targeted research was conducted on both ecotypes to assess their total phenolic, flavonoid contents, and antioxidant capacity (Chapter 5). As we move into the general discussion, we will synthesize the key findings from these experiments, highlighting their implications and discussing avenues for future research. This synthesis will provide a comprehensive overview of how the study's objectives were met and where further investigation is warranted.

6.2. Metabolomic Profiling of *D. dentatus* Ecotypes

While *D. dentatus* is generally valued in traditional medicine across South and Central America; specifically in Guyana there are two ecotypes of *D. dentatus* (Figures 1.3 and 1.4) for which there is an abundance of anecdotal evidence for beneficial effects on specific illnesses such as leishmanial ulcers, diabetes, hepatitis, gastrointestinal problems and claims for erectile dysfunction (ED) therapy (Sauvain et al., 1993; Van Andel T, 2000). However, there is limited scientific evidence to support the pharmacological benefits of *D. dentatus* ecotypes as a treatment for ED. Previous in-depth untargeted metabolomics analyses had limited scope and had not been conducted at the ecotype level to support any therapeutic claims for ED.

The metabolomics analysis of *D. dentatus* red and white ecotypes showed that their metabolite profiles were markedly different, as shown in the detailed results (Chapter 3, Appendix 2). An untargeted, global metabolomic analysis found 637 possible metabolite features. Of these, 107 (16.79%) were unique to the *D. dentatus* red ecotype and 64 (10.05%) were unique to the white ecotype. Further analysis led to the identification of 55 selected compounds (level 2 annotation), including flavonoids (quercetin and kaempferol) derivatives, terpenoids, and some alkaloids (indole alkaloids). There was a statistically significant ($p \leq 0.05$) between the red ecotype

and biosynthesis pathways for secondary metabolites such as sesquiterpene and triterpenoid compounds, galactose, steroid and polyphenols (flavonoids, flavone and flavonol) compounds, underscoring its adaptive emphasis on ecological resilience and interaction (Sauvain et al., 1993; Van Andel T, 2000). These pathways are essential for the synthesis of compounds involved in stress tolerance, signaling, and plant-environment interactions. The enhancement of these pathways in the red ecotype aligns with its higher levels of flavonoids and terpenoids compounds known for their antioxidant, anti-inflammatory, and antimicrobial properties. (Ahmed et al., 2016; Huang et al., 2023).

In contrast, the white ecotype prioritized primary metabolic pathways, including the biosynthesis of valine, leucine, isoleucine and flavonoid reflecting an orientation towards fundamental physiological processes rather than the production of secondary metabolites (Jarial et al., 2018; Lim et al., 2016; Tsai et al., 2015). One important difference was that the red ecotype had 60% more flavonoids than the white ecotype.

The class levels of the nodes annotated by ClassyFire encompass compounds derived from both positive and negative ionization modes from both red and white *D. dentatus*, classified according to the kingdom level (K), superclass level (SC), and class level (C). The contributions of the annotated compounds presented in Chapter 3 (Figure 3.8) are predominantly characterized by the benzenoid, phenylpropanoid, polyketide, and lipid and lipid-like molecule superclasses. This analysis has led to the identification of over 847 compounds, of which 138 have therapeutic potential. Notably, the majority of these compounds are classified as lipids and lipid-like molecules (37.1% of what?), followed by phenylpropanoids and polyketides (20%), and benzenoids (13.7%). Within phenylpropanoids and polyketides, flavonoids dominated at 63.9% respectively (Fig 3.8).

Benzenoids are a group of chemical compounds that have a distinctive structure consisting of a benzene ring. Benzenoids have a considerable impact on pharmacology because of their wide range of biological activity and potential for therapeutic use. Several naturally occurring substances with benzenoid structures display pharmacological capabilities, encompassing anti-inflammatory and antioxidant actions, as well as antibacterial and anticancer activity (Huang et al., 2023; Kuo et al., 2020). Benzenoids possess an aromatic nature that enables them to effectively engage with biological systems, rendering them highly favourable for medication exploration and advancement (Fig 3.8). The study of the pharmacological characteristics of benzenoids entails investigating their modes of operation, ability to be absorbed by the body, and possible adverse reactions, to utilize their healing capabilities for different medical ailments (Huang et al., 2023).

Phenylpropanoids and polyketides are two separate categories of chemicals that have a wide range of structures and are important in pharmacology (Ahmed et al., 2016). Phenylpropanoids, which are generated from phenylalanine, frequently display antioxidant, anti-inflammatory, and antibacterial characteristics. These chemicals, which are present in different plant sources, have a role in plant defence processes and have shown potential therapeutic benefits in humans (Jarial et al., 2018; Tsai et al., 2015).

Polyketides, however, are a category of organic compounds produced through the action of polyketide synthases. These chemicals display a diverse range of pharmacological effects, such as antibacterial, antifungal, and anticancer characteristics. Microorganisms frequently synthesize polyketides, which possess significant pharmacological potential and have consequently been utilized in the creation of several medicinal molecules (Lim et al., 2016).

The elevated relative abundance of polyphenols in the red ecotype, recognized for their antioxidant, anti-inflammatory, and anticancer properties (Bobrysheva et al., 2023; Ewart smith, 2023; Rana et al., 2022), can be linked to CKs through their roles in plant stress responses and phytochemical production. As plant hormones, CKs enhance stress tolerance by modulating antioxidant defenses and can influence the biosynthesis of secondary metabolites, such as polyphenols, through interactions with other hormonal pathways (Liu et al., 2020; Prerostova et al., 2018). CKs promote a favorable environment for polyphenol synthesis by enhancing gene expression in the phenylpropanoid pathway, which is crucial for the production of phenolic compounds (Abdelrahman et al., 2021; Zagoskina et al., 2023). CKs also maintain photosynthetic efficiency under stress conditions, indirectly supporting polyphenol production by ensuring energy availability for secondary metabolite synthesis (Liu et al., 2020; Prerostova et al., 2018). This indirect support for polyphenol production contributes to the plant's antioxidant capacity and stress resilience, potentially explaining why certain ecotypes like the red one exhibit high levels of these beneficial compounds (Abdelrahman et al., 2021; Eyduran et al., 2024).

This profiling provides support to the traditional claims that *D. dentatus* has healing properties and suggests that it might be able to help with oxidative stress-related conditions, which may include erectile dysfunction (Ewart smith, 2023; Xu et al., 2024; Y. Zhang et al., 2024). By distinguishing the chemical diversity between ecotypes, this research paves the way for selecting specific ecotypes for targeted medicinal uses, an approach that could significantly enhance the efficacy of natural product-based treatments (Ewart smith, 2023).

These important findings from Chapter 3 were used to examine the phytohormone's metabolic profiles and the interactions between secondary metabolites in Chapter 4. Overall, these results show that *D. dentatus*, especially the red ecotype, has a lot of substantial therapeutic potential and could be used to develop targeted and effective natural remedies.

6.3. Cytokinin Profiles

The foundation of this thesis is built upon the findings presented in Chapters 2 and 3. These chapters examined compliance and policy frameworks related to the collection of *D. dentatus* ecotypes in Guyana, as well as an untargeted mass spectrometric screening of over 29,944 tentative metabolite features. The results indicated a greater metabolic diversity in the red ecotype when compared to the white ecotype. This investigation into metabolites led us to explore the role of phytohormones, such as CKs, and SA, which are known to regulate the biosynthesis of secondary metabolites in plants. This regulation influences plant defence mechanisms and stress responses (Divekar et al., 2022; Jogawat et al., 2021; Lv et al., 2021a) . The complex interplay between phytohormones and secondary metabolites was further explored due to the recognition of phytohormones' role in regulating secondary metabolic pathways (Jogawat et al., 2021; Lv et al., 2021a). These pathways often produce compounds with antioxidant properties, such as phenylpropanoids and terpenoids (Grzegorczyk-Karolak et al., 2020; Grzegorczyk-Karolak et al., 2023; Hudeček et al., 2023).

Phytohormones, commonly referred to as plant hormones, are signaling molecules synthesized within plants that exist in remarkably low concentrations . These compounds play a critical role in regulating various aspects of plant growth and development, encompassing processes such as embryogenesis, organ size regulation, pathogen defence, stress tolerance, and reproductive development (Hoyerová et al., 2006; Morrison, Knowles, et al., 2015; Schmidt et al., 2024).

While the vast majority of studies on phytohormones concentrate on their roles in regulating plant growth, development, and responses to environmental stressors. These hormones, which include IAA, CKs, GAs, ABA, and ET, are essential for processes such as seed germination, root elongation, and reproductive development. Research also highlights their involvement in stress responses, including the adaptation to abiotic and biotic stresses, with hormones such as ABA, Jas, SA and BRs playing pivotal roles (EL Sabagh et al., 2022; Zheng et al., 2023). Furthermore, investigations examine hormonal crosstalk, microbial interactions, and biotechnological applications aimed at enhancing crop productivity and stress tolerance (EL Sabagh et al., 2022; Zheng et al., 2022).

Chapter 4 delved into the CKs profiles of the red and white ecotypes of *D. dentatus* and its potential impacts on the plant's medicinal properties. The key findings highlight the distinct CK profiles between the red and white ecotypes of *D. dentatus*.

Free-based CKs, such as *t*Z, were markedly elevated in the red ecotype (155.48 ± 20.23 pmol g^-1 DW) compared to the white ecotype (84.52 ± 26.03 pmol g^-1 DW), with *c*Z exhibiting a similar pattern (11.02 ± 2.22 pmol g^-1 DW) in the red ecotype versus (5.82 ± 1.23 pmol g^-1

DW) in the white ecotype. Riboside CKs, including DZR, were also found to be more abundant in the red ecotype (11.85 ± 2.47 pmol g^-1 DW) than in the white ecotype (6.80 ± 0.74 pmol g^-1 DW). The glucoside forms displayed the most pronounced disparity, with *t*Z7G levels in the red ecotype (7161.10 ± 2421.62 pmol g^-1 DW) significantly surpassing those in the white ecotype (0.69 ± 0.19 pmol g^-1 DW). Notably, certain glucosides, such as iP7G and iP9G, were more prevalent in the white ecotype (appendix 3), suggesting distinct CKs storage and transport mechanisms between the two ecotypes.

The red ecotype demonstrated significantly ($p < 0.05$) higher overall levels of CKs compared to the white ecotype. In the red ecotype, 75% of the 20 CKs types identified were upregulated relative to the white ecotype. These differences in CK levels between the two ecotypes were statistically significant, with $p < 0.026$, 0.039, and 0.026. This finding suggests that the red ecotype could possess a more dynamic regulatory mechanism, enabling it to release active CKs when required (Gong et al., 2022; Hošek et al., 2020; Trifunović-Momčilov et al., 2021).

Furthermore, the study uncovered a strong correlation between CKs and secondary metabolites, particularly flavonoids and alkaloids (Fig 4.7).

Alkaloids such as dopamine and tropine displayed strong positive correlations with *t*Z9G and *t*ZR, while hypoxanthine and pipecolinic acid showed similar patterns with certain CKs. Among polyphenols, compounds such as chalconaringenin and naringenin were positively associated with *c*ZOG and *t*Z derivatives, while cyanidin and delphinidin had significant negative correlations with CKs glucosides such as DZOG and DZ9G. Additionally, phenolic compounds, such as vanillic acid and caffeic acid, revealed a mix of positive and negative correlations with various forms of CKs.

This association implies the existence of an integrated network where CKs activity may enhance or modulate the levels of these bioactive compounds, potentially amplifying their therapeutic effects. Given the well-established antioxidant and anti-inflammatory properties of flavonoids and alkaloids, these interactions could position the red ecotype as a particularly valuable resource for pharmacological applications, especially those targeting oxidative stress and inflammatory conditions (Abdelrahman et al., 2021; Chaudhari & Mahajan, 2015; Decendit et al., 1992).

CK signalling molecules that occur at minute levels ($<10^{-8}$M) consist of adenine derivatives with isoprenoid side chains attached to the N^6 position of the adenine ring that significantly influence plant growth and development, including cell division, shoot initiation, and leaf senescence (Fig 4.2). CKs also play a crucial role in the production of secondary metabolites, which are vital for plant defence, stress response, and environmental interactions (Sarkar & Banerjee, 2021). CKs regulate biosynthetic pathways, such as the phenylpropanoid and shikimate pathways, which are essential for the synthesis of phenolic compounds and other secondary metabolites. This regulatory function is often shared with IAA, another key plant hormone (Davies, 2010).

CKs modulate the production of metabolites such as flavonoids and lipids, which are important for stress tolerance (Kieber & Schaller, 2014). The signalling pathways involved include histidine kinases and response regulators, with Arabidopsis Histidine Phosphotransferase proteins (AHP) proteins playing a central role in transmitting signals to regulate gene expression and metabolic processes (Kieber & Schaller, 2014; Kieber & Schaller, 2018; Yener et al., 2019). By influencing gene expression, cytokinins can either activate or repress genes involved in secondary

metabolite biosynthesis, leading to changes in the production of specific metabolites depending on the plant species and environmental conditions (Hwang & Sakakibara, 2006; Sakakibara, 2006b). Overall, cytokinins are valuable tools in biotechnology for enhancing the yield of valuable secondary metabolites and improving plant resilience to environmental stresses (Sakakibara, 2006a).

The insights gained from Chapter 4 have provided information that serves as a foundation for exploring the phenolic and flavonoid contents of both ecotypes in Chapter 5. By understanding the unique CK profiles and their interactions with other bioactive compounds, researchers may be able to develop more effective plant-based treatments for various health issues (Ahmed et al., 2024; Gong et al., 2022). This approach could lead to the creation of novel therapies that harness the natural medicinal properties of *D. dentatus*, potentially offering new solutions for a range of medical conditions.

6.4. Antioxidant and Phenolic Content of *D. dentatus red and white ecotypes*: Implications for Health and Therapeutic Potential

Antioxidant and phenolic content analyses are effective methods for evaluating the potential health benefits of various natural products. These analyses provide valuable insights into the bioactive compounds present in foods, plants, and other organic materials (Delgado et al., 2019; Machu et al., 2015).

The key findings in Chapter 5 reveal that the Guyanese wood vine *D. dentatus* ecotypes possess a high phenolic content and substantial antioxidant capacity. The *D. dentatus* red ecotype

exhibited greater elevated levels of bioactive compounds and antioxidant properties in comparison to the white ecotype. The total phenolic content in the red ecotype (119.70 mg/g) was nearly double that of the white ecotype, (61.08 mg/g). The flavonoid content in the red ecotype (4.15 mg/g) was more than twice that of the white ecotype (1.58 mg/g). These differences underscore the enhanced capacity of the red ecotype to produce secondary metabolites. In terms of antioxidant activity, the red ecotype demonstrated slightly greater effectiveness than the white ecotype, which correlates with its higher phenolic and flavonoid contents. Furthermore, compounds such as apiforol and cyanidin-3-O-glucoside were found to be more abundant in the red ecotype, further highlighting its superior bioactive profile.

This suggests that *D. dentatus* has the potential to serve as a valuable source of natural antioxidants, which can contribute to combating oxidative stress. These compounds play a crucial role in neutralizing free radicals, thereby helping to prevent cellular damage linked to chronic diseases such as cardiovascular disease, cancer, and neurodegenerative disorders (Delgado et al., 2019; Jung et al., 2017; Minarti et al., 2024). The red ecotype, in particular, showed higher concentrations of phenolic compounds compared to the white ecotype, indicating a potentially stronger antioxidant effect.

The high antioxidant capacity of *D. dentatus* red ecotype may support its therapeutic use in traditional medicine for treating various ailments, potentially linked to its ability to mitigate oxidative stress. This property is beneficial in addressing conditions associated with cellular damage from reactive oxygen species, such as inflammation and chronic diseases such as cardiovascular ailments. The findings in Chapter 5 emphasize the therapeutic potential of *D. dentatus*, especially in the development of plant-based treatments that are both effective and

affordable, promoting further research and sustainable use of this native Guyanese Capadulla plant. Finally, the results of the metabolomic profiling, phytohormone analysis, and assessment of antioxidant and phenolic content in different ecotypes of *D. dentatus* show that this woody vine has a lot of therapeutic potential as a medicinal plant. The red and white ecotypes have different chemical makeup and bioactive compound profiles. This study provides better insights into using plants in medicine, especially to treat conditions related to oxidative stress, inflammation, and maybe even erectile dysfunction. The red ecotype's higher levels of polyphenols, antioxidants, active CKs and conjurgates may further underscores its potential as a valuable natural resource for pharmacological applications. By establishing a scientific basis for these traditional medicinal claims, this research not only validates *D. dentatus*'s ethnomedicinal importance but also supports the development of affordable, plant-based therapies that could benefit local communities and modern medicine alike. These insights pave the way for continued research and sustainable applications of this native Guyanese plant in health and wellness. The ethical framework discussed in Chapter 2 ensures that future research can be conducted sustainably, concerning cultural knowledge and biodiversity conservation. Together, these findings contribute to a comprehensive understanding of *D. dentatus* and pave the way for new, plant-based therapies that could benefit both local communities and modern medicinal practices.

6.5. FUTURE DIRECTION

The combined analyses from this thesis yielded new insights in the field of secondary metabolites, CKs and Reactive Oxygen Species (ROS) in *D. dentatus* red and white ecotypes research, as well as the *D. dentatus* research community. Before the onset of this thesis, there was limited information on the metabolomes of *D. dentatus* with the main focus on the leaves (Aponte et al., 2008; Branquinho, Verdan, dos Santos, et al., 2021; Branquinho, Verdan, et al., 2021a; Branquinho, Verdan, Silva-Filho, et al., 2021; Raissa Borges Ishikawa et al., 2017; Raissa Borges Ishikawa et al., 2018; R. Jagessar et al., 2013; Sauvain et al., 1993) demonstrating that, it contains low toxicity in both acute and chronic studies suggests that the leaf extract can be safely utilized at moderate doses in rat models (Branquinho, Verdan, et al., 2021a; Raissa Borges Ishikawa et al., 2018). A review by Lima et al (Lima et al., 2014) of the Dilleniaceae species stated that these plants exhibit numerous pharmacological activities, including anti-inflammatory, antimicrobial, antioxidant, antidiabetic properties and anticancer properties (Lima et al., 2014). This is particularly evident when we look at the metabolic profiles of *D. dentatus* red and white ecotypes found in Guyana south America where the chemical diversity of both ecotypes contains diverse compounds that possess many biological activities. The findings of this thesis yielded new insights into the secondary metabolites and their interaction with CKs regarding functions but also poses many new questions surrounding the regulation, CK interactions, biosynthesis and the molecular mechanisms governing CK involvement in anti-inflammatory, antimicrobial, antioxidant, and antidiabetics and anticancer properties.

In chapters 3,4 and 5 hypotheses that the red ecotype contains a higher relative abundance of secondary metabolites, CKs and antioxidant properties were supported. Chapter 3 indicated that

polyphenolic compounds in *D. dentatus* red and white ecotypes may hold potential as a therapeutic response to ED. Future research on *D. dentatus* ecotypes should emphasize the therapeutic potential of their polyphenolic compounds, particularly in the context of addressing conditions such as ED. Isolating and characterizing specific polyphenols, followed by rigorous in vitro and in vivo studies, could facilitate an evaluation of their efficacy and mechanisms of action. Furthermore, exploring the interactions of these compounds with biological systems may yield valuable insights into their therapeutic roles. Expanding this research to include a comparative analysis of the red and white ecotypes across different seasons and geographical locations would provide a more comprehensive understanding of their metabolite profiles and enhance the reliability of the findings.

Metabolomic and pathway analyses represent promising avenues for future research. Expanding the investigation of significant metabolic pathways, such as flavonoid and sesquiterpenoid biosynthesis, may explain the regulatory mechanisms governing these pathways and their responsiveness to environmental factors. Furthermore, examining compound interactions, including potential synergistic effects, could strengthen the therapeutic potential of *D. dentatus*. Additionally, concentrating on alkaloids, a superclass of this plant that has received comparatively limited scholarly attention, may uncover novel bioactive compounds with unique therapeutic properties.

To translate these findings into practical applications, future research should prioritize clinical studies and investigations into bioavailability. Clinical trials designed to assess the safety, efficacy, and optimal dosage of *D. dentatus* extracts or isolated compounds will be crucial for therapeutic development. Furthermore, studies focused on the bioavailability and metabolism of

key compounds could yield valuable insights into their effectiveness within the human body. An understanding of the genetic and environmental factors that influence metabolite production in red and white ecotypes may also inform cultivation strategies, thereby ensuring consistent yields of bioactive compounds and facilitating the development of sustainable and effective therapeutic applications.

6.6. CONCLUSION

With the completion of this PhD thesis comes a greater knowledge of the *D. dentatus* ecotypes found in Guyana South America. The comparative analysis of the red and white ecotypes of *D. dentatus* reveals significant differences in their phytochemical profiles, phytohormone concentrations, and therapeutic potential. The red ecotype consistently demonstrated higher levels of secondary metabolites, including phenolic and flavonoid compounds, along with elevated CK activity. These characteristics suggest that the red ecotype is metabolically more active and better adapted to environmental challenges, with an enhanced ability to produce bioactive compounds linked to antioxidant, anti-inflammatory, and potential anticancer properties. The high levels of CKs such as *t*Z, *c*Z, and their glucoside forms further highlight the red ecotype's superior capacity for CK storage and activation.

In contrast, the white ecotype demonstrated a stronger emphasis on primary metabolic activities and specific secondary metabolite pathways, such as monoterpenoid biosynthesis, which are associated with antimicrobial and analgesic properties. While its bioactive compound profile is less diverse and abundant compared to the red ecotype, it still holds potential for targeted therapeutic applications. The distinct metabolomic pathways observed between the two ecotypes underscore their unique adaptations, influenced by genetic and environmental factors.

Overall, the findings validate the traditional medicinal use of *D. dentatus*, particularly the red ecotype, and emphasize its potential for developing natural remedies and pharmaceutical applications. Future research should further explore the bioactive compounds and their mechanisms, conduct clinical trials, and investigate sustainable cultivation practices to fully harness the therapeutic potential of both ecotypes.

6.7. REFERENCES

Ahmed, S. I., Hayat, M. Q., Tahir, M., Mansoor, Q., Ismail, M., Keck, K., & Bates, R. B. (2016). Pharmacologically active flavonoids from the anticancer, antioxidant and antimicrobial extracts of Cassia angustifolia Vahl. BMC Complementary and Alternative Medicine, 16(1), 1-9. https://doi.org/10.1186/s12906-016-1443-z

Ahmed, V. A., Rahman, H. S., Mohammed Raheem, M. O., Othman, H. H., Algarawi, M., & Ibnaouf, K. H. (2024). Antidiabetic, antihyperlipidemic, antioxidant effects and regulation of miRNA expression by Dianthus orientalis Adams extract in diabetic rat model. Natural Product Communications, 19(1). https://doi.org/10.1177/1934578X231219691

Aponte, J. C., Vaisberg, A. J., Rojas, R., Caviedes, L., Lewis, W. H., Lamas, G., Sarasara, C., Gilman, R. H., & Hammond, G. B. (2008). Isolation of cytotoxic metabolites from targeted Peruvian Amazonian medicinal plants. Journal of Natural Products, 71(1), 102-105. https://doi.org/10.1021/np070560c

Bobrysheva, T. N., Anisimov, G. S., Zolotoreva, M. S., Bobryshev, D. V., Budkevich, R. O., & Moskalev, A. A. (2023). [Polyphenols as promising bioactive compounds]. Voprosy Pitaniia, 92(1), 92-107. https://doi.org/10.33029/0042-8833-2023-92-1-92-107

Branquinho, L. S., Verdan, M. H., dos Santos, E., Macorini, L. F. B., Maris, R. S., Kuraoka-Oliveira, A. M., Bacha, F. B., Cardoso, C. A. L., Arena, A. C., Silva-Filho, S. E., & Kassuya, C. A. L. (2021). Toxicological evaluation of ethanolic extract of leaves from Doliocarpus dentatus in Swiss mice. Drug and Chemical Toxicology, 0(0), 1-7. https://doi.org/10.1080/01480545.2021.1982638

Branquinho, L. S., Verdan, M. H., Santos, E. d., Neves, S. C. d., Oliveira, R. J., Cardoso, C. A. L., & Kassuya, C. A. L. (2021). Aqueous extract from leaves of Doliocarpus dentatus (Aubl.) Standl. relieves pain without genotoxicity activity. Journal of Ethnopharmacology, 266, 113440. https://doi.org/10.1016/j.jep.2020.113440

Branquinho, L. S., Verdan, M. H., Silva-Filho, S. E., Oliveira, R. J., Cardoso, C. A. L., Arena, A. C., & Kassuya, C. A. L. (2021). Antiarthritic and antinociceptive potential of ethanolic extract from leaves of Doliocarpus dentatus (Aubl.) Standl. in mouse model. Pharmacognosy Research, 13(1), 28-33. https://doi.org/10.4103/pr.pr_79_20

Chaudhari, G. M., & Mahajan, R. T. (2015). Comparative antioxidant activity of twenty traditional Indian medicinal plants and its correlation with total flavonoid and phenolic content.

International Journal of Pharmaceutical Sciences Review and Research, 30(1), 105-111. https://doi.org/10.22270/jddt.v7i5.1513

Delgado, A. M., Issaoui, M., & Chammem, N. (2019). Analysis of main and healthy phenolic compounds in foods. Journal of AOAC International, 102(5), 1356-1364. https://doi.org/10.5740/jaoacint.19-0031

Ewart Smith, A. L., Narine, S. S., & Emery, R. J. N. (2023). Unlocking potentially therapeutic phytochemicals in Capadulla (Doliocarpus dentatus) from Guyana using untargeted mass spectrometry-based metabolomics. Metabolites, 13(10), 1103. https://doi.org/10.3390/metabo13101103

Gong, X., Li, L., Qin, L., Huang, Y., Ye, Y., Wang, M., Wang, Y., Xu, Y., Luo, F., & Mei, H. (2022). Targeted metabolomics reveals impact of N application on accumulation of amino acids, flavonoids and phytohormones in tea shoots under soil nutrition deficiency stress. Forests, 13(10), 1629. https://doi.org/10.3390/f13101629

Hošek, P., Hoyerová, K., Kiran, N. S., Dobrev, P. I., Zahajská, L., Filepová, R., Motyka, V., Müller, K., & Kamínek, M. (2020). Distinct metabolism of N-glucosides of isopentenyladenine and trans-zeatin determines cytokinin metabolic spectrum in Arabidopsis. New Phytologist, 225(6), 2423-2438. https://doi.org/10.1111/nph.16308

Hoyerová, K., Gaudinová, A., Malbeck, J., Dobrev, P. I., Kocábek, T., Šolcová, B., Trávníčková, A., & Kamínek, M. (2006). Efficiency of different methods of extraction and purification of cytokinins. Phytochemistry, 67(11), 1151-1159. https://doi.org/10.1016/j.phytochem.2006.03.010

Huang, Q., Liu, K., Qin, L., & Zhu, B. (2023). Lindera aggregata (Sims) Kosterm: A systematic review of its traditional applications, phytochemical and pharmacological properties, and quality control. Medicinal Plant Biology, 2(1), 20230004. https://doi.org/10.1142/S2949894X23230004

Ishikawa, R. B., Leitão, M. M., Kassuya, R. M., Macorini, L. F., Moreira, F. M. F., Cardoso, C. A. L., Coelho, R. G., Pott, A., Gelfuso, G. M., Croda, J., Oliveira, R. J., & Kassuya, C. A. L. (2017). Anti-inflammatory, antimycobacterial and genotoxic evaluation of Doliocarpus dentatus. Journal of Ethnopharmacology, 204, 18-25. https://doi.org/10.1016/j.jep.2017.04.004

Ishikawa, R. B., Vani, J. M., das Neves, S. C., Rabacow, A. P. M., Kassuya, C. A. L., Croda, J., Cardoso, C. A. L., Monreal, A. C. D. F., Antoniolli, A. C. M. B., Cunha – Laura, A. L., & Oliveira, R. J. (2018). The safe use of Doliocarpus dentatus in the gestational period: Absence of changes in maternal reproductive performance, embryo-fetal development and DNA integrity. Journal of Ethnopharmacology, 217, 1-6. https://doi.org/10.1016/j.jep.2018.01.034

Jagessar, R., Hoolas, G., & Maxwell, A. (2013). Phytochemical screening, isolation of betulinic acid, trigonelline and evaluation of heavy metals ion content of Doliocarpus dentatus. Journal of Natural Products (India), 6, 5-16.

Jarial, R., Thakur, S., Sakinah, M., Zularisam, A., Sharad, A., Kanwar, S., & Singh, L. (2018). Potent anticancer, antioxidant and antibacterial activities of isolated flavonoids from Asplenium nidus. Journal of King Saud University-Science, 30(2), 185-192. https://doi.org/10.1016/j.jksus.2017.01.007

Jung, T. D., Shin, G. H., Kim, J. M., Choi, S. I., Lee, J. H., Lee, S. J., Park, S. J., Woo, K. S., Oh, S. K., & Lee, O. H. (2017). Comparative analysis of γ-oryzanol, β-glucan, total phenolic content and antioxidant activity in fermented rice bran of different varieties. Nutrients, 9(6), 571. https://doi.org/10.3390/nu9060571

Kuo, P.-C., Wu, Y.-H., Hung, H.-Y., Lam, S.-H., Ma, G.-H., Kuo, L.-M., Hwang, T.-L., Kuo, D.-H., & Wu, T.-S. (2020). Anti-inflammatory principles from Lindera aggregata. Bioorganic & Medicinal Chemistry Letters, 30(13), 127224. https://doi.org/10.1016/j.bmcl.2020.127224

Lim, Y. P., Go, M. K., & Yew, W. S. (2016). Exploiting the biosynthetic potential of type III polyketide synthases. Molecules, 21(6), 806. https://doi.org/10.3390/molecules21060806

Lima, C. C., Lemos, R. P. L., & Conserva, L. M. (2014). Dilleniaceae family: An overview of its ethnomedicinal uses, biological and phytochemical profile. Journal of Pharmacognosy and Phytochemistry, 3(2), 181-204. https://doi.org/10.54877/jpj.2014.3.2.370

Macedo, A. L., Boaretto, A. G., da Silva, A. G., Maia, D. S., de Siqueira, J. M., Silva, D. M. d. L. E., & Carollo, C. A. (2021). Evaluation of the effect of Brazilian savanna (Cerrado) seasons in flavonoids and alkaloids accumulation: The case of Duguetia furfuracea. Journal of the Brazilian Chemical Society, 32(7), 1432-1442. https://doi.org/10.21577/0103-5053.20210054

Machu, L., Misurcova, L., Vavra Ambrozova, J., Orsavova, J., Mlcek, J., Sochor, J., & Jurikova, T. (2015). Phenolic content and antioxidant capacity in algal food products. Molecules, 20(1), 1118-1133. https://doi.org/10.3390/molecules20011118

Minarti, M., Ariani, N., Megawati, M., Hidayat, A., Hendra, M., Primahana, G., & Darmawan, A. (2024). Potential antioxidant activity methods DPPH, ABTS, FRAP, total phenol and

total flavonoid levels of Macaranga hypoleuca (Reichb. f. & Zoll.) leaves extract and fractions. E3S Web of Conferences, 396, 01030. https://doi.org/10.1051/e3sconf/202439601030

Morrison, E. N., Knowles, S., Hayward, A., Thorn, R. G., Saville, B. J., & Emery, R. (2015). Detection of phytohormones in temperate forest fungi predicts consistent abscisic acid production and a common pathway for cytokinin biosynthesis. Mycologia, 107(2), 245-257. https://doi.org/10.3852/14-157

Rana, A., Samtiya, M., Dhewa, T., Mishra, V., & Aluko, R. E. (2022). Health benefits of polyphenols: A concise review. Journal of Food Biochemistry, 46(10), e14264. https://doi.org/10.1111/jfbc.14264

Sauvain, M., Dedet, J. P., Kunesch, N., Poisson, J., Gantier, J. C., Gayral, P., & Kunesch, G. (1993). In vitro and in vivo leishmanicidal activities of natural and synthetic quinoids. Phytotherapy Research, 7(2), 167-171. https://doi.org/10.1002/ptr.2650070214

Trifunović-Momčilov, M., Motyka, V., Dobrev, P. I., Marković, M., Milošević, S., Jevremović, S., Dragićević, I. Č., & Subotić, A. (2021). Phytohormone profiles in non-transformed and AtCKX transgenic centaury (Centaurium erythraea Rafn) shoots and roots in response to salinity stress in vitro. Scientific Reports, 11(1), 21471. https://doi.org/10.1038/s41598-021-00934-y

Tsai, P.-J., Huang, W.-C., Hsieh, M.-C., Sung, P.-J., Kuo, Y.-H., & Wu, W.-H. (2015). Flavones isolated from Scutellariae radix suppress Propionibacterium acnes-induced cytokine production in vitro and in vivo. Molecules, 21(1), 15. https://doi.org/10.3390/molecules21010015

van Andel, T. R., & Ruysschaert, S. (2000). Non-timber forest products of the North-West District of Guyana. Part II: A field guide. Tropenbos-Guyana Programme. https://doi.org/10.1007/978-94-015-9642-1

Wu, Z., Shang, X., Liu, G., & Xie, Y. (2023). Comparative analysis of flavonoids, polyphenols and volatiles in roots, stems and leaves of five mangroves. PeerJ, 11, e15529. https://doi.org/10.7717/peerj.15529

Xu, Z., Chu, W., Lei, X., & Chen, C. (2024). Higher oxidative balance score was associated with decreased risk of erectile dysfunction: A population-based study. Nutrition Journal, 23(1), 54. https://doi.org/10.1186/s12937-024-00956-y

Zhang, Y., Su, M., Liu, G., Wu, X., Feng, X., Tang, D., Jiang, H., & Zhang, X. (2024). Chronic sleep deprivation induces erectile dysfunction through increased oxidative stress,

apoptosis, endothelial dysfunction, and corporal fibrosis in a rat model. The Journal of Sexual Medicine. https://doi.org/10.1093/jsxmed/qdae118

Apendex 1 - Permission from copyright holder

Chapter 2 - Compliance With International and National Frameworks Governing Natural Product Research in Guyana

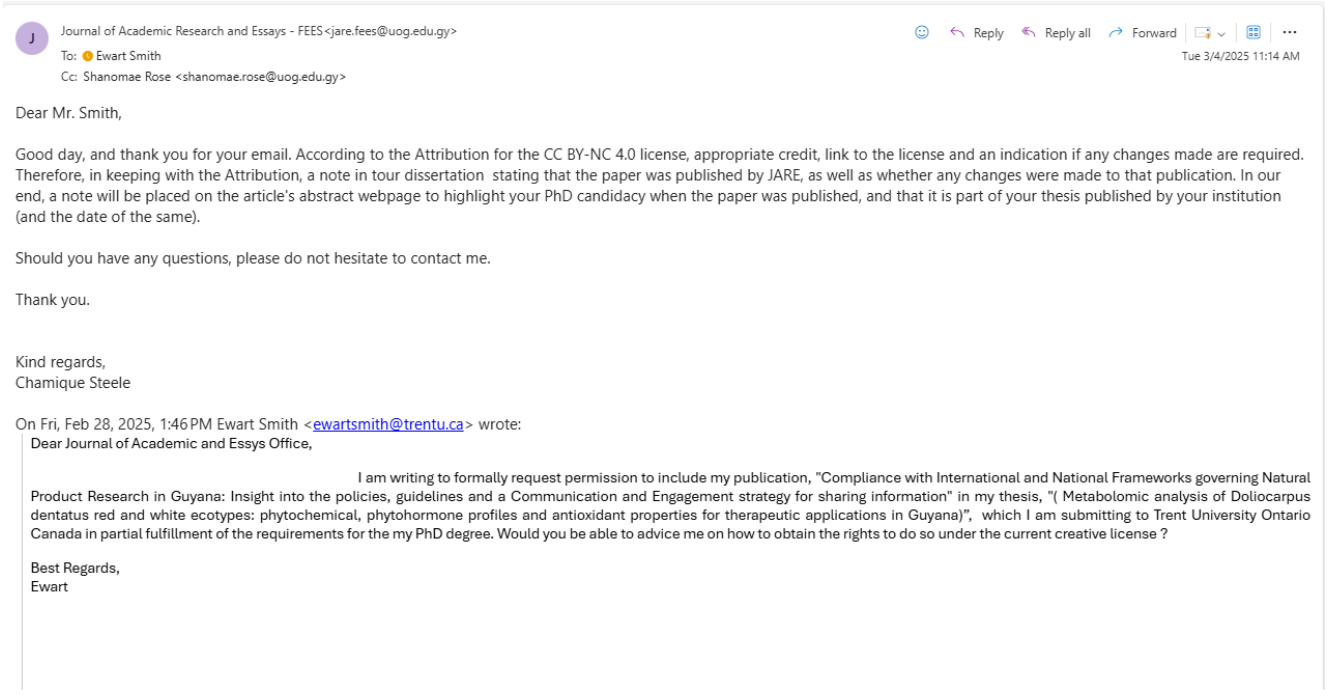

Journal of Academic Research and Essays - FEES<jare.fees@uog.edu.gy>
To: Ewart Smith
Cc: Shanomae Rose <shanomae.rose@uog.edu.gy>

Reply Reply all Forward
Tue 3/4/2025 11:14 AM

Dear Mr. Smith,

Good day, and thank you for your email. According to the Attribution for the CC BY-NC 4.0 license, appropriate credit, link to the license and an indication if any changes made are required. Therefore, in keeping with the Attribution, a note in tour dissertation stating that the paper was published by JARE, as well as whether any changes were made to that publication. In our end, a note will be placed on the article's abstract webpage to highlight your PhD candidacy when the paper was published, and that it is part of your thesis published by your institution (and the date of the same).

Should you have any questions, please do not hesitate to contact me.

Thank you.

Kind regards,
Chamique Steele

On Fri, Feb 28, 2025, 1:46 PM Ewart Smith <ewartsmith@trentu.ca> wrote:

Dear Journal of Academic and Essys Office,

I am writing to formally request permission to include my publication, "Compliance with International and National Frameworks governing Natural Product Research in Guyana: Insight into the policies, guidelines and a Communication and Engagement strategy for sharing information" in my thesis, "(Metabolomic analysis of Doliocarpus dentatus red and white ecotypes: phytochemical, phytohormone profiles and antioxidant properties for therapeutic applications in Guyana)", which I am submitting to Trent University Ontario Canada in partial fulfillment of the requirements for the my PhD degree. Would you be able to advice me on how to obtain the rights to do so under the current creative license ?

Best Regards,
Ewart

Chapter 3 - Unlocking Potentially Therapeutic Phytochemicals in Capadulla (*Doliocarpus dentatus*) from Guyana Using Untargeted Mass Spectrometry-Based Metabolomics

Published in: Metabolites (2023), 13 (1050)

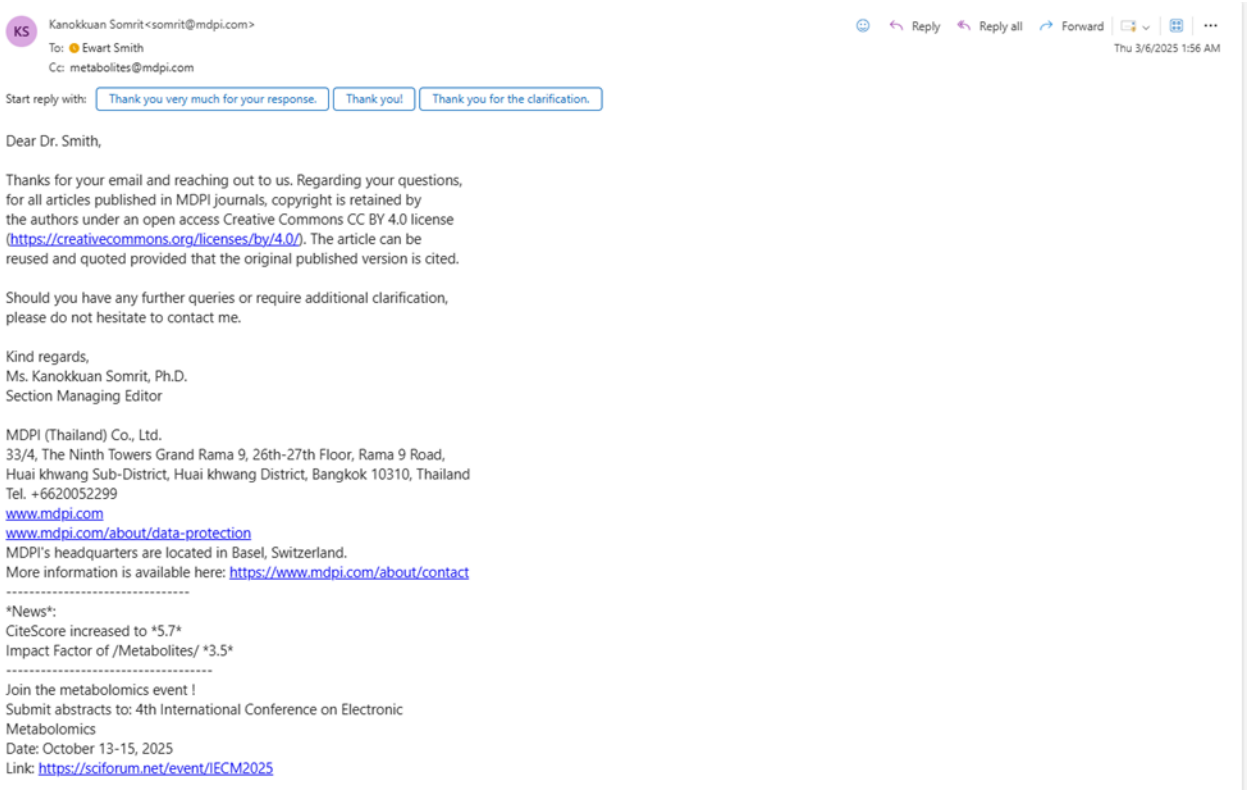

KS Kanokkuan Somrit<somrit@mdpi.com>
To: Ewart Smith
Cc: metabolites@mdpi.com

Reply Reply all Forward
Thu 3/6/2025 1:56 AM

Start reply with: Thank you very much for your response. | Thank you! | Thank you for the clarification.

Dear Dr. Smith,

Thanks for your email and reaching out to us. Regarding your questions, for all articles published in MDPI journals, copyright is retained by the authors under an open access Creative Commons CC BY 4.0 license (https://creativecommons.org/licenses/by/4.0/). The article can be reused and quoted provided that the original published version is cited.

Should you have any further queries or require additional clarification, please do not hesitate to contact me.

Kind regards,
Ms. Kanokkuan Somrit, Ph.D.
Section Managing Editor

MDPI (Thailand) Co., Ltd.
33/4, The Ninth Towers Grand Rama 9, 26th-27th Floor, Rama 9 Road,
Huai khwang Sub-District, Huai khwang District, Bangkok 10310, Thailand
Tel. +6620052299
www.mdpi.com
www.mdpi.com/about/data-protection
MDPI's headquarters are located in Basel, Switzerland.
More information is available here: https://www.mdpi.com/about/contact
---
News:
CiteScore increased to *5.7*
Impact Factor of /Metabolites/ *3.5*

Join the metabolomics event !
Submit abstracts to: 4th International Conference on Electronic Metabolomics
Date: October 13-15, 2025
Link: https://sciforum.net/event/IECM2025

Appendix 2 – Metabolomics

Workflow of tandem mass spectrometry processing for preparation using feature based molecular networking via GNPS.

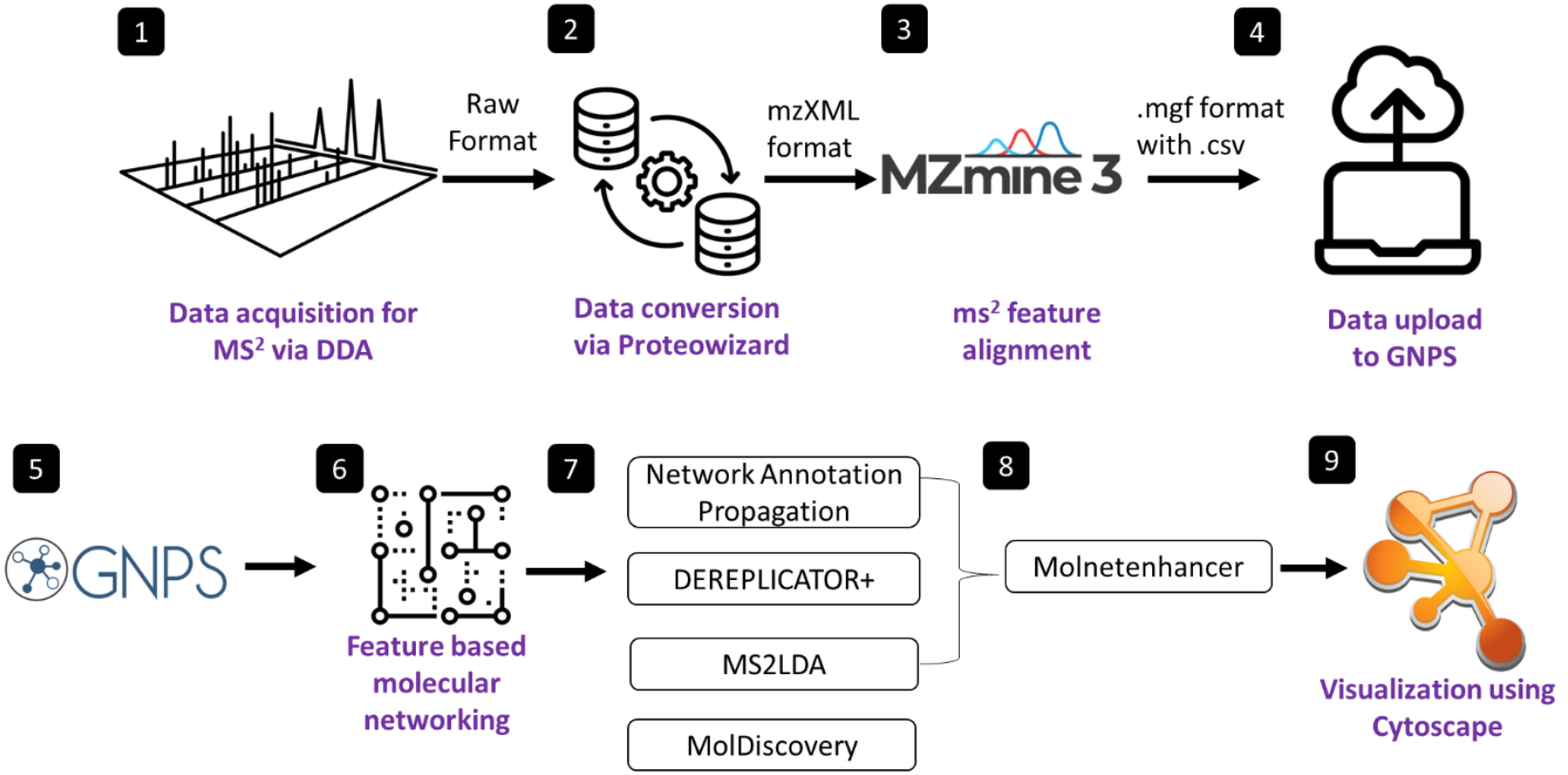

Figure1. 1. Workflow of tandem mass spectrometry processing for preparation using feature based molecular networking via GNPS.

Table. 1: Tentative metabolite identification of compounds that are biofingerprints of interests found in both *D. dentatus* red and white ecotypes. SIRIUS was used as an in silico fragmentation tool for metabolite annotation. Tentative identification of compounds with fragments are at level 3 using SIRIUS, otherwise at level 4 metabolite annotation.

Tentative Identification	Molecular formula	Adduct	Exact mass	Theoretical mass	Experimental mass	Mass error (ppm)	t_R (min)	MS^2	Annotation Level
Resveratrol	$C_{14}H_{12}O_3$	M+H	228.0786	228.0786	228.0773	5.89	4.0	-	4
Quercetin	$C_{15}H_{10}O_7$	M-H	302.0427	301.0354	301.0356	-0.74	4.0	215.0697,149.0241,243.0668	3
Epicatechin 3-O-(3'-O-Methyl gallate)	$C_{23}H_{20}O_{10}$	M+H	456.1056	457.1129	457.1115	3.06	4.6	167.0346,139.0398,123.0440	3
(+)-Catechin	$C_{15}H_{14}O_6$	M+H	290.079	291.0863	291.0851	4.17	4.4	245.0823,203.0717,109.0292	2
Apigenin	$C_{15}H_{10}O_5$	M+H	270.0528	271.0601	271.0591	3.69		215.0698,194.0242,243.0668	3
Proanthocyanidin B2	$C_{30}H_{26}O_{12}$	M+H	578.1424	579.1497	579.1476	3.63	4.5	127.0387, 163.0395,247.0615	3
Leucocyanidin	$C_{15}H_{14}O_7$	M+H	306.074	307.0812	307.0801	3.68	4.1	-	4
Luteolin	$C_{15}H_{10}O_6$	M+H	286.0477	287.0550	287.0541	3.19	4.9	295.0606,167.0695,153.0191	3
Naringenin	$C_{15}H_{12}O_5$	M+H	272.0685	273.0758	273.0746	4.21	5.0		4
Anthocyanidin 3-O-beta-D-sambubioside	$C_{26}H_{29}O_{15}$	M+H	581.1506	582.1579	582.1564	2.61	4.1	-	4
Catechin 3-O-Beta-D-Glucopyranoside	$C_{21}H_{24}O_{11}$	M+H	452.1319	453.1391	453.1371	4.41	4.1	289.0710,245.0823,271.0621	4
Taxifolin	$C_{15}H_{12}O_7$	M+H	304.0583	305.0656	305.0645	3.54	4.3	217.0486, 201.0564,187.0764	3
Quercetin 3-glucoside	$C_{21}H_{20}O_{12}$	M+H	464.0955	465.1028	465.102	1.62	4	-	4
Lyoniside	$C_{27}H_{36}O_{12}$	M+H	552.2207	551.2134	551.2095	7.07	4.3	-	4

Tentative Identification	Molecular formula	Adduct	Exact mass	Theoretical mass	Experimental mass	Mass error (ppm)	t_R (min)	MS^2	Annotation Level
Proanthocyanidin A2	$C_{30}H_{24}O_{12}$	M+H	578.1424	579.1497	579.1476	3.63	4.2	245.0449,287.0565,275.0569	3
Chelidonine	$C_{20}H_{19}NO_5$	M+H	353.1263	354.1336	354.1349	-3.67	5.5	-	4
Trigonelline	$C_7H_7NO_2$	M+H	137.0477	138.0550	138.0544	4.02	0.8	-	4
Kyanmethin	$C_6H_9N_3$	M+H	123.0796	124.0869	124.0865	3.22	7.1	107.0606,810703,79.0545	3
4-Methylpelletierine	$C_{10}H_{13}NO_4$	M+H	211.0845	212.0917	212.0908	4.24	7.1	194.0811,166.0866,109.0287	3
Salsolinol	$C_9H_{11}NO_2$	M+H	165.0790	166.0863	166.0857	3.34	3.9	178.0498,132.0448,105.0338	3
Nicotinamide	$C_6H_6N_2O$	M+H	122.0480	123.0553	123.0548	3.98	0.7	163.0753,145.0652,117.0702	3
Kynurenate	$C_{10}H_7NO_3$	M+H	189.0426	190.0499	190.0491	4.21	4.1	162.0549,144.0438,116.0499	3
Raphanatin	$C_{16}H_{23}N_5O_6$	M+H	381.1648	382.1721	382.1704	4.47	3.8	139.0627,202.1009,145.0509	3
Perillic acid	$C_{10}H_{14}O_2$	M+H	166.0994	167.1067	167.1063	2.13	4.6	214.1010,187.1130,149.0605	3
(+)-Pulegone	$C_{10}H_{16}O$	M+H	152.1201	153.1274	153.1270	2.61	3.7	107.0857,97.0650,95.0860	3
Xerantholide	$C_{15}H_{18}O_3$	M+H	246.1256	247.1329	247.1322	2.83	4.7	214.1010,187.1130,149.0605	3
Kaurane -17,18-dioic acid	$C_{20}H_{30}O_4$	M+H	334.2144	335.2217	335.2204	3.89	4.6	153.0189, 171.0295, 139.0397	3
Betulonic Acid	$C_{30}H_{46}O_3$	M+H	454.3447	455.3520	455.3502	3.89	7	137.1332,95.0861,203.1792	3
Lupenone	$C_{30}H_{48}O$	M-H	424.3705	425.3778	425.3762	3.74	6.9	95.0860,81.0700,137.1332	3
Geniposidic acid	$C_{16}H_{22}O_{10}$	M-H	374.1213	373.1140	373.1115	6.70	3.7	193.0504,343.1048,181.0498	3
Buddlejoside B	$C_{22}H_{26}O_{12}$	M-H	482.1424	481.1351	481.1312	8.21	4.2	169.0138,3130573,151.0042	3
Diospyric Acid B	$C_{30}H_{46}O_6$	M-H	502.3294	501.3222	501.3203	3.72	5.1	439.3207,457.3303,469.3316	3
Glucosol	$C_{30}H_{48}O_4$	M-H	472.3553	471.3480	471.3461	4.00	5.9	427.3587,469.3331,423.3260	3
(-)-Lariciresinol	$C_{20}H_{24}O_6$	M+H	360.1573	361.1646	361.1642	1.01	4.4	-	4
(-)-Pinoresinol	$C_{20}H_{22}O_6$	M+H	358.1416	359.1489	359.1475	3.94	4.7	-	4
Palmatoside G	$C_{25}H_{32}O_{10}$	M+H	492.1995	493.2068	493.2043	5.12	4	-	4
Gallate	$C_7H_6O_5$	M-H	170.0215	169.0142	169.0134	5.01	0.5	125.0245,97.0290,79.0186	3

Tentative Identification	Molecular formula	Adduct	Exact mass	Theoretical mass	Experimental mass	Mass error (ppm)	t_R (min)	MS^2	Annotation Level
2-hydroxy-5-[(3,4,5-trihydroxyoxan-2-yl) oxy] benzoic acid	$C_{12}H_{14}O_8$	M-H	286.0689	285.0616	285.0599	5.96	3.9	152.0106,108.0213,109.0291	3
Lyoniside	$C_{27}H_{36}O_{12}$	M-H-	552.2207	551.2134	551.2095	7.07	4.3	373.1282,404.1492,59.0137	3
Gentisic acid	$C_7H_6O_4$	M-H-	154.0266	153.0193	153.0183	6.74	3	109.0292,110.0010,137.9956	3

Table 1. 1: Tentative metabolite identification of compounds that are biofingerprints of interests unique to *D. dentatus* red ecotype. SIRIUS was used as an in-silico fragmentation tool for metabolite annotation. Tentative identification of compounds with fragments are at level 3 using SIRIUS, otherwise at level 4 metabolite annotation.

Tentative Identification	Molecular formula	Ionization Mode	Exact mass	Theoretical mass	Experimental mass	Mass error (ppm)	t_R (min)	MS^2	Annotation Level
(-)-Epigallocatechin	$C_{15}H_{14}O_7$	M+H	306.0740	307.0812	307.0812	4.33	4.2	-	4
(+)-alpha-Barbatene	$C_{15}H_{24}$	M+H	204.1878	205.1951	205.1943	3.79	5.2	-	4
(+)-Pulegone	$C_{10}H_{16}O$	M+H	152.1201	153.1274	153.1270	2.61	3.7	107.0857,97.0650,95.0860	3
3-alpha(S)-Strictosidine	$C_{27}H_{34}N_2O_9$	M+H	530.2264	531.2337	531.2332	0.95	6	-	4
Afzelin	$C_{21}H_{20}O_{10}$	M+H	432.1056	433.1129	433.1117	2.82	4.5	-	4
alpha-Amyrin	$C_{30}H_{50}O$	M+H	426.3862	427.3934	427.3923	2.67	6.5	-	4
Anthocyanidin 3-O-beta-D-sambubioside	$C_{26}H_{29}O_{15}$	M+H	581.1506	582.1579	582.1564	2.61	4.1	-	4
Cyanidin 3-O-beta-D-sambubioside	$C_{27}H_{31}O_{14}+$	M+H	579.1700	580.1787	580.1841	-9.38	4.6	-	4
Coniferyl Alcohol	$C_{10}H_{12}O_3$	M+H	180.0786	181.0859	181.0853	3.43	5.1	-	4
Gibberellin A_1	$C_{19}H_{24}O_6$	M+H	348.1573	349.1646	349.1671	-7.26	4.0	-	4
Gibberellin A_{19}	$C_{20}H_{26}O_6$	M+H	362.1729	363.1802	363.1788	3.90	5.0	-	4
Katuranin	$C_{15}H_{12}O_6$	M+H	288.0634	287.0561	287.0541	7.00	4.3	215.0697,149.0241,243.0668	3
Leucocyanidin	$C_{15}H_{14}O_7$	M+H	306.074	307.0812	307.0801	3.68	4.1	-	4

Luteolin	$C_{15}H_{10}O_6$	M+H	286.0477	287.0550	287.0541	3.19	4.9	-	4
Naringenin	$C_{15}H_{12}O_5$	M+H	272.0685	273.0758	273.0746	4.21	5.0	-	4
Pheophorbide a	$C_{35}H_{36}N_4O_5$	M+H	592.2686	593.2758	593.2781	-3.80	5.1	-	4
Quercitrin	$C_{21}H_{20}O_{11}$	M+H	448.1006	449.1078	449.1069	2.00	4.5	278.0559,61.0287,71.0494	3

Table 1.2: Tentative metabolite identification of compounds that are biofingerprints of interests unique to *D. dentatus* white ecotype. SIRIUS was used as an in-silico fragmentation tool for metabolite annotation. Tentative identification of compounds with fragments are at level 3 using SIRIUS, otherwise at level 4 metabolite annotation.

Tentative Identification	**Molecular formula**	**Ionization Mode**	**Exact mass**	**Theoretical mass**	**Experimental mass**	**Mass error (ppm)**	**t_R (min)**	**MS^2**	**Annotation Level**
Nicotinic acid	$C_6H_6N_2O$	M+H	122.0480	123.0553	123.0548	3.98	4.7	-	4
Perillyl aldehyde	$C_{10}H_{14}O$	M+H	150.1045	151.1117	151.1113	2.92	4.1	-	4
5-Hydroxyindoleacetaldehyde	$C_{10}H_9NO_2$	M+H	175.0633	176.0706	176.0702	2.30	4.5	-	4
ent-Kaurene	$C_{20}H_{32}$	M+H	272.2504	273.2577	273.2567	3.58	6	-	4
Myricetin	$C_{15}H_{10}O_8$	M+H	318.0376	319.0448	319.0442	2.02	4.1	-	4
Gibberellin A_{51}-catabolite	$C_{19}H_{22}O_5$	M+H	330.1467	331.1540	331.1534	1.81	4.5	-	4
L-Dopa	$C_9H_{11}NO_4$	M+H	197.0688	198.0761	198.0754	3.46	3.8	-	4
Gibberellin A_{20}	$C_{19}H_{24}O_5$	M+H	332.1624	333.1697	333.168	4.95	5.02	-	4
Gibberellin A_4	$C_{20}H_{28}O_6$	M+H	364.1886	364.1886	364.1880	1.62	4.5	-	4
Gibberellin A_{51}	$C_{19}H_{22}O_5$	M+H	330.1467	331.1540	331.1534	1.81	4.5	-	4
Quercetin	$C_{15}H_{10}O_7$	M-H	302.0427	301.0354	301.0356	-0.74	4.01	163.0396,147.0444,137.0237	3

Table 1.3: Tentative metabolite identification of compounds that are biofingerprints of interests found in both *D. dentatus* red and white ecotypes. SIRIUS was used as an in silico fragmentation tool for metabolite annotation. Tentative identification of compounds with fragments are at level 3 using SIRIUS, otherwise at level 4 metabolite annotation.

Tentative Identification	Molecular formula	Ionization Mode	Exact mass	Theoretical mass	Experimental mass	Mass error (ppm)	t_R (min)	MS^2	Annotation Level
5-Hydroxyconiferyl alcohol	$C_{10}H_{12}O_4$	M+H	196.0736	197.081	197.0802	3.04	4.2	-	4
Apigenin	$C_{15}H_{10}O_5$	M+H	270.0528	271.0601	271.0591	3.69	4.5	215.0698,194.0242,243.0668	3
Luteolin	$C_{15}H_{10}O_6$	M+H	286.0477	287.055	287.0541	3.19	4.9	231.0667,213.0561,153.0191	3
Myricetin	$C_{15}H_{10}O_8$	M+H	318.0376	319.0448	319.0442	2.02	4.1	-	4
3,9-Dihydroxypterocarpan	$C_{15}H_{12}O_4$	M+H	256.0736	257.0808	257.0802	2.47	4.74	-	4
(+-)-Dalbergioidin	$C_{15}H_{12}O_6$	M+H	288.0634	289.0707	289.0697	3.34	4.2	-	4
Taxifolin	$C_{15}H_{12}O_7$	M+H	304.0583	305.0656	305.0645	3.54	4.3	217.0486, 01.0564,187.0764	3
Dihydromyricetin	$C_{15}H_{12}O_8$	M+H	320.0532	321.0605	321.0593	3.72	4.1	-	4
(+)-Catechin	$C_{15}H_{14}O_6$	M+H	290.079	291.0863	291.0851	4.17	4.4	139.0398,177.0558,123.0439	2
Leucodelphinidin	$C_{15}H_{14}O_8$	M+H	322.0689	323.0761	323.075	3.54	4.5	-	4
Quercitrin	$C_{21}H_{20}O_{11}$	M+H	448.1006	449.1078	449.1069	2	4.5	278.0559,61.0287,71.0494	3
Quercetin 3-glucoside	$C_{21}H_{20}O_{12}$	M+H	464.0955	465.1028	465.102	1.62	4.4	-	4
Cristacarpin	$C_{21}H_{22}O_5$	M+H	354.1467	355.154	355.1526	3.94	5.04	-	4
Catechin 3-O-Beta-D-Glucopyranoside	$C_{21}H_{24}O_{11}$	M+H	452.1319	453.1391	453.1371	4.41	4.09	139.0399,123.0440,163.0398	3
Fisetin	$C_{22}H_{16}O_8$	M+H	408.0845	409.0918	409.0902	3.91	4.5	257.0437,285.0414,229.0512	3
Epicatechin 3-O-(3'-O-Methylgallate)	$C_{23}H_{20}O_{10}$	M+H	456.1056	457.1129	457.1115	3.06	4.6	167.0346,139.0398,123.0440	3
Anthocyanidin 3-O-beta-D-sambubioside	$C_{26}H_{29}O_{15}$	M+H	581.1506	582.1579	582.1564	2.61	4.1	-	4
Proanthocyanidin A2	$C_{30}H_{24}O_{12}$	M+H	576.1268	577.1341	577.1324	2.94	4.5	245.0449,287.0565,275.0569	3
Gambiriin C	$C_{30}H_{26}O_{11}$	M+H	562.1475	563.1548	563.1536	2.11	4.5	139.0399,147.0445,285.0779	3
Proanthocyanidin B2	$C_{30}H_{26}O_{12}$	M+H	578.1424	579.1497	579.1476	3.63	4.2	127.0387, 63.0395,247.0615	4
Quercetin	$C_{15}H_{10}O_7$	M-H	302.0427	301.0354	301.0356	-0.74	4.06	163.0396,147.0444,137.0237	3
Katuranin	$C_{15}H_{12}O_6$	M-H	288.0634	287.0561	287.0541	7.01	4.3	215.0697,149.0241,243.0668	3
Resveratrol	$C_{14}H_{12}O_3$	M+H	228.0786	228.0786	228.0773	5.89	4.7	-	4
Distylin	$C_{15}H_{12}O_7$	M-H	304.0583	303.051	303.049	6.69	4.27	125.0243,235.0618,258.0396	3
(+)-Catechin	$C_{15}H_{14}O_6$	M-H	290.079	289.0718	289.0695	7.82	4.27	245.0823,203.0717,109.0292	2
Astragalin	$C_{21}H_{20}O_{11}$	M-H	448.1006	447.0933	447.0966	-7.42	4.5	285.0396,284.0330,257.0467	3
Engeletin	$C_{21}H_{22}O_{10}$	M-H	434.1213	433.114	433.1117	5.36	4.61	269.0446,180.0055,152.0107	3
Astilbin	$C_{21}H_{22}O_{11}$	M-H	450.1162	449.1089	449.1089	0.08	5	241.0503,169.0662,199.0403	3
Quercetin 7-(6"-Acetylglucoside)	$C_{23}H_{22}O_{13}$	M-H	506.106	505.0988	505.0989	-0.27	4.13	233.0810,183.0295,215.0709	3
Endotelon	$C_{30}H_{26}O_{12}$	M-H	578.1424	577.1351	577.1324	4.763	4.23	125.0243,245.0823,283.0235	3

Table 1.4. Tentative metabolite identification of terpenoid biofingerprints found in D. dentatus red and white ecotypes. SIRIUS 5.8.3 was used as an in-silico fragmentation tool for metabolite annotation. Tentative identification of compounds with fragments are at level 3 using SIRIUS, otherwise at level 4 metabolite annotation

Tentative Identification	Molecular formula	Ionization Mode	Exact mass	Theoretical mass	Experimental mass	Mass error (ppm)	t_R (min)	MS^2	Annotation Level
Perillic acid	$C_{10}H_{14}O_2$	M+H	166.0994	167.1067	167.1063	2.13	4.6	121.1011,0.93.0699,107.0859	3
(+)-Pulegone	$C_{10}H_{16}O$	M+H	152.1201	153.1274	153.127	2.61	3.7	107.0857,97.0650,95.0860	3
Xerantholide	$C_{15}H_{18}O_3$	M+H	246.1256	247.1329	247.1322	2.83	4.7	214.1010,187.1130,149.0605	3
Alantolactone	$C_{15}H_{20}O_2$	M+H	232.1463	233.1536	233.153	2.6	4.9	-	4
(+)-Thujopsene	$C_{15}H_{24}$	M+H	204.1878	205.1951	205.1943	3.79	4.9	-	4
Deoxyelephantopin	$C_{19}H_{20}O_6$	M+H	344.126	345.1333	345.1319	3.95	4.7	-	4
Deoxymiroestrol	$C_{20}H_{22}O_5$	M+H	342.1467	343.154	343.1526	4.08	5.1	-	4
(-)-Pinoresinol	$C_{20}H_{22}O_6$	M+H	358.1416	359.1489	359.1475	3.94	4.71	-	4
Niveusin C	$C_{20}H_{26}O_7$	M+H	378.1679	379.1751	379.1778	-7.04	4.09	-	4
Gibberellin A12 7-aldehyde	$C_{20}H_{28}O_3$	M+H	316.2038	317.2111	317.2098	4.1	5.7	-	4
Gibberellin A12	$C_{20}H_{28}O_4$	M+H	332.1988	333.206	333.2047	4.01	4.8	-	4
Ent-7-alpha-Hydroxykaur-16-en-19-oic acid	$C_{20}H_{30}O_3$	M+H	318.2195	319.2268	319.2256	3.67	5.9	-	4
(ent-6alpha,7alpha)-6,7-Dihydroxy-16-kauren-19-oic acid	$C_{20}H_{30}O_4$	M+H	334.2144	335.2217	335.2205	3.54	4.5	-	4
Kaurane -17,18-dioic acid	$C_{20}H_{30}O_4$	M+H	334.2144	335.2217	335.2204	3.88	4.6	153.0189, 171.0295, 139.0397	3
ent-Kaurene	$C_{20}H_{32}$	M+H	272.2504	273.2577	273.2567	3.56	6	-	4
Chromolaenide	$C_{22}H_{28}O_7$	M+H	404.1835	405.1908	405.1905	0.69	4.5	-	4
Valtratum	$C_{22}H_{30}O_8$	M+H	422.1941	423.2013	423.1974	9.32	5.4	-	4
Palmatoside G	$C_{25}H_{32}O_{10}$	M+H	492.1995	493.2068	493.2043	5.12	4	-	4
Archangelolide	$C_{29}H_{40}O_{10}$	M+H	548.2621	549.2694	549.2675	3.5	4.6	-	4
Delta7-Avenasterol	$C_{29}H_{48}O$	M+H	412.3705	413.3778	413.3759	4.58	4.9	-	4
Musaroside	$C_{30}H_{44}O_{10}$	M+H	564.2934	565.3007	565.2987	3.58	4.2	-	4
Propapyriogenin A2	$C_{30}H_{44}O_5$	M+H	484.3189	485.3262	485.3247	2.99	5.2	-	4
Betulonic Acid	$C_{30}H_{46}O_3$	M+H	454.3447	455.352	455.3502	3.89	7	137.1332,95.0861,203.1792	3
Lupenone	$C_{30}H_{48}O$	M+H	424.3705	425.3778	425.3762	3.74	6.9	95.0860,81.0700,137.1332	3
L-Valine	$C_5H_{11}NO_2$	M+H	117.079	118.0863	118.0859	3.01	0.6	-	4
Abscisic acid	$C_{15}H_{20}O_4$	M-H	264.1362	263.1289	263.1268	7.91	4.7	-	4
2-trans,6-trans-Farnesal	$C_{15}H_{24}O$	M-H	220.1827	219.1754	219.174	6.56	7.5	-	4
Geniposidic acid	$C_{16}H_{22}O_{10}$	M-H	374.1213	373.114	373.1115	6.7	3.7	193.0504,343.1048,181.0498	3
Secologanin	$C_{17}H_{24}O_{10}$	M-H	388.1369	387.1297	387.1282	3.8	4.14	-	4
Chaparrin	$C_{20}H_{28}O_7$	M-H	380.1835	379.1762	379.1755	1.92	4.9	-	4
Glaucolide B	$C_{21}H_{26}O_{10}$	M-H	438.1526	437.1453	437.1433	4.62	4.2	-	4
Buddlejoside B	$C_{22}H_{26}O_{12}$	M-H	482.1424	481.1351	481.1312	8.21	4.2	169.0138,3130573,151.0042	3
Daphnetoxin	$C_{27}H_{30}O_8$	M-H	482.1941	481.1868	481.1897	-6.05	4.5	-	4
Smilagenin	$C_{27}H_{44}O_3$	M-H	416.329	415.3218	415.3204	3.3	6.9	-	4

Table 1.5: Tentative identification of other compounds outside of alkaloids, terpenoids and flavonoids found in both *D. dentatus* red and white ecotypes. SIRIUS was used as an in silico fragmentation tool for metabolite annotation. Tentative identification of compounds with fragments are at level 3 using SIRIUS, otherwise at level 4 metabolite annotation.

Tentative Identification	Molecular formula	Ionization Mode	Exact mass	Theoretical mass	Experimental mass	Mass error (ppm)	t_R (min)	MS^2	Annotation level
(-)-Lariciresinol	$C_{20}H_{24}O_6$	M+H	360.1573	361.1646	361.1642	1.01	4.4	-	4
Indoleacetic acid	$C_{10}H_9NO_2$	M+H	175.0633	176.0706	176.0701	2.87	5.4	-	4
Adenosine	$C_{10}H_{13}N_5O_4$	M+H	267.0968	268.104	268.1029	4.22	1.7	-	4
1-O-Sinapoyl-beta-D-glucose	$C_{17}H_{22}O_{10}$	M+H	386.1213	387.1286	387.1273	3.29	4.03	-	4
Nordihydroguaiaretic acid	$C_{18}H_{22}O_4$	M+H	302.1518	303.1591	303.1579	3.91	5.7	-	4
Podophyllotoxone	$C_{22}H_{20}O_8$	M+H	412.1158	413.1231	413.1214	4.1	4.43	-	4
Lutein	$C_{40}H_{56}O_2$	M+H	568.428	569.4353	569.4364	-1.92	4.3	-	4
Anthragallol	$C_{14}H_8O_5$	M+H	256.0372	257.0444	257.0435	3.7	4.5	-	4
Biflorin	$C_{16}H_{18}O_9$	M+H	354.0951	355.1024	355.1011	3.54	4.3	-	4
Gartanin	$C_{23}H_{24}O_6$	M+H	396.1573	397.1646	397.163	3.94	5.6	-	4
Marchantin A	$C_{28}H_{24}O_5$	M+H	440.1624	441.1697	441.1717	-4.65	4.3	-	4
Scorzocreticin	$C_{16}H_{14}O_5$	M+H	286.0841	287.0914	287.0905	3.13	4.7	269.0815,257.0826,227.0717	3
Caffeate	$C_9H_8O_4$	M-H	180.0423	179.035	179.0343	3.81	4.3	-	4
1-O-Sinapoyl-beta-D-glucose	$C_{17}H_{22}O_{10}$	M-H	386.1213	385.114	385.1126	3.69	4.4	-	4
5-Hydroxyconiferaldehyde	$C_{10}H_{10}O_5$	M-H	210.0528	209.0455	209.0447	4.05	4.4	-	4
Chlorogenate	$C_{16}H_{18}O_9$	M-H	354.0951	353.0878	353.0858	5.68	4.4	-	4
3-Hydroxypropanoate	$C_3H_6O_3$	M-H	90.0317	89.0244	89.0241	3.56	0.6	-	4
2-Oxobutanoate	$C_4H_6O_3$	M-H	102.0317	101.0244	101.0239	5.12	0.6	-	4
Succinate	$C_4H_6O_4$	M-H	118.0266	117.0193	117.0189	3.69	0.8	-	4
cis-Aconitate	$C_6H_6O_6$	M-H	174.0164	173.0092	173.0083	5	0.6	-	4
Isocitrate	$C_6H_8O_7$	M-H	192.027	191.0197	191.019	3.8	0.6	-	4
Chorismate	$C_{10}H_{10}O_6$	M-H	226.0477	225.0405	225.0397	3.38	4	-	4

Table 1. 6. Pathway impacts of biochemical pathways in *Doliocarpus dentatus* white ecotype as a result of using the mummichog algorithm used in Pathway analysis module in MetaboAnalyst 5.0

Pathways	Total	Expected	Hits	Raw p	-Log10(p)	Holm adjust	False Discovery Rate	Impact
Flavonoid biosynthesis	47	8.2717	23	5.22E-07	6.2822	5.01E-05	5.01E-05	0.35771
Steroid biosynthesis	45	7.9198	18	0.000271	3.5674	0.025183	0.0064988	0.45432
Phenylpropanoid biosynthesis	46	8.0958	14	0.021621	1.6651	1	0.13837	0.49931
Valine, leucine and isoleucine biosynthesis	22	3.8719	13	1.30E-05	4.8856	0.0012362	0.0006246	0.43383
Ubiquinone and other terpenoid-quinone biosynthesis	38	6.6878	13	0.009532	2.0208	0.81971	0.083184	0.44435
Galactose metabolism	27	4.7519	11	0.003727	2.4287	0.32795	0.039752	0.48491
alpha-Linolenic acid metabolism	28	4.9278	11	0.005197	2.2842	0.45218	0.049895	0.65224
Amino sugar and nucleotide sugar metabolism	50	8.7997	11	0.25317	0.59658	1	0.90017	0.03673
Diterpenoid biosynthesis	28	4.9278	10	0.01618	1.791	1	0.11949	0.38809
Tyrosine metabolism	16	2.8159	9	0.000515	3.2878	0.047421	0.0098967	0.47297
Cutin, suberine and wax biosynthesis	18	3.1679	9	0.001575	2.8029	0.1417	0.021593	0.4375
Fructose and mannose metabolism	20	3.5199	8	0.014897	1.8269	1	0.11918	0.12586
Sesquiterpenoid and triterpenoid biosynthesis	24	4.2239	8	0.045824	1.3389	1	0.27494	0.36175
Biosynthesis of unsaturated fatty acids	22	3.8719	7	0.07579	1.1204	1	0.40421	0
Pantothenate and CoA biosynthesis	23	4.0479	7	0.093272	1.0302	1	0.4477	0.2203
Brassinosteroid biosynthesis	26	4.5759	7	0.1577	0.80217	1	0.6308	0.15239

Pathways	Total	Expected	Hits	Raw p	-Log10(p)	Holm adjust	False Discovery Rate	Impact
Flavone and flavonol biosynthesis	10	1.7599	6	0.003146	2.5023	0.27995	0.037745	0.85
Ascorbate and aldarate metabolism	18	3.1679	6	0.080095	1.0964	1	0.40469	0.26865
Citrate cycle (TCA cycle)	20	3.5199	6	0.12342	0.9086	1	0.53858	0.18262
Glyoxylate and dicarboxylate metabolism	29	5.1038	6	0.40343	0.39424	1	1	0.30723
Glycine, serine and threonine metabolism	33	5.8078	6	0.53731	0.26977	1	1	0.10432
Carotenoid biosynthesis	43	7.5678	6	0.79613	0.099017	1	1	0.0365
Purine metabolism	63	11.088	6	0.97766	0.0098126	1	1	0.1955
C5-Branched dibasic acid metabolism	6	1.056	5	0.00084	3.0759	0.076416	0.013436	1
Butanoate metabolism	17	2.9919	5	0.16454	0.78373	1	0.63183	0
Phenylalanine, tyrosine and tryptophan biosynthesis	22	3.8719	5	0.34249	0.46535	1	1	0.21672
Starch and sucrose metabolism	22	3.8719	5	0.34249	0.46535	1	1	0.51292
Aminoacyl-tRNA biosynthesis	46	8.0958	5	0.92905	0.031959	1	1	0.05556
Glucosinolate biosynthesis	65	11.44	5	0.99418	0.002536	1	1	0
Phenylalanine metabolism	11	1.9359	4	0.1114	0.9531	1	0.50927	0.23529
Alanine, aspartate and glutamate metabolism	22	3.8719	4	0.55939	0.25228	1	1	0.07554
Pyruvate metabolism	22	3.8719	4	0.55939	0.25228	1	1	0.24039
Tryptophan metabolism	28	4.9278	4	0.75405	0.1226	1	1	0.2037
Cyanoamino acid metabolism	29	5.1038	4	0.77905	0.10844	1	1	0.23729

Pathways	Total	Expected	Hits	Raw p	-Log10(p)	Holm adjust	False Discovery Rate	Impact
Terpenoid backbone biosynthesis	30	5.2798	4	0.802	0.095826	1	1	0.14525
Valine, leucine and isoleucine degradation	37	6.5118	4	0.9136	0.039246	1	1	0.00991
Cysteine and methionine metabolism	46	8.0958	4	0.97377	0.011545	1	1	0.08428
Linoleic acid metabolism	4	0.70398	3	0.018775	1.7264	1	0.12874	1
Isoquinoline alkaloid biosynthesis	6	1.056	3	0.071241	1.1473	1	0.4023	0
Stilbenoid, diarylheptanoid and gingerol biosynthesis	8	1.408	3	0.15231	0.81729	1	0.6308	0.39705
Arachidonic acid metabolism	12	2.1119	3	0.35578	0.44881	1	1	0
Pentose and glucuronate interconversions	16	2.8159	3	0.55408	0.25643	1	1	0.15625
Arginine biosynthesis	18	3.1679	3	0.63873	0.19468	1	1	0.12816
beta-Alanine metabolism	18	3.1679	3	0.63873	0.19468	1	1	0.31746
Glycerolipid metabolism	21	3.6959	3	0.74343	0.12876	1	1	0.00426
Zeatin biosynthesis	21	3.6959	3	0.74343	0.12876	1	1	0.01491
Thiamine metabolism	22	3.8719	3	0.77249	0.11211	1	1	0.20231
Glycolysis / Gluconeogenesis	26	4.5759	3	0.86292	0.06403	1	1	0.1215
Inositol phosphate metabolism	28	4.9278	3	0.89502	0.048167	1	1	0.10251
Limonene and pinene degradation	5	0.87997	2	0.21423	0.66911	1	0.79102	0
Monobactam biosynthesis	8	1.408	2	0.42454	0.37208	1	1	0
One carbon pool by folate	8	1.408	2	0.42454	0.37208	1	1	0

Pathways	Total	Expected	Hits	Raw p	-Log10(p)	Holm adjust	False Discovery Rate	Impact
Monoterpenoid biosynthesis	9	1.584	2	0.48866	0.31099	1	1	0
Caffeine metabolism	10	1.7599	2	0.54813	0.26112	1	1	0
Selenocompound metabolism	13	2.2879	2	0.69631	0.1572	1	1	0.2437
Sphingolipid metabolism	17	2.9919	2	0.82924	0.081322	1	1	0.24038
Pentose phosphate pathway	19	3.3439	2	0.87381	0.058585	1	1	0
Carbon fixation in photosynthetic organisms	21	3.6959	2	0.90746	0.042172	1	1	0.03607
Glycerophospholipid metabolism	37	6.5118	2	0.99357	0.0028005	1	1	0.06318
Betalain biosynthesis	3	0.52798	1	0.44075	0.3558	1	1	1
Tropane, piperidine and pyridine alkaloid biosynthesis	8	1.408	1	0.78832	0.1033	1	1	0
Lysine biosynthesis	9	1.584	1	0.82578	0.083138	1	1	0.2027
Vitamin B6 metabolism	11	1.9359	1	0.88203	0.054517	1	1	0.03205
Riboflavin metabolism	11	1.9359	1	0.88203	0.054517	1	1	0.06667
Nicotinate and nicotinamide metabolism	13	2.2879	1	0.92017	0.036133	1	1	0
Lysine degradation	18	3.1679	1	0.97	0.013227	1	1	0
Propanoate metabolism	20	3.5199	1	0.97974	0.0088884	1	1	0.08554
Fatty acid elongation	23	4.0479	1	0.98877	0.0049048	1	1	0
Glutathione metabolism	26	4.5759	1	0.99378	0.0027085	1	1	0
Phosphatidylinositol signaling system	26	4.5759	1	0.99378	0.0027085	1	1	0.03285
Folate biosynthesis	27	4.7519	1	0.9949	0.0022221	1	1	0.02624
Arginine and proline metabolism	34	5.9838	1	0.99872	0.0005546	1	1	0.0122

Table 1. 7: Biochemical pathway impacts observed in *Doliocarpus dentatus* red ecotype as a result of using the mummichog algorithm used in Pathway analysis module in MetaboAnalyst 5.0

Pathways	Total	Expected	Hits	Raw p	-Log10(p)	Holm adjust	False Discovery Rate	Impact
Sesquiterpenoid and triterpenoid biosynthesis	24	5.648	19	1.00E-08	7.9991	9.62E-07	9.62E-07	0.57797
Galactose metabolism	27	6.354	20	2.91E-08	7.5357	2.77E-06	1.40E-06	0.82797
Flavonoid biosynthesis	47	11.061	25	7.37E-06	5.1325	0.0006928	0.000236	0.4785
Ascorbate and aldarate metabolism	18	4.236	12	0.0001117	3.952	0.010386	0.00268	0.64179
Biosynthesis of secondary metabolites - other antibiotics	6	1.412	6	0.0001643	3.7843	0.015119	0.003155	1
Steroid biosynthesis	45	10.59	21	0.0004642	3.3333	0.042243	0.006488	0.62018
Fructose and mannose metabolism	20	4.7067	12	0.0004731	3.3251	0.042576	0.006488	0.65819
Flavone and flavonol biosynthesis	10	2.3533	7	0.002327	2.6332	0.2071	0.027924	0.65
Ubiquinone and other terpenoid-quinone biosynthesis	38	8.9427	17	0.0028877	2.5395	0.25411	0.030692	0.55568
Cutin, suberine and wax biosynthesis	18	4.236	10	0.0031971	2.4952	0.27815	0.030692	0.75
Valine, leucine, and isoleucine biosynthesis	22	5.1773	11	0.0058125	2.2356	0.49987	0.0465	0.53039
Starch and sucrose metabolism	22	5.1773	11	0.0058125	2.2356	0.49987	0.0465	0.74456
alpha-Linolenic acid metabolism	28	6.5893	12	0.017648	1.7533	1	0.13032	0.60278
Riboflavin metabolism	11	2.5887	6	0.02533	1.5964	1	0.17369	0.75557
Citrate cycle (TCA cycle)	20	4.7067	9	0.027489	1.5608	1	0.17593	0.39412
C5-Branched dibasic acid metabolism	6	1.412	4	0.030102	1.5214	1	0.18061	0.5
Linoleic acid metabolism	4	0.94134	3	0.04271	1.3695	1	0.23746	1
Diterpenoid biosynthesis	28	6.5893	11	0.044525	1.3514	1	0.23746	0.38321
Amino sugar and nucleotide sugar metabolism	50	11.767	17	0.058165	1.2353	1	0.28261	0.43695

Pathways	Total	Expected	Hits	Raw p	-Log10(p)	Holm adjust	False Discovery Rate	Impact
Glyoxylate and dicarboxylate metabolism	29	6.8247	10	0.12049	0.91905	1	0.50883	0.40321
Alanine, aspartate, and glutamate metabolism	22	5.1773	8	0.12191	0.91397	1	0.50883	0.46044
Arachidonic acid metabolism	12	2.824	5	0.12798	0.89284	1	0.51194	0
Pentose phosphate pathway	19	4.4713	7	0.13585	0.86694	1	0.52167	0.36819
Pantothenate and CoA biosynthesis	23	5.4127	8	0.15051	0.82244	1	0.55572	0.24838
Caffeine metabolism	10	2.3533	4	0.19027	0.72064	1	0.6765	0
Biosynthesis of unsaturated fatty acids	22	5.1773	7	0.24409	0.61245	1	0.83547	0
Glycolysis / Gluconeogenesis	26	6.1187	8	0.25238	0.59794	1	0.83547	0.24829
Phenylpropanoid biosynthesis	46	10.825	13	0.27097	0.56708	1	0.8671	0.44832
Pentose and glucuronate interconversions	16	3.7653	5	0.31708	0.49883	1	0.98193	0.25
Thiamine metabolism	22	5.1773	6	0.41848	0.37833	1	1	0.47399
Phenylalanine metabolism	11	2.5887	3	0.49894	0.30195	1	1	0.23529
Inositol phosphate metabolism	28	6.5893	7	0.50041	0.30068	1	1	0.14853
Phosphonate and phosphinate metabolism	7	1.6473	2	0.51818	0.28552	1	1	0
Valine, leucine, and isoleucine degradation	37	8.7073	9	0.51908	0.28476	1	1	0.05889
Propanoate metabolism	20	4.7067	5	0.52492	0.27991	1	1	0.22404
Cyanoamino acid metabolism	29	6.8247	7	0.54196	0.26604	1	1	0.20339
Zeatin biosynthesis	21	4.942	5	0.57305	0.24181	1	1	0.02847
Carbon fixation in photosynthetic organisms	21	4.942	5	0.57305	0.24181	1	1	0.16543
Sphingolipid metabolism	17	4.0007	4	0.5942	0.22607	1	1	0.40865
Monobactam biosynthesis	8	1.8827	2	0.5959	0.22483	1	1	0

Pathways	Total	Expected	Hits	Raw p	-Log10(p)	Holm adjust	False Discovery Rate	Impact
One carbon pool by folate	8	1.8827	2	0.5959	0.22483	1	1	0
Brassinosteroid biosynthesis	26	6.1187	6	0.59863	0.22284	1	1	0.11429
Pyruvate metabolism	22	5.1773	5	0.61851	0.20865	1	1	0.40463
beta-Alanine metabolism	18	4.236	4	0.64322	0.19164	1	1	0.38889
Synthesis and degradation of ketone bodies	4	0.94134	1	0.65854	0.18142	1	1	0
Indole alkaloid biosynthesis	4	0.94134	1	0.65854	0.18142	1	1	0.5
Monoterpenoid biosynthesis	9	2.118	2	0.66382	0.17795	1	1	0
Lysine biosynthesis	9	2.118	2	0.66382	0.17795	1	1	0.29729
Glycine, serine, and threonine metabolism	33	7.766	7	0.69076	0.16067	1	1	0.10432
Limonene and pinene degradation	5	1.1767	1	0.73911	0.13129	1	1	0
Glycerolipid metabolism	21	4.942	4	0.7657	0.11594	1	1	0.00426
Anthocyanin biosynthesis	11	2.5887	2	0.77187	0.11246	1	1	0
Vitamin B6 metabolism	11	2.5887	2	0.77187	0.11246	1	1	0.03205
Phenylalanine, tyrosine, and tryptophan biosynthesis	22	5.1773	4	0.79841	0.097775	1	1	0.28178
Isoquinoline alkaloid biosynthesis	6	1.412	1	0.80071	0.096522	1	1	0
Arginine biosynthesis	18	4.236	3	0.83362	0.079031	1	1	0.2136
Nicotinate and nicotinamide metabolism	13	3.0593	2	0.84836	0.071418	1	1	0.30707
Tropane, piperidine and pyridine alkaloid biosynthesis	8	1.8827	1	0.88379	0.053651	1	1	0
Stilbenoid, diarylheptanoid and gingerol biosynthesis	8	1.8827	1	0.88379	0.053651	1	1	0.13235
Phosphatidylinositol signaling system	26	6.1187	4	0.89415	0.048589	1	1	0.03545

Pathways	Total	Expected	Hits	Raw p	-Log10(p)	Holm adjust	False Discovery Rate	Impact
Sulfur metabolism	15	3.53	2	0.90082	0.045364	1	1	0.10774
Carotenoid biosynthesis	43	10.119	7	0.91147	0.040259	1	1	0.07053
Tryptophan metabolism	28	6.5893	4	0.92499	0.033863	1	1	0.1713
Terpenoid backbone biosynthesis	30	7.06	4	0.94751	0.023414	1	1	0.17239
Nitrogen metabolism	12	2.824	1	0.96058	0.017465	1	1	0
Selenocompound metabolism	13	3.0593	1	0.96994	0.013257	1	1	0
Fatty acid biosynthesis	56	13.179	8	0.97158	0.01252	1	1	0.01123
Aminoacyl-tRNA biosynthesis	46	10.825	6	0.97634	0.010401	1	1	0.05556
Cysteine and methionine metabolism	46	10.825	6	0.97634	0.010401	1	1	0.17084
Purine metabolism	63	14.826	9	0.97762	0.009828	1	1	0.11117
Histidine metabolism	15	3.53	1	0.98252	0.0076586	1	1	0.13953
Glutathione metabolism	26	6.1187	2	0.99199	0.0034919	1	1	0.05046
Lysine degradation	18	4.236	1	0.99226	0.0033732	1	1	0
Arginine and proline metabolism	34	8.0013	3	0.99341	0.0028701	1	1	0.09001
Glucosinolate biosynthesis	65	15.297	8	0.99344	0.002859	1	1	0.00154
Folate biosynthesis	27	6.354	2	0.9937	0.0027463	1	1	0
Pyrimidine metabolism	38	8.9427	3	0.9973	0.0011744	1	1	0.13096
Fatty acid elongation	23	5.4127	1	0.99802	0.000861	1	1	0
N-Glycan biosynthesis	35	8.2367	2	0.99911	0.0003871	1	1	0.07466
Porphyrin and chlorophyll metabolism	48	11.296	3	0.99973	0.0001153	1	1	0.09842
Fatty acid degradation	37	8.7073	1	0.99996	1.84E-05	1	1	0
Glycerophospholipid metabolism	37	8.7073	1	0.99996	1.84E-05	1	1	0.02629

Appendix 3 – Phytohormone

Table 1: Level 2 metabolite annotation using the feature based molecular networking (FBMN) module of GNPS

Compound	Molecular formula	Adduct	Precursor m/z	Fragments (MS/MS)	Cosine Score
Salicylic acid	$C_7H_6O_3$	$[M+H]^+$	139.04	65.04; 93.03; 111.04	0.95
Homovanillyl alcohol	$C_9H_{12}O_3$	$[M+H-H_2O]^+$	151.07	91.05; 95.05; 119.05	0.65
Genistic Acid	$C_7H_6O_4$	$[M+H]^+$	155.03	65.04; 93.03; 113.96; 131.97	0.87
Gallic Acid	$C_7H_6O_5$	$[M-H]^-$	169.01	81.03; 97.03; 125.02	0.99
Coniferyl aldehyde	$C_{10}H_{10}O_3$	$[M+H]^+$	179.06	55.02; 91.05; 105.07; 119.05; 147.04; 161.06; 179.03	0.73
Quinic acid	$C_7H_{12}O_6$	$[M-H]^-$	191.06	85.03; 87.01; 93.03; 111.01; 127.04	0.71
alpha-Santonin	$C_{15}H_{18}O_3$	$[M+H]^+$	247.13	70.07; 112.08;135.12	0.65
4-Methylphenyl-beta-D-glucopyranoside	$C_{13}H_{18}O_7$	$[M-H]^-$	285.1	71.01; 101.02; 113.03; 123.05	0.90
Epicatechin	$C_{15}H_{14}O_6$	$[M-H]^-$	289.09	109.03; 125.03; 137.03; 179.03; 203.07; 245.08	0.96
Epicatechin	$C_{15}H_{14}O_6$	$[M+H]^+$	291.09	119.05; 123.04; 139.04; 147.04; 165.05; 207.06	0.98
Dianthoside	$C_{12}H_{16}O_8$	$[M+H]^+$	289.1	85.03; 97.03; 109.03; 127.0	0.91
Picraquassioside D	$C_{13}H_{18}O_8$	$[M+H]^+$	303.12	85.03; 109.03; 127.04; 141.07	0.86
trans-Zeatin-O-glucoside	$C_{16}H_{23}N_5O_6$	$[M+H]^+$	382.17	136.06; 202.11; 220.12	0.74
Dapagliflozin	$C_{19}H_{28}O_{10}$	$[M-H]^-$	415.15	59.01; 89.02; 101.02; 119.03	0.79
Stevioside	$C_{17}H_{24}O_{12}$	$[M+H]^+$	421.14	127.0; 289.11	0.92
Epicatechin 3 - gallate	$C_{21}H_{24}O_{11}$	$[M+H]^+$	453.14	85.03; 97.03; 123.04; 139.04; 165.05; 291.09	0.93
Kanokoside A	$C_{21}H_{32}O_{12}$	$[M-H]^-$	475.17	71.01; 89.03; 101.02; 113.03	0.75

Table: 1.2: Level 2 metabolite annotation of compounds in *Doliocarpus dentatus* using the classical molecular networking (CMN) module of GNPS

Compound	Molecular Formula	Adduct	Precursor Mass	Fragments (MS/MS)	Fraction Found	Cosine Score
Pyrogallol	$C_6H_6O_3$	[M+H]+	127.04	81.03; 109.0	Chloroform and Methanol	0.79
Salicylic acid	$C_7H_6O_3$	[M+H]+	139.04	65.04; 93.03; 111.0	Chloroform and Methanol	0.84
Homovanillyl alcohol	$C_9H_{12}O_3$	$[M+H-H_2O]^+$	151.07	91.05; 95.05; 119.05	Chloroform and Methanol	0.81
3,4 Dihydroxymandelate	$C_8H_8O_5$	$[M+H-H_2O]^+$	167.03	111.04; 121.04; 139.04	Chloroform and Methanol	0.60
Vanillic acid	$C_8H_8O_4$	[M+H]+	169.05	65.04; 93.03; 111.04; 125.06	Chloroform and Methanol	0.62
Gallic acid	$C_7H_6O_5$	[M+H]+	171.03	81.03; 109.03; 125.02; 127.0	Chloroform and Methanol	0.85
Esculetin	$C_9H_6O_4$	[M-H]-	177.02	105.04; 133.0	Methanol	0.73
Coniferyl aldehyde	$C_{10}H_{10}O_3$	[M+H]+	179.07	55.02; 119.05; 123.04; 133.08; 147.0	Chloroform and Methanol	0.72
5-Hydroxyisovanillic acid	$C_8H_8O_5$	[M+H]+	185.04	81.04; 109.03; 126.0; 141.06; 153.06	Chloroform	0.65
Genipin	$C_{11}H_{14}O_5$	[M+H]+	209.08	93.07; 121.07; 149.06; 177.06	Chloroform and Methanol	0.67
alpha-Santonin	$C_{15}H_{18}O_3$	[M+H]+	247.13	70.06; 112.0; 135.12	Chloroform	0.72
(+/-)-Catechin/Epicatechin	$C_{15}H_{14}O_6$	[M+H]+	289.07	123.0; 135.04; 187.04	Chloroform and Methanol	0.98
Gallocatechin	$C_{15}H_{14}O_7$	[M-H]-	305.07	109.03; 125.0; 139.0; 165.02; 219.07	Methanol	0.64
Epigallocatechin	$C_{15}H_{14}O_7$	[M+H]+	307.08	139.0; 151.04; 289.07	Chloroform	0.81
Hydroxytyrosol glucuronide	$C_{14}H_{18}O_9$	[M-H]-	329.09	59.01; 71.01; 89.03; 123.0; 153.04	Chloroform and Methanol	0.70
Camptothecin	$C_{20}H_{16}N_2O_4$	[M+Na]+	371.1	73.05; 91.05; 267.00; 285.01	Chloroform and Methanol	0.92
Osmanthuside H	$C_{19}H_{28}O_{11}$	[M-H]-	431.15	59.01; 71.01; 89.03; 101.03	Chloroform	0.69
Flavanomarein	$C_{21}H_{22}O_{11}$	[M-H]-	451.13	179.03; 271.06; 289.0	Chloroform	0.67
Eriodictyol-7-O-glucoside	$C_{21}H_{22}O_{11}$	[M-H]-	451.13	179.03; 205.05; 289.0	Methanol	0.61
Procyanidin B1	$C_{30}H_{26}O_{12}$	[M-H]-	577.13	125.0; 127.03; 161.03; 245.08; 289.07; 407.08	Chloroform and Methanol	0.86
Procyanidin B2	$C_{30}H_{26}O_{12}$	[M+H]+	579.15	123.04; 127.0; 163.04; 247.06; 287.06; 409.09	Chloroform and Methanol	0.94

Table 1. 3 : Level 3 metabolite annotation of compounds in *Doliocarpus dentatus* using SIRIUS v. 5.6.3

Compound	Molecular Formula	Adduct	Precursor Mass	Fragments (MS/MS)	Zodiac Score [%]	SIRIUS Score [%]
2-Furoate	$C_5H_4O_3$	$[M+H]^+$	113.0231	57.0337; 67.0178; 69.0337; 95.0128	100.00	91.47
6-Carboxypyrone-2	C6H4O4	$[M+H]^+$	141.0183	85.0285; 95.0130; 113.0231	100.00	67.52
2,5-Dihydroxyanisol	$C_7H_8O_3$	$[M+H]^+$	141.0552	95.0495; 123.0442; 126.0332; 127.0391	100.00	87.31
3-imidazol-1-ylpropane-1,2-diol	C6H10N2O2	$[M+H]^+$	143.0813	81.0448; 95.0603; 125.0708	100.00	89.74
p-Cresotic acid	C8H8O3	$[M+H-H_2O]^+$	153.0546	67.0544; 79.0543; 91.0542; 107.0488;	100.00	78.57
Gallate/Gallic acid	$C_7H_6O_5$	$[M-H]^-$	169.0151	81.0350; 97.0298; 107.0144; 125.0240	100.00	100.00
L-Quinate/Quinic acid	$C_7H_{12}O_6$	$[M-H]^-$	191.0562	85.0294; 87.0088; 111.0091; 127.0596	100.00	99.35
Ferulate/Ferulic Acid	$C_{10}H_{10}O_4$	$[M+H-H_2O]^+$	195.0652	91.0547; 93.0701; 103.0545; 117.0541	99.85	89.01
Pyrogallol A	C12H12O6	$[M+H]^+$	253.0693	69.0339; 97.0289; 109.0289; 127.0389	100.00	49.77
Catechin/Catergen	$C_{15}H_{14}O_6$	$[M+H]^+$	291.0868	123.0436; 139.0394; 147.0441; 165.0538	100.00	100.00
Epigallocatechin	C16H16O7	$[M+H-H_2O]^+$	321.0969	123.0440; 139.0398; 151.0388; 181.0502	100.00	80.69
Chromone proynyl benzoate	C20H14O5	$[M+H]^+$	335.0927	159.0222; 177.0329	82.92	69.64
7-hydroxycoumarin glucuronide	$C_{15}H_{14}O_9$	$[M+H-H_2O]^+$	339.0711	162.9882; 321.0594	40.25	69.63
Isoferulic acid 3-O-|A-D-glucuronide	$C_{16}H_{18}O_{10}$	$[M+H-H_2O]^+$	371.0973	83.0858; 97.1011	14.87	81.47
Galloyl-oxypropynyl benzoate	C17H14O11	$[M+H-H_2O]^+$	395.0609	57.0703; 377.0489	19.15	69.64
Kaempferol glucoside	C20H18O9	$[M+H-H_2O]^+$	403.1024	205.0283; 254.0389; 265.0500	100.00	77.14
Ellagic acide deivative	C20H14O10	$[M+H-H_2O]^+$	415.066	169.0070; 187.0182; 205.0293; 245.0594	100.00	52.46
Syringyl glucoside	C19H30O10	$[M+H]^+$	419.1922	105.0706; 133.0650; 137.0603; 165.0905	95.93	71.84
Catechin 3-O-beta-D-glycopyranoside	$C_{21}H_{24}O_{11}$	$[M+H]^+$	453.1404	123.0437; 139.0396; 147.0442; 165.0540	99.80	97.66
6-deoxy-Ido(a1-6)Glc(b)-O-galloyl	$C_{19}H_{26}O_{14}$	$[M-H]^-$	477.1274	125.0241;143.0353; 151.0037; 169.0150	93.52	76.67
Kanokoside B	$C_{21}H_{34}O_{12}$	$[M-H]^-$	477.1972	59.0138; 71.0143; 75.0088; 125.0240; 325.1131	99.75	53.62
Rosmarinic acid derivative	C26H24O14	$[M+H]^+$	561.1219	177.0329; 191.0124; 219.0450; 311.0547	99.90	50.37
Cyanidin-3(6""-p-coumarylsambibioside)	$C_{35}H_{34}O_{17}$	$[M-H]^-$	725.1732	125.0292; 183.0292; 289.0726	1.11	49.67

Table 1.4: Bioactive compounds identified *D.dentatus red and white ecotypes* including their adducts, formulas, and relative strengths of various health-promoting properties. The strength of each property is indicated as strong, moderate, or weak based on available scientific evidence.

Compound Class	Compound Name	Adduct	Formula	Bioactive Compounds					
				Antioxidant	Anti-inflammatory	Anticancer	Antimicrobial	Antidiabetic	Cardioprotective
Phenolic Acids	Gallic acid	M+H	$C_7H_6O_5$	Strong	Moderate	Moderate	Moderate	Weak	Weak
Phenolic Acids	Caffeic acid	M+H	$C_9H_8O_4$	Strong	Strong	Moderate	Moderate	Weak	Weak
Phenolic Acids	Ferulic acid	M+H	$C_{10}H_{10}O_4$	Strong	Moderate	Weak	Weak	Weak	Weak
Phenolic Acids	Sinapic acid	M+H	$C_{11}H_{12}O_5$	Strong	Moderate	Weak	Weak	Weak	Weak
Flavonoids	Quercetin	M+H	$C_{15}H_{10}O_7$	Strong	Strong	Strong	Moderate	Moderate	Strong
Flavonoids	Rutin	M+H	$C_{27}H_{30}O_{16}$	Strong	Strong	Moderate	Weak	Moderate	Moderate
Flavonoids	Kaempferol	M+H	$C_{15}H_{10}O_6$	Strong	Strong	Moderate	Weak	Weak	Moderate
Alkaloids	Stachydrine	M+H	$C_7H_{13}NO_2$	Weak	Weak		Weak		
Terpenes	Limonene	M+H	$C_{10}H_{16}$	Moderate	Moderate	Weak	Moderate		

Table 1.4: Peason's correlatiion analysis of Endogenous isotope-labelled cytokinin phytohormones and Secondary metabolites (Alkaloids) scanned for using the Q-Exactive Orbitrap mass spectrometer and their classifications and abbreviations. Secondary metabolites annotation at level 1, 3 and 4.

Secondary metabolites (Compound 1)	Phytohormones (Compound 2)	correlation	P value
5-(2-Hydroxyethyl)-4-methylthiazole	cZ	-0.12756	0.692804
5-(2-Hydroxyethyl)-4-methylthiazole	cZ9G	-0.07889	0.817659
5-(2-Hydroxyethyl)-4-methylthiazole	cZOG	-0.0074	0.981794
5-(2-Hydroxyethyl)-4-methylthiazole	cZR	-0.05588	0.863056
5-(2-Hydroxyethyl)-4-methylthiazole	cZROG	-0.01967	0.951621
5-(2-Hydroxyethyl)-4-methylthiazole	DZ	-0.50078	0.097247
5-(2-Hydroxyethyl)-4-methylthiazole	DZ9G	0.713468	0.009176
5-(2-Hydroxyethyl)-4-methylthiazole	DZOG	-0.16344	0.611775
5-(2-Hydroxyethyl)-4-methylthiazole	DZR	-0.23833	0.455692
5-(2-Hydroxyethyl)-4-methylthiazole	DZROG	-0.16558	0.607046
5-(2-Hydroxyethyl)-4-methylthiazole	iP	0.094048	0.771261
5-(2-Hydroxyethyl)-4-methylthiazole	iP7G	-0.76349	0.006249
5-(2-Hydroxyethyl)-4-methylthiazole	iP9G	-0.58713	0.297943
5-(2-Hydroxyethyl)-4-methylthiazole	iPR	-0.14322	0.657001
5-(2-Hydroxyethyl)-4-methylthiazole	tZ	-0.66805	0.017579
5-(2-Hydroxyethyl)-4-methylthiazole	tZ7G	-0.09338	0.772852
5-(2-Hydroxyethyl)-4-methylthiazole	tZ9G	-0.09785	0.762257
5-(2-Hydroxyethyl)-4-methylthiazole	tZOG	-0.09772	0.762563
5-(2-Hydroxyethyl)-4-methylthiazole	tZR	-0.05585	0.863134
5-(2-Hydroxyethyl)-4-methylthiazole	tZROG	-0.23239	0.467327
Coniferin	cZ	0.700315	0.011205
Coniferin	cZ9G	0.683729	0.020348
Coniferin	cZOG	0.722597	0.007938
Coniferin	cZR	-0.45	0.14214
Coniferin	cZROG	-0.45643	0.135826
Coniferin	DZ	0.4042	0.192513
Coniferin	DZ9G	0.436189	0.156316
Coniferin	DZOG	0.645687	0.023333
Coniferin	DZR	-0.00552	0.986425
Coniferin	DZROG	0.623965	0.030129
Coniferin	iP	-0.33878	0.281388
Coniferin	iP7G	-0.02129	0.95046
Coniferin	iP9G	0.615059	0.269528
Coniferin	iPR	0.334363	0.288112
Coniferin	tZ	-0.087	0.788035
Coniferin	tZ7G	0.704315	0.010556
Coniferin	tZ9G	0.704395	0.010543
Coniferin	tZOG	0.703875	0.010626
Coniferin	tZR	-0.45002	0.142113
Coniferin	tZROG	-0.52647	0.078672
Dopamine	cZ	0.459766	0.132628
Dopamine	cZ9G	0.438124	0.177715
Dopamine	cZOG	0.592033	0.042552
Dopamine	cZR	-0.20149	0.530028
Dopamine	cZROG	-0.14629	0.650075
Dopamine	DZ	0.054773	0.865745
Dopamine	DZ9G	0.675963	0.015816
Dopamine	DZOG	0.312673	0.322412
Dopamine	DZR	-0.11108	0.731091
Dopamine	DZROG	0.323067	0.305707
Dopamine	iP	-0.08197	0.80008
Dopamine	iP7G	-0.61712	0.043106
Dopamine	iP9G	0.351537	0.561807
Dopamine	iPR	0.203323	0.526209
Dopamine	tZ	-0.69556	0.012014
Dopamine	tZ7G	0.474702	0.118903
Dopamine	tZ9G	0.473361	0.120096
Dopamine	tZOG	0.466616	0.126212
Dopamine	tZR	-0.20152	0.529972
Dopamine	tZROG	-0.51246	0.088469
Hypoxanthine	cZ	0.872501	0.000213

Hypoxanthine	cZOG	0.867273	0.000259

Secondary metabolites (Compound 1)	Phytohormones (Compound 2)	correlation	P value
Hypoxanthine	DZOG	0.8668806	0.0002622
Hypoxanthine	DZR	0.2329142	0.4663001
Hypoxanthine	DZROG	0.8183487	0.0011382
Hypoxanthine	iP	-0.2256672	0.4806692
Hypoxanthine	iP7G	0.0753554	0.8257141
Hypoxanthine	iP9G	0.8256286	0.085084
Hypoxanthine	iPR	0.5444941	0.0671892
Hypoxanthine	tZ	-0.0231076	0.9431741
Hypoxanthine	tZ7G	0.8768362	0.0001809
Hypoxanthine	tZ9G	0.8740461	0.0002013
Hypoxanthine	tZOG	0.8750801	0.0001935
Hypoxanthine	tZR	-0.3836968	0.2182138
Hypoxanthine	tZROG	-0.548719	0.0646753
Pipecolinic_acid	cZ	-0.0969726	0.7643234
Pipecolinic_acid	cZ9G	-0.235368	0.4859884
Pipecolinic_acid	cZOG	-0.0082409	0.9797215
Pipecolinic_acid	cZR	-0.2593711	0.4156008
Pipecolinic_acid	cZROG	-0.2711172	0.3940109
Pipecolinic_acid	DZ	-0.2378617	0.4566069
Pipecolinic_acid	DZ9G	0.8067496	0.0015191
Pipecolinic_acid	DZOG	-0.3271398	0.2992953
Pipecolinic_acid	DZR	-0.4042937	0.1923995
Pipecolinic_acid	DZROG	-0.2990586	0.3450292
Pipecolinic_acid	iP	-0.3932739	0.205964
Pipecolinic_acid	iP7G	-0.4973987	0.119533
Pipecolinic_acid	iP9G	-0.5379806	0.3496711
Pipecolinic_acid	iPR	-0.0526872	0.8708188
Pipecolinic_acid	tZ	-0.5524075	0.0625345
Pipecolinic_acid	tZ7G	-0.1373382	0.6703762
Pipecolinic_acid	tZ9G	-0.1435971	0.6561537
Pipecolinic_acid	tZOG	-0.1484681	0.6451569
Pipecolinic_acid	tZR	-0.2594174	0.4155146
Pipecolinic_acid	tZROG	-0.4243021	0.1692149
Trigonelline	cZ	-0.235958	0.4603254
Trigonelline	cZ9G	-0.1747729	0.6072643
Trigonelline	cZOG	-0.1405055	0.6631661
Trigonelline	cZR	0.2591487	0.4160151
Trigonelline	cZROG	0.3616826	0.2480003
Trigonelline	DZ	-0.3247067	0.3031162
Trigonelline	DZ9G	0.3794372	0.2238001
Trigonelline	DZOG	-0.3423787	0.2759837
Trigonelline	DZR	-0.1348327	0.6760979
Trigonelline	DZROG	-0.2506658	0.4319713
Trigonelline	iP	0.219495	0.4930649
Trigonelline	iP7G	-0.5556174	0.0759647
Trigonelline	iP9G	-0.3058003	0.6167995
Trigonelline	iPR	-0.1703558	0.5965694
Trigonelline	tZ	-0.4878919	0.1075895
Trigonelline	tZ7G	-0.2105867	0.5112049
Trigonelline	tZ9G	-0.2071855	0.5182071
Trigonelline	tZOG	-0.2119291	0.5084528
Trigonelline	tZR	0.2591732	0.4159695
Trigonelline	tZROG	0.1472162	0.647977
Tropine	cZ	-0.1443146	0.6545299
Tropine	cZ9G	0.1071048	0.7539462
Tropine	cZOG	-0.0798356	0.8051897
Tropine	cZR	0.0775522	0.8106711
Tropine	cZROG	0.2253174	0.481368
Tropine	DZ	-0.2491567	0.4348406
Tropine	DZ9G	-0.1524897	0.6361264
Tropine	DZOG	-0.045715	0.8878111
Tropine	DZR	-0.0641571	0.8429766
Tropine	DZROG	0.066852	0.8364578
Tropine	iP	0.0085998	0.9788386
Tropine	iP7G	-0.5424838	0.0846768
Tropine	iP9G	-0.0031697	0.9959642
Tropine	iPR	-0.227339	0.4773366
Tropine	tZ	-0.2264373	0.4791327
Tropine	tZ7G	-0.0608917	0.8508877
Tropine	tZ9G	-0.0564823	0.8615901

Table 1.5: Peason's correlatiion analysis of Endogenous isotope-labelled cytokinin phytohormones and Secondary metabolites (Flavoniods) scanned for using the Q-Exactive Orbitrap mass spectrometer and their classifications and abbreviations. Secondary metabolites annotation at level 1,3 and 4.

Secondary metabolites (Compound 1)	Phytohormones (Compound 2)	correlation	P value
(-)-Epigallocatechin	cZ	-0.195178057	0.543254384
(-)-Epigallocatechin	cZ9G	-0.193478763	0.568668861
(-)-Epigallocatechin	cZOG	-0.134146476	0.677667663
(-)-Epigallocatechin	cZR	0.4352881	0.157270425
(-)-Epigallocatechin	cZROG	0.489620643	0.106161779
(-)-Epigallocatechin	DZ	-0.567062088	0.054513737
(-)-Epigallocatechin	DZ9G	0.294437464	0.352894515
(-)-Epigallocatechin	DZOG	-0.363959392	0.244814473
(-)-Epigallocatechin	DZR	0.004155534	0.989773726
(-)-Epigallocatechin	DZROG	-0.294016335	0.353615986
(-)-Epigallocatechin	iP	0.381815077	0.220671127
(-)-Epigallocatechin	iP7G	-0.615426919	0.043846186
(-)-Epigallocatechin	iP9G	-0.307586034	0.614635349
(-)-Epigallocatechin	iPR	-0.035422987	0.912971924
(-)-Epigallocatechin	tZ	-0.517216442	0.085057127
(-)-Epigallocatechin	tZ7G	-0.205337602	0.522028717
(-)-Epigallocatechin	tZ9G	-0.202140684	0.52866893
(-)-Epigallocatechin	tZOG	-0.203966717	0.524871715
(-)-Epigallocatechin	tZR	0.435266982	0.157292855
(-)-Epigallocatechin	tZROG	0.210839557	0.510686034
4-Coumaroylshikimate	cZ	0.064809196	0.84139845
4-Coumaroylshikimate	cZ9G	0.068167137	0.842150021
4-Coumaroylshikimate	cZOG	-0.038600174	0.905195848
4-Coumaroylshikimate	cZR	0.118507882	0.713752053
4-Coumaroylshikimate	cZROG	0.107618329	0.739205385
4-Coumaroylshikimate	DZ	0.676014147	0.015805382
4-Coumaroylshikimate	DZ9G	-0.55868578	0.059004316
4-Coumaroylshikimate	DZOG	0.100712043	0.755475349
4-Coumaroylshikimate	DZR	0.261808308	0.41107361
4-Coumaroylshikimate	DZROG	0.169157099	0.599193661
4-Coumaroylshikimate	iP	-0.005579369	0.986270092
4-Coumaroylshikimate	iP7G	0.886897409	0.000273014
4-Coumaroylshikimate	iP9G	0.952900931	0.012183164
4-Coumaroylshikimate	iPR	0.103504015	0.748886591
4-Coumaroylshikimate	tZ	0.883262512	0.000139919
4-Coumaroylshikimate	tZ7G	0.056199931	0.862276262
4-Coumaroylshikimate	tZ9G	0.064165896	0.842955402
4-Coumaroylshikimate	tZOG	0.058749979	0.856083279
4-Coumaroylshikimate	tZR	0.118502032	0.713765659
4-Coumaroylshikimate	tZROG	0.443345809	0.1488601
Apiforol	cZ	0.314275749	0.319803324
Apiforol	cZ9G	0.301361148	0.367808605
Apiforol	cZOG	0.406176647	0.190138471
Apiforol	cZR	-0.28210042	0.37435258
Apiforol	cZROG	-0.152377385	0.636378015
Apiforol	DZ	0.416259172	0.178311637
Apiforol	DZ9G	0.228990015	0.474055816
Apiforol	DZOG	0.15012647	0.641427601
Apiforol	DZR	-0.226732162	0.478545072
Apiforol	DZROG	0.252909094	0.427722999
Apiforol	iP	-0.471697271	0.121585869
Apiforol	iP7G	-0.243215495	0.471124973
Apiforol	iP9G	0.51295853	0.376775831
Apiforol	iPR	0.073209353	0.821117639
Apiforol	tZ	-0.348931969	0.266289357
Apiforol	tZ7G	0.317885706	0.313972212
Apiforol	tZ9G	0.323617927	0.304834852
Apiforol	tZOG	0.30803274	0.330026725
Apiforol	tZR	-0.282109717	0.374336161
Apiforol	tZROG	-0.273177221	0.390284383
Chalconaringenin	cZ	0.795957251	0.001955048

Chalconaringenin	cZ9G	0.782287512	0.004433264
Chalconaringenin	cZOG	0.831254502	0.000805736
Chalconaringenin	cZR	-0.224721636	0.482558925
Chalconaringenin	DZ	0.383708765	0.218198209
Chalconaringenin	DZ9G	0.321212871	0.308650351
Chalconaringenin	DZOG	0.579038796	0.048516176
Chalconaringenin	DZR	0.131961868	0.682673124
Chalconaringenin	DZROG	0.625559785	0.029586874
Chalconaringenin	iP	-0.220810528	0.490410906
Chalconaringenin	iP7G	-0.140548579	0.680203863
Chalconaringenin	iP9G	0.907757554	0.033161025
Chalconaringenin	iPR	0.531477816	0.075356279
Chalconaringenin	tZ	-0.188042133	0.55837485
Chalconaringenin	tZ7G	0.768313316	0.003509624
Chalconaringenin	tZ9G	0.769554547	0.003424363
Chalconaringenin	tZOG	0.763225705	0.003876055
Chalconaringenin	tZR	-0.224803955	0.482394281
Chalconaringenin	tZROG	-0.474422425	0.119151315
Cyanidin	cZ	-0.695169581	0.012083092
Cyanidin	cZ9G	-0.678954235	0.021599886
Cyanidin	cZOG	-0.651028438	0.021849543
Cyanidin	cZR	0.135854335	0.673762853
Cyanidin	cZROG	0.243099158	0.446450666
Cyanidin	DZ	0.135583565	0.674381446
Cyanidin	DZ9G	-0.402704779	0.19432041
Cyanidin	DZOG	-0.727534806	0.00732332
Cyanidin	DZR	-0.311145755	0.324906938
Cyanidin	DZROG	-0.597120711	0.040364556
Cyanidin	iP	0.003351747	0.991751684
Cyanidin	iP7G	0.07602697	0.824181763
Cyanidin	iP9G	-0.581335783	0.303931861
Cyanidin	iPR	-0.405259544	0.191237683
Cyanidin	tZ	0.076308446	0.813660063
Cyanidin	tZ7G	-0.689682363	0.013074672
Cyanidin	tZ9G	-0.687165881	0.013549006
Cyanidin	tZOG	-0.690892509	0.012850997
Cyanidin	tZR	0.135887173	0.673687846
Cyanidin	tZROG	0.262654076	0.409508341
Cyanidin_3-O-(6-O-p-coumaroyl)glucoside1	cZ	-0.367905294	0.239350534
Cyanidin_3-O-(6-O-p-coumaroyl)glucoside1	cZ9G	-0.3398513	0.306515095
Cyanidin_3-O-(6-O-p-coumaroyl)glucoside1	cZOG	-0.352954153	0.260438203
Cyanidin_3-O-(6-O-p-coumaroyl)glucoside1	cZR	0.525965701	0.079010967
Cyanidin_3-O-(6-O-p-coumaroyl)glucoside1	cZROG	0.548812129	0.064620643
Cyanidin_3-O-(6-O-p-coumaroyl)glucoside1	DZ	-0.733988698	0.006574298
Cyanidin_3-O-(6-O-p-coumaroyl)glucoside1	DZ9G	0.117156719	0.71689632
Cyanidin_3-O-(6-O-p-coumaroyl)glucoside1	DZOG	-0.433104784	0.159600204
Cyanidin_3-O-(6-O-p-coumaroyl)glucoside1	DZR	0.061712185	0.848898706
Cyanidin_3-O-(6-O-p-coumaroyl)glucoside1	DZROG	-0.412341638	0.182850848
Cyanidin_3-O-(6-O-p-coumaroyl)glucoside1	iP	0.542167477	0.068601953
Cyanidin_3-O-(6-O-p-coumaroyl)glucoside1	iP7G	-0.450688489	0.164170912
Cyanidin_3-O-(6-O-p-coumaroyl)glucoside1	iP9G	-0.555931655	0.330537444
Cyanidin_3-O-(6-O-p-coumaroyl)glucoside1	iPR	-0.169001861	0.599533845
Cyanidin_3-O-(6-O-p-coumaroyl)glucoside1	tZ	-0.253835326	0.425974937
Cyanidin_3-O-(6-O-p-coumaroyl)glucoside1	tZ7G	-0.371786289	0.234047583
Cyanidin_3-O-(6-O-p-coumaroyl)glucoside1	tZ9G	-0.369294869	0.237443726
Cyanidin_3-O-(6-O-p-coumaroyl)glucoside1	tZOG	-0.365856354	0.24217863
Cyanidin_3-O-(6-O-p-coumaroyl)glucoside1	tZR	0.525964952	0.079011471
Cyanidin_3-O-(6-O-p-coumaroyl)glucoside1	tZROG	0.397908288	0.200190362
Cyanidin_3-O-beta-D-glucoside	cZ	0.502832507	0.095665694
Cyanidin_3-O-beta-D-glucoside	cZ9G	0.433674016	0.182669803
Cyanidin_3-O-beta-D-glucoside	cZOG	0.589531001	0.043657312
Cyanidin_3-O-beta-D-glucoside	cZR	-0.257078744	0.419881406
Cyanidin_3-O-beta-D-glucoside	cZROG	-0.205636383	0.521409979
Cyanidin_3-O-beta-D-glucoside	DZ	0.320785105	0.309331744
Cyanidin_3-O-beta-D-glucoside	DZ9G	0.401940279	0.195248815
Cyanidin_3-O-beta-D-glucoside	DZOG	0.256265183	0.42140581
Cyanidin_3-O-beta-D-glucoside	DZR	-0.094526256	0.770125984
Cyanidin_3-O-beta-D-glucoside	DZROG	0.339364703	0.280509266
Cyanidin_3-O-beta-D-glucoside	iP	-0.368479648	0.238561296
Cyanidin_3-O-beta-D-glucoside	iP7G	-0.432072617	0.184473356
Cyanidin_3-O-beta-D-glucoside	iP9G	0.664395081	0.221260743

Cyanidin_3-O-beta-D-glucoside	iPR	0.363578548	0.245345687
Cyanidin_3-O-beta-D-glucoside	tZ7G	0.473467406	0.120000813
Cyanidin_3-O-beta-D-glucoside	tZ9G	0.476600267	0.117228922
Cyanidin_3-O-beta-D-glucoside	tZOG	0.463126954	0.129454157
Cyanidin_3-O-beta-D-glucoside	tZR	-0.257144162	0.419758947
Cyanidin_3-O-beta-D-glucoside	tZROG	-0.411412415	0.183937975
Cyanidin_3-O-beta-D-sambubioside	cZ	-0.550286838	0.063759217
Cyanidin_3-O-beta-D-sambubioside	cZ9G	-0.509221743	0.109630667
Cyanidin_3-O-beta-D-sambubioside	cZOG	-0.498677439	0.098888069
Cyanidin_3-O-beta-D-sambubioside	cZR	0.159940123	0.619516937
Cyanidin_3-O-beta-D-sambubioside	cZROG	0.280728488	0.376779779
Cyanidin_3-O-beta-D-sambubioside	DZ	0.188078473	0.558297415
Cyanidin_3-O-beta-D-sambubioside	DZ9G	-0.282592878	0.373483318
Cyanidin_3-O-beta-D-sambubioside	DZOG	-0.639551495	0.025126703
Cyanidin_3-O-beta-D-sambubioside	DZR	-0.218656484	0.494759875
Cyanidin_3-O-beta-D-sambubioside	DZROG	-0.436668726	0.155808411
Cyanidin_3-O-beta-D-sambubioside	iP	-0.036155445	0.911178609
Cyanidin_3-O-beta-D-sambubioside	iP7G	0.023423429	0.945500245
Cyanidin_3-O-beta-D-sambubioside	iP9G	-0.327881351	0.590134139
Cyanidin_3-O-beta-D-sambubioside	iPR	-0.268776007	0.398267777
Cyanidin_3-O-beta-D-sambubioside	tZ	0.155920983	0.628457263
Cyanidin_3-O-beta-D-sambubioside	tZ7G	-0.53788585	0.071255082
Cyanidin_3-O-beta-D-sambubioside	tZ9G	-0.531501214	0.075341016
Cyanidin_3-O-beta-D-sambubioside	tZOG	-0.543165829	0.067993251
Cyanidin_3-O-beta-D-sambubioside	tZR	0.159976585	0.619436045
Cyanidin_3-O-beta-D-sambubioside	tZROG	0.391357021	0.208381457
Cyanidin_3-O-glucoside	cZ	-0.428761779	0.249523246
Cyanidin_3-O-glucoside	cZ9G	-0.409503685	0.273726765
Cyanidin_3-O-glucoside	cZOG	-0.247902829	0.520130358
Cyanidin_3-O-glucoside	cZR	-0.331422456	0.383618262
Cyanidin_3-O-glucoside	cZROG	-0.191699653	0.621235264
Cyanidin_3-O-glucoside	DZ	-0.221420364	0.56695093
Cyanidin_3-O-glucoside	DZ9G	0.653090908	0.056491046
Cyanidin_3-O-glucoside	DZOG	-0.515692584	0.155304682
Cyanidin_3-O-glucoside	DZR	-0.645800623	0.060266922
Cyanidin_3-O-glucoside	DZROG	-0.47009432	0.20162689
Cyanidin_3-O-glucoside	iP	-0.279769073	0.4659368
Cyanidin_3-O-glucoside	iP7G	-0.828987575	0.005736266
Cyanidin_3-O-glucoside	iP9G	-0.901882578	0.098117422
Cyanidin_3-O-glucoside	iPR	-0.414482696	0.267355737
Cyanidin_3-O-glucoside	tZ	-0.849630283	0.003735417
Cyanidin_3-O-glucoside	tZ7G	-0.399619218	0.286606984
Cyanidin_3-O-glucoside	tZ9G	-0.400980173	0.284815297
Cyanidin_3-O-glucoside	tZOG	-0.408873739	0.274538434
Cyanidin_3-O-glucoside	tZR	-0.331422456	0.383618262
Cyanidin_3-O-glucoside	tZROG	-0.592896843	0.09244365
Delphinidin	cZ	-0.594360699	0.04154082
Delphinidin	cZ9G	-0.529358825	0.09402038
Delphinidin	cZOG	-0.591246106	0.042897171
Delphinidin	cZR	0.095268743	0.768363707
Delphinidin	cZROG	0.179240371	0.577257615
Delphinidin	DZ	0.142247501	0.659211827
Delphinidin	DZ9G	-0.681981439	0.014566158
Delphinidin	DZOG	-0.553363123	0.061987919
Delphinidin	DZR	-0.165192002	0.607905536
Delphinidin	DZROG	-0.39028425	0.209741877
Delphinidin	iP	-0.131708469	0.683254486
Delphinidin	iP7G	0.185085004	0.585868225
Delphinidin	iP9G	-0.121942799	0.845123262
Delphinidin	iPR	-0.29500378	0.351925549
Delphinidin	tZ	0.24517148	0.442462217
Delphinidin	tZ7G	-0.571151608	0.052410597
Delphinidin	tZ9G	-0.570125709	0.052932756
Delphinidin	tZOG	-0.573569505	0.051194243
Delphinidin	tZR	0.095333904	0.768209096
Delphinidin	tZROG	0.302001597	0.340069627
Delphinidin_3-O-beta-D-sambubioside	cZ	-0.345382133	0.27151592
Delphinidin_3-O-beta-D-sambubioside	cZ9G	-0.330787408	0.320415456
Delphinidin_3-O-beta-D-sambubioside	cZOG	-0.380160904	0.222845016
Delphinidin_3-O-beta-D-sambubioside	cZR	-0.28077597	0.376695638
Delphinidin_3-O-beta-D-sambubioside	cZROG	-0.280162529	0.377783435

Delphinidin_3-O-beta-D-sambubioside	DZ	0.368569404	0.238438099
Delphinidin_3-O-beta-D-sambubioside	DZ9G	-0.371443696	0.234512859
Delphinidin_3-O-beta-D-sambubioside	DZOG	-0.197985044	0.537354053
Delphinidin_3-O-beta-D-sambubioside	DZR	-0.249886511	0.433451803
Delphinidin_3-O-beta-D-sambubioside	DZROG	-0.235854737	0.46052742
Delphinidin_3-O-beta-D-sambubioside	iP	-0.32392436	0.304350611
Delphinidin_3-O-beta-D-sambubioside	iP7G	0.57447334	0.064537109
Delphinidin_3-O-beta-D-sambubioside	iP9G	-0.352910097	0.560170611
Delphinidin_3-O-beta-D-sambubioside	iPR	-0.351561802	0.262455156
Delphinidin_3-O-beta-D-sambubioside	tZ	0.459320235	0.133052926
Delphinidin_3-O-beta-D-sambubioside	tZ7G	-0.337404459	0.283475166
Delphinidin_3-O-beta-D-sambubioside	tZ9G	-0.340796622	0.278353973
Delphinidin_3-O-beta-D-sambubioside	tZOG	-0.339065134	0.28096137
Delphinidin_3-O-beta-D-sambubioside	tZR	-0.280735381	0.376767565
Delphinidin_3-O-beta-D-sambubioside	tZROG	-0.024645909	0.939397053
Delphinidin_3-O-glucoside	cZ	0.712683014	0.009288587
Delphinidin_3-O-glucoside	cZ9G	0.684903713	0.020048606
Delphinidin_3-O-glucoside	cZOG	0.737960549	0.006142898
Delphinidin_3-O-glucoside	cZR	-0.53212844	0.074932677
Delphinidin_3-O-glucoside	cZROG	-0.585516192	0.045473875
Delphinidin_3-O-glucoside	DZ	0.457192552	0.135092403
Delphinidin_3-O-glucoside	DZ9G	0.273369085	0.389938233
Delphinidin_3-O-glucoside	DZOG	0.613102897	0.034014196
Delphinidin_3-O-glucoside	DZR	0.002079112	0.994883465
Delphinidin_3-O-glucoside	DZROG	0.608884993	0.035615261
Delphinidin_3-O-glucoside	iP	-0.431932261	0.160860375
Delphinidin_3-O-glucoside	iP7G	-0.185677214	0.584648278
Delphinidin_3-O-glucoside	iP9G	0.65660056	0.228712119
Delphinidin_3-O-glucoside	iPR	0.550618702	0.063566467
Delphinidin_3-O-glucoside	tZ	-0.275383544	0.386313339
Delphinidin_3-O-glucoside	tZ7G	0.68773859	0.013439955
Delphinidin_3-O-glucoside	tZ9G	0.683804012	0.014202377
Delphinidin_3-O-glucoside	tZOG	0.685456383	0.013878403
Delphinidin_3-O-glucoside	tZR	-0.53219065	0.07489226
Delphinidin_3-O-glucoside	tZROG	-0.735967161	0.006356657
Genistein	cZ	-0.105920229	0.74319698
Genistein	cZ9G	0.004112645	0.990425091
Genistein	cZOG	-0.14181755	0.660187079
Genistein	cZR	0.458534961	0.133803301
Genistein	cZROG	0.414020795	0.18089651
Genistein	DZ	-0.627118504	0.029063725
Genistein	DZ9G	-0.017939966	0.955869804
Genistein	DZOG	-0.007098312	0.98253267
Genistein	DZR	0.350874573	0.263454002
Genistein	DZROG	-0.008681675	0.978637088
Genistein	iP	0.490911045	0.105104338
Genistein	iP7G	-0.445176494	0.170031265
Genistein	iP9G	-0.343881018	0.57094648
Genistein	iPR	0.148035344	0.646131258
Genistein	tZ	-0.279673718	0.378651391
Genistein	tZ7G	-0.080543297	0.803492461
Genistein	tZ9G	-0.080171251	0.804384622
Genistein	tZOG	-0.071643542	0.82489078
Genistein	tZR	0.458573221	0.133766678
Genistein	tZROG	0.367161848	0.24037442
Homoeriodictyol_chalcone	cZ	0.774194784	0.003119484
Homoeriodictyol_chalcone	cZ9G	0.759568262	0.006687711
Homoeriodictyol_chalcone	cZOG	0.863018801	0.000300426
Homoeriodictyol_chalcone	cZR	-0.35529616	0.257065972
Homoeriodictyol_chalcone	cZROG	-0.370740211	0.235469988
Homoeriodictyol_chalcone	DZ	0.362642203	0.24665462
Homoeriodictyol_chalcone	DZ9G	0.545850757	0.06637473
Homoeriodictyol_chalcone	DZOG	0.646945997	0.022977248
Homoeriodictyol_chalcone	DZR	0.054142232	0.867278752
Homoeriodictyol_chalcone	DZROG	0.632134489	0.027425451
Homoeriodictyol_chalcone	iP	-0.180704189	0.574099786
Homoeriodictyol_chalcone	iP7G	-0.369603242	0.263255288
Homoeriodictyol_chalcone	iP9G	0.774082358	0.124441427
Homoeriodictyol_chalcone	iPR	0.485742186	0.109382567
Homoeriodictyol_chalcone	tZ	-0.470919698	0.122286463
Homoeriodictyol_chalcone	tZ7G	0.774663435	0.003089883

Homoeriodictyol_chalcone	tZ9G	0.771421295	0.00329911
Homoeriodictyol_chalcone	tZOG	0.766629385	0.003627859
Homoeriodictyol_chalcone	tZR	-0.355352182	0.25698562
Homoeriodictyol_chalcone	tZROG	-0.677214916	0.015550008
Kaempferin	cZ	0.144215572	0.654753914
Kaempferin	cZ9G	0.172094056	0.61286888
Kaempferin	cZOG	0.277454578	0.382604747
Kaempferin	cZR	0.047557571	0.88331601
Kaempferin	cZROG	0.179739404	0.5761803
Kaempferin	DZ	0.03394247	0.916597882
Kaempferin	DZ9G	0.235802697	0.460629287
Kaempferin	DZOG	-0.018628034	0.954178775
Kaempferin	DZR	-0.108549235	0.737019673
Kaempferin	DZROG	0.097168265	0.763859827
Kaempferin	iP	-0.026319948	0.935288041
Kaempferin	iP7G	-0.635722086	0.035530319
Kaempferin	iP9G	0.381759277	0.526008248
Kaempferin	iPR	0.081744905	0.800612498
Kaempferin	tZ	-0.667697718	0.017659609
Kaempferin	tZ7G	0.164011372	0.61050868
Kaempferin	tZ9G	0.168183299	0.601328827
Kaempferin	tZOG	0.155224814	0.630010557
Kaempferin	tZR	0.0475563	0.883319111
Kaempferin	tZROG	-0.141284001	0.661397995
Kaempferol_3-O-glucoside	cZ	0.588067477	0.044313447
Kaempferol_3-O-glucoside	cZ9G	0.560248934	0.073041422
Kaempferol_3-O-glucoside	cZOG	0.655049561	0.020778721
Kaempferol_3-O-glucoside	cZR	-0.320709419	0.309452393
Kaempferol_3-O-glucoside	cZROG	-0.280144079	0.377816177
Kaempferol_3-O-glucoside	DZ	0.310566841	0.325855738
Kaempferol_3-O-glucoside	DZ9G	0.391407157	0.208318009
Kaempferol_3-O-glucoside	DZOG	0.419341498	0.174790137
Kaempferol_3-O-glucoside	DZR	-0.035198959	0.913520499
Kaempferol_3-O-glucoside	DZROG	0.50040062	0.097543002
Kaempferol_3-O-glucoside	iP	-0.424764807	0.16870064
Kaempferol_3-O-glucoside	iP7G	-0.392626909	0.232307905
Kaempferol_3-O-glucoside	iP9G	0.670090909	0.215859071
Kaempferol_3-O-glucoside	iPR	0.407357713	0.188728648

Table 1.6: Peason's correlatiion analysis of Endogenous isotope-labelled cytokinin phytohormones and Secondary metabolites (Other phenolics) scanned for using the Q-Exactive Orbitrap mass spectrometer and their classifications and abbreviations. Secondary metabolites annotation at level 1 and 4.

Secondary metabolites (Compound 1)	Phytohormones (Compound 2)	correlation	P value
1-O-Sinapoyl-beta-D-glucose	cZ	0.175931654	0.584421
1-O-Sinapoyl-beta-D-glucose	cZ9G	0.223202523	0.509433
1-O-Sinapoyl-beta-D-glucose	cZOG	0.279541388	0.378887
1-O-Sinapoyl-beta-D-glucose	cZR	-0.020028739	0.950737
1-O-Sinapoyl-beta-D-glucose	cZROG	0.036414727	0.910544
1-O-Sinapoyl-beta-D-glucose	DZ	-0.01728045	0.957491
1-O-Sinapoyl-beta-D-glucose	DZ9G	0.35199981	0.26182
1-O-Sinapoyl-beta-D-glucose	DZOG	0.061484884	0.84945
1-O-Sinapoyl-beta-D-glucose	DZR	-0.011594658	0.971471
1-O-Sinapoyl-beta-D-glucose	DZROG	0.187991738	0.558482
1-O-Sinapoyl-beta-D-glucose	iP	-0.147205418	0.648001
1-O-Sinapoyl-beta-D-glucose	iP7G	-0.64226132	0.033104
1-O-Sinapoyl-beta-D-glucose	iP9G	0.284578928	0.642615
1-O-Sinapoyl-beta-D-glucose	iPR	0.249031772	0.435079
1-O-Sinapoyl-beta-D-glucose	tZ	-0.696528478	0.011846
1-O-Sinapoyl-beta-D-glucose	tZ7G	0.20197569	0.529013
1-O-Sinapoyl-beta-D-glucose	tZ9G	0.20135421	0.530308
1-O-Sinapoyl-beta-D-glucose	tZOG	0.192497725	0.548914
1-O-Sinapoyl-beta-D-glucose	tZR	-0.020012376	0.950777
1-O-Sinapoyl-beta-D-glucose	tZROG	-0.204063807	0.52467
3-O-Methylgallate	cZ	0.368902009	0.237982
3-O-Methylgallate	cZ9G	0.337968397	0.309375
3-O-Methylgallate	cZOG	0.427119667	0.166099
3-O-Methylgallate	cZR	0.109664477	0.734404
3-O-Methylgallate	cZROG	0.096868451	0.76457
3-O-Methylgallate	DZ	-0.144258799	0.654656
3-O-Methylgallate	DZ9G	0.268709628	0.398389
3-O-Methylgallate	DZOG	0.31621634	0.316661
3-O-Methylgallate	DZR	0.14310481	0.657269
3-O-Methylgallate	DZROG	0.21648636	0.499159
3-O-Methylgallate	iP	0.456987091	0.13529
3-O-Methylgallate	iP7G	-0.164644576	0.628552
3-O-Methylgallate	iP9G	0.227157923	0.713281
3-O-Methylgallate	iPR	0.074737988	0.817437
3-O-Methylgallate	tZ	-0.089765371	0.781449
3-O-Methylgallate	tZ7G	0.374081714	0.230944
3-O-Methylgallate	tZ9G	0.372147239	0.233558
3-O-Methylgallate	tZOG	0.371406456	0.234563
3-O-Methylgallate	tZR	0.109615776	0.734518
3-O-Methylgallate	tZROG	-0.194868311	0.543907
5-O-Caffeoylshikimic_acid	cZ	0.138428674	0.667891
5-O-Caffeoylshikimic_acid	cZ9G	0.06328784	0.853339
5-O-Caffeoylshikimic_acid	cZOG	0.305353686	0.334468
5-O-Caffeoylshikimic_acid	cZR	-0.173807641	0.589037
5-O-Caffeoylshikimic_acid	cZROG	-0.110121718	0.733332
5-O-Caffeoylshikimic_acid	DZ	-0.378001804	0.225702
5-O-Caffeoylshikimic_acid	DZ9G	0.561153927	0.057655
5-O-Caffeoylshikimic_acid	DZOG	-0.02293121	0.943607
5-O-Caffeoylshikimic_acid	DZR	-0.329439903	0.295708
5-O-Caffeoylshikimic_acid	DZROG	-0.086398356	0.789481
5-O-Caffeoylshikimic_acid	iP	0.004609636	0.988656
5-O-Caffeoylshikimic_acid	iP7G	-0.926840321	4.08E-05
5-O-Caffeoylshikimic_acid	iP9G	-0.311596226	0.60978
5-O-Caffeoylshikimic_acid	iPR	-0.071418063	0.825434
5-O-Caffeoylshikimic_acid	tZ	-0.944335603	3.83E-06
5-O-Caffeoylshikimic_acid	tZ7G	0.130446268	0.686153
5-O-Caffeoylshikimic_acid	tZ9G	0.124647214	0.699517
5-O-Caffeoylshikimic_acid	tZOG	0.120118841	0.710009
5-O-Caffeoylshikimic_acid	tZR	-0.17385244	0.588939
5-O-Caffeoylshikimic_acid	tZROG	-0.613603162	0.033828

Caffeic_acid	cZ	-0.36569312	0.242405
Caffeic_acid	cZ9G	-0.364415652	0.270534
Caffeic_acid	cZOG	-0.356739106	0.255001
Caffeic_acid	cZR	-0.2195162	0.493022
Caffeic_acid	cZROG	-0.16842269	0.600804
Caffeic_acid	DZ	0.125346988	0.6979
Caffeic_acid	DZ9G	0.068765523	0.831835
Caffeic_acid	DZOG	-0.406283729	0.19001
Caffeic_acid	DZR	-0.341082745	0.277924
Caffeic_acid	DZROG	-0.305304848	0.334549
Caffeic_acid	iP	-0.588675076	0.04404
Caffeic_acid	iP7G	-0.058636982	0.864027
Caffeic_acid	iP9G	-0.368945942	0.54113
Caffeic_acid	iPR	-0.164764682	0.608847
Caffeic_acid	tZ	-0.175492452	0.585374
Caffeic_acid	tZ7G	-0.376764059	0.227349
Caffeic_acid	tZ9G	-0.375282128	0.229331
Caffeic_acid	tZOG	-0.38148715	0.221101
Caffeic_acid	tZR	-0.219482066	0.493091
Caffeic_acid	tZROG	0.030297626	0.925531
Cinnamaldehyde	cZ	-0.076840582	0.812381
Cinnamaldehyde	cZ9G	-0.330489571	0.320878
Cinnamaldehyde	cZOG	-0.101194982	0.754335
Cinnamaldehyde	cZR	-0.419633103	0.174459
Cinnamaldehyde	cZROG	-0.487084979	0.10826
Cinnamaldehyde	DZ	0.063394584	0.844823
Cinnamaldehyde	DZ9G	0.487166318	0.108192
Cinnamaldehyde	DZOG	-0.230847473	0.470377
Cinnamaldehyde	DZR	-0.361953835	0.24762
Cinnamaldehyde	DZROG	-0.257315013	0.419439
Cinnamaldehyde	iP	-0.675178025	0.015985
Cinnamaldehyde	iP7G	-0.066149224	0.846774
Cinnamaldehyde	iP9G	-0.488028749	0.404255
Cinnamaldehyde	iPR	0.077318509	0.811233
Cinnamaldehyde	tZ	-0.260237074	0.413989
Cinnamaldehyde	tZ7G	-0.161684209	0.615652
Cinnamaldehyde	tZ9G	-0.163858864	0.610845
Cinnamaldehyde	tZOG	-0.163988988	0.610558
Cinnamaldehyde	tZR	-0.419701621	0.174382
Cinnamaldehyde	tZROG	-0.328169802	0.297686
Coniferin	cZ	-0.243372795	0.445923
Coniferin	cZ9G	-0.243220685	0.471115
Coniferin	cZOG	-0.117878819	0.715215
Coniferin	cZR	-0.05790396	0.858137
Coniferin	cZROG	0.025936013	0.93623
Coniferin	DZ	-0.066253083	0.837906
Coniferin	DZ9G	0.345227283	0.271745
Coniferin	DZOG	-0.392259884	0.207241
Coniferin	DZR	-0.294089975	0.35349
Coniferin	DZROG	-0.268844326	0.398143
Coniferin	iP	-0.223358175	0.48529
Coniferin	iP7G	-0.604798537	0.048697
Coniferin	iP9G	-0.26620894	0.665099
Coniferin	iPR	-0.060087685	0.852838
Coniferin	tZ	-0.632110385	0.027433
Coniferin	tZ7G	-0.239404358	0.453604
Coniferin	tZ9G	-0.239423425	0.453567
Coniferin	tZOG	-0.252502333	0.428492
Coniferin	tZR	-0.057893833	0.858162
Coniferin	tZROG	-0.103925355	0.747894
Coniferyl_alcohol	cZ	-0.088706272	0.783974
Coniferyl_alcohol	cZ9G	-0.022495911	0.947656
Coniferyl_alcohol	cZOG	0.016275607	0.959961
Coniferyl_alcohol	cZR	-0.065593886	0.8395
Coniferyl_alcohol	cZROG	-0.013208274	0.967503
Coniferyl_alcohol	DZ	-0.207670011	0.517207
Coniferyl_alcohol	DZ9G	0.390438233	0.209546
Coniferyl_alcohol	DZOG	-0.16127539	0.616557
Coniferyl_alcohol	DZR	-0.169373894	0.598719
Coniferyl_alcohol	DZROG	-0.050364243	0.876475
Coniferyl_alcohol	iP	-0.201010719	0.531025

Coniferyl_alcohol	iP7G	-0.683217109	0.02048
Coniferyl_alcohol	iP9G	-0.272522061	0.657358
Coniferyl_alcohol	iPR	0.040798498	0.89982
Coniferyl_alcohol	tZ	-0.721363804	0.008098
Coniferyl_alcohol	tZ7G	-0.057151903	0.859963
Coniferyl_alcohol	tZ9G	-0.061253857	0.85001
Coniferyl_alcohol	tZOG	-0.065553942	0.839597
Coniferyl_alcohol	tZR	-0.065553303	0.839598
Coniferyl_alcohol	tZROG	-0.227528419	0.47696
Coniferyl_aldehyde	cZ	0.102137377	0.75211
Coniferyl_aldehyde	cZ9G	-0.229167384	0.497878
Coniferyl_aldehyde	cZOG	0.081814803	0.800445
Coniferyl_aldehyde	cZR	-0.492224759	0.104035
Coniferyl_aldehyde	cZROG	-0.582217717	0.047006
Coniferyl_aldehyde	DZ	0.173730317	0.589205
Coniferyl_aldehyde	DZ9G	0.551187515	0.063237
Coniferyl_aldehyde	DZOG	-0.086816994	0.788481
Coniferyl_aldehyde	DZR	-0.332500505	0.290973
Coniferyl_aldehyde	DZROG	-0.143825212	0.655637
Coniferyl_aldehyde	iP	-0.673044741	0.01645
Coniferyl_aldehyde	iP7G	-0.047529489	0.889633
Coniferyl_aldehyde	iP9G	-0.355149993	0.557503
Coniferyl_aldehyde	iPR	0.196976331	0.539471
Coniferyl_aldehyde	tZ	-0.267030464	0.401457
Coniferyl_aldehyde	tZ7G	0.001875208	0.995385
Coniferyl_aldehyde	tZ9G	-0.000794594	0.998045
Coniferyl_aldehyde	tZOG	-0.001275987	0.99686
Coniferyl_aldehyde	tZR	-0.492326277	0.103953
Coniferyl_aldehyde	tZROG	-0.468746548	0.124258
Ferulic_acid	cZ	-0.34274381	0.275438
Ferulic_acid	cZ9G	-0.346662412	0.29629
Ferulic_acid	cZOG	-0.304879686	0.335257
Ferulic_acid	cZR	-0.215031897	0.502117
Ferulic_acid	cZROG	-0.187572742	0.559375
Ferulic_acid	DZ	-0.041614583	0.897825
Ferulic_acid	DZ9G	0.296543672	0.349298
Ferulic_acid	DZOG	-0.394038641	0.205004
Ferulic_acid	DZR	-0.339153581	0.280828
Ferulic_acid	DZROG	-0.316051164	0.316928
Ferulic_acid	iP	-0.502175635	0.09617
Ferulic_acid	iP7G	-0.268629111	0.424452
Ferulic_acid	iP9G	-0.474169789	0.419724
Ferulic_acid	iPR	-0.128821499	0.689889
Ferulic_acid	tZ	-0.370464947	0.235845
Ferulic_acid	tZ7G	-0.350118307	0.264556
Ferulic_acid	tZ9G	-0.351669316	0.262299
Ferulic_acid	tZOG	-0.357027202	0.25459
Ferulic_acid	tZR	-0.215002179	0.502177
Ferulic_acid	tZROG	-0.071642381	0.824894
Gentisic_acid	cZ	-0.388785356	0.211652
Gentisic_acid	cZ9G	-0.316072735	0.343686
Gentisic_acid	cZOG	-0.345844106	0.270832
Gentisic_acid	cZR	-0.267586405	0.40044
Gentisic_acid	cZROG	-0.20741269	0.517738
Gentisic_acid	DZ	-0.027363351	0.932728
Gentisic_acid	DZ9G	0.169070942	0.599382
Gentisic_acid	DZOG	-0.235369702	0.461477
Gentisic_acid	DZR	-0.310836282	0.325414
Gentisic_acid	DZROG	-0.241272236	0.449981
Gentisic_acid	iP	-0.265346641	0.404545
Gentisic_acid	iP7G	-0.284107247	0.397165
Gentisic_acid	iP9G	-0.394829749	0.510672
Gentisic_acid	iPR	-0.276416588	0.384461
Gentisic_acid	tZ	-0.186457279	0.561756
Gentisic_acid	tZ7G	-0.353551739	0.259575
Gentisic_acid	tZ9G	-0.350164449	0.264488
Gentisic_acid	tZOG	-0.356421798	0.255454
Gentisic_acid	tZR	-0.267503142	0.400592
Gentisic_acid	tZROG	0.130814191	0.685307
L-Phenylalanine	cZ	-0.356067287	0.255961
L-Phenylalanine	cZ9G	-0.370077435	0.262596

L-Phenylalanine	cZOG	-0.42559435	0.167781
L-Phenylalanine	cZR	-0.188957828	0.556425
L-Phenylalanine	cZROG	-0.191649678	0.550709
L-Phenylalanine	DZ	0.383854241	0.218009
L-Phenylalanine	DZ9G	-0.155127464	0.630228
L-Phenylalanine	DZOG	-0.323547182	0.304947
L-Phenylalanine	DZR	-0.196679335	0.540095
L-Phenylalanine	DZROG	-0.260754715	0.413028
L-Phenylalanine	iP	-0.544224116	0.067352
L-Phenylalanine	iP7G	0.504221195	0.113751
L-Phenylalanine	iP9G	-0.336752164	0.579481
L-Phenylalanine	iPR	-0.157782427	0.624311
L-Phenylalanine	tZ	0.367743833	0.239573
L-Phenylalanine	tZ7G	-0.377022302	0.227005
L-Phenylalanine	tZ9G	-0.374141729	0.230864
L-Phenylalanine	tZOG	-0.378527552	0.225004
L-Phenylalanine	tZR	-0.188930641	0.556483
L-Phenylalanine	tZROG	0.22821662	0.475591
Methylthioadenosine	cZ	0.016300666	0.959899
Methylthioadenosine	cZ9G	-0.161532736	0.635145
Methylthioadenosine	cZOG	-0.138537764	0.667642
Methylthioadenosine	cZR	-0.241404175	0.449726
Methylthioadenosine	cZROG	-0.363695402	0.245183
Methylthioadenosine	DZ	0.412579172	0.182574
Methylthioadenosine	DZ9G	-0.131810912	0.683019
Methylthioadenosine	DZOG	0.05185692	0.87284
Methylthioadenosine	DZR	0.041401664	0.898346
Methylthioadenosine	DZROG	-0.021793986	0.9464
Methylthioadenosine	iP	-0.378228566	0.225401
Methylthioadenosine	iP7G	0.727348381	0.011192
Methylthioadenosine	iP9G	-0.050739552	0.935424
Methylthioadenosine	iPR	0.192777184	0.548322
Methylthioadenosine	tZ	0.58600871	0.045248
Methylthioadenosine	tZ7G	-0.062120335	0.84791
Methylthioadenosine	tZ9G	-0.0572601	0.859701
Methylthioadenosine	tZOG	-0.054374798	0.866713
Methylthioadenosine	tZR	-0.241460498	0.449617
Methylthioadenosine	tZROG	0.168452734	0.600738
p-Coumaroyl_quinic_acid	cZ	-0.181564074	0.572248
p-Coumaroyl_quinic_acid	cZ9G	-0.254857045	0.449463
p-Coumaroyl_quinic_acid	cZOG	-0.30151991	0.340879
p-Coumaroyl_quinic_acid	cZR	-0.121598762	0.706575
p-Coumaroyl_quinic_acid	cZROG	-0.153062118	0.634845
p-Coumaroyl_quinic_acid	DZ	0.490618253	0.105344
p-Coumaroyl_quinic_acid	DZ9G	-0.312834982	0.322147
p-Coumaroyl_quinic_acid	DZOG	-0.145333211	0.652227
p-Coumaroyl_quinic_acid	DZR	-0.072735677	0.822259
p-Coumaroyl_quinic_acid	DZROG	-0.165728653	0.606724
p-Coumaroyl_quinic_acid	iP	-0.38031576	0.222641
p-Coumaroyl_quinic_acid	iP7G	0.877584216	0.000384
p-Coumaroyl_quinic_acid	iP9G	-0.351001948	0.562445
p-Coumaroyl_quinic_acid	tZ	0.710053253	0.009674
p-Coumaroyl_quinic_acid	tZ7G	-0.225305972	0.481391
p-Coumaroyl_quinic_acid	tZ9G	-0.220784352	0.490464
p-Coumaroyl_quinic_acid	tZOG	-0.222401773	0.487209
p-Coumaroyl_quinic_acid	tZR	-0.121613681	0.70654
p-Coumaroyl_quinic_acid	tZROG	0.269808762	0.396387
Sinapaldehyde	cZ	-4.1537E-05	0.999898
Sinapaldehyde	cZ9G	-0.166311628	0.62503
Sinapaldehyde	cZOG	-0.002735405	0.993268
Sinapaldehyde	cZR	-0.428108426	0.165014
Sinapaldehyde	cZROG	-0.490093463	0.105774
Sinapaldehyde	DZ	0.01461412	0.964046
Sinapaldehyde	DZ9G	0.520470669	0.082773
Sinapaldehyde	DZOG	-0.115002713	0.721917
Sinapaldehyde	DZR	-0.306564121	0.332457
Sinapaldehyde	DZROG	-0.127782786	0.692281
Sinapaldehyde	iP	-0.636207144	0.026145
Sinapaldehyde	iP7G	-0.236944632	0.482986
Sinapaldehyde	iP9G	-0.373125667	0.536188
Sinapaldehyde	iPR	0.139341348	0.665813

Sinapaldehyde	tZ	-0.392914865	0.206415
Sinapaldehyde	tZ7G	-0.059130571	0.85516
Sinapaldehyde	tZ9G	-0.062788438	0.846291
Sinapaldehyde	tZOG	-0.062362299	0.847323
Sinapaldehyde	tZR	-0.428152058	0.164966
Sinapaldehyde	tZROG	-0.388249822	0.212337
Sinapyl_alcohol	cZ	-0.261787946	0.411111
Sinapyl_alcohol	cZ9G	-0.233908487	0.488775
Sinapyl_alcohol	cZOG	-0.35053664	0.263946
Sinapyl_alcohol	cZR	-0.173583037	0.589526
Sinapyl_alcohol	cZROG	-0.140884578	0.662305
Sinapyl_alcohol	DZ	0.454133198	0.13806
Sinapyl_alcohol	DZ9G	-0.449018777	0.143115
Sinapyl_alcohol	DZOG	-0.159078359	0.62143
Sinapyl_alcohol	DZR	-0.147188526	0.648039
Sinapyl_alcohol	DZROG	-0.141057171	0.661913
Sinapyl_alcohol	iP	-0.491731792	0.104435
Sinapyl_alcohol	iP7G	0.725103693	0.011572
Sinapyl_alcohol	iP9G	-0.127400608	0.838228
Sinapyl_alcohol	iPR	-0.280111223	0.377874
Sinapyl_alcohol	tZ	0.600081961	0.039129
Sinapyl_alcohol	tZ7G	-0.268102143	0.399497
Sinapyl_alcohol	tZ9G	-0.263154651	0.408583
Sinapyl_alcohol	tZOG	-0.268213426	0.399294
Sinapyl_alcohol	tZR	-0.173542259	0.589615
Sinapyl_alcohol	tZROG	0.290823569	0.359111
Tetrahydrofolate	cZ	-0.411391051	0.237544
Tetrahydrofolate	cZ9G	-0.57942884	0.102022
Tetrahydrofolate	cZOG	-0.314575709	0.376014
Tetrahydrofolate	cZR	-0.001693423	0.996296
Tetrahydrofolate	cZROG	0.036894173	0.919404
Tetrahydrofolate	DZ	-0.230013921	0.52263
Tetrahydrofolate	DZ9G	0.210555001	0.559293
Tetrahydrofolate	DZOG	-0.58481964	0.075769
Tetrahydrofolate	DZR	-0.305020636	0.391457
Tetrahydrofolate	DZROG	-0.54908729	0.100201
Tetrahydrofolate	iP	-0.21665695	0.54769
Tetrahydrofolate	iP7G	-0.629403789	0.069331
Tetrahydrofolate	iP9G	-0.629770013	0.566298
Tetrahydrofolate	iPR	0.101194567	0.78089
Tetrahydrofolate	tZ	-0.684109552	0.029125
Tetrahydrofolate	tZ7G	-0.476159429	0.164169
Tetrahydrofolate	tZ9G	-0.48567768	0.15471
Tetrahydrofolate	tZOG	-0.477386575	0.16293
Tetrahydrofolate	tZR	-0.001705432	0.996269
Tetrahydrofolate	tZROG	-0.193176948	0.592845
trans-5-O-(4-Coumaroyl)-D-quinate	cZ	-0.057533303	0.859037
trans-5-O-(4-Coumaroyl)-D-quinate	cZ9G	-0.091674494	0.788642
trans-5-O-(4-Coumaroyl)-D-quinate	cZOG	-0.178236047	0.579428
trans-5-O-(4-Coumaroyl)-D-quinate	cZR	-0.169500491	0.598441
trans-5-O-(4-Coumaroyl)-D-quinate	cZROG	-0.188888097	0.556573
trans-5-O-(4-Coumaroyl)-D-quinate	DZ	0.406905477	0.189268
trans-5-O-(4-Coumaroyl)-D-quinate	DZ9G	-0.386361412	0.214762
trans-5-O-(4-Coumaroyl)-D-quinate	DZOG	-0.000809084	0.998009
trans-5-O-(4-Coumaroyl)-D-quinate	DZR	-0.043798916	0.892489
trans-5-O-(4-Coumaroyl)-D-quinate	DZROG	-0.021862204	0.946233
trans-5-O-(4-Coumaroyl)-D-quinate	iP	-0.47876682	0.115337
trans-5-O-(4-Coumaroyl)-D-quinate	iP7G	0.778785685	0.004737
trans-5-O-(4-Coumaroyl)-D-quinate	iP9G	0.136853531	0.826298
trans-5-O-(4-Coumaroyl)-D-quinate	tZ	0.629706462	0.02821
trans-5-O-(4-Coumaroyl)-D-quinate	tZ7G	-0.089920357	0.78108
trans-5-O-(4-Coumaroyl)-D-quinate	tZ9G	-0.08627733	0.78977
trans-5-O-(4-Coumaroyl)-D-quinate	tZOG	-0.088167298	0.785259
trans-5-O-(4-Coumaroyl)-D-quinate	tZR	-0.169500402	0.598442
trans-5-O-(4-Coumaroyl)-D-quinate	tZROG	0.193532483	0.546726
Vanillic_acid	cZ	0.205477594	0.521739
Vanillic_acid	cZ9G	0.243213365	0.471129
Vanillic_acid	cZOG	0.221971841	0.488073
Vanillic_acid	cZR	-0.1917431	0.550511
Vanillic_acid	cZROG	-0.197904649	0.537523
Vanillic_acid	DZ	0.622454075	0.030649

Vanillic_acid	DZ9G	0.077084107	0.811796
Vanillic_acid	DZOG	0.211986262	0.508336
Vanillic_acid	DZR	0.081314661	0.801643
Vanillic_acid	DZROG	0.318366522	0.3132
Vanillic_acid	iP	-0.269644177	0.396686
Vanillic_acid	iP7G	0.255424989	0.448418
Vanillic_acid	iP9G	0.366874944	0.543582
Vanillic_acid	iPR	0.241638853	0.449271
Vanillic_acid	tZ	0.1615477	0.615954
Vanillic_acid	tZ7G	0.234305814	0.463564
Vanillic_acid	tZ9G	0.234225645	0.463721
Vanillic_acid	tZOG	0.226287463	0.479432
Vanillic_acid	tZR	-0.191717605	0.550565
Vanillic_acid	tZROG	-0.072896385	0.821872